# Cystic fibrosis defects in intestinal bile acid and guanylin signaling

**Pauline Tresa Ikpa**

The studies presented in this thesis were performed at the Laboratory of Gastroenterology and Hepatology, Erasmus MC University Medical Center Rotterdam, the Netherlands.

This research was funded by:

- The Dutch Cystic Fibrosis Foundation (NCFS).

Printing of this thesis was financially supported by: Erasmus Postgraduate School of Molecular Medicine.

Cover and book layout: Pauline Ikpa

Printed by:Gildeprint

ISBN: 978-94-6233-813-5

# Cystic fibrosis defects in intestinal bile acid and guanylin signaling

Signaal transductie door galzouten en guanylines in cystic fibrosis darmepitheel

**Thesis**
to obtain the degree of Doctor from the
Erasmus University Rotterdam
by command of the
rector magnificus

Prof. dr. H.A.P. Pols

and in accordance with the decision of the Doctorate Board
The public defense shall be held on

The 5th of December 2017 at 11:30am

by

**Pauline Tresa Ikpa**

born in Ikeja, Lagos, Nigeria.

Erasmus University Rotterdam

**Doctoral Committee**

| | |
|---|---|
| **Promotor:** | Prof. dr. M.P. Peppelenbosch |
| **Inner Committee:** | Prof. dr. M. Bruno |
| | Prof. dr. J.C. Escher |
| | Prof. dr. R.P.J. Oude Elferink |
| **Copromotors:** | Dr. M.J.C. Bijvelds |
| | Dr. H.R. de Jonge |

# Contents

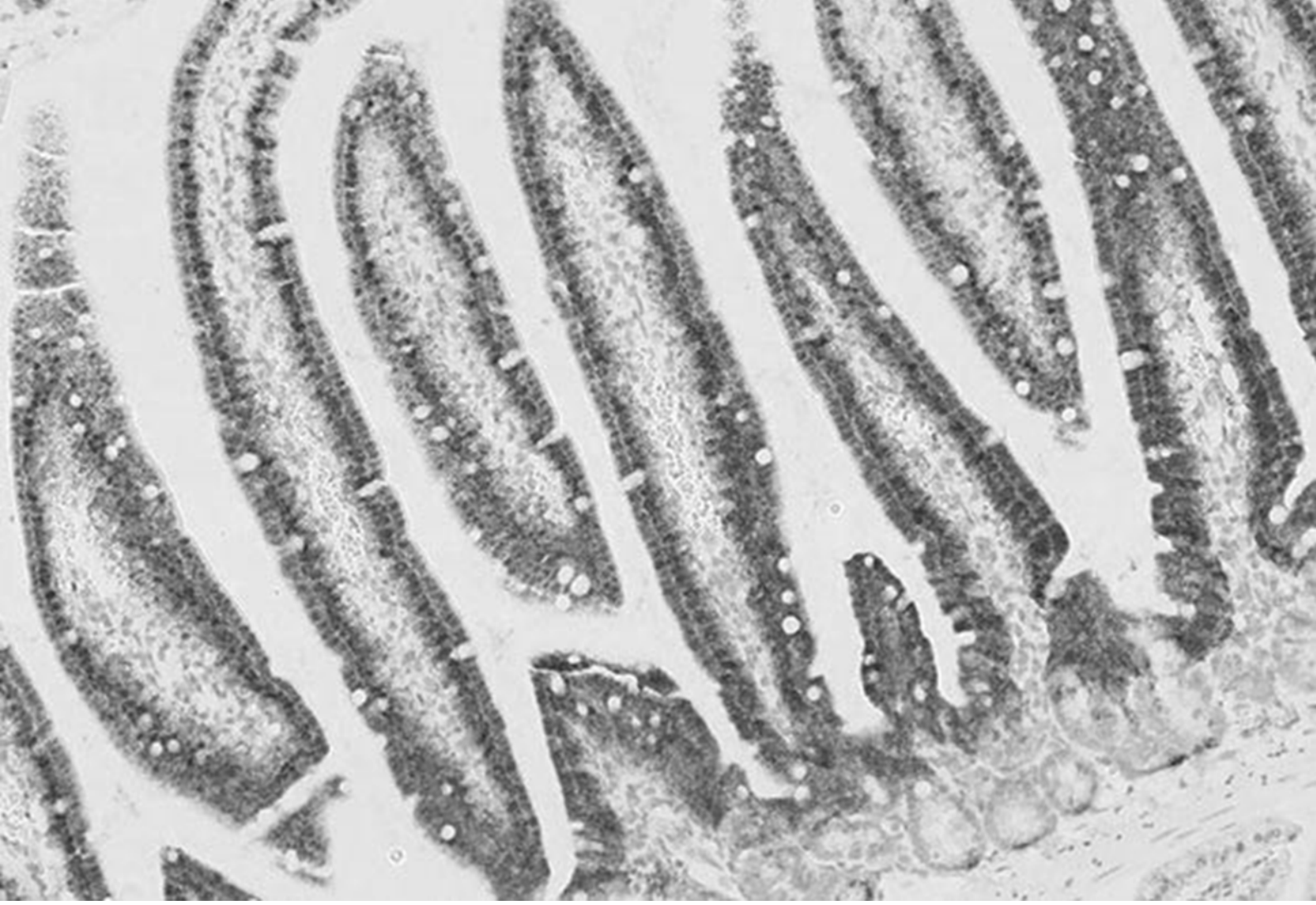

# Chapter 1

# General introduction and outline of the thesis

## General introduction and outline of the thesis

Cystic fibrosis (CF) is a life-threatening autosomal recessive monogenic disease that affects all racial and ethnic groups but is most common among Caucasians, with a carrier frequency of 1:25 (affecting 1 in 2500–4500 newborns) [2, 3]. The major CF pathology is the accumulation of viscous mucus at the epithelial surfaces of affected organs [4, 5]. A major organ affected by CF is the respiratory system, in which accretion of viscous mucus leads to impaired mucociliary clearance, recurrent pulmonary infection, and chronic lung and sinus disease [6]. This pulmonary pathology is the major cause of morbidity and mortality in CF patients [7].

The gastrointestinal pathology of CF includes inflammation of the gut wall, pancreatic insufficiency, malabsorption and malnutrition, bacterial overgrowth and obstruction of the small intestine, and liver disease (focal biliary cirrhosis) [8, 9]. Replacement of pancreatic enzymes and intensive symptomatic pulmonary therapy have improved the treatment of CF, resulting in a progressive increase in the median survival age (currently ~37 years) [10].

### *CFTR Structure*

CF is caused by mutations in the CF gene (also referred to as *ABCC7*) that encodes a chloride ($Cl^-$)/bicarbonate ($HCO_3^-$) conducting channel called the cystic fibrosis transmembrane conductance regulator (CFTR) [11, 12]. CFTR is composed of 1480 amino acid residues arranged in a single polypeptide chain. CFTR is structurally akin to the family of ABC transporters, consisting of 2 transmembrane domains (TMDs), 2 nucleotide-binding domains (NBDs) and a regulatory domain (RD). The presence of the RD makes CFTR unique when compared to other ABC transporters. CFTR contains an N-terminal extension of about 80 residues and a C-terminal extension of about 30 residues. Both extensions are cytoplasmic oriented (Figure 1) [13, 14].

The 2 TMDs, each consisting of 6 membrane-spanning α-helices, are predicted to form a pore that allows the passage of $Cl^-$ and other anions, including $HCO_3^-$ [15, 16]. Phosphorylation of the RD is a prerequisite for CFTR channel gating (opening and closing).

### *CF disease variability*

Presently, over 2000 different mutations have been discovered of which more than 1100 are disease-associated [10] (http://www.genet.sickkids.on.ca/cftr/). CFTR mutations are clustered into six different classes, based on their phenotypic consequences [17-19]. CF-causing mutations can interfere with the biogenesis, transport, activity, and/or stability at the cell surface of CFTR [20]. The most common mutation, F508del, occurring on at least one allele in nearly

90% of all CF patients, has several separate functional defects, i.e. in protein folding (class II),

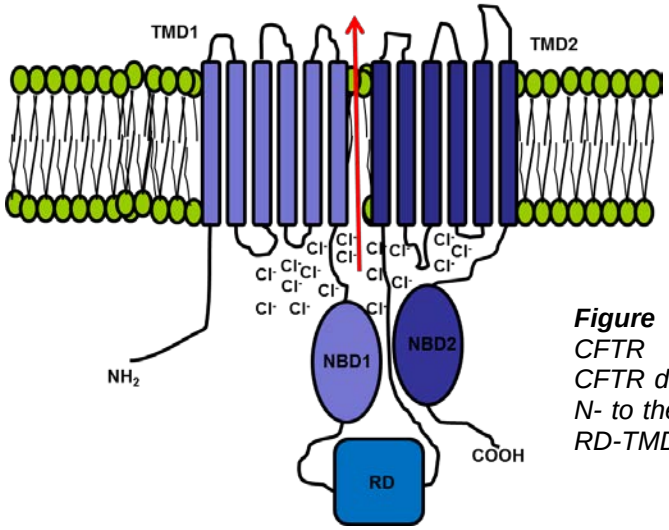


***Figure 1*** *Schematic model of CFTR structure, showing the CFTR domains organized from the N- to the C-terminus TMD1-NBD1-RD-TMD2-NBD2.*

channel gating (class III) and membrane stability (class V). This markedly complicates its pharmacological repair at the protein level. To some extent, these mutation classes also define disease severity. However, although CF is considered a monogenic disease, phenotypic variation among patients, even among those with the same CFTR genotype, is considerable. This variation is a consequence of genetic modifiers and, to a lesser extent, environmental factors [2].

Disease severity and complications also vary considerably among affected organ systems [21], and among individuals carrying different CFTR mutations [22]. For example, patients carrying the G551D mutation rarely suffer from meconium ileus, in contrast to those carrying the F508del or G542X mutation, although all these mutations are associated with pancreatic insufficiency [23-26].

### *CF gastrointestinal disease*

#### *Organization of the intestinal epithelium*

The intestinal lumen is lined by a continuous monolayer of columnar epithelial cells [27], that are structured into proliferative crypts and differentiated villi (small intestine) or surface epithelium (colon). The crypts invaginate into the underlying mesenchyme and the villi project into the intestinal lumen [28]. The crypt-based columnar (CBC) stem cells give rise to rapidly dividing transit-amplifying cells (TACs) which differentiate into 5 different cell types (Figure 2). The absorptive cells, also known as enterocytes, comprise ~90% of the villus cell population.

All differentiated cells migrate towards the top of the villi, except for the Paneth cells that are retained at the base of the crypts. In the crypts, Paneth cells reside interspaced between the CBC stem cells during their life span of ~1 month [29]. These cells protect the epithelium against bacterial infection by secreting lysozyme and other antimicrobial proteins, such as the α-

defensins [30]. In addition, Paneth cells have been shown to express the luminocrinic peptides

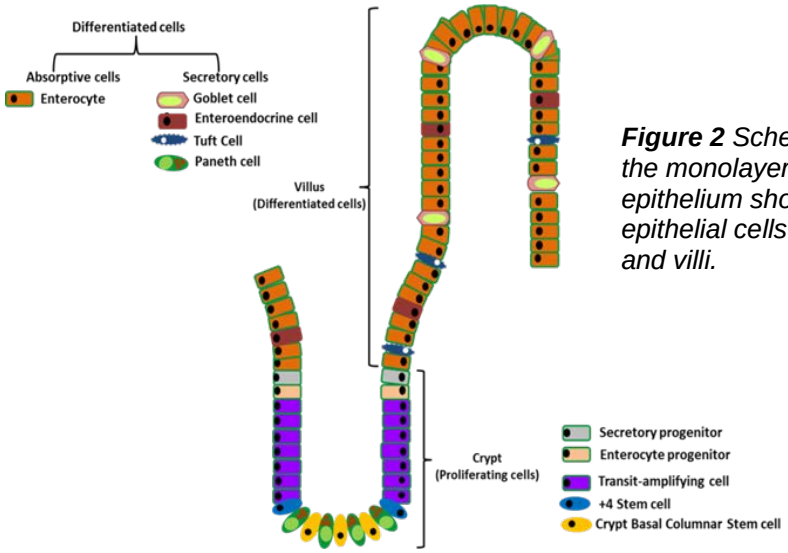


***Figure 2*** *Schematic diagram of the monolayered intestinal epithelium showing the columnar epithelial cells forming the crypts and villi.*

guanylin (*GUCA2A*) and uroguanylin (*GUCA2B*) which fulfill an essential role in intestinal fluid homeostasis [31]. Other cells of the secretory lineage, including enteroendocrine cells and Tuft cells, secrete different classes of peptide hormone such as glucagon-like peptide 1 and 2 (GLP-1, -2), cholecystokinin (CCK), glucose-dependent insulinotropic peptide (GIP), and somatostatin (SST) [28, 31-34].

The colonic epithelium mainly consists of crypts that, like the small intestinal crypts, contain CBC-like proliferative stem cells. These cells produce TACs which differentiate into columnar-, goblet- and enteroendocrine cells. The colonic crypts also contain Paneth-like cells that, however, do not produce anti-microbial peptides [35, 36]. In the human small intestine, cell migration from the base of the crypts to the tip of the villi takes 3-5 days, after which the cells become apoptotic and are shedded. The continuous and rapid renewal of the epithelium from CBC stem cells and TACs is a unique property of the intestine and requires a delicate balance between locally produced growth and differentiation factors.

The intestinal epithelium is structurally and functionally polarized, with segregation of specific plasma membrane (transport) proteins to either the apical or basolateral pole of the cell. Paracellular transport of electrolytes and solutes (e.g. glucose, amino acids, peptides, bile salts) is restricted through cation-selective tight junctional complexes consisting of multiple transmembrane proteins including claudins, occludins and paracellin [37-41]. Many other proteins associate with the tight junction at its cytoplasmic side, thereby changing its selectivity and turning it into a dynamic rather than a static structure [41].

***Fluid homeostasis, electrolyte absorption and secretion, and water flow***

In the gastrointestinal tract, water and electrolyte secretion are central to its physiological function. The gastrointestinal tract drains about 8 liters of fluid per day [42]. The main pathway for apical chloride secretion into the intestinal lumen is CFTR. CFTR is expressed predominantly in the apical membrane of the crypt cells, although a small number of cells with very high expression of CFTR is found scattered throughout the villus epithelium in humans (and rats), but not in mice (Figure 3) [1, 42-44].

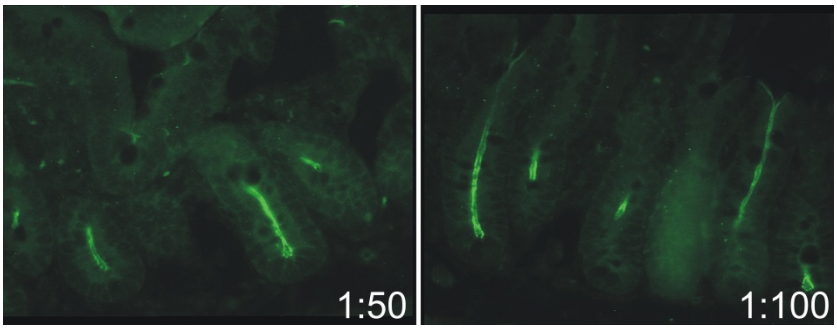


***Figure 3*** *CFTR immunostaining in mouse ileum using two distinct antibody titers. CFTR is localized predominantly at the apical pole of epithelial cells in the crypts, but expression extends to the villi [1].*

Chloride is the predominant electrolyte that contributes to fluid secretion. Chloride secretion initiates paracellular sodium secretion in response to electrical hyperpolarization. This salt secretion triggers eventual osmotic water flow to the lumen. Concurrent with activation of CFTR, sodium absorption via the sodium/proton exchanger NHE3, the major sodium importer in mammalian intestine is inhibited (discussed in more details below) [45]. This combination of chloride secretion and inhibition of NHE3-mediated sodium absorption drives net fluid secretion into the intestinal lumen. Disruption of this process, through yet incompletely resolved mechanisms, results in the many secondary intestinal disease manifestations of CF, e.g. defective mucin expansion and clearance, impaired bacterial clearance and bacterial overgrowth, inflammation, fecal wasting of bile salts, and intestinal obstruction.

In CF, hyperabsorption of sodium through ENaC channels in the airways or through NHE3 in the intestine may contribute to the imbalance of luminal fluid volume and composition [46-51]. NHE3 is responsible for the majority of sodium absorption in the gastrointestinal tract and kidney [45, 52]. In the small intestine, NHE3 activity also provides the acidic micro-climate that drives proton-coupled nutrient absorption mechanisms [53-55]. NHE3 is in a partially activated state under basal conditions, and it is thought to be inhibited in the early digestive period [56]. This inhibition stimulates retention of water in the lumen, which serves to spread

digestive enzymes over the intestinal surface, enhancing enzymatic digestion of nutrients. NHE3 activity is tightly regulated by multiple signaling pathways, leading to rapid cell surface insertion or retrieval of the protein [45, 57]. Inactivation of NHE3 is triggered by protein kinase-mediated, phosphorylation of NHE3 [57, 58]. The importance of NHE3 in intestinal fluid and acid-base homeostasis is underlined by the fact that genetic ablation of NHE3 results in mild diarrhea and systemic acidosis [59, 60].

***Mucus production***

The mucus that lines the surface of the intestinal epithelium is principally produced by goblet cells, which secrete its major component, MUC2. The mucus layer lubricates the epithelial surface, aids digestion, and helps to preserve the intestinal architecture. In addition, the mucus layer forms a barrier between luminal pathogens and epithelial cells. In the healthy intestine, this mucus layer appears to act as a size exclusion filter that prevents bacteria from entering the crypts [61].

Recent studies in CF animal models (mouse [62-64], pig [65], rat [66]) indicate that normal mucus release in the intestine and trachea requires concurrent bicarbonate secretion. Bicarbonate serves to chelate calcium and hydrogen ions that prevent expansion of MUC2, released by the goblet cells. The subsequent detachment of MUC2 from the goblet cells is catalyzed by a metalloprotease, meprin β, which is shedded from neighboring enterocytes in response to bacterial contact or microbial signaling [67]. Thus, a major function of the mucus layer is to entrap pathogens and prevent direct contact with the small intestinal epithelium by promoting their fast transit (“flushing”).

In CF, both CFTR mediated and regulated chloride and bicarbonate secretion is defective, causing the production of a hyper-viscous, immobile mucus layer. The accretion of this *sticky* mucus triggers small intestinal bacterial overgrowth (SIBO) and, together with luminal dehydration, may result in intestinal inflammation and obstruction [16, 46, 64, 68, 69]. In addition, defective bicarbonate production is suggested to lower epithelial surface pH and impede bacterial killing by pH-sensitive defensins. This, in conjunction with protracted nutrient digestion and absorption, further expedites SIBO [46, 68, 69].

***Intestinal obstruction***

Meconium ileus, which affects 10 – 20% of CF newborns, develops perinatally when inspissated secretions obstruct the gastrointestinal lumen of the distal small intestine [47, 48, 70-72]. CF-associated meconium ileus typically presents within 48h after birth as a failure to pass

meconium. Because of the severe obstruction, this complication may be fatal if left untreated [73, 74]. Obstruction of the distal small intestine also affects CF patients in later stages of life. The so-called distal intestinal obstructive syndrome (DIOS) is caused by accumulation of viscous mucoid and faecal material that adheres strongly to the intestinal wall [75-77]. DIOS occurs mostly, but not exclusively, in patients with a history of meconium ileus and pancreatic insufficiency. Delayed gastric emptying and protracted ileal and colonic transit may also contribute to DIOS [78]. A defect in bile acid-induced, CFTR-mediated chloride and bicarbonate secretion may worsen luminal dehydration in the ileum and may account for the predominantly distal location of obstruction . At present, meconium ileus is treated by surgery and DIOS is treated by oral rehydration, using stool softeners [79].

***Small intestinal bacterial overgrowth (SIBO)***

There is an increasing awareness that the gut microbiota plays a key role in gastrointestinal disorders, thereby offering a novel therapeutic target to manage or prevent gastrointestinal conditions [80, 81]. The stagnant mucus in CF creates a niche for abnormal microbial colonization and development of SIBO [82, 83]. In mice, loss of CFTR function is associated with a significant decrease in gut bacterial community richness, and reduced abundance of putative protective species such as *Acinetobacter iwoffii* and a multitude of *Lactobacilliales* members [82-84]. Microorganisms associated with gastrointestinal infection and immunomodulation such as mycobacteria species and *Bacteroides fragilis* are significantly enriched in CF mice. The opportunistic pathogen *B. fragilis* is a frequent cause of gastrointestinal infection and diarrheal disease [85]. Use of antibiotics for CF management also influences the intestinal bacterial community, resulting in enrichment of *Lactobacillaceae* and *Bifidobacteriaceae* strains. Concomitantly, antibiotics, reduce abundance of *Enterobacteriaceae* and *Clostridiaceae* which are associated with SIBO and inflammatory bowel disease [83]. *Enterobacteriaceae* and *Clostridiaceae* may also suppress bacterial species required for maintaining motility and immune homeostasis.

***Intestinal (wall) inflammation***

CF-related intestinal inflammation is already evident in children and young adults [86-88]. Whether the pathogenesis of inflammation in CF–affected organs is of primary or secondary origin, or both, is still under debate [89]. Many factors may contribute to the pathogenesis of CF-related intestinal inflammation, such as chronic pancreatic enzyme supplementation, dysmotility, and SIBO. CF-related intestinal inflammation, which is characterized by high plasma and fecal

levels of the "CF-antigen" calprotectin (MRP8/14), has been associated with a defective immune system [90-92], but may also occur secondary to bacterial infection [93]. Increased levels of inflammatory cytokines, immunoglobulins and other proteins have been found in the intestine of CF-patients with pancreatic-insufficiency [87].

A recent report shows that knockdown of CFTR in intestinal epithelial cell lines induces changes in the inflammatory response system as is manifest by increases in gene expression of IL-6 and IL-8 as well as enhanced activation of the ERK1/2 MAPK, $I_kB\alpha$ and $NF\text{-}_kB$ pathways [89]. This finding suggest that the CFTR defect itself may directly contribute to the propensity to inflammation in the CF intestine.

***Nutrient malabsorption and enhanced fecal bile salt excretion***

Malabsorption of nutrients observed in CF patients is caused principally by pancreatic insufficiency, which results in malnutrition [94]. Nutrient malabsorption was shown to be accompanied by enhanced fecal bile salt excretion in CF patients and CF mice [95-98]. Enhanced fecal bile salt excretion may be attributed to interrupted enterohepatic cycling of bile salts. In CF mice, defective gallbladder emptying may reduce intraluminal bile salt levels and the activity of the farnesoid X receptor (FXR) in the intestine [99]. The FXR target FGF15 is an intestinal hormone that is released into the portal vein and regulates *de novo* bile acid synthesis in the liver by reducing the hepatic expression of CYP7a1 via the FGFR4-ERK-cJUN signal transduction pathway [100]. CYP7a1 is the rate limiting enzyme in the *de novo* synthesis pathway [101, 102]. However, at present it is not known how the FXR signaling pathway affects bile acid homeostasis in CF patients.

***CF Therapies***

***Restoring CFTR function***

Protein-repair therapy in CF aims at rescuing the function of the mutated CFTR protein by improving its expression, folding, trafficking, channel gating and/or membrane stability. Pharmacological targeting of CF disease will often require a combination of therapeutic molecules. This is because (i) one single mutation may interfere with several aspects of CFTR biogenesis and function; (ii) ~40% of all CF patients ("compound heterozygotes") carry a different mutation on each of the CFTR alleles, and (iii) no single molecule is expected to correct the whole spectrum of mutation-induced abnormalities in CF. A clear exception to this rule is the rescue of class III mutant CFTR (G551D and 8 other CFTR gating mutations) by VX-770 (Ivacaftor/Kalydeco®; Vertex), which was shown to be highly effective even in long-term

clinical trials [8, 103, 104]. However, efficient functional rescue of F508del-CFTR requires the combination of a small molecule “corrector” which is capable of improving the folding and trafficking of the F508del-CFTR protein to the cell surface, and a “potentiator” which corrects the opening/gating defect of F508del-CFTR. This is probably why clinical trials, assessing the efficacy of monotherapy with the corrector VX-809 (Lumacaftor) or with the potentiator VX-770 failed to reach their primary endpoint [105, 106].

The combination of VX-809 and VX-770 (named Orkambi®) was shown to be moderately effective in improving CF lung function of homozygous F508del patients, and has recently been approved by the regulatory agencies (FDA and EMA) for this CF cohort [107-110]. The search for small molecule CFTR rescue compounds is still on-going. New drugs may act additive or synergistically with an existing drug such as VX-809 [111-113]. In preclinical studies, synergy is especially prominent with a combination of F508del correctors, i.e. a so called class 1 corrector, acting as a NBD1 domain stabilizer, and a class II corrector, capable of stabilizing the NBD1-TMD2 interface [114]. New correctors may be discovered by high throughput screening (HTS) of new chemical libraries, by the synthesis of common pharmacophoric moieties present in known correctors [115], by the use of a genomic signature approach [116], or by HTS of potential CF drugs by molecular docking [117]. The recent breakthrough in our knowledge of the atomic structure of the full-length CFTR, achieved by single molecule electron cryo-microscopy [118], not only has provided new insights into the structural consequences of CF-causing mutations, but may also facilitate the rational design of novel and more efficient CF therapeutics by this virtual screening approach. In addition, testing of drugs (and drug combinations) on patient-derived cell models may allow the selection of the most effective therapeutic approach(es) for a specific patient i.e. personalized therapy [19]. For this purpose, human bronchial epithelial cells derived from lungs explants or intestinal organoids isolated from rectal biopsies are used in CFTR functional assays, to determine the optimal drug or combination of drugs for an individual patient [119, 120]. Current approaches to CFTR rescue therapies and personalized CF therapies are discussed in more detail in Chapter 2 of this thesis.

***CFTR independent strategies***

Instead of restoring the function of CFTR itself by gene or protein therapy, the CF defect in chloride and bicarbonate secretion may also be bypassed by manipulating the abundance or activity of other ion transport mechanisms whose (in)activity may counteract the phenotypic consequences of CFTR dysfunction. Two approaches under consideration to regain ionic balance and restore luminal alkalinity are (1) activation of alternative chloride channels such as

anoctamins [121, 122] and SLC26A9 [123, 124] and (2) inhibition of sodium-coupled fluid absorption at the level of amiloride-sensitive epithelial sodium channels (ENaC) or the apical sodium/proton exchanger NHE3 [125-127]. The inhibition of NHE3, in contrast to ENaC inhibition, may not only improve luminal hydration, but may additionally promote luminal alkalinization. Therefore, both NHE3 and ENaC may serve as major therapeutic targets in CF [59, 128].

***Improving the intestinal fluid balance by enhancing guanylyl cyclase C signaling***

The luminocrinic peptides guanylin (GN, encoded by the *GUCA2A*) and uroguanylin (UGN, encoded by the *GUCA2B*) are involved in the regulation of salt and water transport across the intestinal epithelia [129]. The precursors of these peptides are secreted by epithelial cells and are extracellularly cleaved to generate the biologically active peptides. GN and UGN are similar in structure and consist of four conserved cysteine residues that form disulfide bonds which are essential for full activity of the peptides (Figure 4).

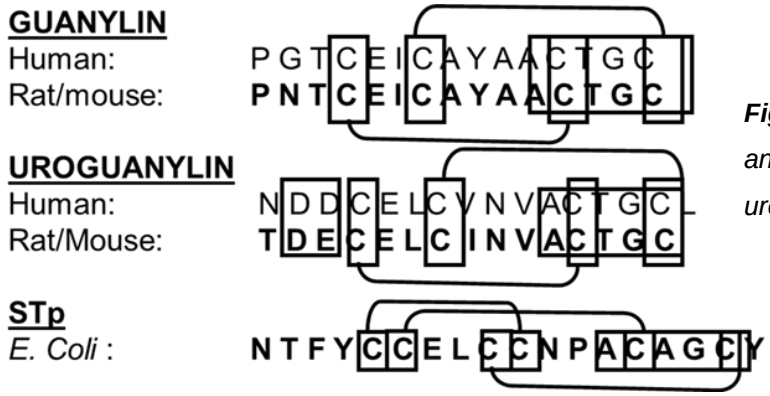


***Figure 4*** *Amino acid sequence and disulfide bonds of guanylin, uroguanylin and ST.*

GN is most active at a slightly alkaline pH while UGN is most active at a pH ~5.5 [130, 131]. The intestinal fluid present along the intestinal tract is of variable pH and this may have influenced the pattern of distribution observed for GN and UGN along the tract [31, 132, 133]. Intestinal secretion of GN and UGN is triggered by a high salt diet [134-136].

Upon luminal secretion and proteolytic cleavage, GN and UGN bind to the extracellular receptor domain of guanylyl cyclase C (GC-C), leading to the conversion of guanosine-5'-triphosphate (GTP) to cyclic guanosine monophosphate (cGMP) [92, 137]. GC-C is also activated by the heat-stable enterotoxin (ST) produced by enterotoxigenic strains of *Escherichia coli* [138]. ST has an extra disulfide bond and this may account for its high potency (Figure 4). GN and UGN are less potent in stimulating chloride secretion than ST as their affinity for GC-C is lower than of ST [139, 140].

Cyclic GMP executes its function by interacting with cGMP-dependent protein kinase type II (PKG-II), cyclic nucleotide-gated channels (CNGs) and cGMP-regulated cyclic nucleotide phosphodiesterases (PDEs) [141-143]. The increase in cGMP production after GC-C activation by GN and UGN regulates intestinal ion and fluid transport [144] by protein kinase-mediated activation of CFTR and inhibition of NHE3. The resultant increase in chloride and bicarbonate secretion and decrease in sodium absorption, stimulates osmotic water secretion and luminal alkalinization (Figure 5) [145, 146].

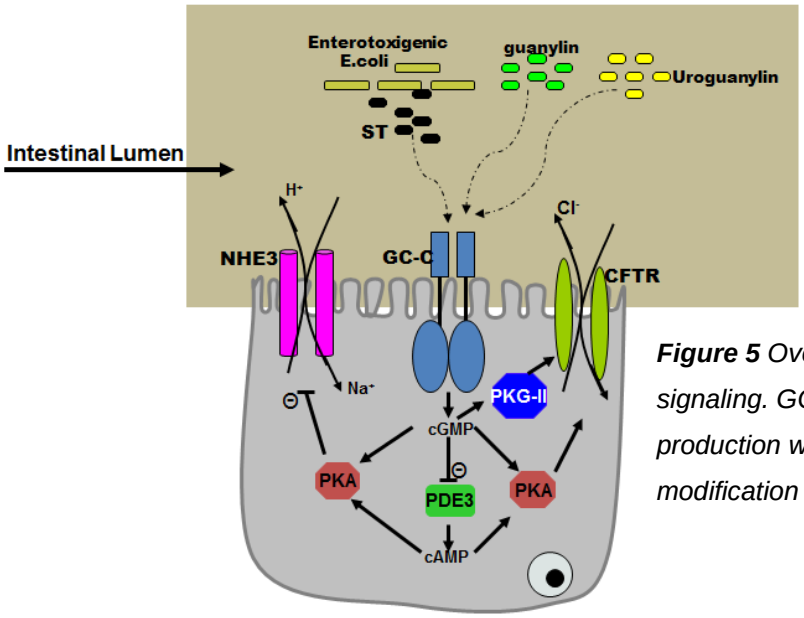


***Figure 5*** *Overview of GC-C/CFTR/NHE3 signaling. GC-C activation leads to cGMP production which results in the modification of CFTR and NHE3.*

GN and UGN were identified in serotonin-positive enterochromaffin cells of the small intestine [147]. However, there are indications that these peptides are also present in other intestinal cell types, including goblet cells [148]. In this thesis we investigated GN and UGN transcript levels in the various intestinal segments and cell types by a novel technique (RNA Scope) and also studied the expression at the protein level (Chapter 4 and 5).

## *Aim and outline of the thesis*

The hallmark of intestinal CF disease is dehydrated epithelial surfaces and mucus plugging emanating from defective CFTR-mediated chloride and bicarbonate secretion [45]. From this primary defect arises a plethora of secondary disease manifestations of which the exact etiology, and the relation to the primary defect is often uncertain. This thesis investigates several aspects of intestinal CF pathology, and aims to provide a rationale for novel therapeutic approaches. A potential alternative therapy proposed in this thesis aims to reduce NHE3-

mediated sodium and fluid absorption and to increase luminal fluidity by guanylin mimetic peptides. As a proof of principle, crossing CFTR- with NHE3-deficient mice has been shown to increase survival and decrease the incidence of intestinal obstruction in the CF mice [59].

The guanylins, through their ability to trigger GC-C/cGMP signaling and NHE3 inhibition may improve luminal hydration and alkalinization in the CF gut. Because the guanylins, in contrast to CFTR correctors and potentiators, act in a CFTR-mutation independent manner, their action could benefit all CF patients. In addition, guanylin/GC-C/cGMP signaling may also activate CFTR-mediated chloride and bicarbonate secretion in patients with residual CFTR activity, e.g. those carrying mutations belonging to class III-V. As discussed above, both chloride and bicarbonate secretion are required to restore the viscoelastic properties of mucus and ensure proper mucus unfolding and detachment.

**Thesis outline**

**Chapter 2** summarizes recent advances made toward personalized therapy in CF. We discuss the emergence and clinical efficacy of new CFTR-targeted drugs that act in a mutation-specific manner. We also discuss developments in *ex vivo* drug testing modes using CF patient derived tissue samples which promise to transform the therapeutic land scape from a trial-and-error prescription to personalized medicine.

In **Chapter 3** we performed transcriptome analysis on intestinal epithelium of CF mice and controls to assess the impact of CF on the intestinal transcriptome. This analysis indicates that SIBO and inflammation are key determinants of the CF-typical intestinal transcriptome.

In **chapter 4** the cellular localization of GN, UGN and GCC in the intestine was investigated, providing evidence for the role of GCC signaling in mucus production and innate immunity.

In **chapter 5** we provide evidence for perturbed GCC signaling in the CF intestine, showing that CF leads to reduced GN and UGN expression. These findings provide a further incentive for exploitation of the guanylyl cyclase-C pathway for restoration of intestinal fluid balance.

In **chapter 6** we investigate the effect of CF disease on FXR signaling and its impact on hepatic bile salt synthesis and fecal bile salt excretion.

**Chapter 7** contains a general discussion of all parts and chapters and also describes the future perspectives.

**References**

[1] Bijvelds MJ, Jorna H, Verkade HJ, Bot AG, Hofmann F, Agellon LB, et al. Activation of CFTR by ASBT-mediated bile salt absorption. Am J Physiol Gastrointest Liver Physiol. 2005;289:G870-9.
[2] Cutting GR. Modifier genetics: cystic fibrosis. Annu Rev Genomics Hum Genet. 2005;6:237-60.
[3] American College of O, Gynecologists Committee on G. ACOG Committee Opinion No. 486: Update on carrier screening for cystic fibrosis. Obstet Gynecol. 2011;117:1028-31.
[4] Cant N, Pollock N, Ford RC. CFTR structure and cystic fibrosis. Int J Biochem Cell B. 2014;52:15-25.
[5] McCarty NA. Permeation through the CFTR chloride channel. J Exp Biol. 2000;203:1947-62.
[6] Sears EH, Gartman EJ, Casserly BP. Treatment options for cystic fibrosis: state of the art and future perspectives. Rev Recent Clin Trials. 2011;6:94-107.
[7] Davies JC, Alton EW, Bush A. Cystic fibrosis. BMJ. 2007;335:1255-9.
[8] Yu J, Chen Z, Ni Y, Li Z. CFTR mutations in men with congenital bilateral absence of the vas deferens (CBAVD): a systemic review and meta-analysis. Hum Reprod. 2012;27:25-35.
[9] Cuppens H, Cassiman JJ. CFTR mutations and polymorphisms in male infertility. Int J Androl. 2004;27:251-6.
[10] Cutting GR. Cystic fibrosis genetics: from molecular understanding to clinical application. Nat Rev Genet. 2015;16:45-56.
[11] Quinton PM. Cystic fibrosis: impaired bicarbonate secretion and mucoviscidosis. Lancet. 2008;372:415-7.
[12] Choi JY, Lee MG, Ko S, Muallem S. Cl(-)-dependent HCO3- transport by cystic fibrosis transmembrane conductance regulator. JOP. 2001;2:243-6.
[13] Hunt JF, Wang C, Ford RC. Cystic Fibrosis Transmembrane Conductance Regulator (ABCC7) Structure. Csh Perspect Med. 2013;3.
[14] Higgins CF. Abc Transporters - from Microorganisms to Man. Annu Rev Cell Biol. 1992;8:67-113.
[15] Gadsby DC, Vergani P, Csanady L. The ABC protein turned chloride channel whose failure causes cystic fibrosis. Nature. 2006;440:477-83.
[16] Riordan JR. CFTR function and prospects for therapy. Annu Rev Biochem. 2008;77:701-26.
[17] Rogan MP, Stoltz DA, Hornick DB. Cystic fibrosis transmembrane conductance regulator intracellular processing, trafficking, and opportunities for mutation-specific treatment. Chest. 2011;139:1480-90.
[18] Derichs N. Targeting a genetic defect: cystic fibrosis transmembrane conductance regulator modulators in cystic fibrosis. Eur Respir Rev. 2013;22:58-65.
[19] Ikpa PT, Bijvelds MJ, de Jonge HR. Cystic fibrosis: toward personalized therapies. Int J Biochem Cell Biol. 2014;52:192-200.
[20] Farinha CM, Matos P. Repairing the basic defect in cystic fibrosis - one approach is not enough. Febs Journal. 2015.
[21] Welsh MJ, Ramsey BW, Accurso FJ, Cutting GR. Cystic fibrosis. In The Metabolic and Molecular Bases of Inheritanced Disease, ed. New York: McGraw-Hill2001.
[22] Ehre C, Ridley C, Thornton DJ. Cystic fibrosis: an inherited disease affecting mucin-producing organs. Int J Biochem Cell Biol. 2014;52:136-45.
[23] Kristidis P, Bozon D, Corey M, Markiewicz D, Rommens J, Tsui LC, et al. Genetic determination of exocrine pancreatic function in cystic fibrosis. Am J Hum Genet. 1992;50:1178-84.

[24] Hamosh A, Corey M. Correlation between Genotype and Phenotype in Patients with Cystic-Fibrosis. New Engl J Med. 1993;329:1308-13.
[25] Feingold J, Guilloud-Bataille M, Registry CCFC. Genetic comparisons of patients with cystic fibrosis with or without meconium ileus. Ann Genet-Paris. 1999;42:147-50.
[26] Ooi CY, Durie PR. Cystic fibrosis transmembrane conductance regulator (CFTR) gene mutations in pancreatitis. J Cyst Fibros. 2012;11:355-62.
[27] Barrett KE, Keely SJ. Chloride secretion by the intestinal epithelium: molecular basis and regulatory aspects. Annu Rev Physiol. 2000;62:535-72.
[28] Elliott EN, Kaestner KH. Epigenetic regulation of the intestinal epithelium. Cell Mol Life Sci. 2015.
[29] Troughton WD, Trier JS. Paneth and goblet cell renewal in mouse duodenal crypts. J Cell Biol. 1969;41:251-68.
[30] Porter EM, Bevins CL, Ghosh D, Ganz T. The multifaceted Paneth cell. Cell Mol Life Sci. 2002;59:156-70.
[31] Ikpa PT, Sleddens HF, Steinbrecher KA, Peppelenbosch MP, de Jonge HR, Smits R, et al. Guanylin and uroguanylin are produced by mouse intestinal epithelial cells of columnar and secretory lineage. Histochem Cell Biol. 2016;146:445-55.
[32] Cheng H, Leblond CP. Origin, differentiation and renewal of the four main epithelial cell types in the mouse small intestine. III. Entero-endocrine cells. Am J Anat. 1974;141:503-19.
[33] Gerbe F, Legraverend C, Jay P. The intestinal epithelium tuft cells: specification and function. Cell Mol Life Sci. 2012;69:2907-17.
[34] Gerbe F, van Es JH, Makrini L, Brulin B, Mellitzer G, Robine S, et al. Distinct ATOH1 and Neurog3 requirements define tuft cells as a new secretory cell type in the intestinal epithelium. J Cell Biol. 2011;192:767-80.
[35] Mantani Y, Nishida M, Yuasa H, Yamamoto K, Takahara E, Omotehara T, et al. Ultrastructural and histochemical study on the Paneth cells in the rat ascending colon. Anat Rec (Hoboken). 2014;297:1462-71.
[36] Noah TK, Donahue B, Shroyer NF. Intestinal development and differentiation. Exp Cell Res. 2011;317:2702-10.
[37] Anderson JM, Van Itallie CM. Tight junctions and the molecular basis for regulation of paracellular permeability. Am J Physiol. 1995;269:G467-75.
[38] Gunzel D, Yu AS. Claudins and the modulation of tight junction permeability. Physiol Rev. 2013;93:525-69.
[39] Krug SM, Schulzke JD, Fromm M. Tight junction, selective permeability, and related diseases. Semin Cell Dev Biol. 2014;36:166-76.
[40] Hou J, Paul DL, Goodenough DA. Paracellin-1 and the modulation of ion selectivity of tight junctions. J Cell Sci. 2005;118:5109-18.
[41] Fanning AS, Mitic LL, Anderson JM. Transmembrane proteins in the tight junction barrier. J Am Soc Nephrol. 1999;10:1337-45.
[42] Barrett KE, Keely SJ. Chloride secretion by the intestinal epithelium: molecular basis and regulatory aspects. Annu Rev Physiol. 2000;62:535-72.
[43] Strong TV, Boehm K, Collins FS. Localization of Cystic-Fibrosis Transmembrane Conductance Regulator Messenger-Rna in the Human Gastrointestinal-Tract by in-Situ Hybridization. Journal of Clinical Investigation. 1994;93:347-54.
[44] Ameen NA, van Donselaar E, Posthuma G, de Jonge H, McLaughlin G, Geuze HJ, et al. Subcellular distribution of CFTR in rat intestine supports a physiologic role for CFTR regulation by vesicle traffic. Histochem Cell Biol. 2000;114:219-28.
[45] Donowitz M, Li X. Regulatory binding partners and complexes of NHE3. Physiol Rev. 2007;87:825-72.

[46] Fridge JL, Conrad C, Gerson L, Castillo RO, Cox K. Risk factors for small bowel bacterial overgrowth in cystic fibrosis. J Pediatr Gastroenterol Nutr. 2007;44:212-8.
[47] Agrons GA, Corse WR, Markowitz RI, Suarez ES, Perry DR. Gastrointestinal manifestations of cystic fibrosis: radiologic-pathologic correlation. Radiographics. 1996;16:871-93.
[48] Eggermont E, De Boeck K. Small-intestinal abnormalities in cystic fibrosis patients. Eur J Pediatr. 1991;150:824-8.
[49] Reddy MM, Light MJ, Quinton PM. Activation of the epithelial Na+ channel (ENaC) requires CFTR Cl- channel function. Nature. 1999;402:301-4.
[50] Briel M, Greger R, Kunzelmann K. Cl- transport by cystic fibrosis transmembrane conductance regulator (CFTR) contributes to the inhibition of epithelial Na+ channels (ENaCs) in Xenopus oocytes co-expressing CFTR and ENaC. J Physiol-London. 1998;508:825-36.
[51] Stutts MJ, Canessa CM, Olsen JC, Hamrick M, Cohn JA, Rossier BC, et al. CFTR as a cAMP-dependent regulator of sodium channels. Science. 1995;269:847-50.
[52] Orlowski J, Grinstein S. Diversity of the mammalian sodium/proton exchanger SLC9 gene family. Pflugers Arch. 2004;447:549-65.
[53] Anderson CM, Thwaites DT. Regulation of intestinal hPepT1 (SLC15A1) activity by phosphodiesterase inhibitors is via inhibition of NHE3 (SLC9A3). Biochim Biophys Acta. 2007;1768:1822-9.
[54] Thwaites DT, Anderson CM. H+-coupled nutrient, micronutrient and drug transporters in the mammalian small intestine. Exp Physiol. 2007;92:603-19.
[55] Gekle M, Freudinger R, Mildenberger S. Inhibition of Na+-H+ exchanger-3 interferes with apical receptor-mediated endocytosis via vesicle fusion. J Physiol. 2001;531:619-29.
[56] Brett CL, Tukaye DN, Mukherjee S, Rao R. The yeast endosomal Na+K+/H+ exchanger Nhx1 regulates cellular pH to control vesicle trafficking. Mol Biol Cell. 2005;16:1396-405.
[57] Donowitz M, Mohan S, Zhu CX, Chen TE, Lin R, Cha B, et al. NHE3 regulatory complexes. J Exp Biol. 2009;212:1638-46.
[58] Cha B, Kim JH, Hut H, Hogema BM, Nadarja J, Zizak M, et al. cGMP inhibition of Na+/H+ antiporter 3 (NHE3) requires PDZ domain adapter NHERF2, a broad specificity protein kinase G-anchoring protein. J Biol Chem. 2005;280:16642-50.
[59] Bradford EM, Sartor MA, Gawenis LR, Clarke LL, Shull GE. Reduced NHE3-mediated Na+ absorption increases survival and decreases the incidence of intestinal obstructions in cystic fibrosis mice. Am J Physiol Gastrointest Liver Physiol. 2009;296:G886-98.
[60] Schultheis PJ, Clarke LL, Meneton P, Miller ML, Soleimani M, Gawenis LR, et al. Renal and intestinal absorptive defects in mice lacking the NHE3 Na+/H+ exchanger. Nat Genet. 1998;19:282-5.
[61] Johansson MEV, Hansson GC. Mucus and the Goblet Cell. Digest Dis. 2013;31:305-9.
[62] Garcia MA, Yang N, Quinton PM. Normal mouse intestinal mucus release requires cystic fibrosis transmembrane regulator-dependent bicarbonate secretion. J Clin Invest. 2009;119:2613-22.
[63] Gustafsson JK, Ermund A, Ambort D, Johansson ME, Nilsson HE, Thorell K, et al. Bicarbonate and functional CFTR channel are required for proper mucin secretion and link cystic fibrosis with its mucus phenotype. J Exp Med. 2012;209:1263-72.
[64] Liu J, Walker NM, Ootani A, Strubberg AM, Clarke LL. Defective goblet cell exocytosis contributes to murine cystic fibrosis-associated intestinal disease. J Clin Invest. 2015;125:1056-68.
[65] Hoegger MJ, Fischer AJ, McMenimen JD, Ostedgaard LS, Tucker AJ, Awadalla MA, et al. Impaired mucus detachment disrupts mucociliary transport in a piglet model of cystic fibrosis. Science. 2014;345:818-22.

[66] Tuggle KL, Birket SE, Cui X, Hong J, Warren J, Reid L, et al. Characterization of defects in ion transport and tissue development in cystic fibrosis transmembrane conductance regulator (CFTR)-knockout rats. PLoS One. 2014;9:e91253.
[67] Schutte A, Ermund A, Becker-Pauly C, Johansson ME, Rodriguez-Pineiro AM, Backhed F, et al. Microbial-induced meprin beta cleavage in MUC2 mucin and a functional CFTR channel are required to release anchored small intestinal mucus. Proc Natl Acad Sci U S A. 2014;111:12396-401.
[68] Pezzulo AA, Tang XX, Hoegger MJ, Alaiwa MH, Ramachandran S, Moninger TO, et al. Reduced airway surface pH impairs bacterial killing in the porcine cystic fibrosis lung. Nature. 2012;487:109-13.
[69] De Lisle RC, Borowitz D. The cystic fibrosis intestine. Cold Spring Harb Perspect Med. 2013;3:a009753.
[70] Karimi A, Gorter RR, Sleeboom C, Kneepkens CM, Heij HA. Issues in the management of simple and complex meconium ileus. Pediatr Surg Int. 2011;27:963-8.
[71] Gorter RR, Karimi A, Sleeboom C, Kneepkens CM, Heij HA. Clinical and genetic characteristics of meconium ileus in newborns with and without cystic fibrosis. J Pediatr Gastroenterol Nutr. 2010;50:569-72.
[72] Chaudry G, Navarro OM, Levine DS, Oudjhane K. Abdominal manifestations of cystic fibrosis in children. Pediatr Radiol. 2006;36:233-40.
[73] Rowe SM, Miller S, Sorscher EJ. Cystic fibrosis. N Engl J Med. 2005;352:1992-2001.
[74] Ziegler MM. Meconium ileus. Curr Probl Surg. 1994;31:731-77.
[75] Dray X, Bienvenu T, Desmazes-Dufeu N, Dusser D, Marteau P, Hubert D. Distal intestinal obstruction syndrome in adults with cystic fibrosis. Clin Gastroenterol Hepatol. 2004;2:498-503.
[76] Houwen RH, van der Doef HP, Sermet I, Munck A, Hauser B, Walkowiak J, et al. Defining DIOS and constipation in cystic fibrosis with a multicentre study on the incidence, characteristics, and treatment of DIOS. J Pediatr Gastroenterol Nutr. 2010;50:38-42.
[77] Blackman SM, Deering-Brose R, McWilliams R, Naughton K, Coleman B, Lai T, et al. Relative contribution of genetic and nongenetic modifiers to intestinal obstruction in cystic fibrosis. Gastroenterology. 2006/10/13 ed2006. p. 1030-9.
[78] Gregory PC. Gastrointestinal pH, motility/transit and permeability in cystic fibrosis. J Pediatr Gastroenterol Nutr. 1996;23:513-23.
[79] Colombo C, Ellemunter H, Houwen R, Munck A, Taylor C, Wilschanski M, et al. Guidelines for the diagnosis and management of distal intestinal obstruction syndrome in cystic fibrosis patients. J Cyst Fibros. 2011;10 Suppl 2:S24-8.
[80] Dahlqvist G, Piessevaux H. Irritable bowel syndrome: the role of the intestinal microbiota, pathogenesis and therapeutic targets. Acta Gastroenterol Belg. 2011;74:375-80.
[81] Goulet O, Joly F. [Intestinal microbiota in short bowel syndrome]
Microbiote intestinal dans le syndrome du grele court. Gastroenterol Clin Biol. 2010;34 Suppl 1:S37-43.
[82] Norkina O, Burnett TG, De Lisle RC. Bacterial overgrowth in the cystic fibrosis transmembrane conductance regulator null mouse small intestine. Infect Immun. 2004;72:6040-9.
[83] Lynch SV, Goldfarb KC, Wild YK, Kong W, De Lisle RC, Brodie EL. Cystic fibrosis transmembrane conductance regulator knockout mice exhibit aberrant gastrointestinal microbiota. Gut Microbes. 2013;4:41-7.
[84] De Lisle RC. Altered transit and bacterial overgrowth in the cystic fibrosis mouse small intestine. Am J Physiol Gastrointest Liver Physiol. 2007;293:G104-11.
[85] Durmaz B, Dalgalar M, Durmaz R. Prevalence of enterotoxigenic Bacteroides fragilis in patients with diarrhea: a controlled study. Anaerobe. 2005;11:318-21.

[86] Raia V, Maiuri L, de Ritis G, de Vizia B, Vacca L, Conte R, et al. Evidence of chronic inflammation in morphologically normal small intestine of cystic fibrosis patients. Pediatr Res. 2000;47:344-50.
[87] Smyth RL, Croft NM, O'Hea U, Marshall TG, Ferguson A. Intestinal inflammation in cystic fibrosis. Arch Dis Child. 2000;82:394-9.
[88] Werlin SL, Benuri-Silbiger I, Kerem E, Adler SN, Goldin E, Zimmerman J, et al. Evidence of intestinal inflammation in patients with cystic fibrosis. J Pediatr Gastroenterol Nutr. 2010;51:304-8.
[89] Crites KS, Morin G, Orlando V, Patey N, Cantin C, Martel J, et al. CFTR Knockdown induces proinflammatory changes in intestinal epithelial cells. J Inflamm (Lond). 2015;12:62.
[90] Bruscia EM, Zhang PX, Ferreira E, Caputo C, Emerson JW, Tuck D, et al. Macrophages directly contribute to the exaggerated inflammatory response in cystic fibrosis transmembrane conductance regulator-/- mice. Am J Respir Cell Mol Biol. 2009;40:295-304.
[91] Perez A, Issler AC, Cotton CU, Kelley TJ, Verkman AS, Davis PB. CFTR inhibition mimics the cystic fibrosis inflammatory profile. Am J Physiol Lung Cell Mol Physiol. 2007;292:L383-95.
[92] Field M, Graf LH, Jr., Laird WJ, Smith PL. Heat-stable enterotoxin of Escherichia coli: in vitro effects on guanylate cyclase activity, cyclic GMP concentration, and ion transport in small intestine. Proc Natl Acad Sci U S A. 1978;75:2800-4.
[93] Heijerman H. Infection and inflammation in cystic fibrosis: a short review. J Cyst Fibros. 2005;4 Suppl 2:3-5.
[94] Kelly T, Buxbaum J. Gastrointestinal Manifestations of Cystic Fibrosis. Dig Dis Sci. 2015;60:1903-13.
[95] Bijvelds MJ, Bronsveld I, Havinga R, Sinaasappel M, de Jonge HR, Verkade HJ. Fat absorption in cystic fibrosis mice is impeded by defective lipolysis and post-lipolytic events. Am J Physiol Gastrointest Liver Physiol. 2005;288:G646-53.
[96] Weber AM, Roy CC, Chartrand L, Lepage G, Dufour OL, Morin CL, et al. Relationship between bile acid malabsorption and pancreatic insufficiency in cystic fibrosis. Gut. 1976;17:295-9.
[97] O'Brien S, Mulcahy H, Fenlon H, O'Broin A, Casey M, Burke A, et al. Intestinal bile acid malabsorption in cystic fibrosis. Gut. 1993;34:1137-41.
[98] Wouthuyzen-Bakker M, Bodewes FA, Verkade HJ. Persistent fat malabsorption in cystic fibrosis; lessons from patients and mice. J Cyst Fibros. 2011;10:150-8.
[99] Debray D, Rainteau D, Barbu V, Rouahi M, El Mourabit H, Lerondel S, et al. Defects in gallbladder emptying and bile Acid homeostasis in mice with cystic fibrosis transmembrane conductance regulator deficiencies. Gastroenterology. 2012;142:1581-91 e6.
[100] Inagaki T, Choi M, Moschetta A, Peng L, Cummins CL, McDonald JG, et al. Fibroblast growth factor 15 functions as an enterohepatic signal to regulate bile acid homeostasis. Cell Metab. 2005;2:217-25.
[101] Song KH, Li T, Owsley E, Strom S, Chiang JY. Bile acids activate fibroblast growth factor 19 signaling in human hepatocytes to inhibit cholesterol 7alpha-hydroxylase gene expression. Hepatology. 2009;49:297-305.
[102] Yu C, Wang F, Jin C, Huang X, McKeehan WL. Independent repression of bile acid synthesis and activation of c-Jun N-terminal kinase (JNK) by activated hepatocyte fibroblast growth factor receptor 4 (FGFR4) and bile acids. J Biol Chem. 2005;280:17707-14.
[103] Rowe SM, Verkman AS. Cystic fibrosis transmembrane regulator correctors and potentiators. Cold Spring Harb Perspect Med. 2013;3.
[104] McKone EF, Borowitz D, Drevinek P, Griese M, Konstan MW, Wainwright C, et al. Long-term safety and efficacy of ivacaftor in patients with cystic fibrosis who have the

Gly551Asp-CFTR mutation: a phase 3, open-label extension study (PERSIST). Lancet Respir Med. 2014;2:902-10.
[105] Clancy JP, Rowe SM, Accurso FJ, Aitken ML, Amin RS, Ashlock MA, et al. Results of a phase IIa study of VX-809, an investigational CFTR corrector compound, in subjects with cystic fibrosis homozygous for the F508del-CFTR mutation. Thorax. 2012;67:12-8.
[106] Flume PA, Liou TG, Borowitz DS, Li H, Yen K, Ordonez CL, et al. Ivacaftor in subjects with cystic fibrosis who are homozygous for the F508del-CFTR mutation. Chest. 2012;142:718-24.
[107] Wainwright CE, Elborn JS, Ramsey BW, Marigowda G, Huang X, Cipolli M, et al. Lumacaftor-Ivacaftor in Patients with Cystic Fibrosis Homozygous for Phe508del CFTR. N Engl J Med. 2015;373:220-31.
[108] Elborn JS, Ramsey BW, Boyle MP, Konstan MW, Huang X, Marigowda G, et al. Efficacy and safety of lumacaftor/ivacaftor combination therapy in patients with cystic fibrosis homozygous for Phe508del CFTR by pulmonary function subgroup: a pooled analysis. Lancet Respir Med. 2016;4:617-26.
[109] Konstan MW, McKone EF, Moss RB, Marigowda G, Tian S, Waltz D, et al. Assessment of safety and efficacy of long-term treatment with combination lumacaftor and ivacaftor therapy in patients with cystic fibrosis homozygous for the F508del-CFTR mutation (PROGRESS): a phase 3, extension study. Lancet Respir Med. 2017;5:107-18.
[110] Boyle MP, Bell SC, Konstan MW, McColley SA, Rowe SM, Rietschel E, et al. A CFTR corrector (lumacaftor) and a CFTR potentiator (ivacaftor) for treatment of patients with cystic fibrosis who have a phe508del CFTR mutation: a phase 2 randomised controlled trial. Lancet Respir Med. 2014;2:527-38.
[111] Farinha CM, King-Underwood J, Sousa M, Correia AR, Henriques BJ, Roxo-Rosa M, et al. Revertants, low temperature, and correctors reveal the mechanism of F508del-CFTR rescue by VX-809 and suggest multiple agents for full correction. Chem Biol. 2013;20:943-55.
[112] Wang Y, Loo TW, Bartlett MC, Clarke DM. Additive effect of multiple pharmacological chaperones on maturation of CFTR processing mutants. Biochem J. 2007;406:257-63.
[113] Phuan PW, Veit G, Tan J, Roldan A, Finkbeiner WE, Lukacs GL, et al. Synergy-based small-molecule screen using a human lung epithelial cell line yields DeltaF508-CFTR correctors that augment VX-809 maximal efficacy. Mol Pharmacol. 2014;86:42-51.
[114] Okiyoneda T, Veit G, Dekkers JF, Bagdany M, Soya N, Xu H, et al. Mechanism-based corrector combination restores DeltaF508-CFTR folding and function. Nat Chem Biol. 2013;9:444-54.
[115] Nieddu E, Pollarolo B, Mazzei MT, Anzaldi M, Schenone S, Pedemonte N, et al. The search for a common structural moiety among selected pharmacological correctors of the mutant CFTR chloride channel. Future Med Chem. 2014;6:1857-68.
[116] Ramachandran S, Osterhaus SR, Karp PH, Welsh MJ, McCray PB, Jr. A genomic signature approach to rescue DeltaF508-cystic fibrosis transmembrane conductance regulator biosynthesis and function. Am J Respir Cell Mol Biol. 2014;51:354-62.
[117] Kalid O, Mense M, Fischman S, Shitrit A, Bihler H, Ben-Zeev E, et al. Small molecule correctors of F508del-CFTR discovered by structure-based virtual screening. J Comput Aided Mol Des. 2010;24:971-91.
[118] Zhang Z, Chen J. Atomic Structure of the Cystic Fibrosis Transmembrane Conductance Regulator. Cell. 2016;167:1586-97 e9.
[119] Awatade NT, Uliyakina I, Farinha CM, Clarke LA, Mendes K, Sole A, et al. Measurements of Functional Responses in Human Primary Lung Cells as a Basis for Personalized Therapy for Cystic Fibrosis. EBioMedicine. 2015;2:147-53.

[120] Dekkers JF, Wiegerinck CL, de Jonge HR, Bronsveld I, Janssens HM, de Winter-de Groot KM, et al. A functional CFTR assay using primary cystic fibrosis intestinal organoids. Nat Med. 2013;19:939-45.
[121] Pedemonte N, Galietta LJ. Structure and function of TMEM16 proteins (anoctamins). Physiol Rev. 2014;94:419-59.
[122] Ma K, Wang H, Yu J, Wei M, Xiao Q. New Insights on the Regulation of Ca2+ -Activated Chloride Channel TMEM16A. J Cell Physiol. 2017;232:707-16.
[123] Mall MA, Galietta LJ. Targeting ion channels in cystic fibrosis. J Cyst Fibros. 2015;14:561-70.
[124] Strug LJ, Gonska T, He G, Keenan K, Ip W, Boelle PY, et al. Cystic fibrosis gene modifier SLC26A9 modulates airway response to CFTR-directed therapeutics. Hum Mol Genet. 2016;25:4590-600.
[125] Kunzelmann K, Schreiber R, Boucherot A. Mechanisms of the inhibition of epithelial Na+ channels by CFTR and purinergic stimulation. Kidney Int. 2001;60:455-61.
[126] Hayashi M, Kita K, Ohashi Y, Aihara E, Takeuchi K. Phosphodiesterase isozymes involved in regulation of HCO3- secretion in isolated mouse duodenum in vitro. Biochem Pharmacol. 2007;74:1507-13.
[127] O'Grady SM, Jiang X, Maniak PJ, Birmachu W, Scribner LR, Bulbulian B, et al. Cyclic AMP-dependent Cl secretion is regulated by multiple phosphodiesterase subtypes in human colonic epithelial cells. J Membr Biol. 2002;185:137-44.
[128] Suaud L, Yan W, Carattino MD, Robay A, Kleyman TR, Rubenstein RC. Regulatory interactions of N1303K-CFTR and ENaC in Xenopus oocytes: evidence that chloride transport is not necessary for inhibition of ENaC. Am J Physiol Cell Physiol. 2007;292:C1553-61.
[129] Forte LR. Guanylin regulatory peptides: structures, biological activities mediated by cyclic GMP and pathobiology. Regul Pept. 1999;81:25-39.
[130] Hamra FK, Eber SL, Chin DT, Currie MG, Forte LR. Regulation of intestinal uroguanylin guanylin receptor-mediated responses by mucosal acidity. P Natl Acad Sci USA. 1997;94:2705-10.
[131] Joo NS, London RM, Kim HD, Forte LR, Clarke LL. Regulation of intestinal Cl- and HCO3- secretion by uroguanylin. Am J Physiol-Gastr L. 1998;274:G633-G44.
[132] Lucas ML, Schneider W, Haberich FJ, Blair JA. Direct Measurement by Ph-Microelectrode of Ph Microclimate in Rat Proximal Jejunum. Proc R Soc Ser B-Bio. 1975;192:39-48.
[133] Whitaker TL, Witte DP, Scott MC, Cohen MB. Uroguanylin and guanylin: distinct but overlapping patterns of messenger RNA expression in mouse intestine. Gastroenterology. 1997;113:1000-6.
[134] Li ZP, Knowles JW, Goyeau D, Prabhakar S, Short DB, Perkins AG, et al. Low salt intake down-regulates the guanylin signaling pathway in rat distal colon. Gastroenterology. 1996;111:1714-21.
[135] Potthast R, Ehler E, Scheving LA, Sindic A, Schlatter E, Kuhn M. High salt intake increases uroguanylin expression in mouse kidney. Endocrinology. 2001;142:3087-97.
[136] Sindic A. Current understanding of guanylin peptides actions. ISRN Nephrol. 2013;2013:813648.
[137] Hughes JM, Murad F, Guerrant RL. Role of Cyclic-Gmp in Mechanism of Action of Heat-Stable Enterotoxin of Escherichia-Coli. Clin Res. 1978;26:A58-A.
[138] Gariepy J, Judd AK, Schoolnik GK. Importance of Disulfide Bridges in the Structure and Activity of Escherichia-Coli Entero-Toxin St1b. P Natl Acad Sci USA. 1987;84:8907-11.
[139] Hamra FK, Forte LR, Eber SL, Pidhorodeckyj NV, Krause WJ, Freeman RH, et al. Uroguanylin - Structure and Activity of a 2nd Endogenous Peptide That Stimulates Intestinal Guanylate-Cyclase. P Natl Acad Sci USA. 1993;90:10464-8.

[140] Forte LR, Eber SL, Turner JT, Freeman RH, Fok KF, Currie MG. Guanylin Stimulation of Cl- Secretion in Human Intestinal T(84) Cells Via Cyclic Guanosine-Monophosphate. Journal of Clinical Investigation. 1993;91:2423-8.
[141] Munzel T, Feil R, Mulsch A, Lohmann SM, Hofmann F, Walter U. Physiology and pathophysiology of vascular signaling controlled by cyclic guanosine 3 ',5 '-cyclic monophosphate-dependent protein kinase. Circulation. 2003;108:2172-83.
[142] Kaupp UB, Seifert R. Cyclic nucleotide-gated ion channels. Physiological Reviews. 2002;82:769-824.
[143] Rybalkin SD, Yan C, Bornfeldt KE, Beavo JA. Cyclic GMP phosphodiesterases and regulation of smooth muscle function. Circ Res. 2003;93:280-91.
[144] Vaandrager AB, De Jonge HR. Effect of cyclic GMP on intestinal transport. Adv Pharmacol. 1994;26:253-83.
[145] Vaandrager AB, Bot AG, Ruth P, Pfeifer A, Hofmann F, De Jonge HR. Differential role of cyclic GMP-dependent protein kinase II in ion transport in murine small intestine and colon. Gastroenterology. 2000;118:108-14.
[146] Vaandrager AB, Bot AG, de Jonge HR. Guanosine 3',5'-cyclic monophosphate-dependent protein kinase II mediates heat-stable enterotoxin-provoked chloride secretion in rat intestine. Gastroenterology. 1997;112:437-43.
[147] Cetin Y, Kuhn M, Kulaksiz H, Adermann K, Bargsten G, Grube D, et al. Enterochromaffin cells of the digestive system: cellular source of guanylin, a guanylate cyclase-activating peptide. Proc Natl Acad Sci U S A. 1994;91:2935-9.
[148] Li Z, Taylor-Blake B, Light AR, Goy MF. Guanylin, an endogenous ligand for C-type guanylate cyclase, is produced by goblet cells in the rat intestine. Gastroenterology. 1995;109:1863-75.

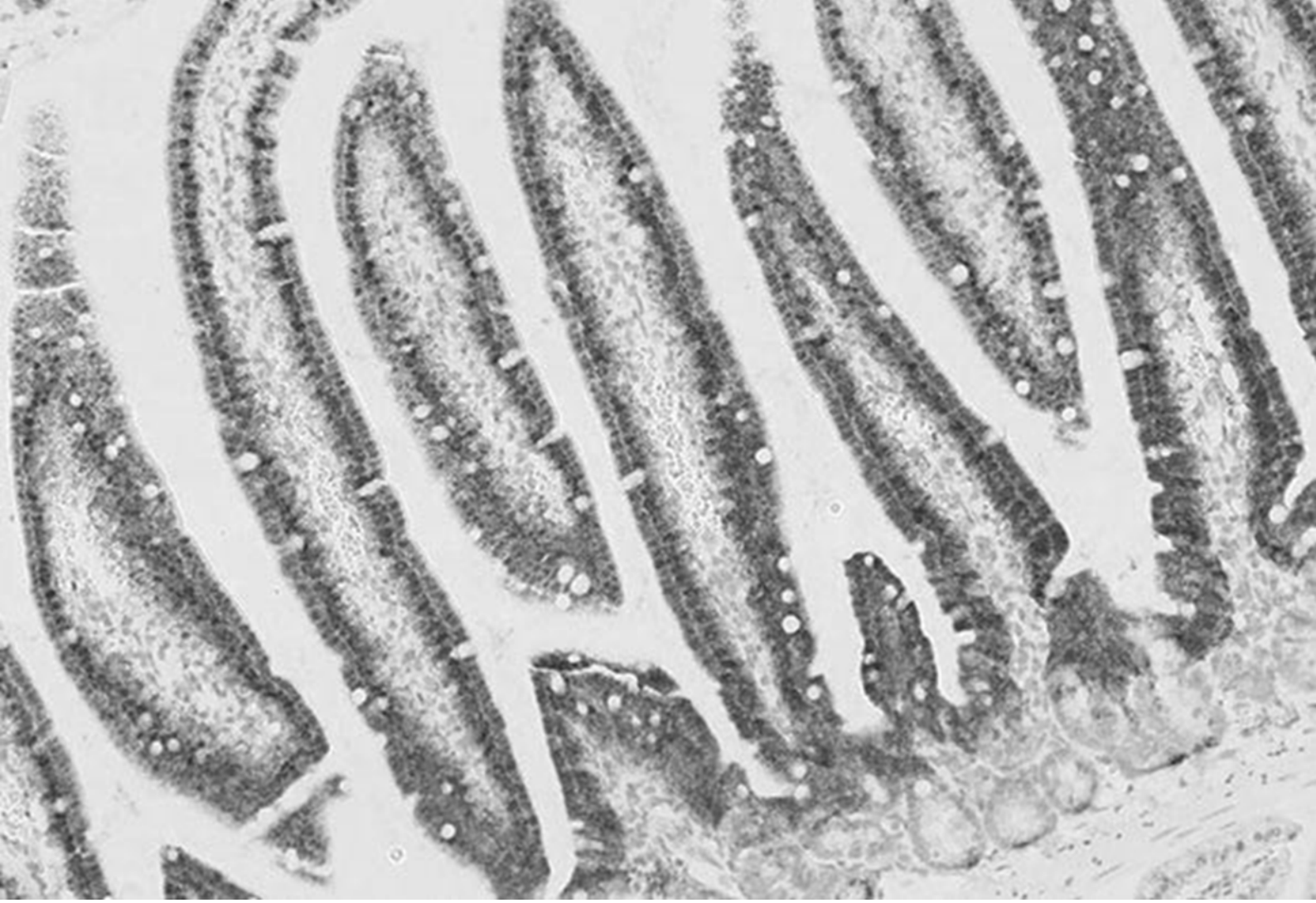

# Chapter 2

# Cystic fibrosis: towards personalized therapies

**P.T. Ikpa, M.J.C. Bijvelds, and H.R. de Jonge**

Erasmus MC University Medical Centre, Department of Gastroenterology & Hepatology, Rotterdam, The Netherlands

**Int J Biochem Cell Biol, 2014. 52: p. 192-200**

## Summary

Cystic fibrosis (CF), the most common, life-threatening monogenetic disease in Caucasians, is caused by mutations in the CFTR gene, encoding a cAMP-and cGMP-regulated epithelial chloride channel. Symptomatic therapies treating end-organ manifestations have increased the life expectancy of CF patients towards a mean of 40 years. The recent development of CFTR-targeted drugs that emerged from high throughput screening and are capable of correcting the basic defect promises to transform the therapeutic landscape from a trial-and-error prescription to personalized medicine. This stratified approach is tailored to a specific functional class of mutations in CFTR, but can be refined further to an individual level by exploiting recent advances in *ex vivo* drug testing methods. These tests range from CFTR functional measurements in rectal biopsies donated by a CF patient to the use of patient-derived intestinal or pulmonary organoids. Such organoids may serve as an inexhaustible source of epithelial cells that can be stored in biobanks and allow medium- to high-throughput screening of CFTR activators, correctors and potentiators on the basis of a simple microscopic assay monitoring organoid swelling. Thus the recent breakthrough in stem cell biology allowing the culturing of mini-organs from individual patients is not only relevant for future stem cell therapy, but may also allow the preclinical testing of new drugs or combinations that are optimally suited for an individual patient.

## Introduction

Cystic fibrosis (CF) is a life-threatening autosomal recessive monogenetic disease caused by mutations in the CFTR gene, encoding a cyclic AMP- and cyclic GMP-regulated and ATP-gated chloride channel [1]. The impact of a defect in CFTR function differs among tissues and cell types [2]. In sweat glands, the decreased reabsorption of sodium chloride by the water-impermeable ductal epithelium results in elevated sweat chloride, a hallmark of CF. In other epithelia, in particular the respiratory and intestinal epithelia as well as the biliary and pancreatic ducts, CFTR dysfunction causes a loss of chloride and bicarbonate secretion, resulting in cellular alkalinity and luminal acidification, impaired decondensation of discharged mucin granules by goblet cells, and defective mucus expansion [3, 4]. The ensuing acidification and dehydration of the mucus layer leads to impaired mucociliary clearance and bacterial killing by epithelial defensins [5]; this predisposes to recurrent infection, inflammation, mucus plugging and luminal obstruction. Loss of CFTR function in monocytes and macrophages, by impairing phagocytosis and intracellular killing of *Pseudomonas aeruginosa*, contributes to the enhanced susceptibility to infection in patients with CF [6-8].

When CF was first described in 1938, the predicted survival age of a CF patient was only 6 months. For patients born in the 1990's median survival is now predicted to exceed 40 years [9]. This impressive gain in life expectancy has resulted largely from advances in early diagnosis and symptomatic treatment of end-organ pathologies based on vast improvements in nutrition, control of airway infections, and physiotherapy (see Fig. 1 for an overview of CF symptomatic treatment). Understandably the discovery of the disease-causing CFTR gene in 1989 created new hope for a curative treatment targeting the basic defect rather than treating CF disease manifestations [10]. The most obvious approach, viral or non-viral gene therapy, would potentially be of benefit to all patients with CF, independent of their genotype. So far however CFTR gene addition or gene replacement, despite promising advances, has not translated into clinical benefits despite more than 20 clinical trials, mainly due to a low expression of the CFTR transgene, inflammatory responses to viral proteins, the development of a humoral immune response preventing successful readministration, and the risk of insertional mutagenesis in case of integrating viral vectors. In contrast, considerable progress has been made in the development of tailored CFTR pharmacotherapy for specific CFTR mutations, and the design of better *in vitro* preclinical assays that allow the selection of the most effective therapeutic approaches on an individual basis, i.e. personalized medicine.

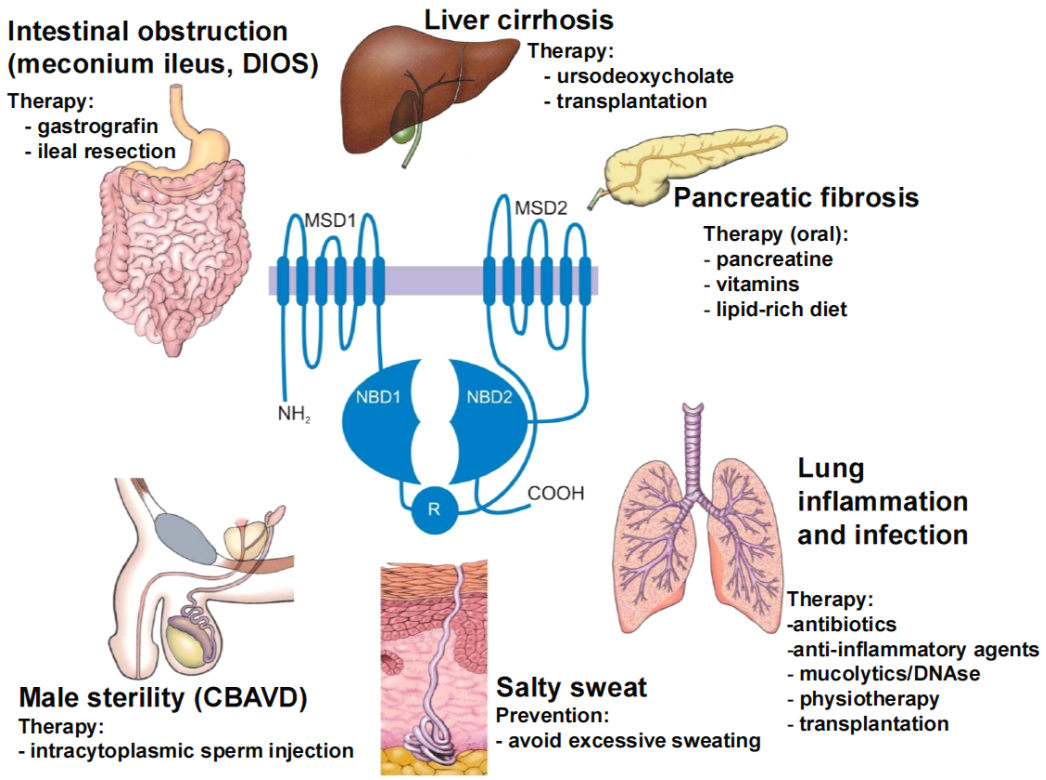


***Fig. 1: Overview of current symptomatic treatments of CF.*** *Inset: CFTR domain structure. MSD, membrane spanning domain; NBD, nucleotide binding domain; R, regulatory domain.*

## *Mutation-specific therapies*

Nearly 2000 mutations in the CFTR gene have been identified that can be subdivided in 6 different classes based on their phenotypic consequences (Fig. 2) [11, 12]. Class I mutations cause defects in full-length protein synthesis due to premature truncations or nonsense alleles, or to severe splicing defects; class II mutations cause folding defects and premature proteasomal degradation, class III shows normal trafficking to the plasma membrane but defective channel gating, class IV results in an impaired channel conductance, class V causes a reduced number of CFTR transcripts, and class VI is characterized by a reduced protein stability and increased turnover of CFTR at the cell surface.

The first three mutation classes are associated with a nearly complete loss of CFTR channel function and are considered severe mutations, whereas mutations in class IV-VI may allow residual CFTR function and are associated with a milder phenotype. F508del, the most common mutation with an allelic frequency of around 90% worldwide, has mixed properties of class II, III and VI and is therefore most difficult to repair at the protein level. Just four other mutations, notably G551D (class III), W1282X, G542X (class I), and N1303K (class II)

have a worldwide prevalence of 1-3% each, whereas only 20 mutations have a frequency above 0.1%.

Before the introduction of high-throughput screening (HTS) as a new technique in CFTR drug discovery, proof of principle showing that mutation-specific repair of CFTR is feasible was reached at the DNA, RNA and protein level. A major advantage of this approach as compared to gene addition by cDNA vectors is that only those cells expressing CFTR endogenously are corrected. Potential deleterious consequences of ectopic expression of the CFTR transgene, such as supraphysiological expression of CFTR in the cells not normally expressing CFTR are avoided, and the need for CFTR promoter constructs or CFTR minigenes that are difficult to transfect and to integrate into viral vectors, is abolished.

## *DNA repair*

One promising approach to reach mutation-specific repair of CFTR at the DNA level is the application of recently developed genomic editing techniques, such as the Zinc-finger nuclease (ZFN), TAL effector nucleases (TALENs), or CRISPR/Cas9 system for genome engineering [13, 14]. Proof of concept for correction of the F508del mutation in exon 11 by

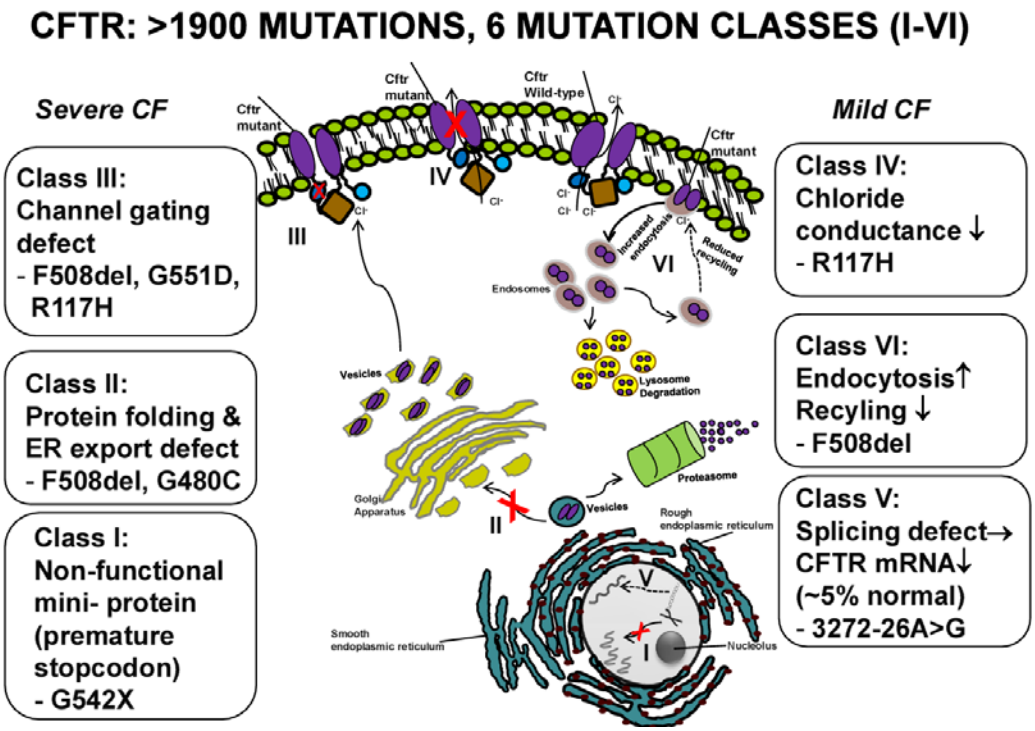


***Fig. 2: Overview of CFTR mutation classes.*** *The functional consequences of the mutations are indicated in the flanking boxes.*

homologous recombination with a donor plasmid encoding wild-type CFTR sequences using CRISPR/Cas9 has been reached recently in human intestinal stem cells [15]. In principle this approach is capable of correcting most if not all other "severe" class I-III mutations, by proper engineering of the 20 nucleotide guide sequence in the single guide RNA that targets the Cas9 nuclease to appropriate cleavage sites. However its direct therapeutic application in CF patients *in vivo* is hampered by the low efficacy of the repair and the mutagenic risk, requiring a time-consuming selection step of the repaired cells that is not feasible *in vivo*.

### *RNA repair*

Partial transcriptional repair of F508del-CFTR and functional restoration of chloride transport in human CF airway cells has been reached by spliceosome-mediated RNA *trans*-splicing technology (SMaRT) using recombinant adenovirus or adeno-associated virus (rAAV) as the delivery vector [16, 17]. Alternatively, insertion of the missing bases (TTT) by hybridization to a 2'-O-methyl RNA-unmodified RNA oligonucleotide duplex has been achieved in a F508del-CFTR expressing cell line [18]. Although RNA repair is transient and only modestly effective, studies of CFTR splicing polymorphisms suggest that 8% of normal CFTR message is sufficient for normal lung function, whereas 5% is associated with relatively mild CF lung disease [19, 20]. Genetic reprogramming of CFTR transcripts by SMaRT or oligonucleotides may in principle be applicable also to other severe CFTR mutations. In addition, the disease-causing effect of CFTR mutations affecting the pre-mRNA splicing of the CFTR gene by disrupting or generating intronic splicing motifs (frequency ~13%), may be reduced in a mutation-specific fashion by bifunctional antisense oligonucleotides providing a *trans*-acting splicing enhancer, or by synthetic exon-specific activators or modified U1 small nuclear RNAs capable of correcting exon skipping [21, 22]. However the clinical utility of these techniques for ameliorating CF lung disease is not yet proven and awaits the development of suitable and safe *in vivo* delivery vectors, for example rAAV engineered to escape neutralizing antibodies, or methods to penetrate the mucus and periciliary layer in the CF lung more effectively [23]. Because oligonucleotide and viral repair techniques are less suitable for oral or systemic delivery, these therapies are likely to remain restricted to aerosolic treatment which targets only the lung compartment, in contrast to the orally applied CF therapeutics discussed hereafter.

## *CFTR protein therapy*

### *Repair of class I mutant CFTR*

Of all CFTR mutations identified, ~10% are nonsense mutations (class I) that result in the creation of premature termination codons (PTCs) and rapid degradation of CFTR transcripts by a quality control mechanism known as nonsense-mediated mRNA decay (NMD) to prevent the synthesis of truncated proteins with potential dominant negative effects [9-11]. Aminoglycoside antibiotics, including tobramycin, gentamycin and amikacin, do not repair the RNA directly but bind to the ribosomes and cause the insertion of a near cognate amino-acyl tRNA into the ribosomal A site. This process suppresses translational fidelity and allows the ribosome to read through the PTC and to produce full-length protein.

Recently the non-aminoglycoside PTC suppressor ataluren (PTC 124; identified by HTS) which is orally bioavailable and non-toxic, has been assessed in a large phase III clinical trial. Despite some success in Phase II testing [24, 25], ataluren did not significantly improve the primary endpoint in Phase III [26]. Several recent *in vitro* reporter assay studies likewise failed to confirm the read-through efficacy of PTC124, and the reliability of the original HTS has been questioned [27]. However encouraging results were obtained recently in preclinical studies using a second generation of synthetic aminoglycosides designed to provide higher readthrough activity with reduced mitochondrial toxicity [26].

### *Repair of conformational defects in the CFTR protein*

Defects in protein conformation, as occur in mutant CFTR, can be rescued by two different approaches: (1) through stabilizing the protein native state with pharmacological chaperones (PCs) that bind directly to the channel protein; and (2) through altering the activity of the transcriptional, folding, or membrane trafficking machinery or blocking the degradation of partially folded, but functional CFTR at the endoplasmic reticulum (ER) or the plasma membrane (PM) by so-called proteostasis regulators (PRs) [28, 29]. Most CFTR trafficking mutants, including F508del, with a few exceptions (e.g. G480C; N287Y), show additional defects in channel gating function, and most PCs and PRs identified thus far only partially normalize the channel conformational defect. Effective protein repair may therefore need the combined use of either PCs or PRs (collectively called ‘correctors’) which promote CFTR exit from the ER and accumulation in the PM, and ‘potentiators’ which improve channel gating [30].

***Structural and functional repair of F508del-CFTR and other class II mutant CFTRs***

It has recently been shown that F508del-CFTR actually contains two distinct folding defects. Studies on second site suppressor mutations and evolved sequences coupled to the F508del residue showed not only misfolding of NBD1 (containing residue 508), but also instability of the NBD1-MSD2 interface [31, 32]. This may explain the rather modest rescue effect of most CFTR correctors available to date, which target only a single defect. Thus multidrug therapy with a combination of a NBD1 domain stabilizer (now mechanistically classified as a "class I corrector") and a NBD1-MSD2 interface stabilizer ("class II corrector") may be required to overcome the previously observed "ceiling" in CFTR protein repair [33]. Conceivably, the parallel targeting of multiple conformational defects by separate small molecule correctors will allow wild-type folding of the mutant protein and obviate the need for a potentiator.

The current collection of preclinically active PCs and PRs is broad and rapidly expanding. It includes not only small molecules but also transcomplementing CFTR fragments [34] and RXR peptides [35].The most promising PC developed so far, VX-809 (Lumacaftor; Vertex Pharmaceuticals) has emerged from HTS in a recombinant cell-based assay and is capable of restoring ~15% CFTR channel activity in primary respiratory epithelia expressing F508del-CFTR [36]. VX-809 is more selective for CFTR than most other folding correctors (for example VRT-325 and corr-4a) and acts early in CFTR biogenesis to interact directly with MSD1 and modulate its conformation [37, 38]. In this way it not only corrects disease-causing mutations in CFTR MSD1 with a high efficacy, but also allosterically suppresses the assembly

defects in CFTR caused by F508del and by several other remote folding mutations in the fourth intracellular loop (ICL4). Therefore VX-809 mono-or combination therapy, by promoting interdomain communication, may restore function to a large number of rare CFTR mutations, aside its main action as a class II F508del-CFTR corrector.

Results of a phase IIa clinical study of VX-809 showed a small but significant reduction of sweat chloride values, but no significant improvement in nasal potential difference (NPD), lung function or maturation of F508del-CFTR in rectal biopsies [39]. VX-809 is reported to normalize the gating of corrected F508del-CFTR but has no direct potentiating action, explaining why acute addition of a potentiator further increased the activity of VX-809-corrected F508del-CFTR (as well as wild-type CFTR) by two-fold [36]. The therapeutic relevance of this gain in activity is presently explored in a phase III clinical study of homozygous F508del CF patients, encouraged by data from a phase II study

showing improved lung function in approximately 50% of the participants undergoing VX-809/VX-770 combi-therapy (see http://www.cff.org).

Aside VX-809, several other small molecule F508del-CFTR correctors may qualify as candidate CF therapeutics, some of which are already in clinical use against other diseases. These include the psoralen-related compound and psoriasis drug trimethylangelicin (TMA), granted orphan designation by the EMA, and acting as a "dual" F508del-CFTR corrector and potentiator, and as a suppressor of IL-8 transcription [40]; the cyanoquinoline CoPo-22 emerging from HTS, with dual corrector and potentiator activities albeit in the micromolar range [41]; *in silico*-selected disruptors of keratin8-F508del NBD1 interaction, functioning as potent correctors of CFTR maturation and trafficking [42]; inhibitors of F508del CFTR-CAL interaction, promoting the formation of a stable F508del CFTR-NHERF1 complex in the plasma membrane [43]; inhibitors of the Hsp90 co-chaperone Aha1 [44]; and sildenafil, a phosphodiesterase type V (PDE5) inhibitor used clinically against erectile dysfunction [45-48]. Sildenafil may increase CFTR activity through cGMP-dependent phosphorylation or through direct cGMP-CFTR interaction, but is also functioning as a relatively weak F508del-CFTR corrector, possibly due to its structural resemblance with the Vertex corrector VRT-325 [49]. Although the rapid expansion of a broad collection of CFTR correctors is encouraging, in most cases additional mechanistic and/or toxicity studies remain to be done before clinical testing can be considered.

***Improvement of CFTR gating by potentiators***

Most CFTR class III gating mutations, including the most common "Keltic" mutation, G551D (frequency ~3%) are localized in the ABC signature sequence or in the Walker A or B motif of the two ATP binding pockets (ABP1 and ABP2) of the NBDs (cf. Fig. 1, center), and cause a defect in ATP-dependent channel gating without abnormalities in synthesis, trafficking or CFTR phosphorylation [50]. Recent insights into the CFTR gating mechanism have revealed the existence of two distinct open states, O1 and O2, with different NBD configurations: a highly stable O1 state, in which with ATP occupies the ABP2 catalytic site, and the more transient O2 state, lacking ATP in ABP2 [51]. VX-770 (Ivacaftor), the first FDA-and EMA-approved CF medication forthcoming from HTS that directly targets CFTR, was found to stabilize the O2 state, thereby promoting ATP-*independent* gating. This nonconventional gating mechanism could be reproduced in purified G551D-CFTR inserted in planar lipid bilayers and proteoliposomes, confirming that VX-770 binds directly to the CFTR protein, most plausibly to the MSDs rather than the NBDs [52]. Stabilizing O2 may

also promote reentry of the channel into the gating cycle and the transition to the O1 state, thereby increasing ATP-dependent gating of WT-CFTR. This new gating model may explain why VX-770 increases the open probability of both WT CFTR and all 10 class III gating mutants tested [53], as well as numerous other CFTR forms with missense mutations or deletions, including F508del and R117H [30, 54].

In several phase III trials oral VX-770 treatment of G551D patients led to rapid, dramatic and sustained improvements in FEV1 and body weight, and a strong reduction of sweat chloride and pulmonary exacerbations (reviewed in Rowe & Verkman). However a 4-month placebo-controlled trial of Ivacaftor in F508del-CFTR homozygous patients only reduced sweat chloride by a small amount [55]. The relative failure of VX-770 monotherapy in F508del patients has been commonly attributed to the very low levels of F508del-CFTR at the cell surface. However recent studies on human bronchial cells suggest an alternative explanation: in these cells, chronic exposure to VX-770 resulted in a dramatic increase in endocytosis and lysosomal degradation of WT- and F508del-CFTR, but not of G551D channels [56]. Whether this phenomenon is limited to VX-770 or is a property of other potentiators too, is not known and warrants further investigation. If occurring also *in vivo*, it may impact the outcome of the ongoing phase III combi-trial of VX-809 and VX-770.

The isoflavone genistein, a major component of soya-rich food, potentiates G551D- and F508del-CFTR channels by binding to the NBDs and promoting ATP-dependent gating [57, 58], but also enhances CFTR phosphorylation at basal cAMP levels [59] and inhibits CFTR endocytosis through an ill-defined mechanism [60]. In contrast, curcumin, another food component and CFTR potentiator, mimics the effect of VX-770 by binding to the MSDs and promoting ATP-independent channel gating [61]. As predicted from their distinct mechanism of action, the combined application of genistein and curcumin in a low concentration range (5-10 µM) synergistically restored the gating defect of G551D of up to ~50% of the WT level [57]. Further clinical studies using combinations of both food components (or combinations of genistein and VX-770, likewise predicted to act synergistically) are needed to determine the therapeutic potential of the combination therapy relative to monotherapy.

## *Towards individualized therapies*

The success of VX-770 monotherapy in G551D patients and improved insights into the mechanism of action of CFTR potentiators and correctors have greatly boosted attempts to develop more potent and specific CFTR modulators targeting a specific class of mutant

CFTR. To define the optimal treatment for an individual patient, genotyping of CFTR is clearly the first step. Subsequently, in case of rare mutations with an unknown phenotype, one approach is to express the protein from a mutated cDNA in a model cell line, for example Fischer rat thyroid cells [54], followed by CFTR localization and functional assays in the absence and presence of CFTR modulators. This method however is unable to report possible differences in corrector and potentiator response among individuals belonging to the same CFTR mutation class, such as caused by polymorphisms in the CFTR gene and CF modifier genes, or by differences in the CFTR interactome. Moreover this technique may be prone to artefacts inherent to CFTR overexpression or to the heterologous cellular background, and is unsuitable for studying splice mutations or complex genotypes, e.g. CF compound heterozygotes. Such confounding factors may explain why some correctors potently act in transfected cell lines but fail in primary epithelial cell cultures [62]

Considering the limitations of heterologous expression systems, the use of native epithelium or primary cell cultures, obtained from CF patients, for CFTR corrector testing seems indicated. Evidently, access to such patient material is limited, and this has hampered its application for this purpose. However recent breakthroughs in the field of stem cell biology now allow large scale cell expansion of non-transformed cells, derived from single biopsies (skin, intestine, respiratory tissue) or blood samples, opening a new chapter for translational CF research.

***Testing CF therapeutics in rectal biopsies and rectal organoids***

As illustrated in Fig. 3, one convenient and minimally invasive technique that is even applicable to CF neonates starts with the harvest of one or more rectal biopsy specimens by forceps or suction, followed by measurements of CFTR-mediated transepithelial chloride and bicarbonate currents ("ICM") in Ussing chambers [63-65]. Both acute and chronic effects of CFTR modulators can be monitored using incubation conditions that maintain tissue viability for at least 20h. Uniquely this technique allows testing of CFTR modulators *ex vivo* in native, non-cultured epithelium, in which, auspiciously, non-CFTR chloride channels minimally contribute to the ICM response. It can also be used to monitor other CF-relevant pathologies, such as intracellular alkalinization and defects in mucin degranulation. Studies on biopsies from class V splice mutation patients indicate that the level of CFTR expression in colonic epithelium is such that only circa 20% of mature, normal CFTR protein in this two-membrane assay (apical chloride exit; basolateral chloride import) suffices to normalize the ICM response (when CFTR is stimulated by saturating forskolin/cAMP levels). This implies

that ICM can detect minute improvements in CFTR function. However, because ICM responses plateau at >20% of normal protein abundance, its dynamic range is rather narrow [64]. To some extent, this range can be expanded by using suboptimal stimulation (low forskolin). Such a strategy may be particularly important to identify corrector effects in biopsies carrying very mild mutations (e.g. R117H) that are associated with less than 80% loss of CFTR function.

A clear limitation of the ICM test is its low capacity (only 4-8 biopsies/patient) and lack of expandability and suitability for large-scale corrector screening. However this problem can be overcome by converting the rectal biopsies into epithelial organoids (also named enteroids) using a 3-D culturing technique developed recently by the Clevers group [66-68]. This primary culture method enables intestinal stem cells to expand into closed and self-renewing organoids containing crypt-like structures and an internal lumen lined by differentiated cells, recapitulating the *in vivo* tissue architecture. Activation of CFTR by the cAMP agonist forskolin drives the secretion of electrolytes and fluid into the lumen of the organoid, resulting in forskolin-induced swelling (FIS) [69]. Luminal expansion is fully blocked by pharmacological CFTR inhibitors and completely absent from CFTR-null organoids, underscoring the validity of FIS as a CFTR-specific assay. Quantification of FIS in calcein green-labeled organoids grown in 96-well plates (up to 80 organoids/well) using live-cell confocal microscopy and imaging software appeared highly reproducible and allowed the testing of up to 32 conditions per experiment in triplicate. Normalized non-corrected FIS rates differed greatly between different CFTR genotypes (non-CF ≈class IV (R117H)>class III>class II (F508del)>class I), and, perhaps less evident, between individuals carrying the same alleles (i.e. F508del/F508del). Similar to the ICM, FIS is a two-membrane assay reaching a “ceiling” at about 20% of “normal” CFTR activity, beyond which apical CFTR activity no longer limits the rate of water secretion. Submaximal stimulation by low forskolin is needed to measure differences in FIS between non-CF and a subgroup of mild mutations (i.e. R117H), and to quantitate rescue effects of CFTR correctors or potentiators above the 20% threshold. As in case of ICM, the assay is highly sensitive which explains why organoids derived from homozygous F508del/F508del patients, without prior corrector treatment, show a definite residual, albeit variable FIS activity (~5% of non-CF, corresponding with ~1% CFTR activity), which can be enhanced by potentiators, such as VX-770 [69].

The FIS assay readily reveals that organoids isolated from different CF patients, even when these carry the same or similar (i.e. same class) CF alleles, may respond differently to

(1) a single corrector or potentiator; (2) a combination of corrector and potentiator (e.g. VX-809 +VX-770 in F508del homozygotes), and (3) a combination of two different correctors (e.g. VRT-325 and Corr-4a) [69]. Even larger individual differences are expected in case of a PR-type of CFTR corrector considering its stronger dependence on cellular background and CFTR interactome in comparison with a PC.

Obviously the FIS assay can only report *intrinsic* differences between CFTR modulator efficacies at the level of intestinal epithelial cells; it cannot account for individual differences in numerous other therapeutically relevant factors *in vivo*, such as pharmacokinetics, infection, inflammation, mesenchyme-epithelium and lymphocyte-epithelium communication, and the frequency and intensity of physiological stimuli, in particular β-adrenergic and VIPergic cAMP agonists. Therefore additional studies designed to correlate drug responses *in vivo* with drug testing by FIS in organoids from the same patient are needed to gain more insight into the predictive value of the FIS assay. Another favorable aspect of organoid cultures is their ability to maintain intact stem cell compartments and (epi)genetic stability even after >40 passages. Repetitive passaging will generate a large number of organoids from individual patients that can be stored in biobanks and used later for testing newly developed CF therapeutics.

***Organoids from airway epithelium as tools for testing CF therapeutics***

Although the intestine and lungs both originate from endoderm during embryonic development, intestinal epithelium cannot be considered simply as a surrogate model for the airways. In contrast to the intestine, the cell turnover in the lungs is very low but accelerates upon tissue injury, causing cryptic stem cells (presumably basal cells) to self-renew and generate luminal cells, including differentiated ciliated cells [70]. Similar to intestinal stem cells, these cells may form spheric structures *in vitro*. More recent studies have shown that this process is reversible, and that fully differentiated epithelial cells, as present in tracheal or bronchial biopsies, can be reprogrammed to reach an adult stem cell-like, indefinite proliferative state [71, 72]. Induction of these karyotype-stable and nontumorigenic “conditionally reprogrammed” cells (CRCs) is reached by isolating cells from small biopsies or cryopreserved tissue by protease dissociation and growing the cells on a layer of fibroblast feeder cells in the presence of a Rho kinase (ROCK) inhibitor. Importantly, these cells maintain their epigenetic memory and, following expansion, shift back to their original differentiated phenotype, including ciliated cells and goblet cells, upon removal of the feeders and the inhibitor. By placing them into an appropriate 3D culture system, they are capable of

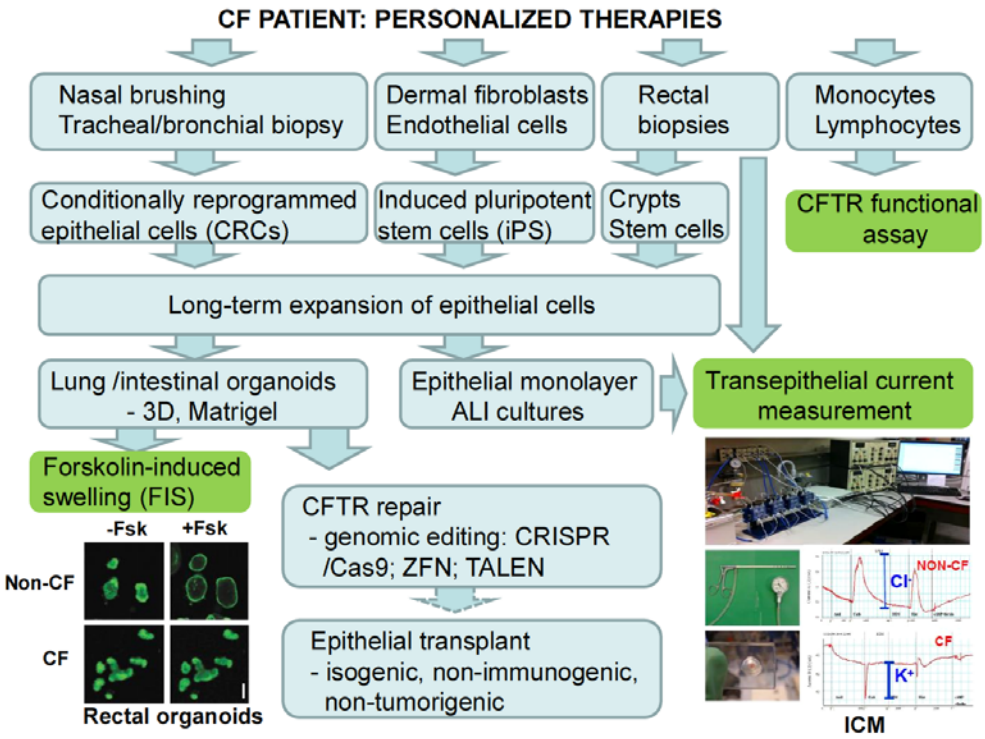


***Fig. 3: Flow diagram depicting the generation of epithelial organoids and monolayers that allow CFTR modulator screening on an individual basis****. Green boxes: functional ex vivo CFTR assays used to select the most effective CFTR modulator (or combinations of modulators) for an individual patient.*

forming spheric lung organoids (grown in Matrigel) or monolayers of epithelial cells (grown as air-liquid interface cultures on filters). These can potentially be used to monitor CFTR activity in FIS assays or transepithelial current measurements, and to study the efficacy of CFTR modulators, in analogy to rectal biopsies and organoids (Fig. 3). Potential hurdles however are the relatively low expression levels of CFTR in human lung epithelial cells, possibly resulting in very low FIS rates and transepithelial currents, and the presence of compensatory non-CFTR channels, e.g. calcium-activated chloride channels, that are much less prominent in the intestine. Clearly further research is needed to evaluate the feasibility of CF drug testing in epithelial monolayers and organoids derived from nasal brushings or bronchial biopsies. If successful, this approach would offer the same advantages for individual drug testing as discussed for rectal organoids, but, considering the severe CF lung pathology, obtained in an even more CF-relevant cell type.

Another option to generate patient-specific airway epithelial cells for testing CF therapeutics starts with the creation of induced pluripotent stem cell (iPSC) lines from dermal fibroblasts donated by the CF patient, followed by an *in vitro* directed differentiation protocol

using growth factors that mimic endoderm developmental pathways, and culturing the cells under Air-Liquid-Interface (ALI) conditions on permeable substrates [73]. However, although a subpopulation of cells did express CFTR and showed CFTR activity in an iodide efflux assay, the cell culturing procedure was highly time-consuming, and the assay was not robust enough to demonstrate clear effects of a VX-809 like corrector.

***Testing CF therapeutics in immune cells***

The "personalized medicine" approaches discussed so far are restricted to epithelial cells and organoids; however, CFTR is also expressed at low but functionally important amounts in non-epithelial cells including myeloid cells [6], in particular monocytes [7, 8], macrophages [74] and lymphocytes [75]. CFTR defects in these cells may contribute to abnormalities in the innate immune defense of CF patients [76], implying that restoration of CFTR function by orally available CFTR correctors and potentiatiors may be of prime importance in preventing inflammation and infection. Though our present knowledge of CFTR biosynthesis, processing and function in immune cells is fairly limited [7], studying the effect of CFTR modulators in cells isolated from individual CF patients is clinically highly relevant. This can be done on a small scale using monocytes isolated freshly from blood samples of the patient, or following expansion of lymphocyte cell lines immortalized with Epstein-Barr virus, using fluorescent membrane potential sensing probes or other live assays to monitor CFTR activity (Fig. 3).

## Summary and future prospects and challenges

The development of mutation-specific and personalized therapies for CF is progressing rapidly, spurred by major technical advances at various levels. Firstly, the introduction of reliable newborn screening methods allows early evaluation of the efficacy of CFTR-restoring drugs, and optimization of treatment at the personal level, before overt disease progression sets in. Secondly, the advent of new generation DNA sequencing techniques, which allow the rapid detection of mutations within the full length of the CFTR gene, including introns and the promoter region. Thirdly, the development by HTS and other approaches, of an ever-expanding collection of CFTR protein correctors and potentiators, with proof of clinical efficacy established for at least one compound, the CFTR potentiator VX-770. Due to the oral bioavailablity of these new CF therapeutics, CFTR repair is no longer restricted to the lungs, as is the case for most DNA- and RNA-based mutation repair

techniques, but is feasible in virtually all CF-relevant cell types, including bile ducts, intestine, sweat glands and immune cells.

Finally, the development of novel techniques to generate almost unlimited numbers of epithelial cells and organoids from stem cells in the intestine and from conditionally reprogrammed stem cells in the airways, and the introduction of simple, robust and high-throughput assays to measure CFTR activity in organoids by FIS, has made it possible to perform pre-clinical CFTR modulator screens in cells originating from individual CF patients. This approach is clearly superior to modulator assays in heterologous mutant CFTR expression systems because (i) it allows the detection of modulator responses for individual CF patients, irrespective of the mutation, and of possible differences in response to the same modulator between CF patients; (2) CFTR correction is assessed in a native cellular and genetic background, closely reflecting the *in vivo* condition; (3) artefacts of CFTR under- or overexpression are avoided. Moreover, the option to store cells or organoids from individual CF patients in biobanks implies that only a single donation of a small amount of tissue is needed to allow repetitive preclinical optimization of treatment with existing CF therapeutics or with new drugs emerging from drug development programs. It should be emphasized, however, that the value of the new preclinical drug screening tests for predicting the efficacy of a CF drug in the clinic still awaits thorough verification by comparisons of *in vitro versus in vivo* drug responses in a large number of CF patients belonging to different mutation classes.

Patient-specific epithelial organoids also hold promise for regenerative medicine approaches to treat CF lung disease (Fig. 3). The feasibility of *in vivo* epithelial transplantation was demonstrated recently in a mouse model showing long-term (>6 months) repair of chemically-induced lesions in the colon of immunocompromised recipient mice by functional engraftment of colonic organoids expanded *in vitro* from a single adult colonic stem cell [77]. By combining this approach with mutation-specific repair of CFTR in the patient's own tracheal/bronchial organoids, as has been done successfully in human intestinal organoids using the CRISPR/Cas9 genome editing system, stepwise replacement of CF epithelium by isogenic, non-immunogenic and non-tumorigenic epithelial transplants may perhaps become feasible in the far future.

## REFERENCES

[1] Riordan JR. CFTR function and prospects for therapy. Annu Rev Biochem. 2008;77:701-26.
[2] Antunovic SS, Lukac M, Vujovic D. Longitudinal cystic fibrosis care. Clin Pharmacol Ther. 2013;93:86-97.
[3] Quinton PM. Role of epithelial HCO3(-) transport in mucin secretion: lessons from cystic fibrosis. Am J Physiol Cell Physiol. 2010;299:C1222-33.
[4] De Lisle RC, Borowitz D. The cystic fibrosis intestine. Cold Spring Harb Perspect Med. 2013;3:a009753.
[5] Pezzulo AA, Tang XX, Hoegger MJ, Alaiwa MH, Ramachandran S, Moninger TO, et al. Reduced airway surface pH impairs bacterial killing in the porcine cystic fibrosis lung. Nature. 2012;487:109-13.
[6] Bonfield TL, Hodges CA, Cotton CU, Drumm ML. Absence of the cystic fibrosis transmembrane regulator (Cftr) from myeloid-derived cells slows resolution of inflammation and infection. J Leukoc Biol. 2012;92:1111-22.
[7] Sorio C, Buffelli M, Angiari C, Ettorre M, Johansson J, Vezzalini M, et al. Defective CFTR expression and function are detectable in blood monocytes: development of a new blood test for cystic fibrosis. PLoS One. 2011;6:e22212.
[8] Van de Weert-van Leeuwen PB, Van Meegen MA, Speirs JJ, Pals DJ, Rooijakkers SH, Van der Ent CK, et al. Optimal complement-mediated phagocytosis of Pseudomonas aeruginosa by monocytes is cystic fibrosis transmembrane conductance regulator-dependent. Am J Respir Cell Mol Biol. 2013;49:463-70.
[9] Wilschanski M. Novel therapeutic approaches for cystic fibrosis. Discov Med. 2013;15:127-33.
[10] Clancy JP, Jain M. Personalized medicine in cystic fibrosis: dawning of a new era. Am J Respir Crit Care Med. 2012;186:593-7.
[11] Derichs N. Targeting a genetic defect: cystic fibrosis transmembrane conductance regulator modulators in cystic fibrosis. Eur Respir Rev. 2013;22:58-65.
[12] Rogan MP, Stoltz DA, Hornick DB. Cystic fibrosis transmembrane conductance regulator intracellular processing, trafficking, and opportunities for mutation-specific treatment. Chest. 2011;139:1480-90.
[13] Joung JK, Sander JD. TALENs: a widely applicable technology for targeted genome editing. Nat Rev Mol Cell Biol. 2013;14:49-55.
[14] Lee CM, Flynn R, Hollywood JA, Scallan MF, Harrison PT. Correction of the DeltaF508 Mutation in the Cystic Fibrosis Transmembrane Conductance Regulator Gene by Zinc-Finger Nuclease Homology-Directed Repair. Biores Open Access. 2012;1:99-108.
[15] Schwank G, Koo BK, Sasselli V, Dekkers JF, Heo I, Demircan T, et al. Functional Repair of CFTR by CRISPR/Cas9 in Intestinal Stem Cell Organoids of Cystic Fibrosis Patients. Cell Stem Cell. 2013;13:653-8.
[16] Mansfield SG, Clark RH, Puttaraju M, Kole J, Cohn JA, Mitchell LG, et al. 5' exon replacement and repair by spliceosome-mediated RNA trans-splicing. Rna. 2003;9:1290-7.
[17] Liu X, Luo M, Zhang LN, Yan Z, Zak R, Ding W, et al. Spliceosome-mediated RNA trans-splicing with recombinant adeno-associated virus partially restores cystic fibrosis transmembrane conductance regulator function to polarized human cystic fibrosis airway epithelial cells. Hum Gene Ther. 2005;16:1116-23.
[18] Zamecnik PC, Raychowdhury MK, Tabatadze DR, Cantiello HF. Reversal of cystic fibrosis phenotype in a cultured Delta508 cystic fibrosis transmembrane conductance regulator cell line by oligonucleotide insertion. Proc Natl Acad Sci U S A. 2004;101:8150-5.

[19] Ramalho AS, Beck S, Meyer M, Penque D, Cutting GR, Amaral MD. Five percent of normal cystic fibrosis transmembrane conductance regulator mRNA ameliorates the severity of pulmonary disease in cystic fibrosis. Am J Respir Cell Mol Biol. 2002;27:619-27.
[20] Chu CS, Trapnell BC, Curristin SM, Cutting GR, Crystal RG. Extensive posttranscriptional deletion of the coding sequences for part of nucleotide-binding fold 1 in respiratory epithelial mRNA transcripts of the cystic fibrosis transmembrane conductance regulator gene is not associated with the clinical manifestations of cystic fibrosis. J Clin Invest. 1992;90:785-90.
[21] Nissim-Rafinia M, Aviram M, Randell SH, Shushi L, Ozeri E, Chiba-Falek O, et al. Restoration of the cystic fibrosis transmembrane conductance regulator function by splicing modulation. EMBO Rep. 2004;5:1071-7.
[22] Fernandez Alanis E, Pinotti M, Dal Mas A, Balestra D, Cavallari N, Rogalska ME, et al. An exon-specific U1 small nuclear RNA (snRNA) strategy to correct splicing defects. Hum Mol Genet. 2012;21:2389-98.
[23] Hida K, Lai SK, Suk JS, Won SY, Boyle MP, Hanes J. Common gene therapy viral vectors do not efficiently penetrate sputum from cystic fibrosis patients. PLoS One. 2011;6:e19919.
[24] Wilschanski M, Miller LL, Shoseyov D, Blau H, Rivlin J, Aviram M, et al. Chronic ataluren (PTC124) treatment of nonsense mutation cystic fibrosis. Eur Respir J. 2011;38:59-69.
[25] Sermet-Gaudelus I, Boeck KD, Casimir GJ, Vermeulen F, Leal T, Mogenet A, et al. Ataluren (PTC124) induces cystic fibrosis transmembrane conductance regulator protein expression and activity in children with nonsense mutation cystic fibrosis. Am J Respir Crit Care Med. 2010;182:1262-72.
[26] Xue X, Mutyam V, Tang L, Biswas S, Du M, Jackson LA, et al. Synthetic Aminoglycosides Efficiently Suppress CFTR Nonsense Mutations and are Enhanced by Ivacaftor. Am J Respir Cell Mol Biol. 2013.
[27] McElroy SP, Nomura T, Torrie LS, Warbrick E, Gartner U, Wood G, et al. A lack of premature termination codon read-through efficacy of PTC124 (Ataluren) in a diverse array of reporter assays. PLoS Biol. 2013;11:e1001593.
[28] Lukacs GL, Verkman AS. CFTR: folding, misfolding and correcting the DeltaF508 conformational defect. Trends Mol Med. 2012;18:81-91.
[29] Okiyoneda T, Lukacs GL. Fixing cystic fibrosis by correcting CFTR domain assembly. J Cell Biol. 2012;199:199-204.
[30] Rowe SM, Verkman AS. Cystic fibrosis transmembrane regulator correctors and potentiators. Cold Spring Harb Perspect Med. 2013;3.
[31] Mendoza JL, Schmidt A, Li Q, Nuvaga E, Barrett T, Bridges RJ, et al. Requirements for efficient correction of DeltaF508 CFTR revealed by analyses of evolved sequences. Cell. 2012;148:164-74.
[32] Rabeh WM, Bossard F, Xu H, Okiyoneda T, Bagdany M, Mulvihill CM, et al. Correction of both NBD1 energetics and domain interface is required to restore DeltaF508 CFTR folding and function. Cell. 2012;148:150-63.
[33] Okiyoneda T, Veit G, Dekkers JF, Bagdany M, Soya N, Xu H, et al. Mechanism-based corrector combination restores DeltaF508-CFTR folding and function. Nat Chem Biol. 2013;9:444-54.
[34] Cormet-Boyaka E, Jablonsky M, Naren AP, Jackson PL, Muccio DD, Kirk KL. Rescuing cystic fibrosis transmembrane conductance regulator (CFTR)-processing mutants by transcomplementation. Proc Natl Acad Sci U S A. 2004;101:8221-6.

[35] Kim Chiaw P, Huan LJ, Gagnon S, Ly D, Sweezey N, Rotin D, et al. Functional rescue of DeltaF508-CFTR by peptides designed to mimic sorting motifs. Chem Biol. 2009;16:520-30.
[36] Van Goor F, Hadida S, Grootenhuis PD, Burton B, Stack JH, Straley KS, et al. Correction of the F508del-CFTR protein processing defect in vitro by the investigational drug VX-809. Proc Natl Acad Sci U S A. 2011;108:18843-8.
[37] Ren HY, Grove DE, De La Rosa O, Houck SA, Sopha P, Van Goor F, et al. VX-809 corrects folding defects in cystic fibrosis transmembrane conductance regulator protein through action on membrane-spanning domain 1. Mol Biol Cell. 2013;24:3016-24.
[38] Loo TW, Bartlett MC, Clarke DM. Corrector VX-809 stabilizes the first transmembrane domain of CFTR. Biochem Pharmacol. 2013;86:612-9.
[39] Clancy JP, Rowe SM, Accurso FJ, Aitken ML, Amin RS, Ashlock MA, et al. Results of a phase IIa study of VX-809, an investigational CFTR corrector compound, in subjects with cystic fibrosis homozygous for the F508del-CFTR mutation. Thorax. 2012;67:12-8.
[40] Tamanini A, Borgatti M, Finotti A, Piccagli L, Bezzerri V, Favia M, et al. Trimethylangelicin reduces IL-8 transcription and potentiates CFTR function. Am J Physiol Lung Cell Mol Physiol. 2011;300:L380-90.
[41] Phuan PW, Yang B, Knapp JM, Wood AB, Lukacs GL, Kurth MJ, et al. Cyanoquinolines with independent corrector and potentiator activities restore DeltaPhe508-cystic fibrosis transmembrane conductance regulator chloride channel function in cystic fibrosis. Mol Pharmacol. 2011;80:683-93.
[42] Odolczyk N, Fritsch J, Norez C, Servel N, da Cunha MF, Bitam S, et al. Discovery of novel potent DeltaF508-CFTR correctors that target the nucleotide binding domain. EMBO Mol Med. 2013;5:1484-501.
[43] Wolde M, Fellows A, Cheng J, Kivenson A, Coutermarsh B, Talebian L, et al. Targeting CAL as a negative regulator of DeltaF508-CFTR cell-surface expression: an RNA interference and structure-based mutagenetic approach. J Biol Chem. 2007;282:8099-109.
[44] Koulov AV, LaPointe P, Lu B, Razvi A, Coppinger J, Dong MQ, et al. Biological and structural basis for Aha1 regulation of Hsp90 ATPase activity in maintaining proteostasis in the human disease cystic fibrosis. Mol Biol Cell. 2010;21:871-84.
[45] Noel S, Dhooghe B, Leal T. PDE5 Inhibitors as Potential Tools in the Treatment of Cystic Fibrosis. Front Pharmacol. 2012;3:167.
[46] Leier G, Bangel-Ruland N, Sobczak K, Knieper Y, Weber WM. Sildenafil acts as potentiator and corrector of CFTR but might be not suitable for the treatment of CF lung disease. Cell Physiol Biochem. 2012;29:775-90.
[47] Lubamba B, Lecourt H, Lebacq J, Lebecque P, De Jonge H, Wallemacq P, et al. Preclinical evidence that sildenafil and vardenafil activate chloride transport in cystic fibrosis. Am J Respir Crit Care Med. 2008;177:506-15.
[48] Dhooghe B, Noel S, Bouzin C, Behets-Wydemans G, Leal T. Correction of Chloride Transport and Mislocalization of CFTR Protein by Vardenafil in the Gastrointestinal Tract of Cystic Fibrosis Mice. PLoS One. 2013;8:e77314.
[49] Kalid O, Mense M, Fischman S, Shitrit A, Bihler H, Ben-Zeev E, et al. Small molecule correctors of F508del-CFTR discovered by structure-based virtual screening. J Comput Aided Mol Des. 2010;24:971-91.
[50] Yu YC, Miki H, Nakamura Y, Hanyuda A, Matsuzaki Y, Abe Y, et al. Curcumin and genistein additively potentiate G551D-CFTR. J Cyst Fibros. 2011;10:243-52.
[51] Jih KY, Hwang TC. Vx-770 potentiates CFTR function by promoting decoupling between the gating cycle and ATP hydrolysis cycle. Proc Natl Acad Sci U S A. 2013;110:4404-9.

[52] Eckford PD, Li C, Ramjeesingh M, Bear CE. Cystic fibrosis transmembrane conductance regulator (CFTR) potentiator VX-770 (ivacaftor) opens the defective channel gate of mutant CFTR in a phosphorylation-dependent but ATP-independent manner. J Biol Chem. 2012;287:36639-49.
[53] Yu H, Burton B, Huang CJ, Worley J, Cao D, Johnson JP, Jr., et al. Ivacaftor potentiation of multiple CFTR channels with gating mutations. J Cyst Fibros. 2012;11:237-45.
[54] Van Goor F, Yu H, Burton B, Hoffman BJ. Effect of ivacaftor on CFTR forms with missense mutations associated with defects in protein processing or function. J Cyst Fibros. 2013.
[55] Flume PA, Liou TG, Borowitz DS, Li H, Yen K, Ordonez CL, et al. Ivacaftor in subjects with cystic fibrosis who are homozygous for the F508del-CFTR mutation. Chest. 2012;142:718-24.
[56] Cholon DM QN, Fulcher ML, Randell SH, Boucher RC, Gentzsch M. Potentiator ivacaftor impedes pharmacological correction of F508del CFTR. Pediatr Pulmonol Suppl. 2013;36:225.
[57] Sohma Y, Yu YC, Hwang TC. Curcumin and genistein: the combined effects on disease-associated CFTR mutants and their clinical implications. Curr Pharm Des. 2013;19:3521-8.
[58] French PJ, Bijman J, Bot AG, Boomaars WE, Scholte BJ, de Jonge HR. Genistein activates CFTR Cl- channels via a tyrosine kinase- and protein phosphatase-independent mechanism. Am J Physiol. 1997;273:C747-53.
[59] Pyle LC, Ehrhardt A, Mitchell LH, Fan L, Ren A, Naren AP, et al. Regulatory domain phosphorylation to distinguish the mechanistic basis underlying acute CFTR modulators. Am J Physiol Lung Cell Mol Physiol. 2011;301:L587-97.
[60] Lim CH, Bijvelds MJ, Nigg A, Schoonderwoerd K, Houtsmuller AB, de Jonge HR, et al. Cholesterol depletion and genistein as tools to promote F508delCFTR retention at the plasma membrane. Cell Physiol Biochem. 2007;20:473-82.
[61] Wang W, Bernard K, Li G, Kirk KL. Curcumin opens cystic fibrosis transmembrane conductance regulator channels by a novel mechanism that requires neither ATP binding nor dimerization of the nucleotide-binding domains. J Biol Chem. 2007;282:4533-44.
[62] Pedemonte N, Tomati V, Sondo E, Galietta LJ. Influence of cell background on pharmacological rescue of mutant CFTR. Am J Physiol Cell Physiol. 2010;298:C866-74.
[63] Clancy JP, Szczesniak RD, Ashlock MA, Ernst SE, Fan L, Hornick DB, et al. Multicenter intestinal current measurements in rectal biopsies from CF and non-CF subjects to monitor CFTR function. PLoS One. 2013;8:e73905.
[64] De Boeck K, Derichs N, Fajac I, de Jonge HR, Bronsveld I, Sermet I, et al. New clinical diagnostic procedures for cystic fibrosis in Europe. J Cyst Fibros. 2011;10 Suppl 2:S53-66.
[65] De Jonge HR, Ballmann M, Veeze H, Bronsveld I, Stanke F, Tummler B, et al. Ex vivo CF diagnosis by intestinal current measurements (ICM) in small aperture, circulating Ussing chambers. J Cyst Fibros. 2004;3 Suppl 2:159-63.
[66] Sato T, Vries RG, Snippert HJ, van de Wetering M, Barker N, Stange DE, et al. Single Lgr5 stem cells build crypt-villus structures in vitro without a mesenchymal niche. Nature. 2009;459:262-5.
[67] Sato T, Stange DE, Ferrante M, Vries RG, Van Es JH, Van den Brink S, et al. Long-term expansion of epithelial organoids from human colon, adenoma, adenocarcinoma, and Barrett's epithelium. Gastroenterology. 2011;141:1762-72.
[68] Sato T, Clevers H. Growing self-organizing mini-guts from a single intestinal stem cell: mechanism and applications. Science. 2013;340:1190-4.

[69] Dekkers JF, Wiegerinck CL, de Jonge HR, Bronsveld I, Janssens HM, de Winter-de Groot KM, et al. A functional CFTR assay using primary cystic fibrosis intestinal organoids. Nat Med. 2013;19:939-45.
[70] Rock JR, Onaitis MW, Rawlins EL, Lu Y, Clark CP, Xue Y, et al. Basal cells as stem cells of the mouse trachea and human airway epithelium. Proc Natl Acad Sci U S A. 2009;106:12771-5.
[71] Liu X, Ory V, Chapman S, Yuan H, Albanese C, Kallakury B, et al. ROCK inhibitor and feeder cells induce the conditional reprogramming of epithelial cells. Am J Pathol. 2012;180:599-607.
[72] Suprynowicz FA, Upadhyay G, Krawczyk E, Kramer SC, Hebert JD, Liu X, et al. Conditionally reprogrammed cells represent a stem-like state of adult epithelial cells. Proc Natl Acad Sci U S A. 2012;109:20035-40.
[73] Wong AP, Bear CE, Chin S, Pasceri P, Thompson TO, Huan LJ, et al. Directed differentiation of human pluripotent stem cells into mature airway epithelia expressing functional CFTR protein. Nat Biotechnol. 2012;30:876-82.
[74] Deriy LV, Gomez EA, Zhang G, Beacham DW, Hopson JA, Gallan AJ, et al. Disease-causing mutations in the cystic fibrosis transmembrane conductance regulator determine the functional responses of alveolar macrophages. J Biol Chem. 2009;284:35926-38.
[75] Krauss RD, Bubien JK, Drumm ML, Zheng T, Peiper SC, Collins FS, et al. Transfection of wild-type CFTR into cystic fibrosis lymphocytes restores chloride conductance at G1 of the cell cycle. Embo J. 1992;11:875-83.
[76] Tang XX, Fok KL, Chen H, Chan KS, Tsang LL, Rowlands DK, et al. Lymphocyte CFTR promotes epithelial bicarbonate secretion for bacterial killing. J Cell Physiol. 2012;227:3887-94.
[77] Yui S, Nakamura T, Sato T, Nemoto Y, Mizutani T, Zheng X, et al. Functional engraftment of colon epithelium expanded in vitro from a single adult Lgr5(+) stem cell. Nat Med. 2012;18:618-23.

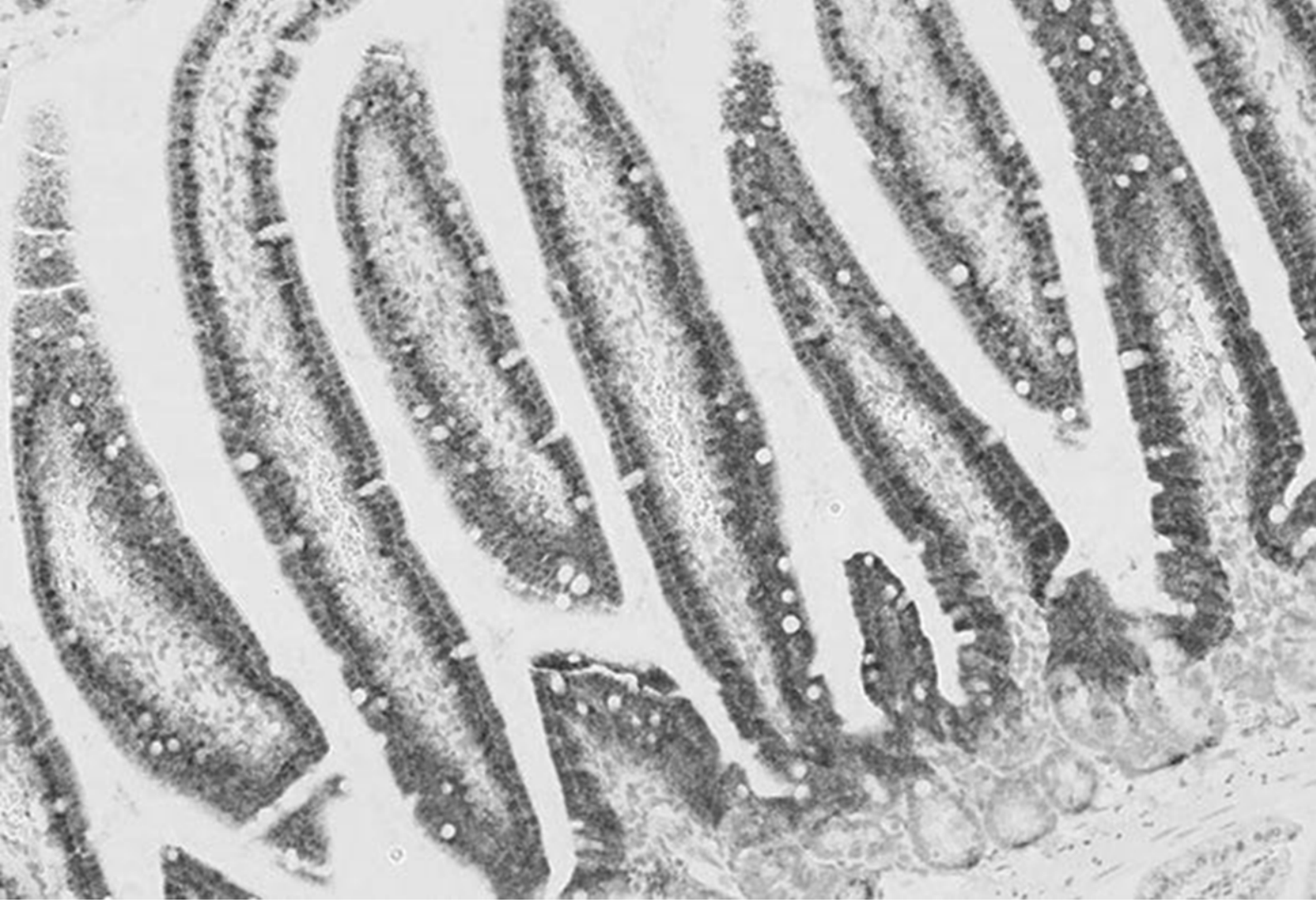

# Chapter 3

# Transcriptome analysis of the distal small intestine of *Cftr* null mice

**P.T. Ikpa[1], K. Dulla[2], H.R. de Jonge[1], and M.J.C. Bijvelds[1]**

[1]Department of Gastroenterology and Hepatology, Erasmus MC University Medical Center, PO Box 2040, 3000CA Rotterdam, The Netherlands. [2]ProQR Therapeutics N.V., Darwinweg 24, 2333CR Leiden, The Netherlands.

**Abstract**

Transcriptome analysis was performed on the distal small intestine of cystic fibrosis (CF; Cftr -/-) mice and littermate controls (Cftr N/N) reared on a conventional (solid) diet. Transcriptome data were analyzed using the Ingenuity Pathway Analysis (IPA) software application to delineate the impact of CFTR dysfunction on cellular signaling networks. The IPA analysis showed that the most strongly affected pathways are involved in antigen presentation, and T and B cell maturation/activation, and indicated a bacterial endotoxin-provoked activation of the innate and adaptive immune response. IPA indicated that this immune response, through activation of the c-Jun N-terminal kinase (JNK) and nuclear factor κB (NFκB) pathways, represses signaling via the retinoid X receptor (RXR). Indeed, among the most strongly down-regulated genes in the CF ileum are the farnesoid X receptor (FXR) targets *Nr0b2* (Shp) and *Fgf15*, the pregnane X receptor (PXR) targets *Ces2a/b*, several members of the cytochrome P450 family, and many other genes involved in lipid metabolism/transport that are controlled by ligand-dependent nuclear receptors that form obligate heterodimers with RXR. In addition, we observed dysregulation of genes involved in nutrient and solute uptake, including strong down-regulation of *Cubn* (cobalamin/intrinsic factor receptor), *Lct* (lactase) and *Slc28a1* (concentrative nucleoside transporter 1), as well as strong up-regulation of the amino acid transporter/CF modifier gene *Slc6a14*. Antibiotic administration reversed most of the CF-typical changes in ileal gene expression, attenuated the inflammatory response and largely restored RXR signaling. Our data indicate that the gut microbiota has a pervasive, but readily reversible, effect on intestinal gene expression in CF mice, and suggest that dysbiosis perturbs intestinal lipid and bile acid handling, and nutrient absorption in CF.

**Introduction**

The intestinal pathology of cystic fibrosis is characterized by luminal dehydration, luminal surface acidification, and accretion of viscous mucus [1]. Mucus accumulation and dehydration are thought to play a key role in the development of the CF-typical obstruction of the distal small intestine. The abnormally viscous mucus layer that lines the epithelium may also provide a niche for bacterial colonization, leading to small intestinal bacterial overgrowth (SIBO) [2]. SIBO is relatively common among CF patients and may affect the luminal processing and uptake of nutrients (lipids in particular) and bile acids, potentially contributing to their malabsorption and to the growth retardation observed in CF. SIBO is likely to markedly impact host-microbe interactions, and trigger a local, innate immune response [3]. This is most evident from studies on CF mouse models, which report evidence for both SIBO and inflammation of the gut wall, which is amenable to antibiotic treatment [4, 5].

A limited number of studies have systematically assessed the effect of the CF condition on intestinal gene expression, using a DNA microarray approach [4, 6, 7]. Applied to a Cftr *null* mouse model with a severe intestinal phenotype (i.e. a strong predisposition to develop a lethal obstruction in early life), these microarray studies have shown that CF is associated with marked changes in intestinal gene expression. Some of these changes appear to be directly related to SIBO and inflammation, e.g. the up-regulation of genes involved in host-microbe interactions [4]. For other differentially regulated genes the link with SIBO and inflammation is less evident. For instance, it was shown that antibiotic treatment did not correct the reduction in the expression of genes involved in the processing/uptake of macro- and micro-nutrients, although it did improve weight gain [5, 7].

These studies assessing the CF intestinal transcriptome have yielded important insights into the pathophysiology of CF-related intestinal disease. However, one limitation is that they were performed on animals reared on a lipid-enriched, low-carbohydrate/protein elemental liquid diet (Peptamen), which may have intrinsic effects on the CF gastrointestinal phenotype and the gut microbiota [8, 9]. Also, only one of these studies specifically assessed gene expression in the distal small intestine, i.e. the region which is most susceptible to obstruction and SIBO, and has a key role in bile acid uptake [6]. In the present study, to exclude confounding effects of the dietary regimen, we assessed the ileal transcriptome of CF mice reared on a solid diet with a standard nutrient formulation. The CF mouse model used by us differs from the one presented in previous CF-related transcriptome analyses in that, probably because of secondary genetic and environmental factors, it does rarely suffer lethal intestinal obstructions in the adult stage, even when maintained on a conventional regimen (i.e. a solid chow and drinking water without added

osmolytes). We employed a next-generation sequencing technique, RNAseq, that allows the quantification of RNA transcripts with single base-pair resolution, whilst maintaining a high dynamic detection range. To minimize variation in gene expression resulting from secondary genetic and environmental factors, we used sex (and age) matched littermate couples that, from birth onwards, were housed together. Furthermore, recent advancements in the analysis of high-throughput gene expression data, specifically the application of algorithms that assess causal networks that are assimilated based on prior published research, enabled us to identify differentially regulated signaling pathways and their upstream modulators [10].

## Methods

### *Animal procedures and tissue collection*

CF mice ($Cftr^{tm1Cam}$; congenic FVB/n) and littermate controls were housed together in individually ventilated cages, in an environmentally controlled facility at the Erasmus MC, Rotterdam. Animals were reared on a low fiber diet (C1013; Altromin) and a polyethylene glycol/electrolyte drinking solution to prevent intestinal obstruction in early life [11]. In some instances, animals were administered drinking water supplemented with ciprofloxacin (0.3 g/L) and metronidazole (0.5 g/L) for 15 days [12]. Before tissue collection, animals were kept on normal drinking water (or, when applicable, drinking water supplemented with antibiotics) for >4 days. This procedure is well tolerated by adult (>12 weeks) CF mice. Intake of food and water was monitored during this period, and shown to be comparable between genotypes (not shown). Experiments were approved of by the Ethical Committee for Animal Experiments of the Erasmus MC.

### *RNA Isolation*

Animals were anaesthetized (ketamine 120 mg/kg, xylazine 20 mg/kg; i.p.), and the intestinal tract was collected and flushed with ice-cold saline. Ileal sections (3-5 mm in length) were collected at 5-6 cm proximal to the ileocecal valve. Sampling from a CF animal (*Cftr* -/-) and a sex-matched littermate control (*Cftr* N/N) was performed within a time window of 20 min, and between 12:00-14:00h, to control for diurnal variations in gene expression. Tissue was homogenized with a rotor-stator homogenizer in Trizol reagent (Qiagen), and total RNA was extracted using the Nucleospin RNA kit (Macherey-Nagel). After the integrity of the extracted RNA was verified by gel electrophoresis, cDNA was synthesized using the PrimeScript RT master mix (Takara Bio).

***Transcriptome sequencing and pathway analysis***

Transcriptome sequencing was performed at the Beijing Genomics Institute (BGI). In brief, mRNA was isolated from total ileal tissue. The mRNA extracts (200 ng) were fragmented and subsequently used for cDNA synthesis. The resulting cDNA library was sequenced using an HiSeq 2000 sequencer (TruSeq SBS KIT-HS V3; Illumina). Data were processed with CLC genomic workbench 7.5 (CLC Bio), and the sequence reads were mapped to the Genome Reference Consortium (GRC) genome data set GRCm38.76, using default parameters. Data depict reads per 1000 base pair transcript per million mapped reads (RPKM).

For identification of differentially regulated canonical signaling pathways in the ileum of CF mice, compared to controls, transcriptome data from 3 couples (2F/1M) were used. For each couple and transcript, expression in the Cftr -/- animal was calculated relative to the respective control. Identification of differentially regulated signaling pathways was based on those genes that, on average, were up- or down-regulated by a factor of ≥2 (see *Data analysis*). To assess the effect of the antibiotic treatment on ileal gene expression, for each genotype, the expression in one treated animal was expressed relative to the average expression level in the untreated animals, and the analysis was performed on genes that were up- or down-regulated by a factor of ≥2.

***Data analysis***

Transcriptome data were analyzed using the Ingenuity® web-based software application (Version 1.10; Qiagen). Ingenuity pathway analysis (IPA) and upstream regulator analysis (URA) was applied to identify differentially regulated pathways and their upstream modulators, as described in detail elsewhere [10]. In brief, to identify differentially regulated pathways, the enrichment of the dataset with up- or down-regulated genes comprised within a signal transduction network was assessed using Fisher's exact test (overlap P-value). To assess the activation state of a pathway and its upstream regulator, the consistency of the match between the observed and the predicted (based on established interactions within a network) expression pattern was calculated (activation Z-score). A positive Z-score signifies a regulator in the active state, a negative score indicates that its activity is repressed.

Statistical differences in mean transcript levels were evaluated by the (paired) ratio t-test. Data shown are mean ± SE.

## Results

### *Identification of canonical signaling pathways affected by CF*

We compared the ileal transcriptome of CF mice and wildtype littermates by IPA. This identified >100 differentially regulated canonical signaling pathways. The most affected canonical pathways (based on the overlap P-value) in the CF ileum are listed below (Figure 1).

### *Activation of the innate and adaptive immune response in the CF ileum*

The IPA indicated a highly significant differential regulation of genes involved in antigen presentation, activation of T helper cells, and B cell development (Figure 1; Table S1). This points towards the activation of an innate and adaptive immune response, resulting from an altered host-microbe (pathogen) interaction in the CF gut (Figure 2A). Among the up-regulated genes are those involved in antigen association with MHC molecules and their presentation to T cells, and several (co-)receptors and cytokines that stimulate differentiation of naïve CD4+ cells into T helper cells (Figure 2B). In contrast, the gene encoding the TGF-β co-receptor ALK7 (ACVR1C) is down-regulated, which may further promote the immune response [13]. Consistent with T helper cell activation, many genes in the B-cell development and iCOS-iCOSL signaling in T helper cells pathways were also up-regulated, suggesting an increase in the production/recruitment of cells involved in the adaptive immune response (Table S1).

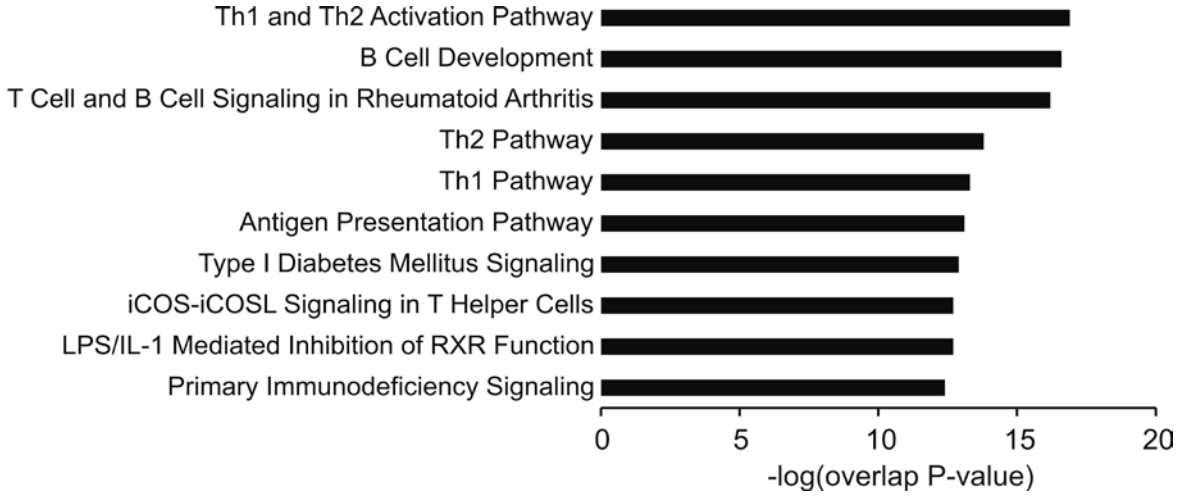


***Figure 1*** *Differential regulation of canonical signal transduction pathways in the murine CF ileum. IPA was used to assess the enrichment of the dataset with up- or down-regulated genes that make up predefined signal transduction networks. The top canonical pathways, based on overlap P-value, are shown.*

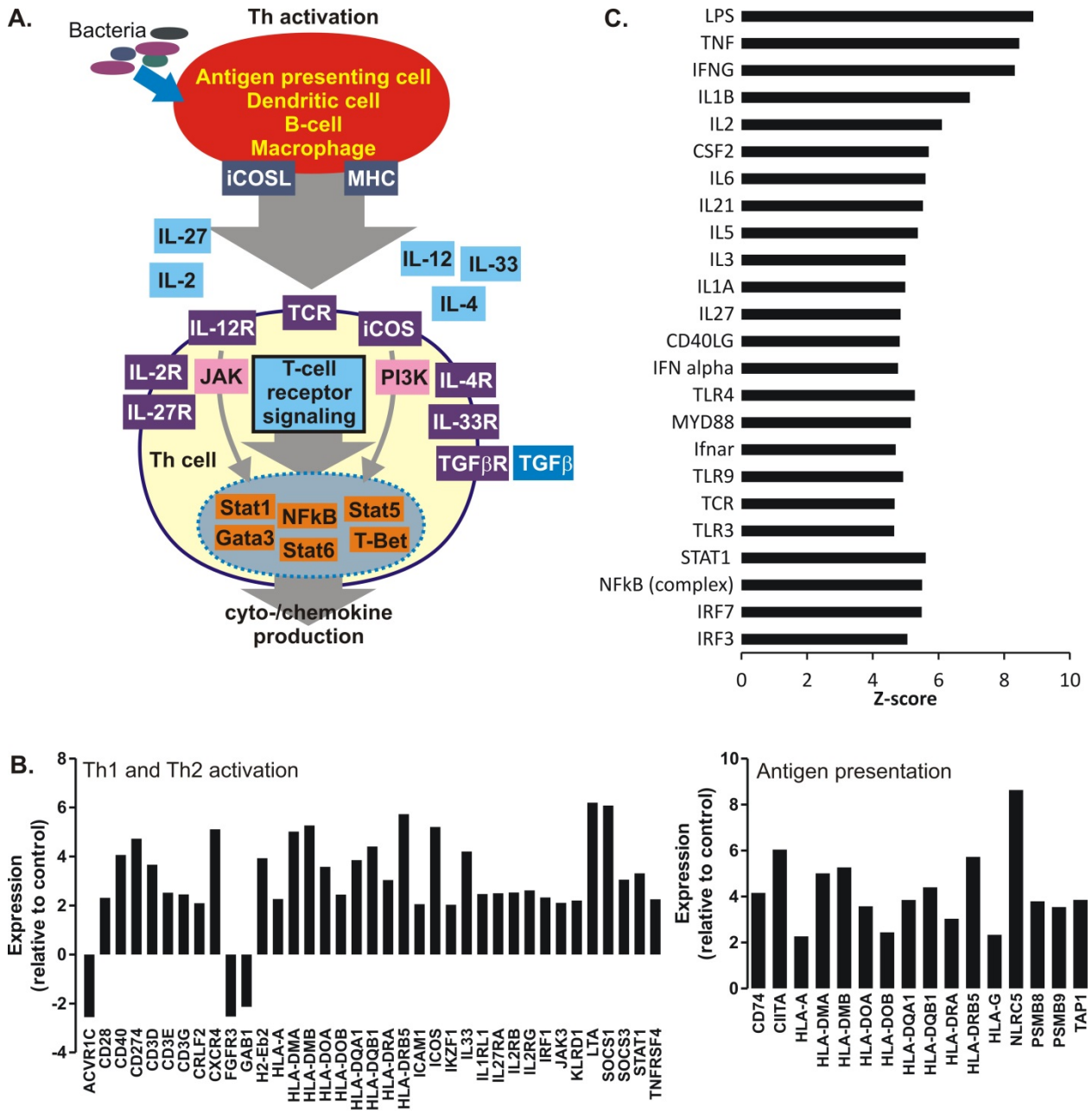


***Figure 2*** *A. Antigen presentation to, and activation of, CD4+ T cells. Upon contact with microorganisms or their products, antigen-presenting cells produce specific cues that trigger differentiation of naïve CD4+ cells into one of several T helper cell subtypes. The MHC complex is involved in the processing of antigens and their presentation to the T cell receptor (TCR) complex. In conjunction with stimulation of the TCR, specific interleukins are essential for the priming of T helper cells. The iCOSL-iCOS (inducible T-cell co-stimulator ligand/receptor) interaction contributes to the regulation of activated T cells. CD4+ cell priming is regulated by activation of several transcription factors, including Stat1, T-Bet, Gata3 and Stat5. TGF-β has an immune-suppressive action and inhibits differentiation of T cells. B. Transcript levels of genes involved in antigen presentation and the Th1 and Th2 activation pathway in the CF ileum, relative to a paired Cftr N/N animal. Many of the up-regulated genes encode proteins involved in antigen processing or (co-)receptors and ligands that form the immunological synapse between antigen-presenting and CD4+ cells. C. The URA indicated that immune modulatory receptor ligands, their (co-)receptors, and transcription factors are activated in the CF ileum*

The URA suggested that the activation of this inflammatory response is caused by exposure to bacterial lipopolysaccharide (LPS) produced by gram-negative bacteria, which,

through Toll-like receptor (TLR) stimulation, leads to activation of pro-inflammatory transcription factors (interferon regulatory factor, IRF3/7; nuclear factor κB, NFκB; signal transducer and activator of transcription, STAT1), and the production of pro-inflammatory cytokines (IFNγ, IL-1β, TNFα; Figure 2C).

In this context, it is of interest that alkaline phosphatase (*Alpi*) transcript levels were significantly lowered in the ileum of CF mice (407 ± 69 vs. 228 ± 34 RPKM in control and CF mice, respectively; $P < 0.05$, $N = 3$). Intestinal alkaline phosphatase was shown to have anti-inflammatory actions, conceivably through catalyzing dephosphorylation of LPS and other endotoxins [14]. We also observed that *Fut2* transcript levels were significantly higher in CF mice than controls (0.3 ± 0.04 vs. 7.4 ± 2.3 RPKM in control and CF mice, respectively; $P < 0.05$, $N = 3$). This fucosyltransferase plays a role in host-microbe interactions and is induced by bacterial colonization of the gut [15]. Increased expression of *Fut2* has previously been observed in CF mice [16].

***LPS represses the activity of ligand-dependent nuclear receptors in the CF ileum***

The IPA further indicated that the release of LPS and IL-1β inhibits the activity of the retinoid X receptors (RXRα/β) in the CF ileum (Figure 1; Table S1). This is in accordance with previous studies that have shown that LPS reduces nuclear localization of hepatic RXRα and represses induction of its target genes [17, 18]. This repression is thought to be mediated by activation of the c-Jun N-terminal kinase (JNK) and NFκB pathways (Figure 3A). RXRs form obligate heterodimers with type II ligand-dependent nuclear receptors, including FXR (NR1H4), LXR (NR1H2/3), PXR (NR1I2) and PPARα/δ/γ. Indeed, we observed significant down-regulation of genes involved in the metabolism and transport of fatty acids, bile acids, sterols and xenobiotics (Figure 3B; Table S1). Among the most strongly down-regulated genes are the PXR-induced carboxylesterases *Ces2a/b*, and the FXR targets *Fgf15* and *Nr0b2*, involved in intestinal bile acid transport and hepatic bile acid synthesis. This set also includes members of the ATP binding cassette family such as *Abca1*, *Abcb1a*, *Abcg5*, *Abcg8*, which encode proteins that facilitate transport of sterols and xenobiotics to the intestinal lumen [19-21]. Also down-regulated are genes of the aldehyde hydrogenase and the cytochrome P450 family, involved in xenobiotic and lipid metabolism, and the fatty acid binding proteins involved in the transport of fatty acids. In line with these data, the URA indicated that the activity of these ligand-dependent nuclear receptors is repressed (Figure 3C).

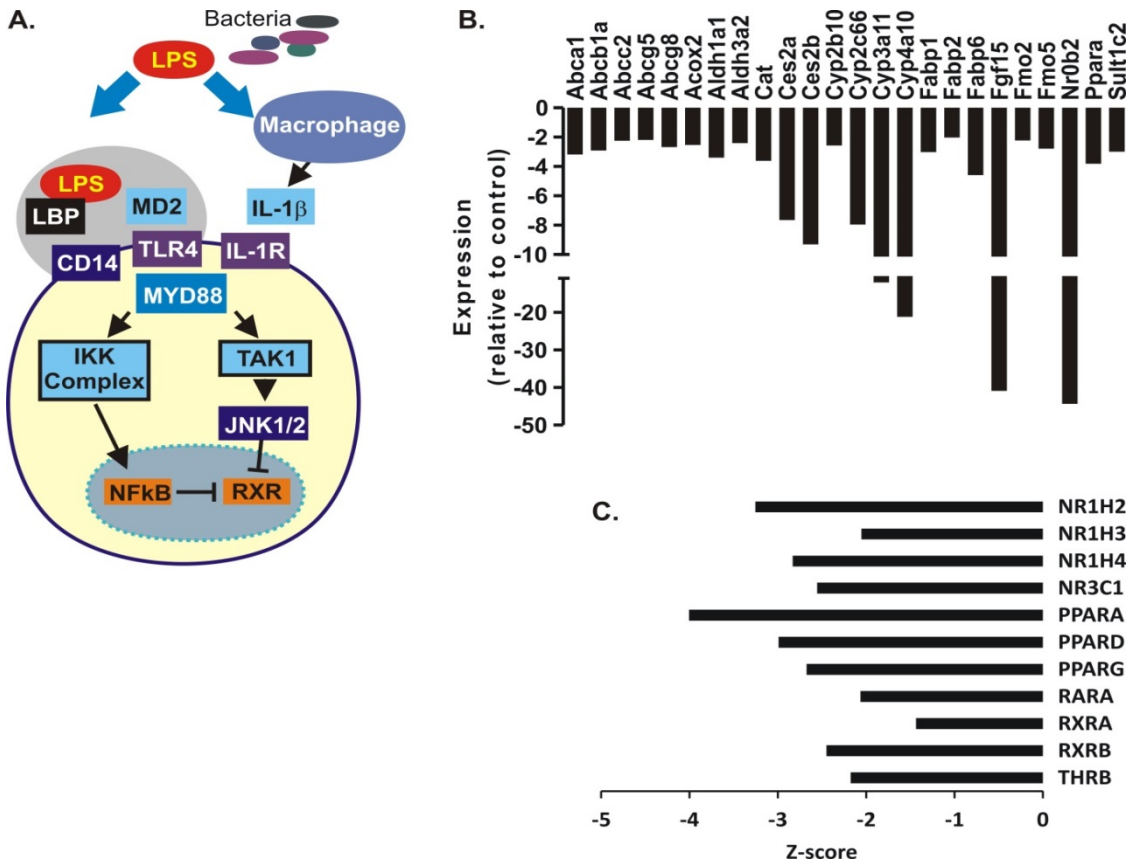


***Figure 3*** *LPS/IL-1β-mediated inhibition of RXR. A. LPS, bound to the LPS-binding protein (LBP), activates the CD14/TRL4/MD2 receptor complex. This stimulates the production of pro-inflammatory cytokines (IL-1β, TNFα) by immune cells. Stimulation of intestinal cells by LPS and pro-inflammatory cytokines leads to the recruitment of the IKK (inhibitor of NFκB kinase) and TAK1 (TGFβ-activated kinase 1) complexes, and activation of NFκB and JNK, which decreases RXR transcriptional activity. B. Because RXR dimerizes with type II ligand-dependent nuclear receptors, including FXR, LXR, PXR, RAR, CAR and PPAR, this leads to down-regulation of an array of genes involved in the metabolism and transport of fatty acids, sterols, bile acids and xenobiotics. C. The URA indicated that many ligand-dependent nuclear receptors in the CF ileum are in an inactive state.*

### *CF is associated with down-regulation of genes involved in the absorption of monosaccharides, amino acids and B vitamins*

In view of the reduced expression of genes involved in lipid transport, we also investigated whether the transcriptome data show evidence for impaired intestinal translocation of other nutrients. We observed a strong reduction in transcript levels of lactase (*Lct*), a disaccharidase ectoenzyme located at the brush border membrane of intestinal epithelial cells (Figure 4).

Trehalase (*Treh*) transcript levels were also reduced, albeit to a more moderate extent. In contrast, expression of other brush border disaccharidases, i.e. maltase-glucoamylase (*Mgam*) and sucrose-isomaltase (*Sis*), was similar in CF and control mice. Further, we found that the expression of the major monosaccharide transporters located in the brush border membrane,

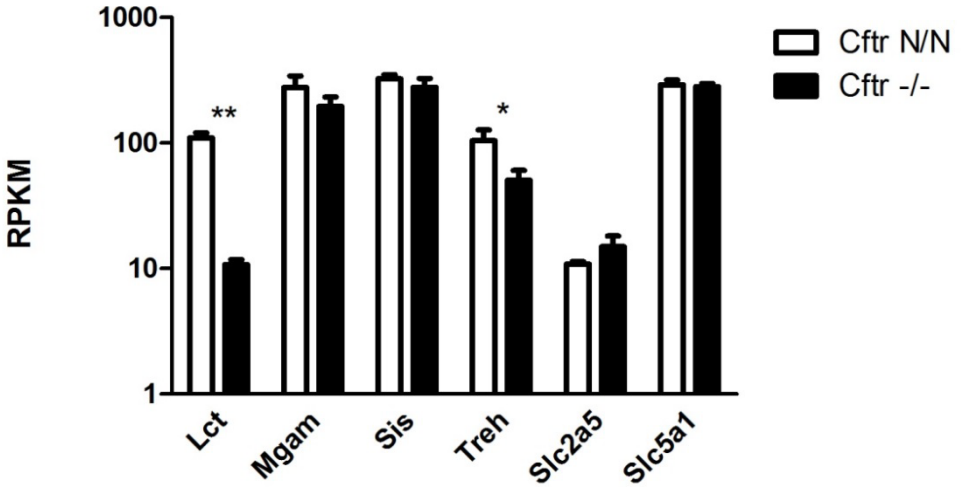


***Figure 4*** *Transcript level of genes encoding membrane proteins involved in the enzymatic release and uptake of monosaccharides. *P < 0.05; **P < 0.01; N=3.*

GLUT5 (*Slc2a5*) and SGLT1 (*Slc5a1*), was similar in both genotypes. Of the major aminopeptidases, only glutamyl aminopeptidase (*Enpep*) transcript levels showed a moderate reduction in the CF ileum, compared to controls, whereas the expression of alanyl aminopeptidase (*Anpep*) was unchanged (Figure 5).

The expression of the sodium-dependent neutral amino acid transporter (*Slc6a19*) was modestly reduced in CF mice. No statistically significant difference was observed in the expression of the PEPT1 dipeptide transporter (*Slc15a1*). Intriguingly, we noted strong induction of ATB0,+ (*Slc6a14*), a broad-specificity amino acid transporter, in the CF intestine: whereas expression was negligible (<1 RPKM) in ileum of controls, this gene was robustly expressed in the ileum of CF mice.

The ileum plays a crucial role in the enterohepatic circulation of bile acids and cobalamin (vitamin B12). Therefore, we also investigated the expression of plasma membrane proteins

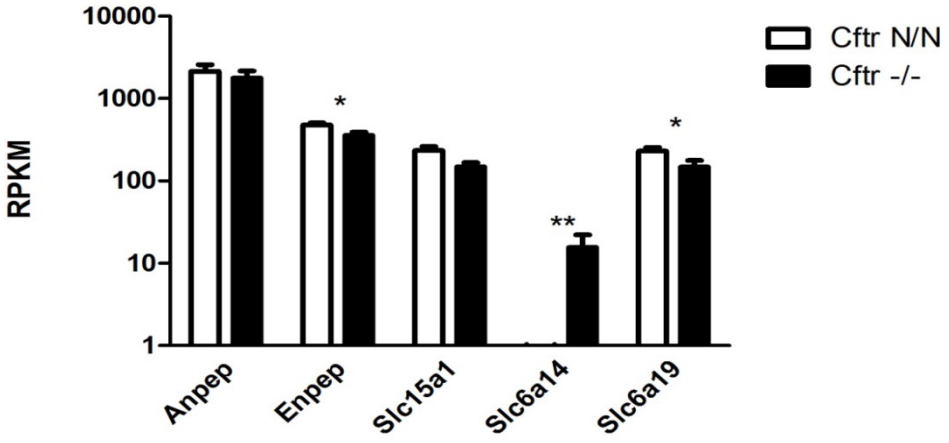


***Figure 5*** *Transcript level of genes encoding membrane proteins involved in the enzymatic release and uptake of oligopeptides and amino acids. *P < 0.05; **P < 0.01; N=3*

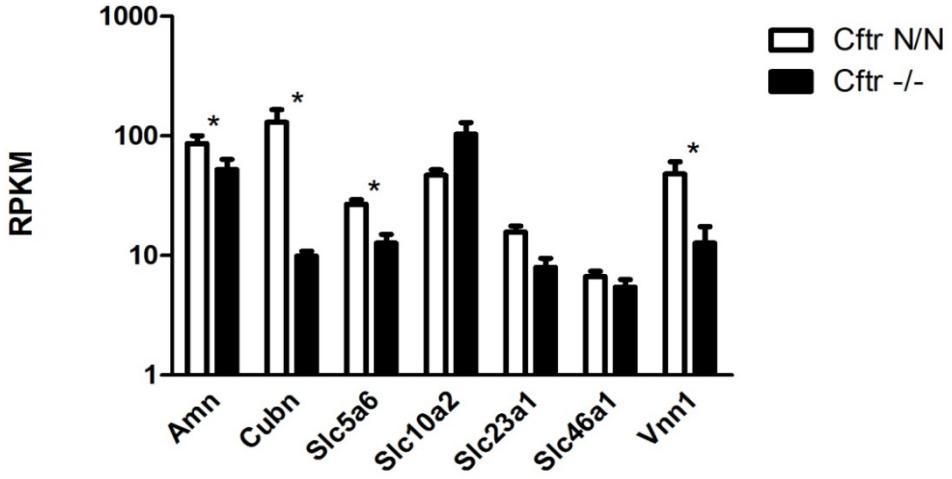


**Figure 6** *Transcript level of genes encoding membrane proteins involved in the uptake of vitamins and bile acids. *P < 0.05; N=3.*

involved in the uptake of this and other water-soluble vitamins, and of the sodium-dependent apical bile acid transporter (*Slc10a2*). We found that transcript levels of *Cubn*, which encodes the cobalamin receptor cubilin, were strongly (>10-fold) reduced in the CF ileum, compared to control tissue, whereas the transcript levels of amnionless (*Amn*), which is also thought to be involved in cobalamin uptake, were more moderately reduced (Figure 6).

Further, we observed a moderate reduction in the expression of the sodium-dependent multivitamin transporter (*Slc5a6*), principally involved in biotin and panthothenic acid uptake. The expression of the pantetheine hydrolase ectoenzyme vanin-1 (*Vnn1*), a PPARα target required for intraluminal production of panthothenic acid from its non-absorbable precursors, was also markedly (>3-fold) lower in the CF ileum than in control tissue [22]. The expression of ascorbic and folic acid transporters (*Slc23a1* and *Slc46a1*, respectively) and of *Slc10a2* was not affected.

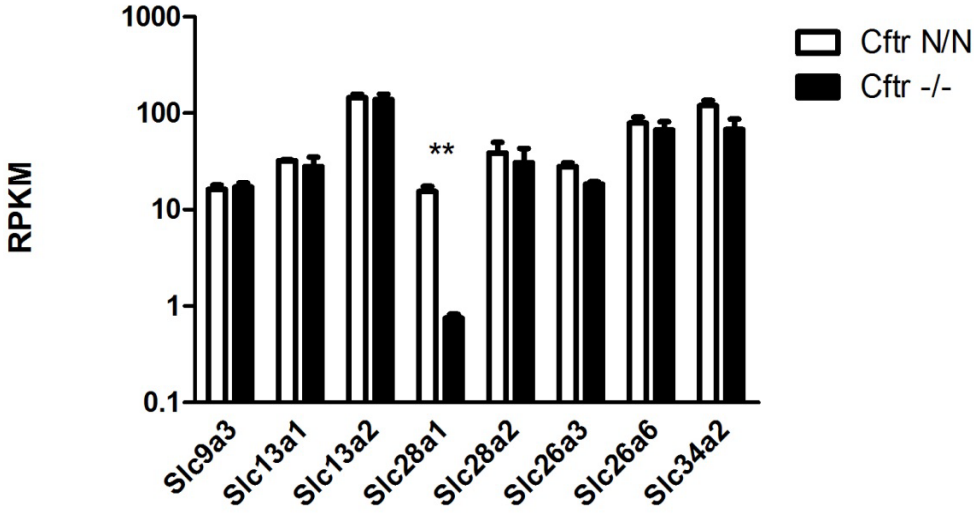


***Figure 7*** *Transcript level of genes encoding solute transporters involved in the uptake of sodium, chloride, nucleosides, phosphate and sulfate. **P < 0.01; N=3.*

Finally, we assessed the expression of some major intestinal solute transporters. These facilitate either sodium and chloride uptake via proton (*Slc9a3*) and bicarbonate (*Slc26a3*, *Slc26a6*) antiport, respectively, or mediate sulfate/citrate/succinate (*Slc13a1/2*), nucleoside (*Slc28a1/2*) and phosphate (*Slc34a2*) uptake via sodium symport. This analysis showed that transcript levels of the concentrative nucleoside transporter 1 (CNT1; *Slc28a1*) were significantly (ca. 20-fold) lower in CF than in control tissue (Figure 7). The expression of the other genes in this category was not notably affected.

***Effect of antibiotic treatment on intestinal gene expression in CF mice***

Assuming that increased exposure of the intestinal epithelium to bacterial endotoxins does indeed lead to repression of signaling through RXR and other ligand-dependent nuclear

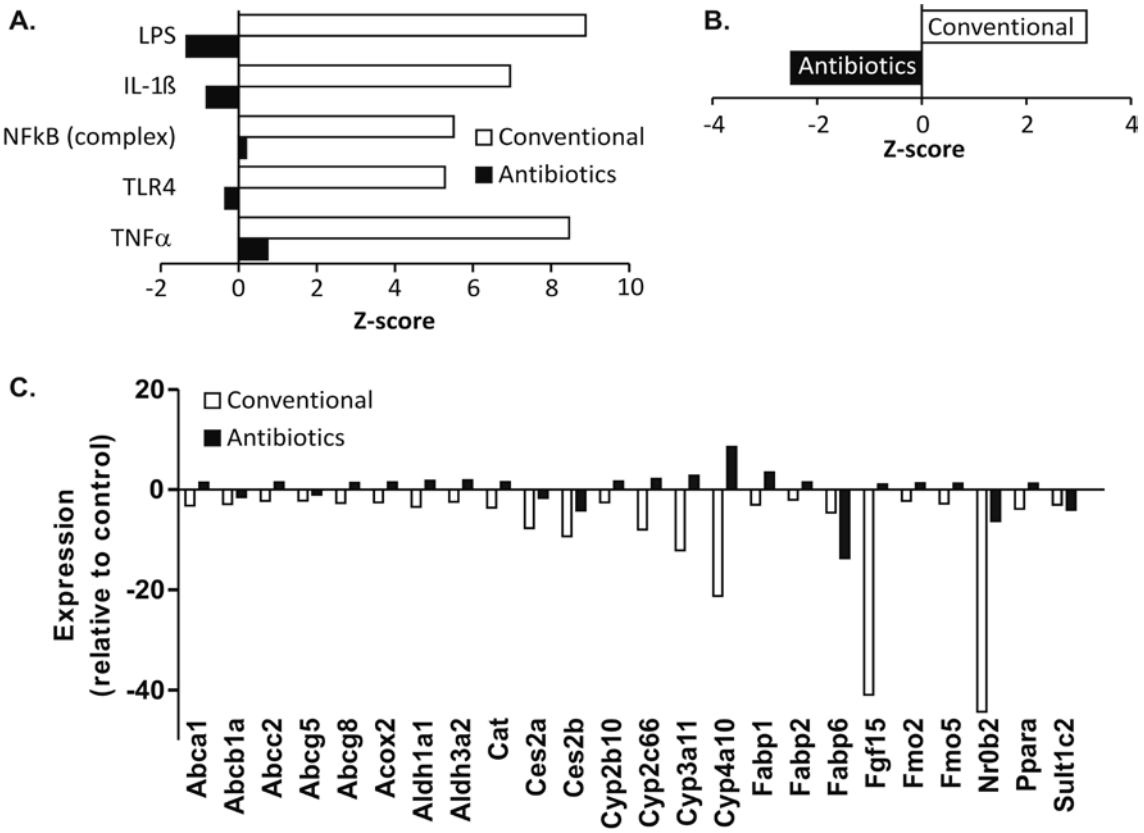


***Figure 8*** *Effect of antibiotic treatment on the inflammatory response and on ligand-dependent nuclear receptor activity. A. The URA was used to assess the effect of antibiotic treatment on the activation state of inflammation modulators in the CF ileum, relative to ileum of control mice. For comparison, the activation state in conventionally reared CF mice is included (data as in Figure 2C). Antibiotic treatment reduced the activation state of these modulators down to the level observed in (untreated) wildtype ileum. B. Activation state of the LPS/IL-1β-mediated inhibition of RXR pathway in CF mice, compared to wildtype mice, before and after antibiotic treatment. Antibiotic treatment reversed the activation of the LPS/IL-1β-mediated inhibition of RXR pathway. C. Effect of antibiotic treatment on the expression of genes involved in the metabolism and transport of fatty acids, sterols, bile acids and xenobiotics. Transcript levels are shown relative to Cftr N/N mice. Antibiotic treatment reversed the down-regulation of most genes, restoring transcript levels closely to those found in Cftr N/N mice*

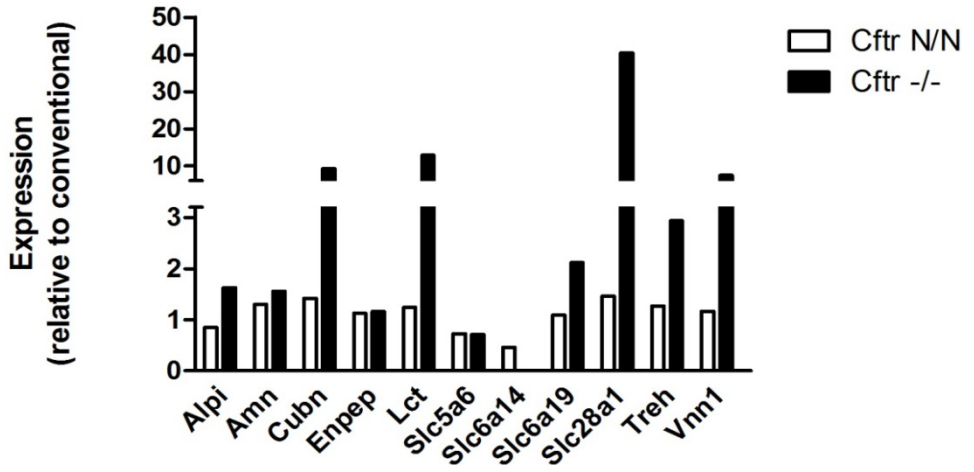


***Figure 9*** *Effect of antibiotic treatment on transcript levels of genes encoding brush border ectoenzymes, solute transporters or receptors that are differentially regulated in CF mice and controls. Data show transcript levels relative to conventionally reared animals*

receptors, we reasoned that measures to counteract SIBO would restore their activity. To test this, we treated animals with an antibiotic regimen that was previously shown to reduce the bacterial load in CF whilst increasing community diversity, leading to a convergence of the microbiome composition of CF and wildtype mice [12]. The URA was used to assess the effect of this regimen on the activation state of key inflammation modulators in the CF ileum. This analysis showed that, whereas these modulators were in the activated state in conventionally reared CF animals, the antibiotic treatment reduced their activity to (or below) the level observed in the ileum of conventionally reared wildtype mice (Figure 8A). This strongly suggests that antibiotic treatment effectively reduces exposure to LPS and attenuates the attendant immune response to the levels normally observed in the mouse intestine. Consistent with reduced LPS exposure and IL-1β production, the repression of RXR activity observed in conventionally reared CF mice was lost after antibiotic treatment (Figure 8B), and the expression of most genes controlled by RXR heterodimeric nuclear receptors was restored (Figure 8C).

We also investigated whether antibiotic treatment could reverse the observed changes in the expression of genes involved in the absorption of monosaccharides, amino acids, nucleosides and B vitamins. Indeed, antibiotic treatment strongly stimulated expression of *Cubn*, *Lct*, *Slc28a1* and *Vnn1* in CF mice, and led to a more moderate induction of *Alpi*, *Slc6a19* and *Treh* (Figure 9). In contrast, *Slc6a14* transcript levels were strongly reduced by antibiotic treatment. In wildtype mice, antibiotic treatment had comparatively little effect on the expression of these genes. Thus, these data show that antibiotic treatment corrects anomalous gene expression in the CF ileum.

***Normal expression of villus markers in the CF intestine***

CF has been associated with enhanced crypt cell proliferation, leading to expansion of the crypt compartment [6, 23]. We hypothesized that delayed maturation of the absorptive, columnar epithelial cells (enterocytes) may contribute to the observed reduction in transcript levels of genes involved in nutrient uptake, as these are typically substantially higher in the upper epithelial (villus) compartment than in the crypts. To investigate this, we assessed transcript levels of genes which were previously found to be expressed at >60-fold higher levels in the villi than in the crypts of mouse ileum [24]. Congruent with our hypothesis, this set of 15 genes included *Lct* and *Nr0b2*, i.e. genes that are strongly down-regulated in CF ileum. However, none of the other transcripts in this set showed a significant reduction in the CF condition, which argues against substantial changes in enterocyte maturation (Figure 10).

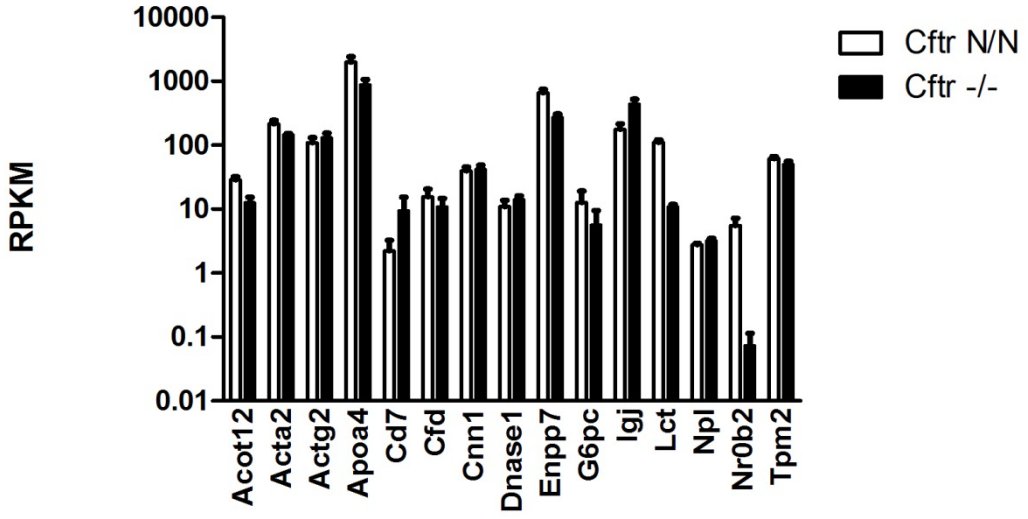


***Figure 10*** *Transcript level of typical villus markers in CF mice and controls. Transcript levels of these genes were previously shown to be >60 fold higher in the villi than in the crypts of mouse ileum.*

**Discussion**

It has been proposed that, in CF, intestinal dysbiosis is a key factor in the onset of intestinal inflammation and the activation of the immune system [25, 26]. Presently, transcriptome analysis showed unequivocal evidence for altered host-microbe interactions and the activation of an innate and adaptive immune response in the distal small intestine of a CF mouse model, which is triggered by bacterial endotoxins. Gut inflammation was associated with a marked overall reduction in the activity of (type II) ligand-dependent nuclear receptors, which is predicted to strongly affect fatty acid, sterol, bile acid and xenobiotic metabolism and transport. Apart from these marked effects on lipid handling, we noted that CF is associated with

reduced expression of a limited set of genes involved in the absorption of other nutrients. Most of these changes in gene expression could be corrected by antibiotic treatment, suggesting dysbiosis has a pervasive effect on the CF intestinal transcriptome.

The IPA indicated that signaling through ligand-dependent nuclear receptors is markedly repressed in the CF intestine, as a consequence of LPS/TLR-mediated activation of pro-inflammatory signaling pathways that lead to repression of RXR. LPS, a component of the outer membrane of gram-negative bacteria, triggers the production of pro-inflammatory cytokines by macrophages and other immune cells by activation of the LPS core receptor complex (Figure 3) [27]. LPS and pro-inflammatory cytokines have been shown to decrease the nuclear levels of hepatic RXRα and, consequently, its activity, in a JNK-dependent manner [17]. Down-regulation of *Alpi* and *Nr0b2* (encoding the SHP nuclear receptor), may contribute to the inflammatory response, as alkaline phosphatase and SHP activity was shown to inhibit LPS/TLR signaling [14, 28, 29]. Collectively, these data suggest that, in CF, SIBO-provoked enhanced production of LPS represses ligand-dependent receptor signaling.

The gut microbiota is known to modulate the activity of the bile acid receptor FXR in the ileum by intra-luminal conversion of primary bile acids, which limits the level of FXR-antagonistic species, but may also reduce uptake of the FXR-activating type [30, 31]. Our data indicate that dysbiosis, in addition, may repress FXR through its effects on the host immune response and RXR activity. RXR heterodimer nuclear receptors play a key role in the metabolism of fatty acids, sterols, bile acids and xenobiotics. Altered fatty acid, sterol and bile acid transport and metabolism are typical of CF, suggesting that intestinal repression of RXR may contribute to the development of CF-related pathologies [32-34]. For instance, a deficiency of the intestinal FXR target FGF15, or loss of the receptor for this hormone (FGFR4), was shown to enhance fecal excretion of bile acids, and to deplete the gall bladder, respectively [35, 36]. Similarly, the changes in the expression of genes involved in intestinal lipid physiology we present here may play a role in aberrant fatty acid and cholesterol transport and the changes in tissue lipid composition observed in CF patients and mouse models [34, 37, 38]. Repression of RXR may also contribute to the previously reported loss of intestinal PPARγ activity in CF mice, and to the presently observed reduction in *Alpi* transcripts, as this gene is targeted by the thyroid hormone receptor-RXR heterodimer [39-41].

Apart from these wide-ranging effects on the expression of genes involved in lipid handling, we also observed discrete changes in the expression of genes involved in the absorption of monosaccharides, amino acids, nucleosides and B vitamins. The most significant changes were observed in the transcript levels of *Cubn*, *Lct*, *Slc28a1* (all markedly reduced in CF

ileum), and *Slc6a14* (strongly increased in CF ileum). Lowered intestinal expression of *Cubn* and *Lct* has been found in earlier transcriptome analyses on CF mice [4, 6], and lowered intestinal lactase, as well as alkaline phosphatase, levels have previously been reported for CF patients [42]. We noted that the down-regulation of *Cubn* and *Lct* observed in the CF ileum can be reversed by antibiotic treatment, suggesting that the CF microbiome also modulates the expression of these genes. Consistent with a role of bacterial products, it has been shown that LPS-provoked acute endotoxemia reduces *Cubn* expression in the kidney [43]. Intriguingly, in CF mice, cubilin protein levels in the proximal tubules were also reduced, resulting in a mild (low molecular weight) proteinuria, but *Cubn* expression was apparently not affected [44]. Up-regulation of intestinal *Slc6a14* expression has previously been reported for patients suffering from ulcerative colitis and for *Vibrio cholerae* infected subjects, which suggests that the regulation of this gene is also linked to host-pathogen interactions and inflammation [45, 46]. In line with his notion, we found that antibiotic treatment strongly repressed *Slc6a14* expression in the CF ileum. Interestingly, genome-wide association studies on CF cohorts have shown that single nucleotide polymorphisms at loci near the *SLC6A14* gene are associated with meconium ileus [47]. Although the functional consequences of this genetic polymorphism are unknown, it is conceivable that enhanced SLC6A14-mediated uptake of solutes and stimulation of attendant osmotic water transport compounds the CF fluid secretory defect and exacerbates luminal dehydration.

Expression of genes that encode proteins involved in nutrient processing/uptake is particularly high in fully matured enterocytes, located at or near the tips of the villi. Therefore, a reduction in the transcript levels of these genes may signal an underlying defect in enterocyte maturation [7]. Arguing against such a wide-ranging defect is the observation that the expression of many typical villus markers (i.e. genes which are expressed at much higher level in villus than in crypt cells) is apparently normal in the CF intestine. Consequently, it is improbable that defective cell maturation fully accounts for the observed changes in gene expression. This is also indicated by the observation that, although *Lct* expression is strongly reduced in CF mice, the expression of other ectoenzymes located at the brush border of mature enterocytes, like *Anpep*, *Mgam* and *Sis*, was not affected. Therefore, if present, this mechanism does appear to affect only specific aspects of enterocyte maturation, and it is conceivable that the intestinal micro-environment provides specific cues which direct cell programming. Our data suggest that the gut microbiota is a key determinant of this maturation program.

**References**

[1] Assis DN, Freedman SD. Gastrointestinal disorders in Cystic Fibrosis. Clin Chest Med. 2016;37:109-18.
[2] Fridge JL, Conrad C, Gerson L, Castillo RO, Cox K. Risk factors for small bowel bacterial overgrowth in cystic fibrosis. J Pediatr Gastroenterol Nutr. 2007;44:212-8.
[3] Munck A. Cystic fibrosis: evidence for gut inflammation. Int J Biochem Cell Biol. 2014;52:180-3.
[4] Norkina O, Kaur S, Ziemer D, De Lisle RC. Inflammation of the cystic fibrosis mouse small intestine. Am J Physiol. 2004;286:G1032-G41.
[5] Norkina O, Burnett TG, De Lisle RC. Bacterial overgrowth in the cystic fibrosis transmembrane conductance regulator null mouse small intestine. Infect Immun. 2004;72:6040-9.
[6] Canale-Zambrano JC, Poffenberger MC, Cory SM, Humes DG, Haston CK. Intestinal phenotype of variable-weight cystic fibrosis knockout mice. Am J Physiol. 2007;293:G222-G9.
[7] De Lisle RC. Decreased expression of enterocyte nutrient-assimilation genes and proteins in the cystic fibrosis mouse small intestine. J Pediatr Gastroenterol Nutr. 2016;62:627-34.
[8] Kayama S, Mitsuyama M, Sato N, Hatakeyama K. Overgrowth and translocation of Escherichia coli from intestine during prolonged enteral feeding in rats. J Gastroenterol. 2000;35:15-9.
[9] Cottart CH, Bonvin E, Rey C, Wendum D, Bernaudin JF, Dumont S, et al. Impact of nutrition on phenotype in CFTR-deficient mice. Pediatr Res. 2007;62:528-32.
[10] Krämer A, Green J, Pollard J, Jr., Tugendreich S. Causal analysis approaches in Ingenuity Pathway Analysis. Bioinformatics. 2014;30:523-30.
[11] Xiao F, Li J, Singh AK, Riederer B, Wang J, Sultan A, et al. Rescue of epithelial HCO3- secretion in murine intestine by apical membrane expression of the cystic fibrosis transmembrane conductance regulator mutant F508del. J Physiol. 2012;590:5317-34.
[12] Lynch SV, Goldfarb KC, Wild YK, Kong W, De Lisle RC, Brodie EL. Cystic fibrosis transmembrane conductance regulator knockout mice exhibit aberrant gastrointestinal microbiota. Gut Microbes. 2013;4:41-7.
[13] Yoshimura A, Wakabayashi Y, Mori T. Cellular and molecular basis for the regulation of inflammation by TGF-beta. J Biochem. 2010;147:781-92.
[14] Estaki M, DeCoffe D, Gibson DL. Interplay between intestinal alkaline phosphatase, diet, gut microbes and immunity. World J Gastroenterol. 2014;20:15650-6.
[15] Goto Y, Uematsu S, Kiyono H. Epithelial glycosylation in gut homeostasis and inflammation. Nat Immunol. 2016;17:1244-51.
[16] Thomsson KA, Hinojosa-Kurtzberg M, Axelsson KA, Domino SE, Lowe JB, Gendler SJ, et al. Intestinal mucins from cystic fibrosis mice show increased fucosylation due to an induced Fucalpha1-2 glycosyltransferase. Biochem J. 2002;367:609-16.
[17] Ghose R, Zimmerman TL, Thevananther S, Karpen SJ. Endotoxin leads to rapid subcellular re-localization of hepatic RXRalpha: A novel mechanism for reduced hepatic gene expression in inflammation. Nucl Recept. 2004;2:4.
[18] Gu X, Ke S, Liu D, Sheng T, Thomas PE, Rabson AB, et al. Role of NF-kappaB in regulation of PXR-mediated gene expression: a mechanism for the suppression of cytochrome P-450 3A4 by proinflammatory agents. J Biol Chem. 2006;281:17882-9.
[19] Repa JJ, Berge KE, Pomajzl C, Richardson JA, Hobbs H, Mangelsdorf DJ. Regulation of ATP-binding cassette sterol transporters ABCG5 and ABCG8 by the liver X receptors alpha and beta. J Biol Chem. 2002;277:18793-800.
[20] Repa JJ, Turley SD, Lobaccaro JA, Medina J, Li L, Lustig K, et al. Regulation of absorption and ABC1-mediated efflux of cholesterol by RXR heterodimers. Science. 2000;289:1524-9.

[21] Sharpe LJ, Cook EC, Zelcer N, Brown AJ. The UPS and downs of cholesterol homeostasis. Trends Biochem Sci. 2014;39:527-35.
[22] Van Diepen JA, Jansen PA, Ballak DB, Hijmans A, Hooiveld GJ, Rommelaere S, et al. PPAR-alpha dependent regulation of vanin-1 mediates hepatic lipid metabolism. J Hepatol. 2014;61:366-72.
[23] Gallagher AM, Gottlieb RA. Proliferation, not apoptosis, alters epithelial cell migration in small intestine of CFTR null mice. Am J Physiol. 2001;281:G681-G7.
[24] Middendorp S, Schneeberger K, Wiegerinck CL, Mokry M, Akkerman RD, van Wijngaarden S, et al. Adult stem cells in the small intestine are intrinsically programmed with their location-specific function. Stem Cells. 2014;32:1083-91.
[25] Nielsen S, Needham B, Leach ST, Day AS, Jaffe A, Thomas T, et al. Disrupted progression of the intestinal microbiota with age in children with cystic fibrosis. Sci Rep. 2016;6:24857.
[26] Garg M, Ooi CY. The enigmatic gut in cystic fibrosis: linking inflammation, dysbiosis, and the increased risk of malignancy. Curr Gastroenterol Rep. 2017;19:6.
[27] Park BS, Lee JO. Recognition of lipopolysaccharide pattern by TLR4 complexes. Exp Mol Med. 2013;45:e66.
[28] Yuk JM, Shin DM, Lee HM, Kim JJ, Kim SW, Jin HS, et al. The orphan nuclear receptor SHP acts as a negative regulator in inflammatory signaling triggered by Toll-like receptors. Nat Immunol. 2011;12:742-51.
[29] Chen KT, Malo MS, Moss AK, Zeller S, Johnson P, Ebrahimi F, et al. Identification of specific targets for the gut mucosal defense factor intestinal alkaline phosphatase. Am J Physiol Gastrointest Liver Physiol. 2010;299:G467-75.
[30] Sayin SI, Wahlstrom A, Felin J, Jantti S, Marschall HU, Bamberg K, et al. Gut microbiota regulates bile acid metabolism by reducing the levels of tauro-beta-muricholic acid, a naturally occurring FXR antagonist. Cell Metab. 2013;17:225-35.
[31] Degirolamo C, Rainaldi S, Bovenga F, Murzilli S, Moschetta A. Microbiota modification with probiotics induces hepatic bile acid synthesis via downregulation of the Fxr-Fgf15 axis in mice. Cell Rep. 2014;7:12-8.
[32] Freedman SD, Shea JC, Blanco PG, Alvarez JG. Fatty acids in cystic fibrosis. Curr Opin Pulm Med. 2000;6:530-2.
[33] Weizman Z, Durie PR, Kopelman HR, Vesely SM, Forstner GG. Bile acid secretion in cystic fibrosis: evidence for a defect unrelated to fat malabsorption. Gut. 1986;27:1043-8.
[34] Strandvik B. Fatty acid metabolism in cystic fibrosis. N Engl J Med. 2004;350:605-7.
[35] Yu C, Wang F, Kan M, Jin C, Jones RB, Weinstein M, et al. Elevated cholesterol metabolism and bile acid synthesis in mice lacking membrane tyrosine kinase receptor FGFR4. J Biol Chem. 2000;275:15482-9.
[36] Inagaki T, Choi M, Moschetta A, Peng L, Cummins CL, McDonald JG, et al. Fibroblast growth factor 15 functions as an enterohepatic signal to regulate bile acid homeostasis. Cell Metab. 2005;2:217-25.
[37] Freedman SD, Katz MH, Parker EM, Laposata M, Urman MY, Alvarez JG. A membrane lipid imbalance plays a role in the phenotypic expression of cystic fibrosis in cftr(-/-) mice. Proc Natl Acad Sci U S A. 1999;96:13995-4000.
[38] Bederman I, Perez A, Henderson L, Freedman JA, Poleman J, Guentert D, et al. Altered de novo lipogenesis contributes to low adipose stores in cystic fibrosis mice. Am J Physiol Gastrointest Liver Physiol. 2012;303:G507-18.
[39] Ollero M, Junaidi O, Zaman MM, Tzameli I, Ferrando AA, Andersson C, et al. Decreased expression of peroxisome proliferator activated receptor gamma in cftr-/- mice. J Cell Physiol. 2004;200:235-44.

[40] Harmon GS, Dumlao DS, Ng DT, Barrett KE, Dennis EA, Dong H, et al. Pharmacological correction of a defect in PPAR-gamma signaling ameliorates disease severity in Cftr-deficient mice. Nat Med. 2010;16:313-8.
[41] Malo MS, Zhang W, Alkhoury F, Pushpakaran P, Abedrapo MA, Mozumder M, et al. Thyroid hormone positively regulates the enterocyte differentiation marker intestinal alkaline phosphatase gene via an atypical response element. Mol Endocrinol. 2004;18:1941-62.
[42] Van Biervliet S, Eggermont E, Carchon H, Veereman G, Deboeck K. Small intestinal brush border enzymes in cystic fibrosis. Acta Gastroenterol Belg. 1999;62:267-71.
[43] Schreiber A, Theilig F, Schweda F, Hocherl K. Acute endotoxemia in mice induces downregulation of megalin and cubilin in the kidney. Kidney Int. 2012;82:53-9.
[44] Jouret F, Bernard A, Hermans C, Dom G, Terryn S, Leal T, et al. Cystic fibrosis is associated with a defect in apical receptor-mediated endocytosis in mouse and human kidney. J Am Soc Nephrol. 2007;18:707-18.
[45] Eriksson A, Flach CF, Lindgren A, Kvifors E, Lange S. Five mucosal transcripts of interest in ulcerative colitis identified by quantitative real-time PCR: a prospective study. BMC Gastroenterol. 2008;8:34.
[46] Flach CF, Qadri F, Bhuiyan TR, Alam NH, Jennische E, Holmgren J, et al. Differential expression of intestinal membrane transporters in cholera patients. FEBS Lett. 2007;581:3183-8.
[47] Sun L, Rommens JM, Corvol H, Li W, Li X, Chiang TA, et al. Multiple apical plasma membrane constituents are associated with susceptibility to meconium ileus in individuals with cystic fibrosis. Nat Genet. 2012;44:562-9.

## SUPPLEMENTARY DATA

**Table S1**: Differentially regulated canonical pathways in the CF ileum.

| Gene Symbol Human | Gene Name | Gene Symbol Mouse | Expression: Fold change |
|---|---|---|---|
| **Antigen presentation** | | | |
| CD74 | CD74 molecule | Cd74 | 4.162 |
| CIITA | class II major histocompatibility complex transactivator | Ciita | 6.042 |
| HLA-A | major histocompatibility complex. class I. A | H2-Q7 | 2.267 |
| HLA-DMA | major histocompatibility complex. class II. DM alpha | H2-DMa | 5.015 |
| HLA-DMB | major histocompatibility complex. class II. DM beta | H2-DMb1 | 5.267 |
| HLA-DOA | major histocompatibility complex. class II. DO alpha | H2-Oa | 3.583 |
| HLA-DOB | major histocompatibility complex. class II. DO beta | H2-Ob | 2.444 |
| HLA-DQA1 | major histocompatibility complex. class II. DQ alpha 1 | H2-Aa | 3.854 |
| HLA-DQB1 | major histocompatibility complex. class II. DQ beta 1 | H2-Ab1 | 4.405 |
| HLA-DRA | major histocompatibility complex. class II. DR alpha | H2-Ea-ps | 3.037 |
| HLA-DRB5 | major histocompatibility complex. class II. DR beta 5 | H2-Eb1 | 5.732 |
| HLA-G | major histocompatibility complex. class I. G | H2-M3 | 2.341 |
| NLRC5 | NLR family CARD domain containing 5 | Nlrc5 | 8.639 |
| PSMB8 | proteasome subunit beta 8 | Psmb8 | 3.793 |
| PSMB9 | proteasome subunit beta 9 | Psmb9 | 3.547 |
| TAP1 | transporter 1. ATP binding cassette subfamily B member | Tap1 | 3.858 |
| **B cell development** | | | |
| CD19 | CD19 molecule | Cd19 | 14.814 |
| CD40 | CD40 molecule | Cd40 | 4.061 |
| CD79A | CD79a molecule | Cd79a | 6.106 |
| CD79B | CD79b molecule | Cd79b | 6.633 |
| H2-Eb2 | histocompatibility 2. class II antigen E beta2 | H2-Eb2 | 3.934 |
| HLA-A | major histocompatibility complex. class I. A | H2-Q7 | 2.267 |
| HLA-DMA | major histocompatibility complex. class II. DM alpha | H2-DMa | 5.015 |
| HLA-DMB | major histocompatibility complex. class II. DM beta | H2-DMb1 | 5.267 |
| HLA-DOA | major histocompatibility complex. class II. DO alpha | H2-Oa | 3.583 |
| HLA-DOB | major histocompatibility complex. class II. DO beta | H2-Ob | 2.444 |
| HLA-DQA1 | major histocompatibility complex. class II. DQ alpha 1 | H2-Aa | 3.854 |
| HLA-DQB1 | major histocompatibility complex. class II. DQ beta 1 | H2-Ab1 | 4.405 |
| HLA-DRA | major histocompatibility complex. class II. DR alpha | H2-Ea-ps | 3.037 |
| HLA-DRB5 | major histocompatibility complex. class II. DR beta 5 | H2-Eb1 | 5.732 |
| Ighg2b | immunoglobulin heavy constant gamma 2B | Ighg2b | 10.012 |
| IGHM | immunoglobulin heavy constant mu | Ighm | 4.157 |
| IL7 | interleukin 7 | Il7 | 3.374 |
| SPN | sialophorin | Spn | 2.867 |
| **iCOS-iCOSL signaling in Th cells** | | | |
| CD28 | CD28 molecule | Cd28 | 2.315 |
| CD40 | CD40 molecule | Cd40 | 4.061 |
| CD3D | CD3d molecule | Cd3d | 3.669 |
| CD3E | CD3e molecule | Cd3e | 2.522 |
| CD3G | CD3g molecule | Cd3g | 2.457 |
| FGFR3 | fibroblast growth factor receptor 3 | Fgfr3 | -2.531 |
| GAB1 | GRB2 associated binding protein 1 | Gab1 | -2.137 |
| GRAP2 | GRB2-related adaptor protein 2 | Grap2 | 2.017 |

| | | | |
|---|---|---|---|
| H2-Eb2 | histocompatibility 2. class II antigen E beta2 | H2-Eb2 | 3.934 |
| HLA-A | major histocompatibility complex. class I. A | H2-Q7 | 2.267 |
| HLA-DMA | major histocompatibility complex. class II. DM alpha | H2-DMa | 5.015 |
| HLA-DMB | major histocompatibility complex. class II. DM beta | H2-DMb1 | 5.267 |
| HLA-DOA | major histocompatibility complex. class II. DO alpha | H2-Oa | 3.583 |
| HLA-DOB | major histocompatibility complex. class II. DO beta | H2-Ob | 2.444 |
| HLA-DQA1 | major histocompatibility complex. class II. DQ alpha 1 | H2-Aa | 3.854 |
| HLA-DQB1 | major histocompatibility complex. class II. DQ beta 1 | H2-Ab1 | 4.405 |
| HLA-DRA | major histocompatibility complex. class II. DR alpha | H2-Ea-ps | 3.037 |
| HLA-DRB5 | major histocompatibility complex. class II. DR beta 5 | H2-Eb1 | 5.732 |
| ICOS | inducible T-cell costimulator | Icos | 5.209 |
| IL2RB | interleukin 2 receptor subunit beta | Il2rb | 2.533 |
| IL2RG | interleukin 2 receptor subunit gamma | Il2rg | 2.62 |
| ITK | IL2 inducible T-cell kinase | Itk | 2.065 |
| LAT | linker for activation of T-cells | Lat | 3.191 |
| LCK | LCK proto-oncogene. Src family tyrosine kinase | Lck | 2.496 |
| LCP2 | lymphocyte cytosolic protein 2 | Lcp2 | 2.189 |
| ZAP70 | zeta chain of T-cell receptor associated protein kinase 70 | Zap70 | 3.071 |

**Th1 and Th2 activation**

| | | | |
|---|---|---|---|
| ACVR1C | activin A receptor type 1C | Acvr1c | -2.559 |
| CD28 | CD28 molecule | Cd28 | 2.315 |
| CD40 | CD40 molecule | Cd40 | 4.061 |
| CD274 | CD274 molecule | Cd274 | 4.73 |
| CD3D | CD3d molecule | Cd3d | 3.669 |
| CD3E | CD3e molecule | Cd3e | 2.522 |
| CD3G | CD3g molecule | Cd3g | 2.457 |
| CRLF2 | cytokine receptor-like factor 2 | Crlf2 | 2.093 |
| CXCR4 | C-X-C motif chemokine receptor 4 | Cxcr4 | 5.114 |
| FGFR3 | fibroblast growth factor receptor 3 | Fgfr3 | -2.531 |
| GAB1 | GRB2 associated binding protein 1 | Gab1 | -2.137 |
| H2-Eb2 | histocompatibility 2. class II antigen E beta2 | H2-Eb2 | 3.934 |
| HLA-A | major histocompatibility complex. class I. A | H2-Q7 | 2.267 |
| HLA-DMA | major histocompatibility complex. class II. DM alpha | H2-DMa | 5.015 |
| HLA-DMB | major histocompatibility complex. class II. DM beta | H2-DMb1 | 5.267 |
| HLA-DOA | major histocompatibility complex. class II. DO alpha | H2-Oa | 3.583 |
| HLA-DOB | major histocompatibility complex. class II. DO beta | H2-Ob | 2.444 |
| HLA-DQA1 | major histocompatibility complex. class II. DQ alpha 1 | H2-Aa | 3.854 |
| HLA-DQB1 | major histocompatibility complex. class II. DQ beta 1 | H2-Ab1 | 4.405 |
| HLA-DRA | major histocompatibility complex. class II. DR alpha | H2-Ea-ps | 3.037 |
| HLA-DRB5 | major histocompatibility complex. class II. DR beta 5 | H2-Eb1 | 5.732 |
| ICAM1 | intercellular adhesion molecule 1 | Icam1 | 2.056 |
| ICOS | inducible T-cell costimulator | Icos | 5.209 |
| IKZF1 | IKAROS family zinc finger 1 | Ikzf1 | 2.032 |
| IL33 | interleukin 33 | Il33 | 4.208 |
| IL1RL1 | interleukin 1 receptor like 1 | Il1rl1 | 2.47 |
| IL27RA | interleukin 27 receptor subunit alpha | Il27ra | 2.5 |
| IL2RB | interleukin 2 receptor subunit beta | Il2rb | 2.533 |
| IL2RG | interleukin 2 receptor subunit gamma | Il2rg | 2.62 |
| IRF1 | interferon regulatory factor 1 | Irf1 | 2.329 |
| JAK3 | Janus kinase 3 | Jak3 | 2.106 |
| KLRD1 | killer cell lectin like receptor D1 | Klrd1 | 2.207 |
| LTA | lymphotoxin alpha | Lta | 6.198 |
| SOCS1 | suppressor of cytokine signaling 1 | Socs1 | 6.08 |

| | | | |
|---|---|---|---|
| SOCS3 | suppressor of cytokine signaling 3 | Socs3 | 3.053 |
| STAT1 | signal transducer and activator of transcription 1 | Stat1 | 3.316 |
| TNFRSF4 | TNF receptor superfamily member 4 | Tnfrsf4 | 2.254 |
| | | | |
| **LPS-IL-1 mediated inhibition of RXR function** | | | |
| ABCA1 | ATP binding cassette subfamily A member 1 | Abca1 | -3.189 |
| ABCB1 | ATP binding cassette subfamily B member 1 | Abcb1a | -2.904 |
| ABCC2 | ATP binding cassette subfamily C member 2 | Abcc2 | -2.237 |
| ABCG5 | ATP binding cassette subfamily G member 5 | Abcg5 | -2.198 |
| ABCG8 | ATP binding cassette subfamily G member 8 | Abcg8 | -2.677 |
| ACOX2 | acyl-CoA oxidase 2 | Acox2 | -2.524 |
| ALDH1A1 | aldehyde dehydrogenase 1 family member A1 | Aldh1a1 | -3.399 |
| ALDH3A2 | aldehyde dehydrogenase 3 family member A2 | Aldh3a2 | -2.412 |
| ALDH4A1 | aldehyde dehydrogenase 4 family member A1 | Aldh4a1 | 2.137 |
| CAT | catalase | Cat | -3.622 |
| CD14 | CD14 molecule | Cd14 | 3.364 |
| CHST3 | carbohydrate sulfotransferase 3 | Chst3 | 23.983 |
| CHST4 | carbohydrate sulfotransferase 4 | Chst4 | 3.539 |
| CHST10 | carbohydrate sulfotransferase 10 | Chst10 | 3.18 |
| CYP2B6 | cytochrome P450 family 2 subfamily B member 6 | Cyp2b10 | -2.566 |
| CYP2C9 | cytochrome P450 family 2 subfamily C member 9 | Cyp2c66 | -7.949 |
| CYP3A5 | cytochrome P450 family 3 subfamily A member 5 | Cyp3a11 | -12.095 |
| CYP4A11 | cytochrome P450 family 4 subfamily A member 11 | Cyp4a10 | -21.224 |
| FABP1 | fatty acid binding protein 1 | Fabp1 | -3.019 |
| FABP2 | fatty acid binding protein 2 | Fabp2 | -2.032 |
| FABP6 | fatty acid binding protein 6 | Fabp6 | -4.583 |
| FMO2 | flavin containing monooxygenase 2 | Fmo2 | -2.23 |
| FMO5 | flavin containing monooxygenase 5 | Fmo5 | -2.792 |
| GAL3ST2 | galactose-3-O-sulfotransferase 2 | Gal3st2 | -2.855 |
| GSTA5 | glutathione S-transferase alpha 5 | Gm10639 | 2.343 |
| GSTP1 | glutathione S-transferase pi 1 | Gstp2 | 2.081 |
| IL33 | interleukin 33 | Il33 | 4.208 |
| IL1RL1 | interleukin 1 receptor like 1 | Il1rl1 | 2.47 |
| IL1RN | interleukin 1 receptor antagonist | Il1rn | 2.977 |
| IL4I1 | interleukin 4 induced 1 | Il4i1 | 2.834 |
| NGFR | nerve growth factor receptor | Ngfr | -2.271 |
| NR0B2 | nuclear receptor subfamily 0 group B member 2 | Nr0b2 | -44.334 |
| PPARA | peroxisome proliferator activated receptor alpha | Ppara | -3.81 |
| SMOX | spermine oxidase | Smox | 2.001 |
| SULT1C2 | sulfotransferase family 1C member 2 | Sult1c2 | -2.988 |
| TNF | tumor necrosis factor | Tnf | 4.137 |
| | | | |
| **FXR/RXR activation** | | | |
| ABCC2 | ATP binding cassette subfamily C member 2 | Abcc2 | -2.237 |
| ABCG5 | ATP binding cassette subfamily G member 5 | Abcg5 | -2.198 |
| ABCG8 | ATP binding cassette subfamily G member 8 | Abcg8 | -2.677 |
| AGT | angiotensinogen | Agt | -2.902 |
| APOA4 | apolipoprotein A4 | Apoa4 | -2.237 |
| BAAT | bile acid-CoA:amino acid N-acyltransferase | Baat | -2.022 |
| CLU | clusterin | Clu | 3.391 |
| FABP6 | fatty acid binding protein 6 | Fabp6 | -4.583 |
| FBP1 | fructose-bisphosphatase 1 | Fbp1 | -3.53 |
| FGF19 | fibroblast growth factor 19 | Fgf15 | -40.903 |
| G6PC | glucose-6-phosphatase catalytic subunit | G6pc | -2.944 |

| | | | |
|---|---|---|---|
| IL33 | interleukin 33 | Il33 | 4.208 |
| IL1RN | interleukin 1 receptor antagonist | Il1rn | 2.977 |
| MLXIPL | MLX interacting protein like | Mlxipl | -2.124 |
| NR0B2 | nuclear receptor subfamily 0 group B member 2 | Nr0b2 | -44.334 |
| PPARA | peroxisome proliferator activated receptor alpha | Ppara | -3.81 |
| RBP4 | retinol binding protein 4 | Rbp4 | 2.111 |
| SAA1 | serum amyloid A1 | Saa1 | 21.654 |
| SERPINA1 | serpin family A member 1 | Serpina1b | 4.477 |
| SLC10A2 | solute carrier family 10 member 2 | Slc10a2 | 2.29 |
| TNF | tumor necrosis factor | Tnf | 4.137 |
| TTR | transthyretin | Ttr | 11.339 |

**LXR/RXR activation**

| | | | |
|---|---|---|---|
| ABCA1 | ATP binding cassette subfamily A member 1 | Abca1 | -3.189 |
| ABCG5 | ATP binding cassette subfamily G member 5 | Abcg5 | -2.198 |
| ABCG8 | ATP binding cassette subfamily G member 8 | Abcg8 | -2.677 |
| AGT | angiotensinogen | Agt | -2.902 |
| APOA4 | apolipoprotein A4 | Apoa4 | -2.237 |
| ARG2 | arginase 2 | Arg2 | -2.303 |
| CD14 | CD14 molecule | Cd14 | 3.364 |
| CLU | clusterin | Clu | 3.391 |
| IL33 | interleukin 33 | Il33 | 4.208 |
| IL1RL1 | interleukin 1 receptor like 1 | Il1rl1 | 2.47 |
| IL1RN | interleukin 1 receptor antagonist | Il1rn | 2.977 |
| LYZ | lysozyme | Lyz2 | 2.477 |
| MLXIPL | MLX interacting protein like | Mlxipl | -2.124 |
| MYLIP | myosin regulatory light chain interacting protein | Mylip | -2.415 |
| NGFR | nerve growth factor receptor | Ngfr | -2.271 |
| NOS2 | nitric oxide synthase 2 | Nos2 | 3.976 |
| RBP4 | retinol binding protein 4 | Rbp4 | 2.111 |
| SAA1 | serum amyloid A1 | Saa1 | 21.654 |
| SERPINA1 | serpin family A member 1 | Serpina1b | 4.477 |
| TNF | tumor necrosis factor | Tnf | 4.137 |
| TTR | transthyretin | Ttr | 11.339 |

**PXR/RXR activation**

| | | | |
|---|---|---|---|
| ABCB1 | ATP binding cassette subfamily B member 1 | Abcb1a | -2.904 |
| ABCC2 | ATP binding cassette subfamily C member 2 | Abcc2 | -2.237 |
| ALDH1A1 | aldehyde dehydrogenase 1 family member A1 | Aldh1a1 | -3.399 |
| Aldh1a7 | aldehyde dehydrogenase family 1. subfamily A7 | Aldh1a7 | -2.73 |
| ALDH3A2 | aldehyde dehydrogenase 3 family member A2 | Aldh3a2 | -2.412 |
| CES- | Carboxylesterase 2A | Ces2a | -7.656 |
| CES- | Carboxylesterase 2B | Ces2b | -9.311 |
| CYP2B6 | cytochrome P450 family 2 subfamily B member 6 | Cyp2b10 | -2.566 |
| CYP2C9 | cytochrome P450 family 2 subfamily C member 9 | Cyp2c66 | -7.949 |
| CYP3A5 | cytochrome P450 family 3 subfamily A member 5 | Cyp3a11 | -12.095 |
| G6PC | glucose-6-phosphatase catalytic subunit | G6pc | -2.944 |
| INSR | insulin receptor | Insr | -2.207 |
| NR0B2 | nuclear receptor subfamily 0 group B member 2 | Nr0b2 | -44.334 |
| PPARA | peroxisome proliferator activated receptor alpha | Ppara | -3.81 |
| TNF | tumor necrosis factor | Tnf | 4.137 |

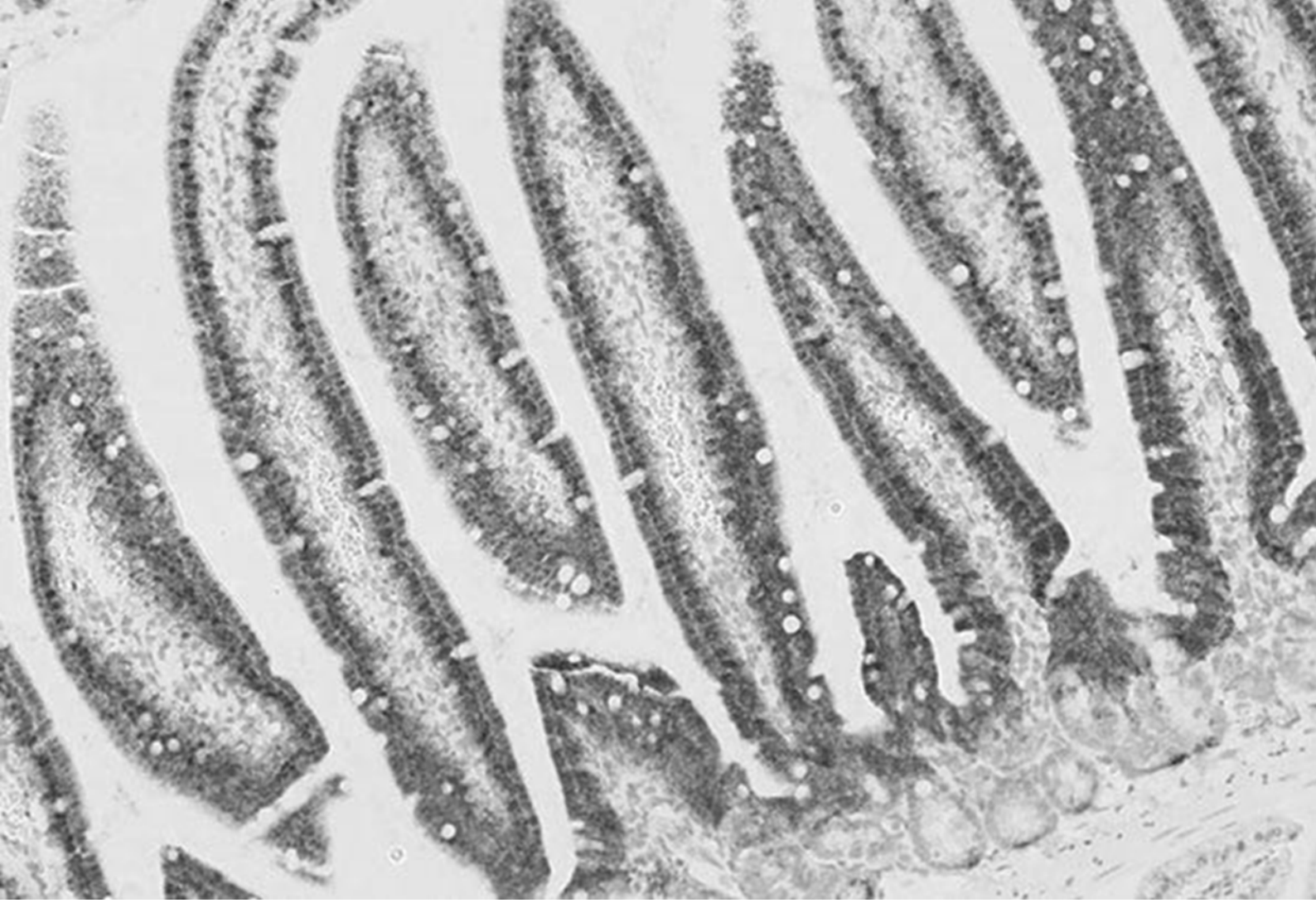

# Chapter 4

# Guanylin and uroguanylin are produced by mouse intestinal epithelial cells of columnar and secretory lineage

**Pauline T. Ikpa [a], Hein F.B.M. Sleddens [b], Kris A. Steinbrecher [c], Maikel P. Peppelenbosch [a], Hugo R. de Jonge [a], Ron Smits [a,1], Marcel J.C. Bijvelds [a,1]**

[a] Department of Gastroenterology and Hepatology,. [b] Department of Pathology, Erasmus MC University Medical Center, PO Box 2040, 3000CA Rotterdam, The Netherlands. [c] Division of Gastroenterology, Hepatology and Nutrition, Cincinnati Children's Hospital Medical Center, Cincinnati, OH 45229, USA [1] Equal contribution

***Histochem Cell Biol, 2016. 146(4): p. 445-55.***

**Abstract**

Guanylin (GN) and uroguanylin (UGN), through activation of guanylyl cyclase C (GCC), serve to control intestinal fluid homeostasis. Both peptides are produced in the intestinal epithelium, but their cellular origin has not been fully charted. Using quantitative PCR and an improved in situ hybridization technique (RNAscope) we have assessed the expression of GN (*Guca2a*), UGN (*Guca2b*), and GCC (*Gucy2c*) in mouse intestine. In the crypts of Lieberkühn, expression of *Guca2a* and *Guca2b* was restricted to cells of secretory lineage, at the crypt's base, and to a region above, previously identified as a common origin of cellular differentiation. In this compartment, comparatively uniform levels of *Guca2a* and *Guca2b* expression were observed throughout the length of the gut. In contrast, *Guca2a* and *Guca2b* expression in the villus/surface region was more variable, and reflected the distinct, but overlapping expression pattern observed previously. Accordingly, in jejunum and ileum, *Guca2a* and *Guca2b* were abundantly expressed by enterocytes, whereas in colon only *Guca2a* transcript was found in the surface region. In duodenum, only low levels of *Guca2b* transcript were observed in columnar cells, and *Guca2a* expression was restricted entirely to cells of the secretory lineage. *Gucy2c* was shown to be expressed relatively uniformly along the rostrocaudal and crypt-villus axes, and was also found in the duodenal glands. Our study reveals novel aspects of the cellular localization of the GCC signaling axis that, apart from its role in the regulation of fluid balance, link it to pH regulation, cell cycle control, and host defense.

Key terms: cyclic guanosine monophosphate, enteroendocrine cells, guanylyl cyclase C, intestinal fluid transport

## Introduction

Signal transduction through the receptor-enzyme guanylyl cyclase C (GCC) serves to control intestinal fluid balance. Activation of the luminal, extracellular receptor domain by one of two locally produced peptides, guanylin (GN) and uroguanylin (UGN), leads to a surge in cellular cGMP levels, which prompts osmotic water transport to the intestinal lumen by protein kinase-mediated stimulation of anion secretion through the cystic fibrosis transmembrane conductance regulator (CFTR) anion channel and inhibition of sodium absorption through the sodium-proton exchanger type 3 (NHE3) [1]. This pivotal role of GCC signaling in intestinal fluid balance is most poignantly illustrated by gain- and loss-of-function mutations in *GUCY2C* (encoding GCC), which have been shown to cause secretory diarrhea and intestinal obstruction, respectively [2-4]. Furthermore, GCC is activated by the (U)GN mimetic heat-stable toxin (STa) produced by enterotoxigenic *Escherichia coli*, a frequent cause of infectious diarrhea.

Apart from its role in the regulation of fluid homeostasis, GCC signaling may also regulate luminal pH. GCC stimulation strongly enhances duodenal bicarbonate secretion, and some data suggest that luminal acid may stimulate UGN release from duodenal enteroendocrine cells [5-10]. Evidently, in proximal intestine, such a feedback loop may aid the neutralization of the acid load entering from the stomach. In addition, it has become apparent that local bicarbonate production is crucial for the proper expansion of the mucins produced by goblet cells, and, consequently, the physiochemical properties of the mucus layer covering the epithelium along the entire tract [11, 12]. Possibly connected to its effect on mucin unfolding and fluid transport, loss of GCC signaling was shown to impair epithelial barrier function, and innate host responses to bacterial pathogens [13, 14].

Lastly, GCC signaling may modulate the cell cycle in small intestinal and colonic epithelium. Mice deficient in either GN, GCC, or the cGMP-dependent protein kinase operating downstream of GCC (PRKG2), exhibit enhanced cell proliferation in the crypts, and a reduction in the amount of cells of the secretory lineage [15-17]. It has also been suggested that loss of GCC signaling predisposes to tumor development [18].

The convergence of such apparently disparate physiological processes at the level of GCC suggests a strict compartmentalization of signaling routes. In this context, it is of interest that various distinct cell types within the intestinal epithelium have been proposed to produce GN and UGN. Mostly, these studies indicate production by cells from the secretory (granulocytic) lineage. In human small intestine, GN transcript was localized to the Paneth cells, whereas in the rat, GN transcript and protein was detected in goblet cells, and UGN transcript

was found in enterochromaffin (EC) cells [19-22]. In rat colon, GN was expressed by goblet cells, but also by the columnar cells of the surface epithelium, whereas in guinea pig, GN immunoreactivity was restricted to EC cells [20, 23, 24]. Finally, in mouse intestine, UGN transcript was localized exclusively to the villus, whereas GN transcript was found in both the villi and crypts of the small intestine, and in the surface epithelium of colon [25]. These disparate results may signify marked differences in the localization, and, perhaps, the physiological role, of GN and UGN between species, and different anatomical regions. In addition, they may reflect the technical limitations of classical in situ hybridization and immunological methods.

Our study aimed to ascertain the expression pattern of GN, UGN, and GCC, using quantitative PCR and an improved in situ hybridization technique, which drastically improves sensitivity. While our study, in the main, corroborates previously reported patterns of GN, UGN, and GCC partitioning along the rostrocaudal axis of the intestine, these technical advances have allowed us to chart these patterns in more detail, revealing previously unappreciated differences in the expression pattern of duodenum versus jejunum, and the cell lineages involved in the production of GN, UGN, and GCC.

## Materials and methods

### Animals

Mice (FVB) were maintained in an environmentally controlled facility at the Erasmus MC, Rotterdam. All experiments were performed on animals, 8-16 weeks of age, and were approved of by the Ethical Committee for Animal Experiments of the Erasmus MC.

### Tissue collection

Mice were anaesthetized (ketamine 100 mg/kg, xylazine 20 mg/kg; i.p.), and the intestinal tract was collected and flushed with ice-cold saline. All tissue was harvested between 12:00-14:00h, to control for diurnal variations in gene expression.

For assessing the partitioning of transcript along the rostrocaudal axis of the intestinal tract, 6 equidistant segments (length: 0.5 cm) of small intestine, and 2 segments of the colon were excised. The small intestine was sampled, starting 1 cm caudal to the pyloric sphincter, and up to 1 cm proximal to the ileocecal valve. Colon was sampled at 1/3 and 2/3 of its entire length. Tissue was flash frozen in liquid nitrogen and stored at -80°C.

For RNAscope analysis, and lectin UEA1 (*Ulex europeaus* agglutinin 1) staining (see below), the excised intestine was flushed with ice-cold saline, cut open lengthwise, rolled into a

Swiss-roll, and immersed in PBS-buffered formalin (10%) for 24h at 4°C. After fixation, tissue was embedded in paraffin, according to established protocols.

**Quantitative Polymerase Chain Reaction (qPCR):**

Tissue was homogenized with a rotor-stator homogenizer in Trizol reagent (Qiagen), and total RNA was extracted using the Nucleospin RNA kit (Macherey-Nagel). After the integrity of the extracted RNA was verified by gel electrophoresis, cDNA was synthesized using the PrimeScript RT master mix (Takara Bio).

Quantitative PCR (primer sequences shown in Table S1) was performed on cDNA, using the SYBR Select master mix (Applied Bio System). Median values from assays performed in triplicate were used to determine the expression levels of *Guca2a*, *Guca2b* and *Gucy2c*, relative to *Gapdh*.

***In situ* hybridization by RNAscope**

Probes for detection of murine GN, UGN and GCC transcript were purchased from Advanced Cell Diagnostics (product code: 427996, 428006, and 436596, respectively). Because, other than in conventional in situ hybridization, multiple independent probes have to hybridize to the target sequence in tandem in order for signal amplification to occur, RNAscope ensures selective amplification of target-specific signals [26]. RNAscope was performed according to the instructions of the manufacturer of the probes and the reagent kit (VS Reagent Kit 320600; Advanced Cell Diagnostics), on proteinase K (0.1%, 5 min at 37°C) treated paraffin sections (5 µm). Detection of the ubiquitously expressed gene *Ppib* (peptidylprolyl isomerase B) served to ensure that tissue sections were correctly primed for probe hybridization (Advanced Cell Diagnostics, product code: 313919).

**Histochemical detection of lysozyme and fucose-glycoprotein**

For detection of fucose-glycoprotein producing cells, sections used for RNAscope were re-hydrated in PBS, treated with a biotin blocking reagent (Dako), and incubated (1 h, at room temparature) with biotinylated lectin UEA1 (Vector Labs). Lectin UEA1 labeled carbohydrate moieties were visualized with a streptavidin-conjugated fluorescent probe (Alexa Fluor 594; Life Technologies). In negative controls, incubation with lectin UEA1 was omitted. Slides were mounted with Prolong Gold Antifade reagent (Life Technologies), and stored at 4°C.

## Results

### *Partitioning of Guca2a, Guca2b, and Gucy2c transcript along the rostrocaudal axis of the mouse intestinal tract*

Quantitative PCR analysis showed that *Guca2a* transcript levels gradually increased along the rostrocaudal axis of the small intestine, and peaked in the proximal colon (Fig. 1a). In contrast, *Guca2b* transcript levels were low in colon. *Guca2b* levels were also low in the duodenum, but rose steeply along the rostrocaudal axis, and peaked in the middle to distal part of the small intestine (Fig. 1b). *Gucy2c* was expressed at much lower (>10-fold) levels than *Guca2a* or *Guca2b*, and was partitioned more uniformly (Fig. 1c). Distribution of these transcripts was similar in male and female mice (not shown).

The RNAscope technique was used to visualize *Guca2a*, *Guca2b* and *Gucy2c* transcripts in longitudinal sections of mouse intestine. This methodology employs up to 20 pairs of oligonucleotide probes per transcript, of which the paired probes need to hybridize in close proximity in order for signal amplification to occur. As a consequence, this technique provides a strongly improved signal to noise ratio compared with conventional in situ hybridization techniques [26]. The distribution pattern that emerged for these transcripts closely matched the expression profile assessed by qPCR analysis, i.e. the gradual increase of *Guca2a* and *Guca2b* expression from duodenum to the distal small intestine, the high expression of *Guca2a*, but low expression of *Guca2b*, in colon, and the comparatively low expression of *Gucy2c* (Fig. 2).

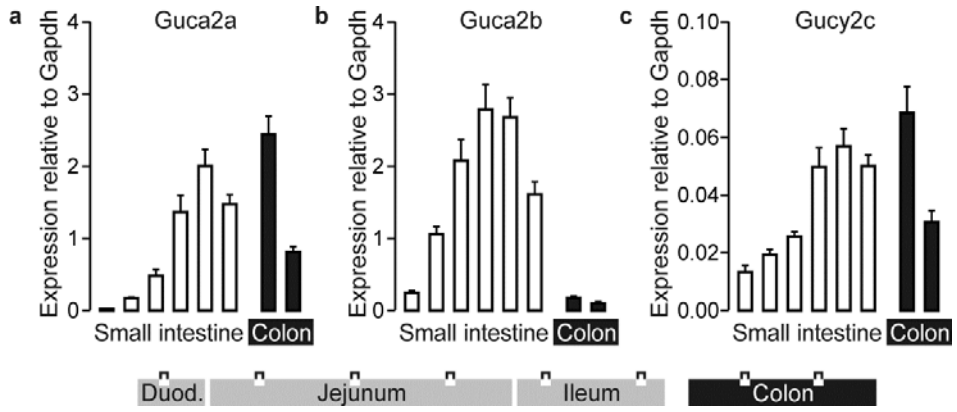


***Figure 1*** *Partitioning of Guca2a (a), Guca2b (b), and Gucy2c (c) transcript along the rostrocaudal axis of the mouse intestinal tract. Transcript levels in 6 equidistant sections of small intestine, and 2 sections of colon (see diagram) were assessed by qPCR, using expression of Gapdh as a reference. Data depict means ± standard error. N=6*

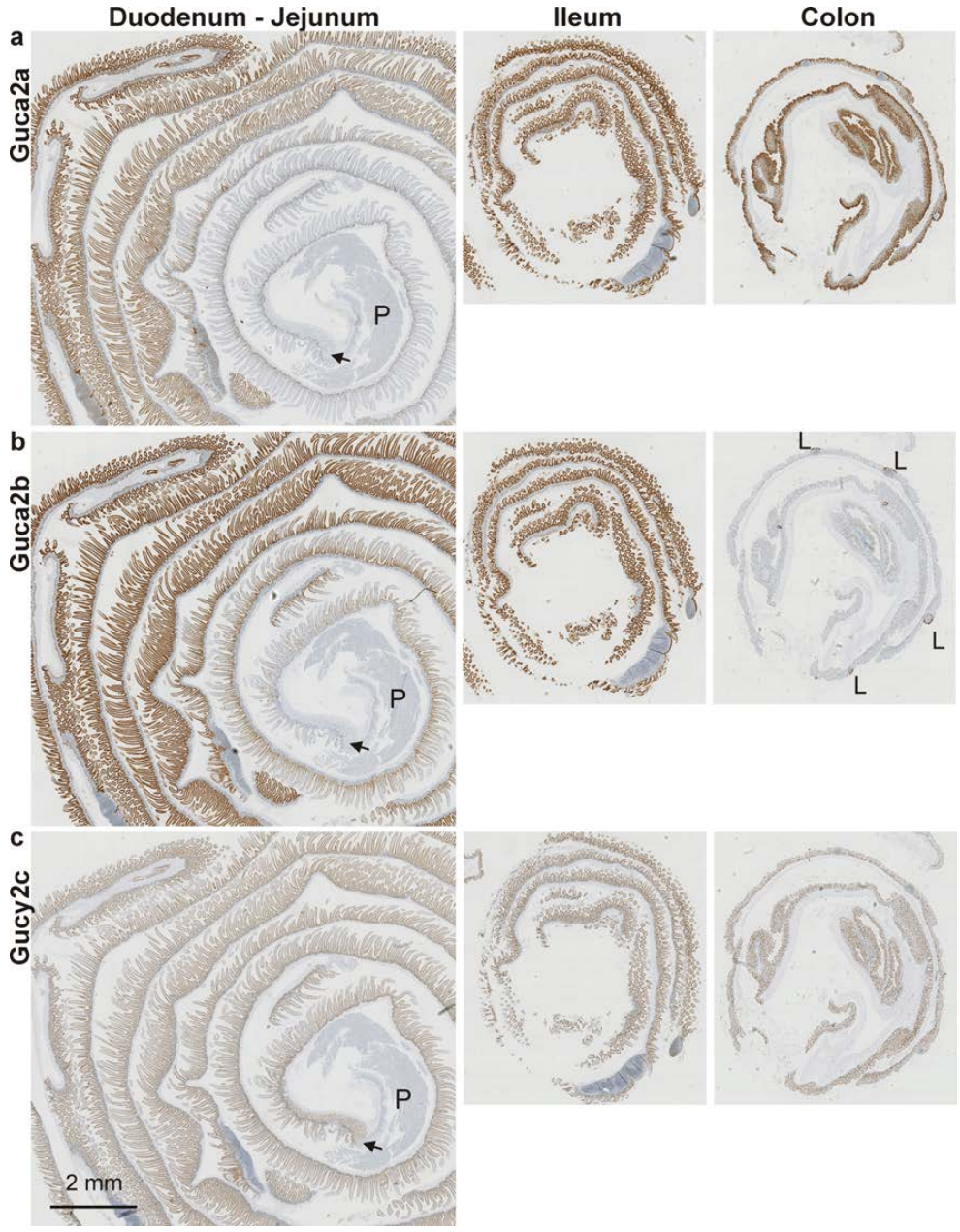


***Figure 2*** *Partitioning of Guca2a (a), Guca2b (b), and Gucy2c (c) transcript in intestinal mucosa. Intestinal tissue was paraffin-embedded in a "Swiss roll" configuration and was probed by RNAscope. The arrow indicates the transition from gastric to duodenal epithelium. P: pancreatic tissue. L: Lymphoid tissue*

This agreement strongly suggests specific hybridization of the probes. In addition, probe hybridization was restricted to intestinal epithelial cells, i.e. absent from underlying connective and muscle tissue, consistent with the discrete epithelial expression pattern of these genes. Our data also corroborate the previously observed high levels of focal *Guca2b* expression in regions of the colonic epithelium that border on lymphoid tissue (Fig. 2b colon section, Fig. 4j) [25].

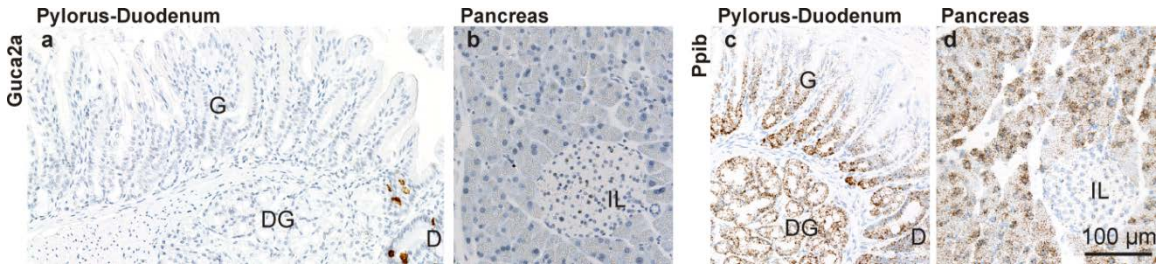


***Figure 3*** *Partitioning of Guca2a and Ppib transcript in the pyloric-duodenal region and in pancreas. a,b: Guca2a expression was found in the duodenum (D), in cells at the base of the crypts of Lieberkühn, but was not detected in the gastric (G) or the duodenal glands (DG), or in the pancreas. c,d: Detection of Ppib transcript in glandular epithelia in the pyloric-duodenal region and pancreas. IL: Islet of Langerhans*

Specificity of the *Guca2a* probes was further corroborated by RNAscope performed on intestinal tissue of *Guca2a* null mice, in which only sparse punctuate staining was found in the nuclei (indicating weak hybridization with DNA), and the cytoplasmic region (indicating weak hybridization with truncated *Guca2a* transcripts; Fig. S1).

The observed rostrocaudal distribution patterns of GN, UGN and GCC are congruent with those previously reported for rat intestine [27], but differ somewhat from those reported in a previous mouse study, in which the levels of *Guca2b* expression in duodenum and jejunum were shown to be similar [25]. However, in this previous study, tissue from the proximal 3 cm of the mouse small intestine was pooled to assess duodenal expression, whereas we used a section between 1 and 1.5 cm distal to the pylorus. As is apparent from the RNAscope data (Fig. 2b), the expression level of *Guca2b* steeply increases within the first few centimeters of the small intestine, indicating that these apparent differences may be due largely to the different sampling strategies. Furthermore, it is conceivable that these differences reflect the effect of an unidentified environmental factor (i.e. diurnal rhythm, food intake and composition, etc.) on duodenal *Guca2b* expression.

We did not detect *Guca2a* transcript in gastric or in pancreatic epithelia (Fig. 2a, 3), nor did we detect expression of *Guca2b* or *Gucy2c* in these tissues (Fig. 2b,c). This contrasts with previous observations on guinea pig, in which GN immunoreactivity was observed in pyloric EC cells [23], and with observations on human and rat pancreatic tissue, in which GN, UGN, and GCC transcript and protein were detected [28, 29]. RT-PCR analysis confirmed that, compared to the gut, these glandular tissues contain only very low levels of these three transcripts (not shown). Such transcripts of low abundance may not be detectable by in situ hybridization, particularly in the pancreas, which contains high levels of ribonucleases [30]. However, arguing against significant mRNA loss prior to tissue fixation, we could readily detect *Ppib* transcript, in

both the stomach and the pancreas (Fig. 3c,d). Therefore, we tentatively conclude that expression of the GCC signaling axis is low in mouse-, compared to human pancreas. Interestingly, this apparent difference in the pancreatic expression of the GCC signaling axis between these species mirrors a previously observed disparity in the regulation of ductal anion and fluid secretion: whereas in the human pancreas the GCC signaling axis is thought to control the activity of the phosphorylation-regulated CFTR anion channel, anion and fluid secretion in the murine exocrine pancreas is principally governed by $Ca^{2+}$-dependent anion channels, which operate independently of the GCC pathway [28, 31].

***Partitioning of Guca2a and Guca2b transcript along the crypt-villus and crypt-surface axis of the mouse small intestine and colon, respectively***

Along the entire length of the small intestine, high *Guca2a* transcript levels were found in cell clusters at the base of the crypts, and in solitary cells that line the lateral sides of the crypts (Fig. 4a-d). In the proximal small intestine, expression in the villus region was restricted to a distinct, sparsely distributed cell type (Fig. 4a). Very little expression was found in columnar, absorptive villus cells (enterocytes). However, in the proximal jejunum, expression of *Guca2a* in the villus became more prominent, and was found in most columnar cells. *Guca2a* expression in the villus region further increased along the rostrocaudal axis, and distal jejunum and ileum showed abundant *Guca2a* expression in enterocytes (Fig. 4b,c). In colon, *Guca2a* transcript was found along the entire crypt-surface axis, but appeared to be most abundantly expressed by cells lining the lateral sides of the crypts, and the surface. Strong expression was also found in cell clusters at the base of the crypts (Fig. 4d). *Guca2a* was also strongly expressed by the follicle-associated epithelium overlying lymphoid aggregates, in both small and large intestine (Fig. 4e).

Like for *Guca2a*, *Guca2b* transcript was found in cells at the base and the lateral sides of the crypts, along the length of the small intestine (Fig. 4f-h). However, the level of cellular expression, and the amount of cells that expressed *Guca2b* in the crypts, appeared somewhat lower than for *Guca2a*. In the duodenum, *Guca2b* expression started to emerge at the base of the villi, and involved the entire height of the villus in more distal sections of the small intestine (Fig. 4f-h). In colon, *Guca2b* expression was restricted to individual cells, or small clusters of cells, in the crypts (Fig. 4i). Although small in number, the level of expression per single cell was relatively high, and comparable to the level in *Guca2b* expressing cells in the crypts of the small intestine. As for *Guca2a*, we observed strong *Guca2b* expression in the follicle-associated epithelium overlying lymphoid tissue, in both small and large intestine (Fig. 2b colon section, Fig. 4j).

***Partitioning of Gucy2c transcript along the crypt-villus and crypt-surface axis of the mouse small intestine and colon, respectively***

Gucy2c was expressed relatively uniformly, in both the crypt and villus region of the epithelium (Fig. 4k-n). As for *Guca2a* and *Guca2b*, *Gucy2c* probe hybridization was restricted to intestinal epithelial cells. Expression in these cells was relatively uniform; only at the tip of the villi, expression seemed to wane slightly (similar was observed for *Guca2a* and *Guca2b*). No specific subset of cells was shown to be enriched in (or depleted of) *Gucy2c* transcript.

Further, we found *Gucy2c* transcripts in the duodenal glands (Fig. 4o). Previously, by autoradiographic demonstration of STa specific binding sites in the intestinal mucosa, the presence of GCC in the duodenal glands of the North American opossum had been inferred [32]. However, similar studies performed on human duodenal mucosa failed to demonstrate specific STa binding [33]. Remarkably, the duodenal glands did not contain *Guca2a* or *Guca2b* transcript, indicating that local GCC activation relies on GN or UGN produced elsewhere.

***Localization of Guca2a and Guca2b in cells of secretory lineage***

In the small intestine, the *Guca2a* and *Guca2b* expressing cells at the base of the crypt were found to contain secretory granules and (in part) co-localized with Paneth cells (Fig. 5a,f). In contrast, *Guca2a* or *Guca2b* expression was not observed in the adjacent stem cells. A previous in situ hybridization study suggested that apparent *Guca2b* localization at the base of the crypts was a result of autofluorescence of the Paneth cells [25], but since RNAscope uses an enzymatic detection method this cannot have confounded our observations. Moreover our detection of *Guca2a* and *Guca2b* in Paneth cells is consistent with studies using a fluorescence-activated cell sorting technique to isolate specific epithelial cell lineages [34, 35]. This showed that *Guca2a* and *Guca2b* rank in the 90$^{th}$ percentile of most highly expressed genes in murine Paneth cells, and that Paneth cells are highly enriched in these transcripts, relative to stem cells (NCBI GEO datasets GSE5156 and GSE25109). In addition, these datasets reveal that *Gucy2c* is expressed at near equal levels in Paneth and stem cells, congruent with the relatively uniform distribution of *Gucy2c* transcript in crypt epithelium (Fig. 4k-n).

*Guca2a* and *Guca2b* transcript were also found in cells at the base of the crypts in colon (Fig. 5b,g). These cells appear to occupy the same niche as the Paneth cells of the small intestine, suggesting they represent the cKit-positive Paneth-like cells identified previously [36]. In earlier studies, only *Guca2a* transcript had been detected in this compartment, possibly because the low sensitivity of conventional in situ hybridization techniques precluded detection of the less abundant *Guca2b* transcripts [25].

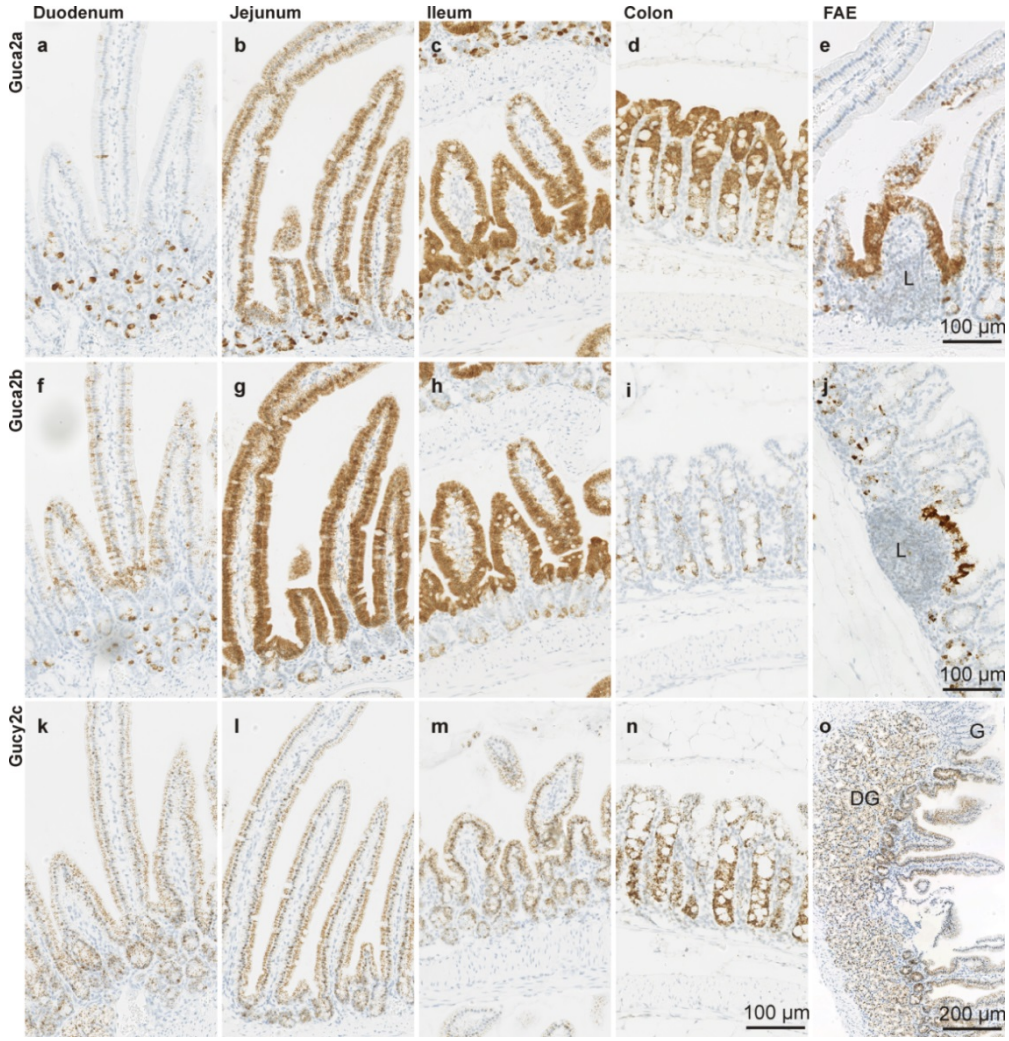


***Figure 4*** *Localization of Guca2a (a-d), Guca2b (f-i), and Gucy2c (k-n) transcript in intestinal epithelium. e: Guca2a expression in follicle-associated epithelium in proximal jejunum. j: Guca2b expression in follicle-associated epithelium in colon. o: Gucy2c expression in the region of transition from the gastric (G) to duodenal mucosa, with duodenal glands (DG) below. L: Lymphoid tissue*

Lectin UEA1 staining confirmed that the cells at the base of the crypts, and other *Guca2a*- and *Guca2b*-positive cells in the crypts and villus region of duodenum were of secretory lineage (Fig. 5e). Based on their numbers, localization, and typical shape, these *Guca2a* and *Guca2b* expressing cells in the villus appear to include brush (tuft) cells (Fig. 5c,h). Previously, a murine duodenal enteroendocrine cell type secreting β-endorphin in response to acidic or hyperosmotic stimulation was identified [7]. Interestingly, this cell type also contained UGN (but, based on immunological detection methods, not GN). In rat, apart from goblet cells, some enteroendocrine cell types also seemed to contain immunoreactive GN, although the specificity of the signal was questioned by the authors [24]. Collectively, these data strongly

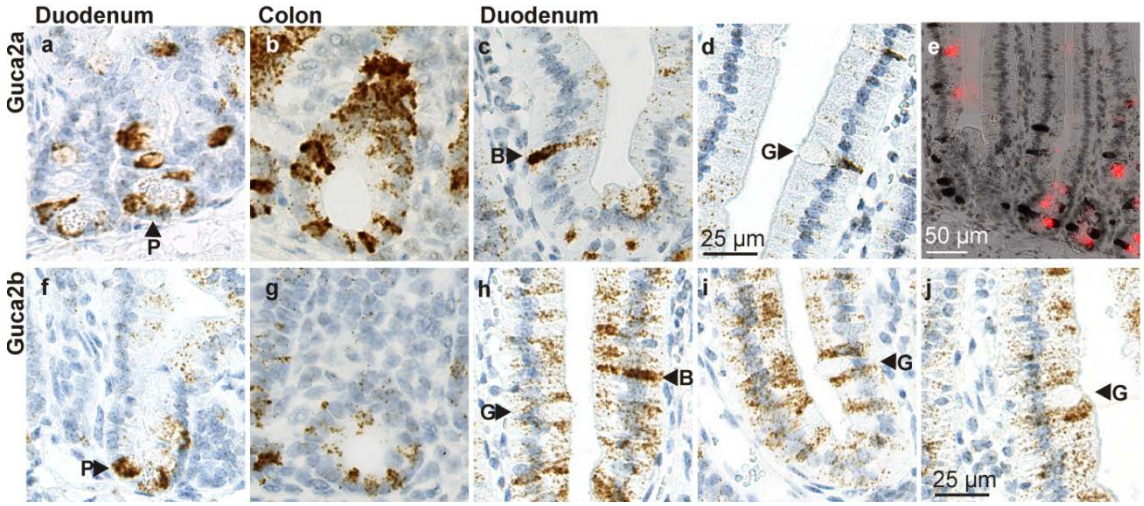


***Figure 5*** *Guca2a and Guca2b expression by cells of the secretory lineage in the duodenum and colon. a: Guca2a expression in Paneth cells in duodenum. b: Guca2a expression in cells at the base and the neck region of the crypts in colon. c: Guca2a expression in a duodenal brush cell. d: Guca2a expression in a duodenal goblet cell. e: Co-staining of Guca2a transcript (dark brown) and lectin UEA1-binding fucose-glycoproteins (bright red) in duodenum. f: Guca2b expression in Paneth cells in duodenum. g: Guca2b expression in cells at the base of the crypts in colon. h: Guca2b expression in a duodenal brush cell. No Guca2b transcript was observed in goblet cells. i,j: Guca2b levels were generally low in columnar cells, but comparatively high in columnar cells adjoining goblet cells. B: brush cell; G: goblet cell P: Paneth cell*

suggest that distinct brush cell populations co-exist in the murine duodenal epithelium, expressing *Guca2a* or *Guca2b*.

In addition, *Guca2a* expression was found in a subset of goblet cells in the lower villus (Fig. 5d). This suggests that GN may be released concurrently with the mucin containing granules produced by goblet cells. No *Guca2b* was found in goblet cells, but in the duodenum, where *Guca2b* expression is generally low, columnar cells that adjoined goblet cells seemed to have relatively (compared to more remote columnar cells) high *Guca2b* expression, suggesting that UGN release from these cells may play a role in goblet cell function (Fig. 5h-j). These findings are in line with studies on rat, which detected GN, but not UGN, in a subset of goblet cells of the rat small intestine and colon [20, 24].

**Discussion**

An improved in situ hybridization technique (RNAscope) has allowed us to reveal novel aspects of the localization of the GCC signaling axis in the murine intestinal tract. We demonstrate strong expression of *Guca2a* and *Guca2b* transcript in cells of secretory lineage, in

particular Paneth cells located at the base of the crypts and chemosensory brush cells in the lower villus. Strikingly, the general pattern of *Guca2a* and *Guca2b* expression in this lineage is relatively uniform along the entire intestine: even in the proximal part, which was thought to produce little GN, we observed prominent *Guca2a* expression in Paneth and brush cells, whereas in colon, which was thought to produce little UGN, robust *Guca2b* expression was found in Paneth-like cells at the base of the crypts.

In contrast to this relatively stable expression pattern in the crypts, expression in the villus/surface compartment showed more variation between anatomical regions, as expression of *Guca2a* and *Guca2b* extends to cells from the columnar (absorptive) lineage. It is chiefly the expression in this compartment that reiterates the previously reported pattern of GN and UGN distribution. i.e. a predominance of UGN in the proximal gut, and of GN in the colon [25, 27]. As has been noted before, this pattern is consistent with the observation that GN is a relatively (in comparison to UGN) poor GCC ligand at the low pH prevailing in the proximal small intestine [25]. Nevertheless, prominent expression of *Guca2a* is found in the crypts of the proximal small intestine, suggesting that the pH in this area may be maintained at more neutral values (aided by local bicarbonate secretion).

Along the length of the small intestine, *Guca2a* and *Guca2b* transcripts were found in Paneth cells, or, in case of the colon, in cells which appear to occupy the same position as these. *Guca2a* expression appeared more pronounced than *Guca2b*, but the localization pattern was similar. Previous in situ hybridization studies showed a similar distribution of *Guca2a* at the base of the crypts in jejunum and ileum of mice, although the exact cell types involved could not be ascertained [25]. *Guca2a* and *Guca2b* expression by murine Paneth cells was also indicated in studies that employed cell sorting techniques to isolate epithelial cells representing different lineages [34, 35]. Furthermore, GN transcript was localized to human Paneth cells [19].

It has been suggested that GN-stimulated fluid secretion emanating from the lower crypt may have a cleansing effect that supports the action of the bactericidal products of the Paneth cells [19]. In further support of innate immunity, GN and/or UGN release from Paneth cells may trigger bicarbonate secretion from neighboring CFTR-containing columnar cells, facilitating expansion of condensed mucins, and, consequently, the formation of the protective mucus layer covering the epithelium [11, 12]. In accordance with this notion, it has been shown that GCC signaling reduces susceptibility to infection by attaching/effacing bacterial pathogens [13]. GN stored in goblet cells (and UGN in adjoining columnar cells) may serve a similar role. When released together with the mucin granules, a synchronized activation of GCC-dependent bicarbonate secretion from adjacent enterocytes (as goblet cells seem to contain little CFTR)

may aid the proper expansion of the secreted condensed mucin granules. Consistent with this hypothesis, exocytosis from goblet cells is under cholinergic control, and it has been shown that cholinergic input also stimulates GN release in rat colon [37, 38].

Apart from producing antibacterial products, Paneth cells also produce various factors that modulate stem cell function. It is conceivable that GN and UGN may also contribute to this modulation. In mice, it has been shown that GN, PRKG2, or GCC deficiency leads to enhanced crypt cell proliferation, and that GCC deficiency reduces goblet and Paneth cell numbers in mouse small intestine, whereas PRKG2 deficiency reduces goblet cell numbers in colon [15-17]. These results suggest that GCC signaling directs differentiation to a secretory lineage. Indeed, PRKG2 has been shown to control the activity of the transcription factor Sox9, which is a key determinant of Paneth cell formation [39-41]. Because of their close contact to stem cells and their progenitors, the Paneth cells are a likely source of the ligands that control GCC activity in this niche. Consistent with this model, both our present data and previous studies (NCBI GEO datasets GSE5156 and GSE25109) indicate that *Gucy2c* expression in the crypts extends to the stem cells, whereas Guca2a and Guca2b expression is restricted to cells of the secretory lineage [34, 35].

In duodenum, prominent expression of *Guca2a* and *Guca2b* in the villi is mostly confined to just the few cells of secretory lineage. Apart from Paneth and goblet cells, this includes brush cells. UGN, but not GN, has previously been localized to murine brush cells [7]. Brush cells are known to monitor the composition of the lumen, and it was shown that this particular subset of UGN-containing duodenal brush cells secretes β-endorphin into the lumen upon acidic or hypertonic stimulation [7, 42]. We propose that the UGN stored in this cell type may also be released upon exposure to these luminal stimuli. In support, an increase in bicarbonate secretion was observed in mouse duodenum upon lowering of the luminal pH, which may be attributed to endogenous (U)GN release, as GN and UGN are known to strongly stimulate duodenal bicarbonate secretion [5, 8, 10]. This assumption is also consistent with the observation that (I) luminal hypertonicity stimulates the release of GN and UGN, and inhibits NHE3-mediated sodium absorption [43, 44], and (II) enteral salt loading may induce intra-arterial UGN release from the intestinal mucosa (to stimulate renal natriuresis) [45]. Collectively, these data suggest that GN and UGN are released from distinct subsets of brush cells upon acidic or hypertonic stimulation, and that their release serves to regulate luminal pH and osmolarity.

We observed expression of *Gucy2c*, but not of *Guca2a* or *Guca2b*, in the duodenal glands. This GCC pool may be targeted by GN and/or UGN released into the duodenal lumen

(although diffusion of peptides into the glands is likely to be opposed by secretory fluid movement), and/or by systemic GN and UGN. In support of the latter option, intra-arterial GN or UGN has been shown to trigger duodenal bicarbonate secretion [6]. Indeed, systemic UGN has been shown to elicit additional GCC-dependent effects, notably in neuro-endocrine tissues [46, 47]. In further support of such actions in the gut, it was shown that, contra-luminal administration of STa to duodenal enteroids provoked GCC-mediated inhibition of $Na^+$,$H^+$ antiport activity, strongly suggesting that such oligopeptides are translocated across the epithelium, although the presence of GCC at the basolateral aspect of polarized intestinal epithelial cells cannot be excluded completely [48].

Distal from the duodenum, prominent *Guca2a* and *Guca2b* expression is found in the columnar (absorptive) cells of the villus. Strong expression of *Guca2a* and *Guca2b* in the villus has been observed before in mice, but not in rat or guinea pig [16, 17, 19, 21, 23]. Thus, the increase in total expression of *Guca2a* and *Guca2b* distal from the duodenum can be mainly attributed to expression initiated in enterocytes. This expression pattern is similar to that of the transcription factor *Cdx2*, suggesting that this, or other intestine-specific transcription factors, control *Guca2a* and *Guca2b* expression in enterocytes [49]. GN and/or UGN released in this region is unlikely to enter the crypts, which contain most of the CFTR-mediated anion-secretory capacity, and a function in the villus compartment seems indicated. Apart from activating a sub-pool of CFTR, GN and UGN may limit sodium absorption through NHE3, which is highly expressed in mature enterocytes and is inhibited through cGMP-dependent protein phosphorylation [48]. Assuming that peptides released at the surface of the villi would diffuse more rapidly into the bulk luminal content than those secreted in the crypts, local GCC activity and ion transport may simply be controlled by the level to which its ligands are diluted upon their release; GCC stimulation would peak at a low level of hydration, when a high concentration of its ligands is maintained at the epithelial surface. This may constitute a relatively straightforward mechanism to maintain fluid homeostasis, which does not so much rely on a stimulus-controlled release of GN and UGN, but on a continual secretion from columnar cells in the villus. It is of interest that the combined *Guca2a* and *Guca2b* expression in this compartment is particularly high in the distal small intestine, a region which appears especially prone to dehydration and obstruction caused by GCC deficiency [2].

In the colon, strong *Guca2a* expression was found in cells positioned at the lateral sides of the crypts. At the base of the crypts, expression was markedly lower, and confined to a Paneth-like cell type [36]. The distal colon in particular contains high numbers of goblet cells, and these also appeared to express *Guca2a*. As in the small intestine, GN release from goblet

cells may play a role in mucin expansion. *Guca2b* expression was low in colon, but was retained in solitary cells in the crypts. Strikingly, high *Guca2a* and *Guca2b* expression was found in those parts of the epithelium that were in contact with lymphoid tissue. This particular expression pattern has been observed before for *Guca2b* in the ileocecal region of mice [25]. Because the follicle-associated epithelium also shows strong expression of genes encoding specific ion channels, i.e. *Cftr*, *Clca2, Kcnj15* and *Kcna1* [50], and we also found weak expression of *Gucy2c* in this region, it is conceivable that GN and UGN regulate ion transport across the follicle-associated epithelium through autocrine signaling.

In summary, the present study charts *Guca2a*, *Guca2b*, and *Gucy2c* expression along the entire murine intestinal tract. Whereas *Gucy2c* expression is relatively uniform along the rostrocaudal and crypt-villus axes, strong regional differences exist in the expression of its ligands. These differences mostly reflect varying levels of expression in the upper regions of the epithelium. *Gucy2c* expression was found in the duodenal glands, suggesting it serves a role in UGN/GN-dependent duodenal bicarbonate secretion. Further, we show distinct expression of *Guca2a* and *Guca2b* in Paneth cells and brush cells, suggesting that GN and UGN play a role in chemoreception, stem cell proliferation, and host defense.

## References

[1] Vaandrager AB. Structure and function of the heat-stable enterotoxin receptor/guanylyl cyclase C. Mol Cell Biochem. 2002;230:73-83.
[2] Romi H, Cohen I, Landau D, Alkrinawi S, Yerushalmi B, Hershkovitz R, et al. Meconium ileus caused by mutations in GUCY2C, encoding the CFTR-activating guanylate cyclase 2C. Am J Hum Genet. 2012;90:893-9.
[3] Fiskerstrand T, Arshad N, Haukanes BI, Tronstad RR, Pham KD, Johansson S, et al. Familial diarrhea syndrome caused by an activating GUCY2C mutation. N Engl J Med. 2012;366:1586-95.
[4] Muller T, Rasool I, Heinz-Erian P, Mildenberger E, Hulstrunk C, Muller A, et al. Congenital secretory diarrhoea caused by activating germline mutations in GUCY2C. Gut. 2015.
[5] Guba M, Kuhn M, Forssmann WG, Classen M, Gregor M, Seidler U. Guanylin strongly stimulates rat duodenal $HCO_3^-$ secretion: proposed mechanism and comparison with other secretagogues. Gastroenterology. 1996;111:1558-68.
[6] Bengtsson MW, Jedstedt G, Flemstrom G. Duodenal bicarbonate secretion in rats: stimulation by intra-arterial and luminal guanylin and uroguanylin. Acta Physiol (Oxf). 2007;191:309-17.
[7] Kokrashvili Z, Rodriguez D, Yevshayeva V, Zhou H, Margolskee RF, Mosinger B. Release of endogenous opioids from duodenal enteroendocrine cells requires Trpm5. Gastroenterology. 2009;137:598-606.
[8] Joo NS, London RM, Kim HD, Forte LR, Clarke LL. Regulation of intestinal $Cl^-$ and $HCO_3^-$ secretion by uroguanylin. Am J Physiol. 1998;274:G633-G44.
[9] Rao SP, Sellers Z, Crombie DL, Hogan DL, Mann EA, Childs D, et al. A role for guanylate cyclase C (GC-C) in acid-stimulated duodenal mucosal bicarbonate secretion. Am J Physiol. 2004;286:G95-G101.
[10] Singh AK, Sjoblom M, Zheng W, Krabbenhoft A, Riederer B, Rausch B, et al. CFTR and its key role in in vivo resting and luminal acid-induced duodenal $HCO_3^-$ secretion. Acta Physiol (Oxf). 2008.
[11] Garcia MA, Yang N, Quinton PM. Normal mouse intestinal mucus release requires cystic fibrosis transmembrane regulator-dependent bicarbonate secretion. J Clin Invest. 2009;119:2613-22.
[12] Gustafsson JK, Ermund A, Ambort D, Johansson ME, Nilsson HE, Thorell K, et al. Bicarbonate and functional CFTR channel are required for proper mucin secretion and link cystic fibrosis with its mucus phenotype. J Exp Med. 2012;209:1263-72.
[13] Mann EA, Harmel-Laws E, Cohen MB, Steinbrecher KA. Guanylate cyclase C limits systemic dissemination of a murine enteric pathogen. BMC Gastroenterol. 2013;13:135.
[14] Han X, Mann E, Gilbert S, Guan Y, Steinbrecher KA, Montrose MH, et al. Loss of guanylyl cyclase C (GCC) signaling leads to dysfunctional intestinal barrier. PLoS One. 2011;6:e16139.
[15] Li P, Lin JE, Chervoneva I, Schulz S, Waldman SA, Pitari GM. Homeostatic control of the crypt-villus axis by the bacterial enterotoxin receptor guanylyl cyclase C restricts the proliferating compartment in intestine. Am J Pathol. 2007;171:1847-58.
[16] Steinbrecher KA, Wowk SA, Rudolph JA, Witte DP, Cohen MB. Targeted inactivation of the mouse guanylin gene results in altered dynamics of colonic epithelial proliferation. Am J Pathol. 2002;161:2169-78.
[17] Wang R, Kwon IK, Thangaraju M, Singh N, Liu K, Jay P, et al. Type 2 cGMP-dependent protein kinase regulates proliferation and differentiation in the colonic mucosa. Am J Physiol. 2012;303:G209-G19.
[18] Li P, Schulz S, Bombonati A, Palazzo JP, Hyslop TM, Xu Y, et al. Guanylyl cyclase C suppresses intestinal tumorigenesis by restricting proliferation and maintaining genomic integrity. Gastroenterology. 2007;133:599-607.
[19] De Sauvage FJ, Keshav S, Kuang WJ, Gillett N, Henzel W, Goeddel DV. Precursor structure, expression, and tissue distribution of human guanylin. Proc Natl Acad Sci U S A. 1992;89:9089-93.
[20] Cohen MB, Witte DP, Hawkins JA, Currie MG. Immunohistochemical localization of guanylin in the rat small intestine and colon. Biochem Biophys Res Commun. 1995;209:803-8.
[21] Perkins A, Goy MF, Li Z. Uroguanylin is expressed by enterochromaffin cells in the rat gastrointestinal tract. Gastroenterology. 1997;113:1007-14.
[22] Date Y, Nakazato M, Yamaguchi H, Miyazato M, Matsukura S. Tissue distribution and plasma concentration of human guanylin. Intern Med. 1996;35:171-5.

[23] Cetin Y, Kuhn M, Kulaksiz H, Adermann K, Bargsten G, Grube D, et al. Enterochromaffin cells of the digestive system: cellular source of guanylin, a guanylate cyclase-activating peptide. Proc Natl Acad Sci U S A. 1994;91:2935-9.
[24] Li Z, Taylor-Blake B, Light AR, Goy MF. Guanylin, an endogenous ligand for C-type guanylate cyclase, is produced by goblet cells in the rat intestine. Gastroenterology. 1995;109:1863-75.
[25] Whitaker TL, Witte DP, Scott MC, Cohen MB. Uroguanylin and guanylin: distinct but overlapping patterns of messenger RNA expression in mouse intestine. Gastroenterology. 1997;113:1000-6.
[26] Wang F, Flanagan J, Su N, Wang LC, Bui S, Nielson A, et al. RNAscope: a novel in situ RNA analysis platform for formalin-fixed, paraffin-embedded tissues. J Mol Diagn. 2012;14:22-9.
[27] Qian X, Prabhakar S, Nandi A, Visweswariah SS, Goy MF. Expression of GC-C, a receptor-guanylate cyclase, and its endogenous ligands uroguanylin and guanylin along the rostrocaudal axis of the intestine. Endocrinology. 2000;141:3210-24.
[28] Kulaksiz H, Schmid A, Honscheid M, Eissele R, Klempnauer J, Cetin Y. Guanylin in the human pancreas: a novel luminocrine regulatory pathway of electrolyte secretion via cGMP and CFTR in the ductal system. Histochem Cell Biol. 2001;115:131-45.
[29] Kulaksiz H, Cetin Y. The electrolyte/fluid secretion stimulatory peptides guanylin and uroguanylin and their common functional coupling proteins in the rat pancreas: a correlative study of expression and cell-specific localization. Pancreas. 2002;25:170-5.
[30] Azevedo-Pouly AC, Elgamal OA, Schmittgen TD. RNA isolation from mouse pancreas: a ribonuclease-rich tissue. J Vis Exp. 2014:e51779.
[31] Winpenny JP, Verdon B, McAlroy HL, Colledge WH, Ratcliff R, Evans MJ, et al. Calcium-activated chloride conductance is not increased in pancreatic duct cells of CF mice. Pflugers Arch. 1995;430:26-33.
[32] Krause WJ, Freeman RH, Fort LR. Autoradiographic demonstration of specific binding sites for E. coli enterotoxin in various epithelia of the North American opossum. Cell Tissue Res. 1990;260:387-94.
[33] Krause WJ, Cullingford GL, Freeman RH, Eber SL, Richardson KC, Fok KF, et al. Distribution of heat-stable enterotoxin/guanylin receptors in the intestinal tract of man and other mammals. J Anat. 1994;184:407-17.
[34] Sato T, van Es JH, Snippert HJ, Stange DE, Vries RG, van den Born M, et al. Paneth cells constitute the niche for Lgr5 stem cells in intestinal crypts. Nature. 2011;469:415-8.
[35] Cash HL, Whitham CV, Behrendt CL, Hooper LV. Symbiotic bacteria direct expression of an intestinal bactericidal lectin. Science. 2006;313:1126-30.
[36] Rothenberg ME, Nusse Y, Kalisky T, Lee JJ, Dalerba P, Scheeren F, et al. Identification of a cKit(+) colonic crypt base secretory cell that supports Lgr5(+) stem cells in mice. Gastroenterology. 2012;142:1195-205 e6.
[37] Martin S, Adermann K, Forssmann WG, Kuhn M. Regulated, side-directed secretion of proguanylin from isolated rat colonic mucosa. Endocrinology. 1999;140:5022-9.
[38] Phillips TE. Both crypt and villus intestinal goblet cells secrete mucin in response to cholinergic stimulation. Am J Physiol. 1992;262:G327-31.
[39] Mori-Akiyama Y, van den Born M, van Es JH, Hamilton SR, Adams HP, Zhang J, et al. SOX9 is required for the differentiation of paneth cells in the intestinal epithelium. Gastroenterology. 2007;133:539-46.
[40] Swartling FJ, Ferletta M, Kastemar M, Weiss WA, Westermark B. Cyclic GMP-dependent protein kinase II inhibits cell proliferation, Sox9 expression and Akt phosphorylation in human glioma cell lines. Oncogene. 2009;28:3121-31.
[41] Chikuda H, Kugimiya F, Hoshi K, Ikeda T, Ogasawara T, Shimoaka T, et al. Cyclic GMP-dependent protein kinase II is a molecular switch from proliferation to hypertrophic differentiation of chondrocytes. Genes Dev. 2004;18:2418-29.
[42] Ronnestad I, Akiba Y, Kaji I, Kaunitz JD. Duodenal luminal nutrient sensing. Curr Opin Pharmacol. 2014;19:67-75.
[43] Gawenis LR, Franklin CL, Simpson JE, Palmer BA, Walker NM, Wiggins TM, et al. cAMP inhibition of murine intestinal $Na^+/H^+$ exchange requires CFTR-mediated cell shrinkage of villus epithelium. Gastroenterology. 2003;125:1148-63.
[44] Steinbrecher KA, Mann EA, Giannella RA, Cohen MB. Increases in guanylin and uroguanylin in a mouse model of osmotic diarrhea are guanylate cyclase C-independent. Gastroenterology. 2001;121:1191-202.

[45] Lorenz JN, Nieman M, Sabo J, Sanford LP, Hawkins JA, Elitsur N, et al. Uroguanylin knockout mice have increased blood pressure and impaired natriuretic response to enteral NaCl load. J Clin Invest. 2003;112:1244-54.
[46] Valentino MA, Lin JE, Snook AE, Li P, Kim GW, Marszalowicz G, et al. A uroguanylin-GUCY2C endocrine axis regulates feeding in mice. J Clin Invest. 2011;121:3578-88.
[47] Gong R, Ding C, Hu J, Lu Y, Liu F, Mann E, et al. Role for the membrane receptor guanylyl cyclase-C in attention deficiency and hyperactive behavior. Science. 2011;333:1642-6.
[48] Foulke-Abel J, In J, Yin J, Zachos NC, Kovbasnjuk O, Estes MK, et al. Human enteroids as a model of upper small intestinal ion transport physiology and pathophysiology. Gastroenterology. 2016;150:638-49.
[49] Fang R, Olds LC, Sibley E. Spatio-temporal patterns of intestine-specific transcription factor expression during postnatal mouse gut development. Gene Expr Patterns. 2006;6:426-32.
[50] Kobayashi A, Donaldson DS, Kanaya T, Fukuda S, Baillie JK, Freeman TC, et al. Identification of novel genes selectively expressed in the follicle-associated epithelium from the meta-analysis of transcriptomics data from multiple mouse cell and tissue populations. DNA Res. 2012;19:407-22.

## Supplementary

### Table 1 Sequence of the primers used for qPCR.

| Protein | Gene | Forward primer | Reverse Primer |
|---|---|---|---|
| GN | *Guca2a* | GATCCTGCAGAGGCTAGAGG | AAGGCAAGCGATGTCACTCT |
| UGN | *Guca2b* | AGGAGATGTCCAATCCCCAG | ACAGTTCACATTCGTCGGTGG |
| GCC | *Gucy2c* | TGTGAACGCGACTTTCATCTAC | GCAGCCCATCTTATGATCTCTTG |
| GAPDH | *Gapdh* | TTCCAGTATGACTCCACTCACGG | TGAAGACACCAGTAGACTCCACGAC |

.

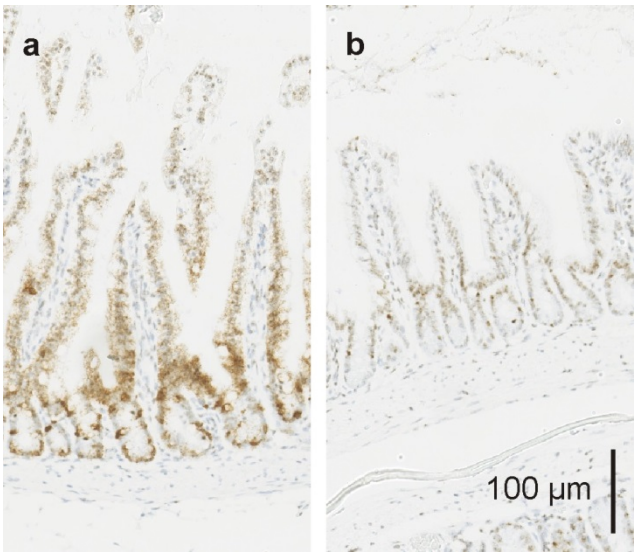


**Figure Supplementary 1 (S1).** RNAscope analysis of *Guca2a* transcript in jejunal tissue of normal (a) and *Guca2a* null (b) mice. In control mice, *Guca2a* staining matched the pattern shown in Figure 3, but in *Guca2a* null mice, only sparse punctuate staining was found in the nuclei (indicating hybridization with DNA), and cytoplasmic region (indicating weak hybridization with truncated *Guca2a* transcripts)

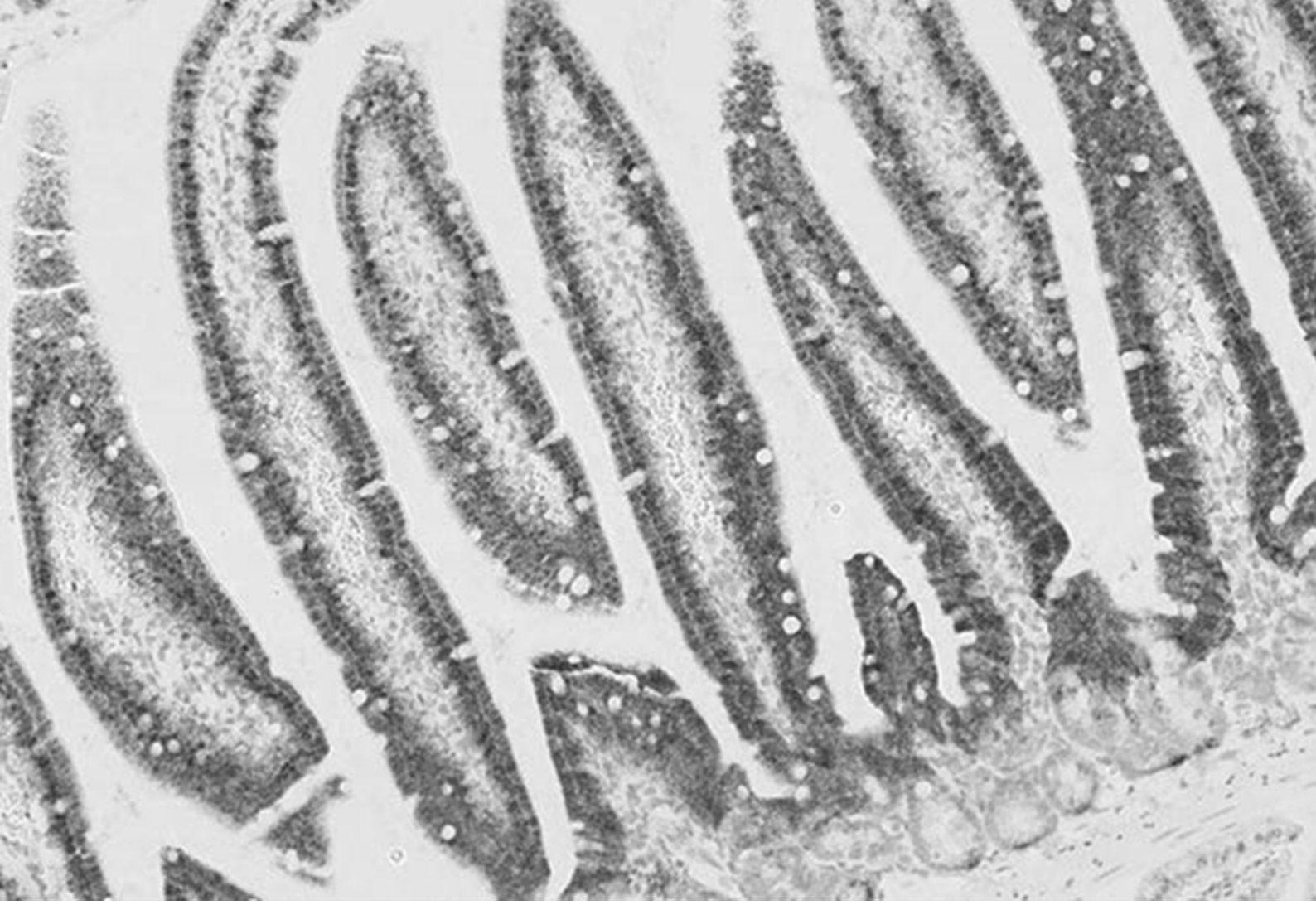

# Chapter 5

# Impaired intestinal guanylyl cyclase C signaling in cystic fibrosis mice

**Pauline T. Ikpa[1], Sabine Middendorp[2], Natascha D. A. Nieuwenhuijze[1], Kelly F. Meijsen[1], Hugo R. de Jonge[1], Marcel J.C. Bijvelds[1]**

[1] Department of Gastroenterology and Hepatology, Erasmus MC University Medical Center, PO Box 2040, 3000CA Rotterdam, The Netherlands

[2] Division of Pediatrics, Department of Pediatric Gastroenterology, Wilhelmina Children's Hospital, University Medical Center Utrecht, Regenerative Medicine Center Utrecht, Uppsalalaan 6, 3584 CT Utrecht, The Netherlands

**Abstract**

Cystic fibrosis (CF) related gastrointestinal disease is characterized by dehydration of the epithelial surfaces, a reduction in the luminal surface pH, and mucus plugging, often culminating in impaction of the distal small intestine contents and bacterial overgrowth (SIBO). We hypothesized that this pathology affects the production of the luminocrine peptides guanylin (GN) and uroguanylin (UGN), which, through activation of the guanylyl cyclase C (GCC), control intestinal fluid homeostasis. To address this question, we investigated gene and protein expression of GN, UGN and GCC in intestinal tissue of CF (*Cftr null*) and wildtype mice reared on a conventional diet or after oral antibiotic treatment. We found that expression of GN, UGN and GCC was markedly reduced in the distal small intestine of CF mice, compared to tissue of wildtype mice. Corresponding with low GN and UGN transcript levels, the level of the secreted peptide precursors were also reduced in the CF ileum. Expression of GN and UGN was restored in primary organoids cultures of CF intestinal epithelium, suggesting that the down-regulation of the GCC signaling axis results from secondary disease manifestations. Indeed, intestinal dysbiosis was indicated by a marked induction of genes involved in host-microbe interactions, and antibiotic treatment restored GN and UGN transcript levels to those observed in wildtype mice. We conclude that CF-related changes in the gut microbiota suppress signaling through the pro-secretory (U)GN-GCC signaling axis, suggesting that impaired GCC signaling may contribute to luminal dehydration and acidification in CF.

## Introduction

Dehydration of the epithelial surfaces, mucus plugging, and obstruction of the distal small intestine are hallmarks of cystic fibrosis (CF) related gastrointestinal disease. This pathology is caused by loss-of-function mutations in the gene encoding the CF transmembrane conductance regulator (CFTR) anion channel. CFTR mediates chloride and bicarbonate transport to the intestinal lumen and the biliary and exocrine pancreatic ducts. Both a reduction in the resultant osmotic water transport and a decrease in surface pH, which is a critical determinant of the physiochemical properties of the mucus layer lining the luminal surfaces, are thought to contribute to the gastrointestinal phenotype [1]. In turn, anomalous mucus production and luminal dehydration lead to impaired pancreatic enzyme delivery, malabsorption and intestinal obstruction. Combined, these factors may elicit distinct alterations in the gut microbiota (*dysbiosis*).

In the intestine, CFTR operates downstream of several intricately interwoven signaling pathways that control intestinal fluid balance and acid-base homeostasis [2]. One of these pathways is controlled by the release of 2 luminocrine factors, the cysteine-rich peptides guanylin (GN) and uroguanylin (UGN), by the intestinal epithelium. These peptides control the activity of the receptor-enzyme guanylyl cyclase C (GCC), which is located on the luminal membrane of epithelial cells throughout the length of the gut [3-5]. GCC stimulation increases cellular cyclic guanosine monophosphate (cGMP) levels, which prompts protein kinase mediated phosphorylation/activation of CFTR, and, consequently, chloride and bicarbonate secretion. Concurrent phosphorylation/inhibition of the sodium-proton exchanger type 3 (NHE3) leads to luminal retention of sodium, which is thought to contribute significantly to the pro-secretory effect of cGMP- and cyclic AMP-linked (neuro-)endocrine pathways [2]. The importance of the GCC signaling axis for intestinal fluid homeostasis is underlined by the fact that loss-of-function mutations in GCC lead to a CF-like phenotype, i.e. a predisposition to develop obstruction of the distal small intestine [6].

Apart from regulating intestinal fluid homeostasis, the GCC signaling axis may also play a role in host-microbe interactions and the innate immune response to pathogens. This involvement may, in part, reflect the role of GCC in luminal pH regulation. Acid-stimulated GCC activation was shown to trigger strong CFTR-dependent bicarbonate secretion [7, 8]. This luminal alkalization was shown to be crucial for proper unfolding of condensed mucins, and the CF-typical changes in the physiochemical properties of the mucus layer are thought to precipitate mucus plugging and bacterial colonization of the small intestine [1, 9]. In addition, it is probable that GCC signaling has further roles in the regulation of innate immunity: GN and UGN are

highly expressed in Paneth cells, and, by stimulating local fluid secretion, may oppose microbial invasion of the crypts of Lieberkühn [5, 10]. This fluid movement may also aid the dispersion of the anti-microbial products produced by Paneth cells. Consistent with such a role, it was shown that loss of GCC activity compromises the epithelial barrier and the innate host response to pathogens in mice [11, 12].

GN and UGN are expressed by several different epithelial cell types of the secretory lineage, including some enteroendocrine types [5, 13]. This suggests that their production and release may be controlled through a chemosensory mechanism, i.e. by luminal input. Indeed, it was shown that luminal hyperosmotic fluid triggers the expression of GN and UGN in mouse small intestine, whereas intake of a high-fat diet was shown to suppress UGN and GN expression in the gut [14-16]. Of interest, inflammation of the gut wall is associated with down-regulation of the GCC signaling axis, suggesting that local chemo-/cytokine production affects (U)GN production and GCC signaling [17-19].

Considering the potential effect of luminal salinity, pH, inflammation, and the gut microbiota on GN and UGN production, we hypothesized that the CF condition may alter GN and UGN expression. An increase in either GN or UGN production, resulting from a decrease in luminal pH and the low hydration level of the luminal surface, would enhance GCC signaling, and counteract the CF fluid secretory defect, principally by reducing sodium uptake through NHE3. In contrast, dysbiosis and inflammation may attenuate GCC activity and promote further luminal dehydration. To test these different scenarios, we assessed the expression of GN, UGN, and GCC along the intestinal tract of CF mice and littermate controls.

## Materials and methods

### *Animals*

CF mice ($Cftr^{tm1Cam}$; FVB) and littermate controls were maintained in an environmentally controlled facility at the Erasmus MC, Rotterdam. Animals were reared on a low fiber diet (C1013; Altromin) and a polyethylene glycol/electrolyte drinking solution to prevent intestinal obstruction [20]. All experiments were performed on animals >12 weeks of age, and were approved of by the Ethical Committee for Animal Experiments of the Erasmus MC.

### *Tissue collection*

Prior to tissue collection, animals were weaned of the osmotic laxative and kept on normal drinking water for >4 days. Animals were anaesthetized (ketamine 100 mg/kg, xylazine 20 mg/kg; i.p.), and the intestinal tract was collected and flushed with ice-cold saline. Sampling

from a CF mouse and a sex-matched littermate control was performed within a time window of 20 min, and between 12:00-14:00h, to control for diurnal variations in gene expression.

For assessing the partitioning of transcript along the rostrocaudal axis of the intestinal tract, segments (length: 0.5 cm) were excised from small intestine and the colon. The small intestine was sampled 1 cm caudal to the pyloric sphincter (duodenum), half-length (jejunum) and at 6 and 1 cm proximal to the ileocecal valve (ileum). Colon was sampled at 1/3 of its entire length. Tissue was flash frozen in liquid nitrogen and stored at -80°C.

***Organoid culture***

Organoids were derived from mouse ileum, and cultured in serum-free medium containing epidermal growth factor, noggin, and R-spondin, as described in detail elsewhere [21].

***Quantitative Polymerase Chain Reaction (qPCR) and transcriptome sequencing***

Tissue and organoids were homogenized with a rotor-stator homogenizer in Trizol reagent (Qiagen), and total RNA was extracted using the Nucleospin kit (Macherey-Nagel). After the integrity of the extracted RNA was verified by gel electrophoresis, cDNA was synthesized using the PrimeScript RT master mix (Takara Bio).

Quantitative PCR (primer sequences in Table S1) was performed on cDNA, using the SYBR Select master mix (Applied Bio System). Median values from assays performed in triplicate were used to determine the expression levels of *Guca2a* (GN), *Guca2b* (UGN) and *Gucy2c* (GCC), relative to *Gapdh*. To correct for regional differences in gene expression in the distal small intestine, mean values of the relative expression levels at the 2 ileal sampling locations are presented.

Transcriptome sequencing was performed at the Beijing Genomics Institute (BGI). In brief, mRNA was isolated from total tissue or organoid RNA extracts (200 ng), fragmented, and, subsequently used for cDNA synthesis. The resulting cDNA library was sequenced using an HiSeq 2000 sequencer (TruSeq SBS KIT-HS V3; Illumina). Data analysis was performed using CLC genomic workbench 7.5 (CLC Bio), and the sequence reads were mapped to the Genome Reference Consortium (GRC) genome data set GRCm38.76, using default parameters. Data depict reads per 1000 base pair transcript per million mapped reads (RPKM). Data are available through the NCBI-GEO record GSE92991.

***Western Analysis***

Epithelial cell lysates were prepared from 6 cm sections of the distal ileum. The segment was cut open lengthwise and cut in to sections of circa 5 mm in length. Sections were extensively washed in ice-cold phosphate buffered saline (PBS), supplemented with a protease inhibitor cocktail (Roche), and subsequently incubated with EDTA (2.5 mmol/L) in 20 mL PBS (4°C), on a bench-top roller to dissociate the epithelial cell layer. After 30 min, dissociation was completed by brief, vigorous shaking, and crypt/villus fragments and single cells were filtered through a cell strainer (70 μm) to remove tissue debris. Subsequently, the filtered epithelial fraction was collected by centrifugation (300x g, 5 min) and lysed by brief sonication in ice-cooled lysis buffer, NaCl (150 mmol/L), Tris/HCl pH 7.6 (25 mmol/L), Triton X100 (1%), sodium deoxycholate (1%), SDS (0.1%), NaF (5 mmol/L), $Na_3VO_4$ (3 mmol/L), supplemented with protease inhibitor cocktail. Lysates were subjected to SDS-PAGE, and proteins were transferred to nitrocellulose membrane. GN and UGN prohormone was detected by Western analysis, using the previously characterized antisera #2538 and #6910, respectively [22, 23]. Detection of β-actin served as loading control (SC47778; Santa Cruz).

***Statistical Analysis***

The statistical significance of differences between mean expression levels of *Guca2a*, *Guca2b* and *Gucy2c* in CF and wildtype tissue was analyzed by one-way Anova followed by Bonferroni's multiple comparison test on selected pairs of data sets (Graphpad Prism 5, Graphpad Software). The statistical significance of differences between transcript levels was analyzed using the (paired) ratio *t*-test.

**Results**

***Reduced expression of Guca2a, Guca2b and Gucy2c in the CF intestine***

We assessed expression of *Guca2a, Guca2b and Gucy2c* along the rostrocaudal axis of the intestinal tract, in CF mice (Cftr -/-) and littermate controls (Cftr N/N). We noted that, in the distal small intestine, expression of all 3 genes was >2-fold lower in CF mice than in control littermates (Figure 1). In contrast, expression in other parts of the intestinal tract was comparable between CF mice and controls, except that *Guca2b* expression was also moderately lowered in the jejunum of CF mice (Figure 1). The rostrocaudal distribution pattern of *Guca2a, Guca2b* and *Gucy2c* observed, matches with previous reports on the partitioning of these transcripts in rat and mouse intestine [4, 5, 24, 25]. Our transcriptome analysis showed that *Guca2a* and *Guca2b* rank among the most highly expressed genes in mouse ileum, and confirmed that their transcript

levels are markedly lower in CF mice, compared to controls (not shown). The levels of *Gucy2c* transcript were considerably lower than of its ligands, and peaked in the distal part of the intestinal tract (Figure 1c).

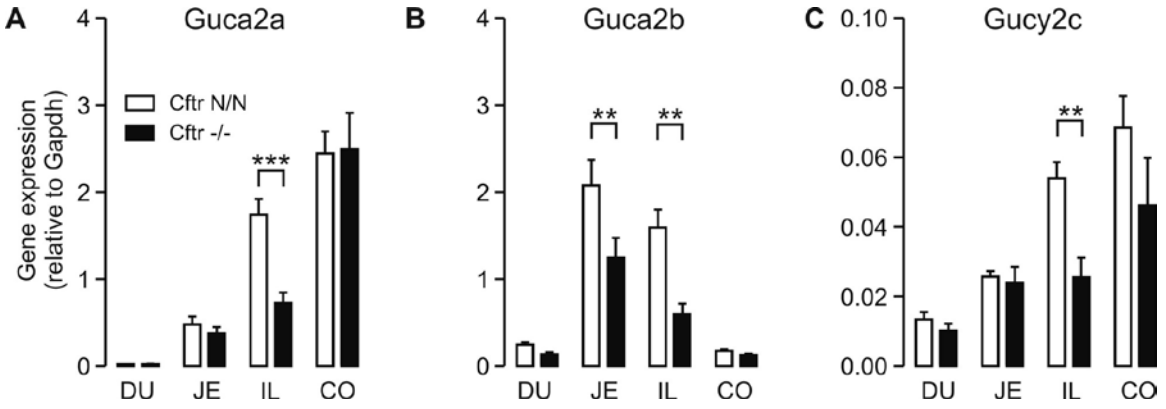


***Figure 1*** *Expression of Guca2a (A), Guca2b (B), and Gucy2c (C) in the small intestine and colon of CF mice (Cftr -/-) and littermate controls (Cftr N/N) was assessed by qPCR. N=5-6. Values depict mean ± standard error. ** P < 0.01; *** P < 0.001*

To assess whether such marked reductions in transcript levels translate to lowered protein levels, we quantified the levels of the secreted precursors of GN and UGN in intestinal epithelial cells by Western analysis. This analysis showed that the levels of pro-GN and pro-UGN present in ileal tissue of CF mice were markedly lower than in the corresponding samples of littermate controls (Figure 2).

Previously, we have shown that, in the distal small intestine, *Guca2a* and *Guca2b* are expressed by Paneth cells and other cells of the secretory lineage, and by mature columnar cells in the upper (villus) regions of the epithelium [5]. Because CF was shown to affect both proliferation and apoptosis in the intestinal epithelium, we considered that CF may lead to a

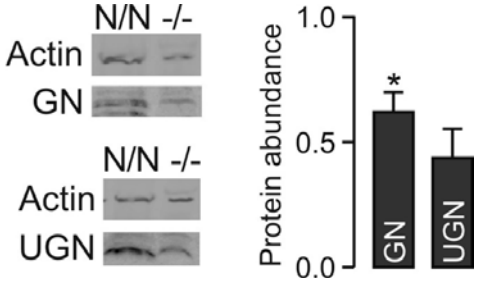


***Figure 2*** *GN and UGN prohormone level in the distal small intestine of CF mice and controls. Western analysis of pro-GN and pro-UGN was performed on epithelial cell lysates prepared from ileum of CF animals (-/-) and sex-matched littermate controls (N/N). For quantitation, signal intensity was normalized against the β-actin signal of the same sample. The bar graph shows protein abundance in Cftr -/- animals relative, to controls. N = 4. * P < 0.05*

relative reduction in specific GN or UGN producing cell types [26, 27]. However, we have previously assessed transcript levels of typical villus markers (i.e. genes which are highly expressed in the villi, relative to the crypts) and found no evidence for delayed cell maturation in the CF ileum (Chapter 3). Further, transcriptome analysis showed that the expression of transcription factors that direct differentiation to the secretory (granulocytic) lineage (*Atoh1*, *Klf4, Sox9* and *Spdef*), or of typical enteroendocrine cell markers (*Chga, Lyz1*) was not reduced in the CF ileum, which argues against a specific reduction in GN and/or UGN producing cells of the secretory lineage (Figure 3) [28, 29]. Consistent with these findings, we found that goblet cell numbers were normal or even slightly increased in the CF ileum, compared to control tissue (Figure S1).

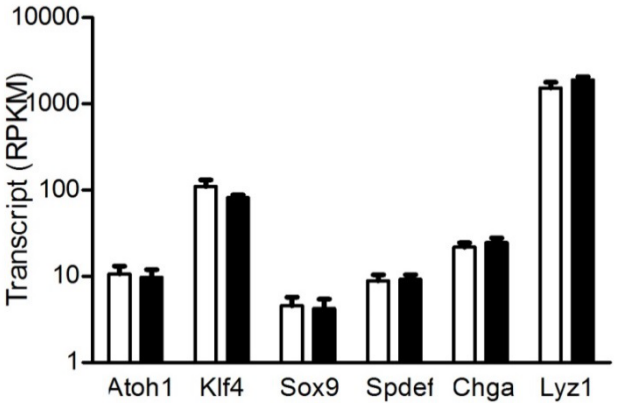


***Figure 3.*** *Transcript levels of selected genes in the distal small intestine of CF mice and controls that are specifically expressed in cells of the secretory lineage (Atoh1, Klf4, Sox9, Spdef), enterochromaffin cells (Chga), and Paneth cells (Lyz1). N = 3.*

Next, we asked whether these apparent changes in the expression of *Guca2a*, *Guca2b* and *Gucy2c* are intrinsic to loss of CFTR anion channel function, or may be caused by secondary disease manifestations (e.g. inflammation, dysbiosis). We reasoned that if it is an epithelial-autonomous defect, it should be preserved in primary cultures of CF intestinal epithelial cells. Therefore, we obtained organoid cultures from ileal stem cells, to determine transcript levels of *Guca2a*, *Guca2b* and *Gucy2c* in intestinal epithelial cells in the absence of confounding environmental factors. A paired comparison of CF and control organoids (obtained from littermates) showed that the differences in gene expression between genotypes observed in native tissue were lost in cultured epithelial cells (Figure 4).

***Antibiotic treatment corrects Guca2a and Guca2b expression in the CF intestine***

Because differences in expression of the GCC signaling axis between CF and control ileum are lost in organoid cultures, we hypothesized that changes in the intestinal environment secondary to loss of CFTR function, and absent under cell culture conditions, prompt *Guca2a* and *Guca2b* down-regulation. One such factor may be inflammation of the gut wall, which

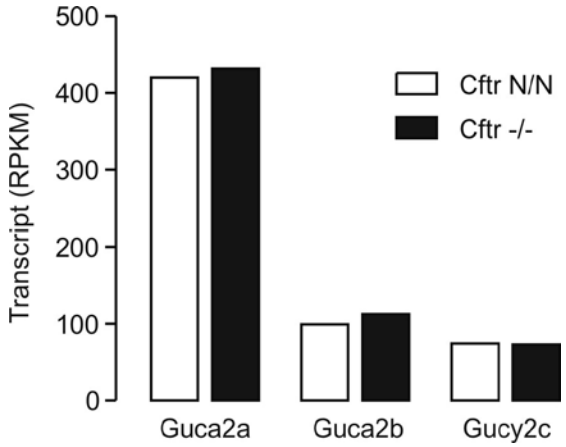


***Figure 5.*** *Transcript numbers of Guca2a, Guca2b, and Gucy2c in organoids derived from ileum of CF (Cftr -/-) and wildtype (Cftr N/N) mice.*

previously has been shown to lead to down-regulation of GN and UGN in the setting of inflammatory bowel disease (IBD) [18, 19]. In CF, inflammation of the gut wall is thought to result from small intestinal bacterial overgrowth (SIBO), and aberrant Paneth/goblet cell function and mucus production/unfolding [1, 30, 31]. Indeed, transcriptome analysis clearly indicated the activation of an (innate) immune response in the CF ileum, as many genes involved in host-pathogen interactions were up-regulated, including those encoding the lipopolysaccharide co-receptor CD14, and the antimicrobial peptides muclin (*Dmbt1*), REG3β/γ and RELM-β (*Retnlb*; Figure 5).

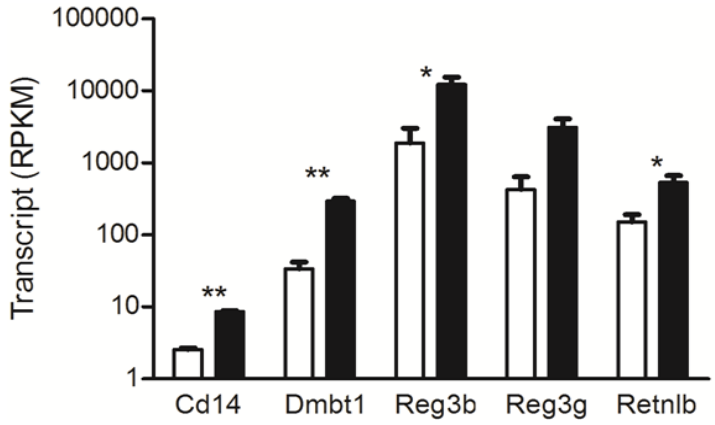


***Figure 4.*** *Transcript levels of selected genes involved in host-pathogen interactions in the distal small intestine of CF mice and controls. * P < 0.05; ** P < 0.01; N = 3.*

To investigate whether dysbiosis is involved in the down-regulation of the GCC signaling axis, we treated CF mice with antibiotics. The antibiotic regimen applied has previously been shown not to fully eradicate the microbiota but to reduce bacterial overgrowth and increase community diversity in CF mice [32]. We found that this mild regimen increased the expression of both *Guca2a* and *Guca2b* in the CF ileum, up to the level observed in antibiotic-treated control mice, in which antibiotics did not increase *Guca2a* or *Guca2b* expression (Figure 6).

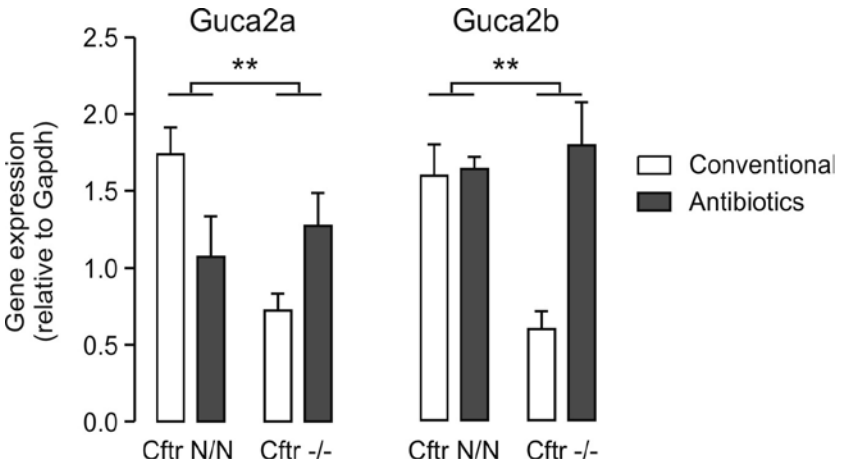


***Figure 6.*** *Effect of antibiotic treatment on expression of Guca2a and Guca2b in the ileum of CF mice and controls. Two-way ANOVA indicated a statistically significant interaction between antibiotic treatment and Cftr genotype for Guca2a and Guca2b, expression, implying that loss of CFTR affects the response to antibiotic treatment. ** P < 0.01; N = 4-6*

**Discussion**

GN and UGN are highly abundant intestinal luminocrine factors that control intestinal fluid transport by stimulating epithelial salt and fluid secretion. The key finding of our study is that the expression of both of these peptides is markedly reduced in the CF intestine, in particular in the distal small intestine. We surmise that diminished production of GN and UGN, by reducing GCC activity and cGMP production, may contribute to the dehydration and acidification of the CF intestine.

It has been shown previously that the dissolution of secretory granules produced by Paneth cells is impaired in CF mice [31]. This was associated with a concurrent downregulation of genes encoding some of the antimicrobial peptides produced by this cell type, and it was proposed that impaired post-exocytotic processing of secretory granules might exert feedback control on gene expression [31]. Because this cell lineage is an important source of GN and UGN, it is conceivable that the reduction in *Guca2a* and *Guca2b* transcript levels shown here are, similarly, caused by defects in the process of exocytosis, and feedback control on gene expression [5]. For goblet cells (a source of GN in mice), defects in the release and processing of secretory granules have been attributed to impaired regulation of the pH of the secretory granules and their luminal environment, which appears to link these defects directly to loss of CFTR activity [30]. However, we observed that *Guca2a* and *Guca2b* down-regulation was resolved in cultured epithelial cells, which argues against an intrinsic cellular defect. Instead, this suggests that changes in the intestinal environment secondary to loss of CFTR function, and lost in organoid cultures, prompt down-regulation of GCC signaling.

Indeed, the observation that antibiotic treatment normalized *Guca2a* and *Guca2b* expression in CF mice suggests that CF-related changes in the gut microbiota play a role in the repression of these genes. Congruently, it was shown that colonization of the gut by a gram-negative pathogen, *Citrobacter rodentium*, markedly represses *Guca2a* expression in mouse colon [11]. Conversely, this study also showed that GCC deficiency aggravates the deleterious effects of *C. rodentium* infection on the intestinal epithelium, implying a role of the GCC signaling axis in the innate immune response to enteric pathogens. Consistent with such a role, we found that acute exposure of intestinal epithelium to lipopolysaccharide (*ex vivo*), a product of gram-negative bacteria, moderately induced *Guca2a* and *Guca2b* (unpublished data). Thus, these results suggest that the initial response to bacterial pathogens is an activation of GCC signaling, but that prolonged colonization, possibly through the attendant inflammatory response, leads to attenuation of GCC signaling. That chronic inflammation may down-regulate the GCC signaling axis is also suggested by the observation that, in patients suffering from IBD, expression of GN and UGN is generally low [18, 19].

Reduced GCC signaling in CF intestine may have several consequences for CF pathology. Foremost, loss of GCC/cGMP-dependent NHE3 inhibition may enhance sodium and water uptake, and reduce the extracellular pH [33]. Furthermore, it has been shown that some UGN-dependent bicarbonate secretion persists in *Cftr* null mice [34]. This UGN-dependent, CFTR-independent bicarbonate secretion will be reduced by low GCC stimulation, and this may further contribute to the deregulation of luminal pH in CF. These effects are expected to aggravate the mucus inspissation and dehydration of the luminal surface that typifies CF. They may also contribute to the dysbiosis that is common in CF, as GCC is a key component of the host defense response triggered by enteric pathogens [11]. In this context, it is of interest that down-regulation of the GCC signaling axis is most evident in the distal small intestine, which seems especially predisposed to develop obstruction and SIBO.

Secondly, GCC signaling, through activation of the cGMP-dependent protein kinase PRKG2, modulates cell cycle progression in intestinal epithelium [3, 35]. Mice deficient in GN, GCC or PRKG2 show signs of enhanced proliferation, and subtle changes in the cellular composition of the epithelium [36-38]. Consistent with impaired GCC signaling, the intestinal epithelium of CF mice also displays enhanced cell proliferation and/or a reduced rate of apoptosis [26, 27].

In summary, our data suggest that CF may be associated with impaired GCC signaling resulting from reduced intestinal GN and UGN production. Impaired GCC signaling may contribute to the intestinal manifestations of CF, like luminal dehydration and acidification.

Because the GCC receptor, except for distal small intestine, is normally expressed in the CF intestine, GCC signaling may be enhanced by (oral) supplementation with exogenous ligands [39]. Such treatment may compensate for the shortage of endogenous ligand, repress sodium absorption and partly restore the intestinal fluid balance. In addition, it may have a beneficial effect on mucin unfolding and the gut microbiota.

**Acknowledgements**

The authors are indebted to Dr. Michael F. Goy (University of North Carolina at Chapel Hill) for kind donation of the proguanylin and prouroguanylin antisera. This study was supported by the Dutch Cystic Fibrosis Foundation (NCFS).

**References**

[1] Garcia MA, Yang N, Quinton PM. Normal mouse intestinal mucus release requires cystic fibrosis transmembrane regulator-dependent bicarbonate secretion. J Clin Invest. 2009;119:2613-22.
[2] Field M. Intestinal ion transport and the pathophysiology of diarrhea. J Clin Invest. 2003;111:931-43.
[3] Brierley SM. Guanylate cyclase-C receptor activation: unexpected biology. Curr Opin Pharmacol. 2012;12:632-40.
[4] Qian X, Prabhakar S, Nandi A, Visweswariah SS, Goy MF. Expression of GC-C, a receptor-guanylate cyclase, and its endogenous ligands uroguanylin and guanylin along the rostrocaudal axis of the intestine. Endocrinology. 2000;141:3210-24.
[5] Ikpa PT, Sleddens HFBM, Steinbrecher KA, Peppelenbosch MP, De Jonge HR, Smits R, et al. Guanylin and uroguanylin are produced by mouse intestinal epithelial cells of columnar and secretory lineage. Histochem Cell Biol. 2016;146:445-55.
[6] Romi H, Cohen I, Landau D, Alkrinawi S, Yerushalmi B, Hershkovitz R, et al. Meconium ileus caused by mutations in GUCY2C, encoding the CFTR-activating guanylate cyclase 2C. Am J Hum Genet. 2012;90:893-9.
[7] Guba M, Kuhn M, Forssmann WG, Classen M, Gregor M, Seidler U. Guanylin strongly stimulates rat duodenal $HCO_3^-$ secretion: proposed mechanism and comparison with other secretagogues. Gastroenterology. 1996;111:1558-68.
[8] Rao SP, Sellers Z, Crombie DL, Hogan DL, Mann EA, Childs D, et al. A role for guanylate cyclase C (GC-C) in acid-stimulated duodenal mucosal bicarbonate secretion. Am J Physiol. 2004;286:G95-G101.
[9] Gustafsson JK, Ermund A, Ambort D, Johansson ME, Nilsson HE, Thorell K, et al. Bicarbonate and functional CFTR channel are required for proper mucin secretion and link cystic fibrosis with its mucus phenotype. J Exp Med. 2012;209:1263-72.
[10] De Sauvage FJ, Keshav S, Kuang WJ, Gillett N, Henzel W, Goeddel DV. Precursor structure, expression, and tissue distribution of human guanylin. Proc Natl Acad Sci U S A. 1992;89:9089-93.
[11] Mann EA, Harmel-Laws E, Cohen MB, Steinbrecher KA. Guanylate cyclase C limits systemic dissemination of a murine enteric pathogen. BMC Gastroenterol. 2013;13:135.
[12] Han X, Mann E, Gilbert S, Guan Y, Steinbrecher KA, Montrose MH, et al. Loss of guanylyl cyclase C (GCC) signaling leads to dysfunctional intestinal barrier. PLoS One. 2011;6:e16139.
[13] Kokrashvili Z, Rodriguez D, Yevshayeva V, Zhou H, Margolskee RF, Mosinger B. Release of endogenous opioids from duodenal enteroendocrine cells requires Trpm5. Gastroenterology. 2009;137:598-606.
[14] Steinbrecher KA, Mann EA, Giannella RA, Cohen MB. Increases in guanylin and uroguanylin in a mouse model of osmotic diarrhea are guanylate cyclase C-independent. Gastroenterology. 2001;121:1191-202.
[15] Lin JE, Colon-Gonzalez F, Blomain E, Kim GW, Aing A, Stoecker B, et al. Obesity-induced colorectal cancer is driven by caloric silencing of the guanylin-GUCY2C paracrine Ssignaling axis. Cancer Res. 2016;76:339-46.
[16] Simoes-Silva L, Moreira-Rodrigues M, Quelhas-Santos J, Fernandes-Cerqueira C, Pestana M, Soares-Silva I, et al. Intestinal and renal guanylin peptides system in hypertensive obese mice. Exp Biol Med (Maywood). 2013;238:90-7.
[17] Harmel-Laws E, Mann EA, Cohen MB, Steinbrecher KA. Guanylate cyclase C deficiency causes severe inflammation in a murine model of spontaneous colitis. PLoS One. 2013;8:e79180.
[18] Brenna O, Bruland T, Furnes MW, Granlund A, Drozdov I, Emgard J, et al. The guanylate cyclase-C signaling pathway is down-regulated in inflammatory bowel disease. Scand J Gastroenterol. 2015;50:1241-52.

[19] Lan D, Niu J, Miao J, Dong X, Wang H, Yang G, et al. Expression of guanylate cyclase-C, guanylin, and uroguanylin is downregulated proportionally to the ulcerative colitis disease activity index. Sci Rep. 2016;6:25034.
[20] Xiao F, Li J, Singh AK, Riederer B, Wang J, Sultan A, et al. Cystic fibrosis transmembrane conductance regulator mutant F508del membrane expression rescues epithelial HCO3- secretion in murine intestine. J Physiol. 2012.
[21] Dekkers JF, Wiegerinck CL, De Jonge HR, Bronsveld I, Janssens HM, De Winter-de Groot KM, et al. A functional CFTR assay using primary cystic fibrosis intestinal organoids. Nat Med. 2013;19:939-45.
[22] Perkins A, Goy MF, Li Z. Uroguanylin is expressed by enterochromaffin cells in the rat gastrointestinal tract. Gastroenterology. 1997;113:1007-14.
[23] Li Z, Taylor-Blake B, Light AR, Goy MF. Guanylin, an endogenous ligand for C-type guanylate cyclase, is produced by goblet cells in the rat intestine. Gastroenterology. 1995;109:1863-75.
[24] Whitaker TL, Witte DP, Scott MC, Cohen MB. Uroguanylin and guanylin: distinct but overlapping patterns of messenger RNA expression in mouse intestine. Gastroenterology. 1997;113:1000-6.
[25] Li Z, Goy MF. Peptide-regulated guanylate cyclase pathways in rat colon: in situ localization of GCA, GCC, and guanylin mRNA. Am J Physiol. 1993;265:G394-402.
[26] Gallagher AM, Gottlieb RA. Proliferation, not apoptosis, alters epithelial cell migration in small intestine of CFTR null mice. Am J Physiol. 2001;281:G681-G7.
[27] Canale-Zambrano JC, Poffenberger MC, Cory SM, Humes DG, Haston CK. Intestinal phenotype of variable-weight cystic fibrosis knockout mice. Am J Physiol. 2007;293:G222-G9.
[28] Gerbe F, Legraverend C, Jay P. The intestinal epithelium tuft cells: specification and function. Cell Mol Life Sci. 2012;69:2907-17.
[29] Middendorp S, Schneeberger K, Wiegerinck CL, Mokry M, Akkerman RD, van Wijngaarden S, et al. Adult stem cells in the small intestine are intrinsically programmed with their location-specific function. Stem Cells. 2014;32:1083-91.
[30] Liu J, Walker NM, Ootani A, Strubberg AM, Clarke LL. Defective goblet cell exocytosis contributes to murine cystic fibrosis-associated intestinal disease. J Clin Invest. 2015;125:1056-68.
[31] Clarke LL, Gawenis LR, Bradford EM, Judd LM, Boyle KT, Simpson JE, et al. Abnormal Paneth cell granule dissolution and compromised resistance to bacterial colonization in the intestine of CF mice. Am J Physiol. 2004;286:G1050-G8.
[32] Lynch SV, Goldfarb KC, Wild YK, Kong W, De Lisle RC, Brodie EL. Cystic fibrosis transmembrane conductance regulator knockout mice exhibit aberrant gastrointestinal microbiota. Gut Microbes. 2013;4:41-7.
[33] Bradford EM, Sartor MA, Gawenis LR, Clarke LL, Shull GE. Reduced NHE3-mediated $Na^+$ absorption increases survival and decreases the incidence of intestinal obstructions in cystic fibrosis mice. Am J Physiol. 2009;296:G886-G98.
[34] Joo NS, London RM, Kim HD, Forte LR, Clarke LL. Regulation of intestinal $Cl^-$ and $HCO_3^-$ secretion by uroguanylin. Am J Physiol. 1998;274:G633-G44.
[35] Kim GW, Lin JE, Waldman SA. GUCY2C: at the intersection of obesity and cancer. Trends Endocrinol Metab. 2013;24:165-73.
[36] Steinbrecher KA, Wowk SA, Rudolph JA, Witte DP, Cohen MB. Targeted inactivation of the mouse guanylin gene results in altered dynamics of colonic epithelial proliferation. Am J Pathol. 2002;161:2169-78.
[37] Lin JE, Li P, Snook AE, Schulz S, Dasgupta A, Hyslop TM, et al. The hormone receptor GUCY2C suppresses intestinal tumor formation by inhibiting AKT signaling. Gastroenterology. 2010;138:241-54.

[38] Wang R, Kwon IK, Thangaraju M, Singh N, Liu K, Jay P, et al. Type 2 cGMP-dependent protein kinase regulates proliferation and differentiation in the colonic mucosa. Am J Physiol. 2012;303:G209-G19.
[39] Bryant AP, Busby RW, Bartolini WP, Cordero EA, Hannig G, Kessler MM, et al. Linaclotide is a potent and selective guanylate cyclase C agonist that elicits pharmacological effects locally in the gastrointestinal tract. Life Sci. 2010;86:760-5.

## Supplementary data

### *Supplementary materials and methods*

### *Histochemical detection of goblet cells*

Paraffin sections (5µm) were stained (30 min) with Alcian blue solution (1% Alcian blue 8GX in 3% acetic acid solution, pH 2.5), washed in water, and subsequently counterstained (5 min) with nuclear fast red solution (0.1% nuclear fast red, 5% aluminum sulfate). After rinsing in water, sections were mounted in Pertex mounting medium (Histolab Products AB), and stored at room temperature.

**Table S1**

**Sequence of the primers used for qPCR.**

| Genes | Accession | Forward primer | Reverse Primer |
|---|---|---|---|
| *Guca2a* | NM008190.1 | GATCCTGCAGAGGCTAGAGG | AAGGCAAGCGATGTCACTCT |
| *Guca2b* | NM008191.2 | AGGAGATGTCCAATCCCCAG | ACAGTTCACATTCGTCGGTGG |
| *Gucy2c* | NM001127318.1 | TGTGAACGCGACTTTCATCTAC | GCAGCCCATCTTATGATCTCTTG |
| *Gapdh* | NM008084.3 | TTCCAGTATGACTCCACTCACGG | TGAAGACACCAGTAGACTCCACGAC |

**Supplementary results**

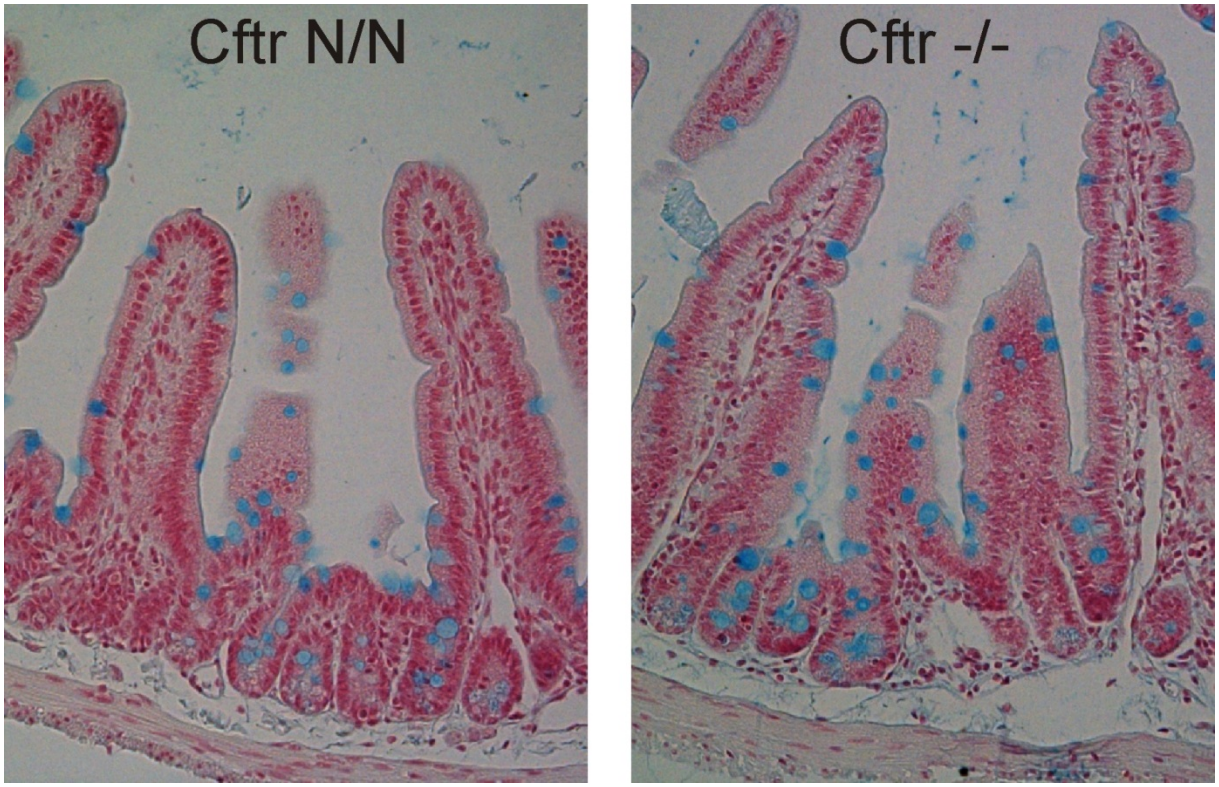


***Figure S1****. Detection of goblet cells in mouse ileum. Representative tissue sections of a CF animal (Cftr -/-) and littermate control (Cftr N/N) were stained with Alcian blue to identify the mucopolysaccharide containing goblet cells (blue staining). (original magnification: 20x)*

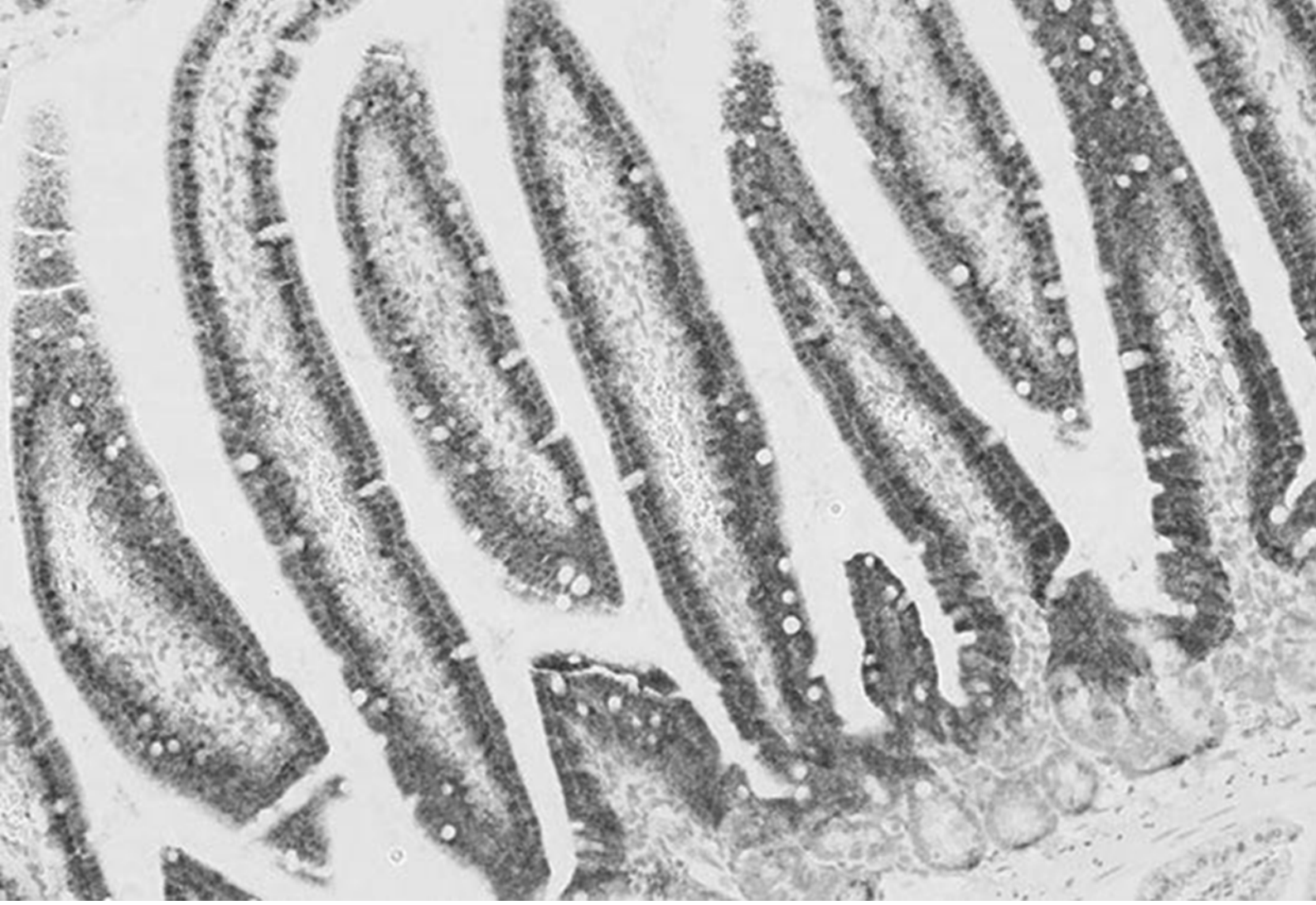

# Chapter 6.

# Impaired intestinal farnesoid X receptor signaling in cystic fibrosis mice

**Pauline T. Ikpa[1], Marcela Doktorova[2], Kelly F. Meijsen[1], Natascha D. A. Nieuwenhuijze[1], Kalyan Dulla[3], Henkjan J. Verkade[2], Johan W. Jonker[2], Hugo R. de Jonge[1], Marcel J. C. Bijvelds[1]**

[1]Department of Gastroenterology and Hepatology, Erasmus MC University Medical Center, PO Box 2040, 3000CA Rotterdam, The Netherlands. [2]Section of Molecular Metabolism and Nutrition, Department of Pediatrics, University of Groningen, University Medical Center Groningen, Hanzeplein 1, 9713 GZ Groningen, The Netherlands. [3]ProQR Therapeutics N.V., Darwinweg 24, 2333CR Leiden, The Netherlands.

**Summary**

Bile acid (BA) metabolism is regulated by the BA-activated farnesoid X receptor (FXR), which controls hepatic BA synthesis and cell proliferation via the intestinal hormone fibroblast growth factor 19 (FGF19). Because cystic fibrosis (CF) is associated with anomalous BA handling and biliary cirrhosis, we investigated FXR signaling in CF. We found that ileal *Fgf15* (the murine FGF19 ortholog) expression was markedly lower in CF (*Cftr null*) mice than in controls, although luminal BA composition, and expression and localization of the apical sodium-dependent BA transporter were not affected. *Ex vivo*, BAs induced *Fgf15* up to normal levels in the CF ileum, but suppression was reinstated when tissue was exposed to bacterial lipopolysaccharide (LPS). Transcriptome sequencing and pathway analysis revealed a marked activation of the innate and adaptive immune responses in the CF intestine, and indicated LPS-provoked inhibition of signaling through FXR's obligate heterodimeric partner, the retinoid X receptor (RXR). Antibiotic treatment reversed the up-regulation of inflammatory markers, and restored intestinal FXR/RXR-signaling. Loss of intestinal FXR/RXR activity was associated with a markedly blunted hepatic trophic response to oral BA supplementation, and with impaired repression of *Cyp7a1*, the gene encoding the rate-limiting enzyme in BA synthesis. We conclude that, in CF mice, the gut microbiota suppresses intestinal RXR activity, and, consequently, FXR-dependent hepatic cell proliferation and feedback control of BA synthesis.

**KEYWORDS** Bile acids and salts; Gut microbiota; Fibroblast Growth Factors; Receptors, Cytoplasmic and Nuclear

**Introduction**

Bile acids (BAs) are amphiphilic molecules synthesized from cholesterol in the liver. Upon release into the proximal small intestine, BAs aid the absorption of dietary lipids, after which they are reabsorbed, mainly through active uptake in the distal ileum via the apical sodium-dependent BA transporter (ASBT; encoded by *SLC10A2*) [1]. Although very little of the load entering the intestine escapes re-uptake, small amounts of BA pass through the colon and are excreted in the feces. Fecal loss is compensated for by *de novo* synthesis, which is regulated through a finely tuned homeostatic control mechanism, to maintain a near constant body BA pool. One of the key elements of this control mechanism is the activation of the farnesoid X receptor (FXR) in ileal epithelial cells by reclaimed BAs [2, 3]. Intestinal FXR activation induces the expression of an array of genes involved in BA transport and metabolism. Most importantly, BA reabsorption triggers the production and release of fibroblast growth factor 19 (FGF19). This hormone, through activation of its hepatic receptor (FGFR4), represses expression of *CYP7A1*, the gene encoding the cholesterol 7α-hydroxylase that catalyzes the rate-limiting step in cholic acid (CA) synthesis [4]. The importance of this feedback loop is underlined by the observation that in FGF15 (the murine FGF19 ortholog) deficient mice, hepatic BA synthesis and intestinal delivery are stimulated to a level that exceeds the capacity for reabsorption, resulting in enhanced fecal excretion [5]. In addition, FGF15/19 has trophic effects in the liver, which are crucial for liver regeneration after injury [6, 7]. Through its effects on hepatic BA synthesis and cell proliferation, FGF15/19 signaling may prevent cholestasis-induced liver damage [8].

Cystic fibrosis (CF), an autosomal, recessive disease caused by mutations in the CF transmembrane conductance regulator (CFTR) gene, is characterized by focal biliary cirrhosis, which in a subgroup of patients (circa 30%) progresses to a clinically significant, advanced stage of CF-related liver disease (CFLD) [9]. Principally, this cholangiopathy is thought to be caused by obstruction of the intrahepatic bile ducts by mucoid secretions and accumulation of hydrophobic BAs, but other factors, like exposure to gut-derived endotoxins, may also contribute [9-11]. Bile of CF patients shows a relative increase in CA levels and a decrease in the levels of secondary BAs, which is indicative of enhanced *de novo* synthesis [12]. This is also implied by the observation that the body BA pool size of CF patients is normal to large, despite the fact that in many, fecal BA excretion is abnormally high [12]. Fecal BA wasting, high biliary CA levels, and a mild cholangiopathy are also observed in most CF mouse models [13-15]. These observations suggest that, perhaps because of interrupted enterohepatic cycling of BAs, the FXR/FGF19 signaling pathway is suppressed in CF. Indeed, strongly reduced ileal *Asbt* and

*Fgf15* expression, indicative of reduced BA uptake and FXR activation, was reported for one CF mouse model [16]. In this instance, low FXR/FGF15 signaling was attributed to defective gallbladder emptying, which severely limited intestinal delivery of BAs. Further, more circumstantial, evidence for attenuated FXR/FGF15 signaling in CF is provided by one of our previous studies, in which it was shown that dietary CA supplementation, which is known to induce hepatocyte proliferation through an FXR/FGF15-dependent pathway, triggers a markedly blunted response in CF mice [6, 7, 17]. Assuming that the virtual absence of this response in our CF mice is indeed linked to a low intestinal FGF15 production, our data imply that enhanced intestinal delivery of BAs (as per diet) does not fully correct FXR/FGF15 signaling. This led us to speculate that, apart from defective gallbladder emptying, other factors may contribute to impaired FXR/FGF15 signaling.

In recent years it has become apparent that the gut microbiota, through modulation of intestinal FXR signaling, is a key regulator of BA metabolism. In mice, intra-luminal microbial BA conversion appears to be a key determinant of BA uptake and FXR activity, as both eradication of the microflora and colonization of the gut by probiotics were shown to markedly repress *Fgf15* induction [18-20]. Further, it was shown that bacterial endotoxins, by activation of the nuclear factor κB (NFκB) pathway, repress hepatic FXR signaling, and that FGF15 production is reduced in inflamed intestinal tissue [21-23]. Because murine CF models display distinct quantitative and qualitative changes in the gut microbiota (*dysbiosis*) and inflammation of the gut wall [24-26], it is conceivable that BA biotransformation or exposure to endotoxins leads to a loss of FXR-dependent feedback control of hepatic BA synthesis.

Presently, we have investigated the role of the gut microbiota in intestinal FXR signaling in CF mice. We show that intestinal FXR signaling is markedly attenuated in CF mice, despite normal luminal BA levels, and that repression of FXR signaling persists upon supra-physiological BA dosage, but that constraining bacterial colonization by antibiotic treatment reduces the expression of inflammation markers and normalizes *Fgf15* expression and BA synthesis.

## Results

### *Intestinal FXR signaling is impaired in CF mice*

The expression of FXR targets *Fgf15* and *Shp* (*Nr0b2*) was markedly lower in the ileum of CF mice as compared to littermate controls, whereas expression of *Fxr* (*Nr1h4*) itself was similar between genotypes (Figure 1A). Congruent with low intestinal FGF15 production, hepatic expression of *Cyp7a1* was enhanced in CF mice.

We hypothesized that a shortage of activating ligands may have attenuated FXR signaling, possibly as a result of reduced ASBT-mediated BA uptake. Therefore, we assessed the expression and localization of ASBT. In the distal ileum, the mRNA level of *Asbt* (*Slc10a2*) was similar in CF mice and controls (Figure 1B). A high ASBT protein abundance was detected in ileal brush border membrane preparations of CF mice and controls (Figure 1C). By immunohistochemistry, ASBT was localized at the apical plasma membrane of enterocytes in the villi, and this pattern was unaffected by CFTR deficiency (Figure 1D). When ileal tissue sheets of CF mice and controls were exposed to TC, *Fgf15* was induced to a similar extent in both groups (Figure 1E). These findings argue against a primary defect in cellular BA uptake.

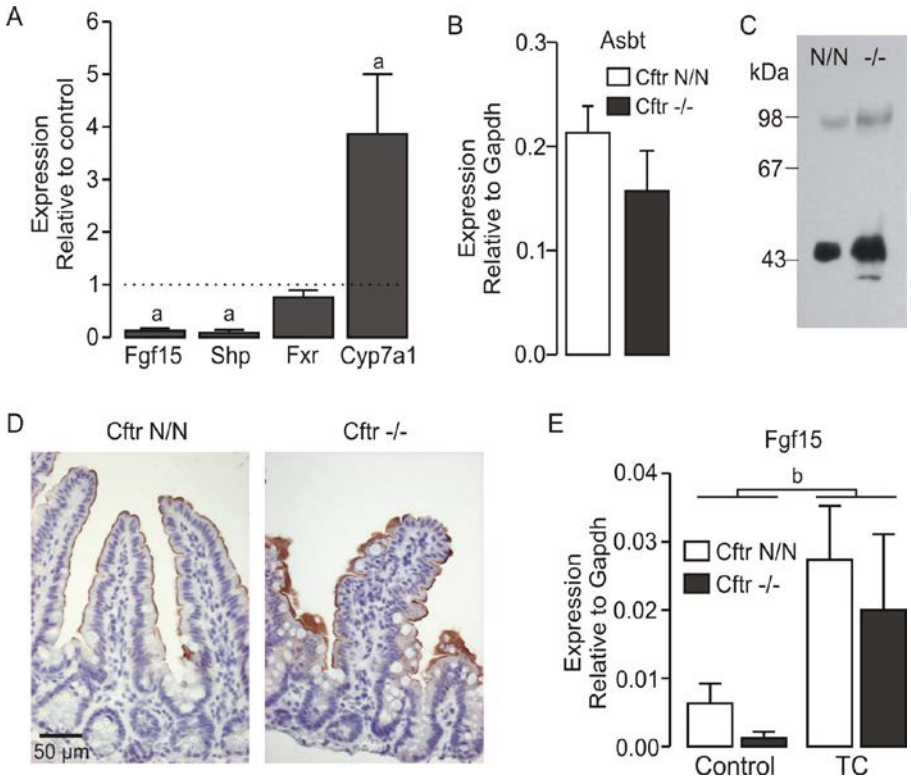


***Figure 1*** *FXR activity, ASBT localization, and TC-dependent gene induction in the CF ileum. A. Expression of Fxr and its target genes, Fgf15 and Shp, in the ileum, and of Cyp7a1 in the liver of CF mice (Cftr -/-) and controls (Cftr N/N). Data represent expression in a CF animal relative to an age/sex-matched littermate control.* [a]*A (paired) ratio t test indicated that Fgf15 (p = 0.005) and Shp (p = 0.006) expression were significantly reduced in CF mice, relative to controls, whereas expression of Cyp7a1 was increased (p = 0.002). Fxr expression was not affected. n = 5-8. B. Expression of Asbt in ileum of CF mice (Cftr -/-) and controls (Cftr N/N). C. ASBT protein was detected in brush border membranes prepared from CF (-/-) and control (N/N) ileum. Both the monomeric (46 kDa) and dimeric form were detected. Numerals to the left of the blot refer to the molecular mass (kDa) of protein standards. D. Immunohistochemical detection of ASBT. ASBT was localized at the apical aspect of epithelial cells of the villi in CF mice (Cftr -/-) and controls (Cftr N/N). E. Induction of gene expression by TC in ileal tissue sections of CF mice (Cftr -/-) and controls (Cftr N/N).* [b]*Two-way ANOVA indicated that TC treatment significantly enhanced Fgf15 expression (p = 0.01), independent of genotype. n = 3-5.*

***CFTR deficiency affects the composition, but not the size, of the luminal BA pool***

Because, *ex vivo*, FXR could be fully activated by exogenous BAs, we hypothesized that, *in vivo*, FXR activation may be curtailed by a low luminal BA level, as was suggested previously [16]. Therefore, we assessed the levels of the major BAs in the small intestinal lumen and in gastrointestinal tissues. This analysis showed that the BA content of the small intestinal lumen was similar in CF mice and controls (Figure 2A). The total amount of BA contained in the 4 compartments analyzed (representing most of the total pool) was also similar between genotypes. However, the composition of the luminal BA pool was changed by CFTR deficiency: β-MCA levels were markedly lower, whereas CA levels were higher than in control mice (Figure 2B). We have previously observed that hepatic CA synthesis is enhanced in CF mice, leading to a similar shift in the biliary β-MCA/CA ratio [15]. Low ileal *Fgf15* expression, enhanced hepatic BA synthesis, and low biliary β-MCA/CA ratios have been linked to enhanced intra-luminal conversion (deconjugation, dehydroxylation) of BAs upon gut microbiota modulation by probiotic bacterial strains [20]. Because CF mice display a distinct dysbiosis [24], it is conceivable that the reduced β-MCA/CA ratio observed in CF mice, similarly, results from enhanced BA biotransformation, interrupted enterohepatic cycling and increased *de novo* synthesis. However, arguing against enhanced intraluminal biotransformation, the level of the secondary BA deoxycholic acid (DCA) in the small intestinal lumen was similar in CF mice and controls (Figure 2B). Therefore, whereas the luminal BA composition in CF mice is indicative of enhanced hepatic BA synthesis, in line with attenuated FXR/FGF15 signaling, it does not provide evidence for reduced intestinal BA delivery or enhanced BA biotransformation.

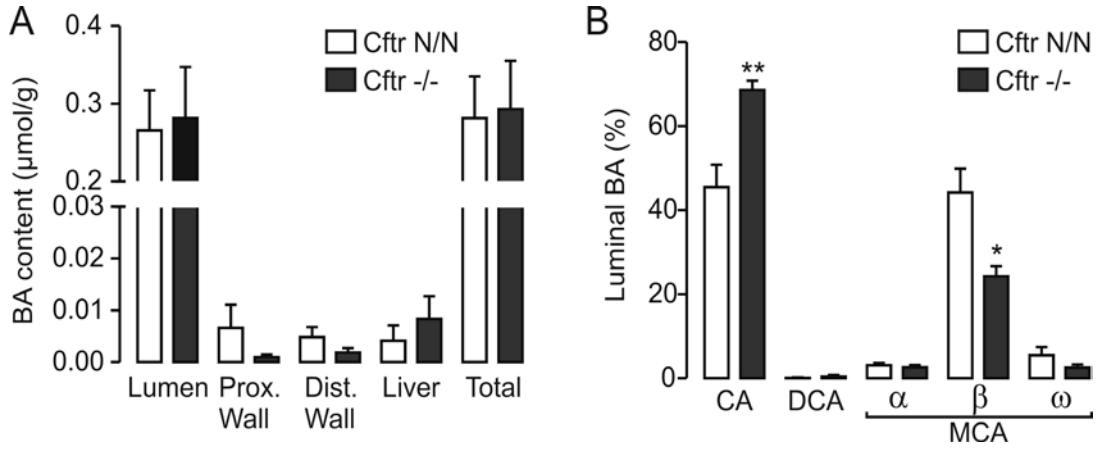


***Figure 2*** *Partitioning of BAs in gastrointestinal tissues and composition of the luminal BA pool. A. BA content, normalized to body mass, of the small intestinal lumen and gastrointestinal tissues in CF mice (Cftr -/-) and controls (Cftr N/N). The total levels shown are a summation of the 4 separate compartments analyzed. B. The relative contribution of the major BAs to the luminal pool. *p < 0.05, **p < 0.01, n = 4.*

***Antibiotic treatment corrects FXR signaling in CF mice***

In view of the tentative role of the gut microbiota in the regulation of FXR activity in CF mice, we assessed the effect of antibiotic treatment on FXR signaling. Previously, it was shown that complete eradication of the microflora strongly reduces *Fgf15* expression, as the gut microbiota appears to control the level of the FXR antagonist tauro-β-MCA [18]. Therefore we applied an antibiotic regimen that was previously shown not to fully eradicate the microflora, but to reduce small intestinal bacterial overgrowth, and increase bacterial community diversity in CF mice [25]. We found that, in CF mice, *Fgf15* and *Shp* expression were markedly enhanced by this particular regimen, up to the level observed in control animals, in which antibiotic treatment did not induce *Fgf15* or *Shp* (Figure 3A). In fact, antibiotic treatment appeared to moderately reduce the expression of *Fgf15* in controls, which may indicate that even this mild regimen leads to increased tauro-β-MCA levels and suppression of FXR activity. If present, this antagonistic action of tauro-β-MCA is apparently offset by a dominant FXR stimulatory effect in CF mice. Concomitant with induction of *Fgf15*, hepatic expression of *Cyp7a1* was reduced in CF mice (Figure 3B). These results strongly suggest that a CF-related dysbiosis, that is lost or reduced after antibiotic treatment, impairs intestinal FXR signaling.

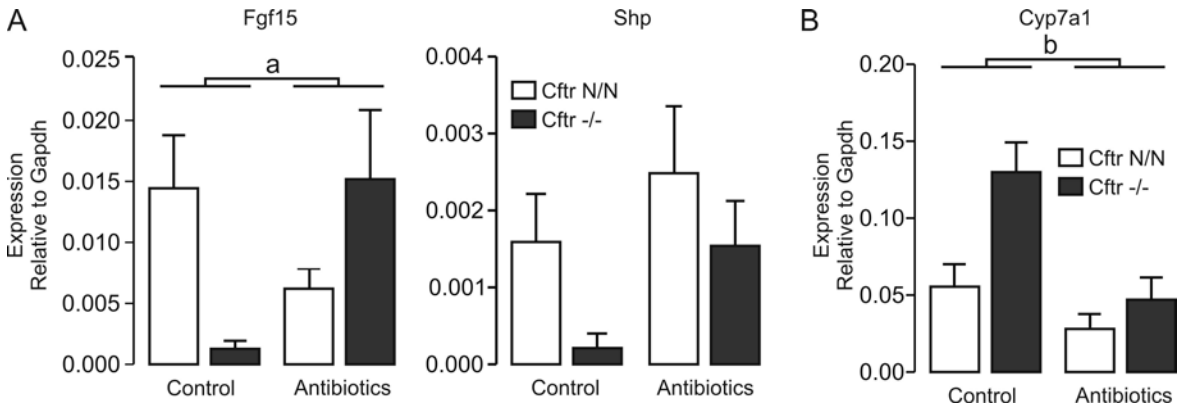


***Figure 3*** *The effect of antibiotic treatment on intestinal and hepatic gene expression. A. The effect of antibiotic treatment on ileal Fgf15 and Shp expression in CF mice (Cftr -/-) and littermate controls (Cftr N/N).* [a]*Two-way ANOVA indicated a statistically significant interaction between antibiotic treatment and Cftr genotype for Fgf15 expression (p = 0.03), implying that loss of CFTR affects the response to antibiotic treatment. n = 4-6. B. The effect of antibiotic treatment on hepatic Cyp7a1 expression.* [b]*Antibiotic treatment reduced Cyp7a1 expression (p = 0.02). n = 3-8.*

***Bacterial LPS abrogates FXR-dependent Fgf15 induction***

We considered that, apart from through its effect on BA biotransformation and uptake, the CF microbiota may reduce FXR activity via other mechanisms. Previously, it was shown that the activity of the retinoid X receptor (RXR) in the liver is attenuated by specific cytokines that are produced upon exposure to bacterial LPS [27-29]. As FXR forms an obligate heterodimer with RXR, we hypothesized that LPS may also impair intestinal FXR/RXR function. To test this hypothesis, we assessed the effect of LPS on *Fgf15* induction by the synthetic FXR agonist

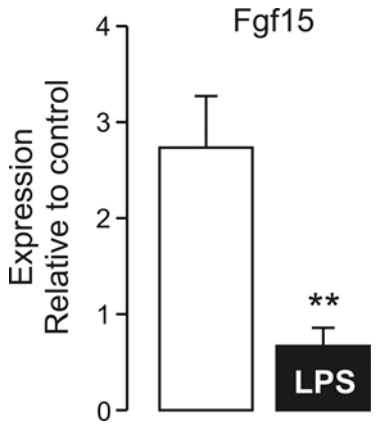


***Figure 4*** *Bacterial LPS inhibits FXR-dependent Fgf15 induction in mouse ileum. Induction of Fgf15 expression by GW4064 in the presence or absence of LPS. Data depict the level of gene expression relative to the level of expression in the absence of GW4064. **p < 0.01, n = 4.*

GW4064. These experiments showed that LPS exposure completely abrogated GW4064-dependent *Fgf15* expression in the ileum (Figure 4). These results are consistent with a previous study showing that pro-inflammatory cytokines (IL-1β, TNFα) suppress FXR activity in mouse ileum through an NFκB-dependent route [30], and indicate that the gut microbiota may suppress FXR/RXR signaling by triggering an endotoxin-provoked inflammatory response.

***The ileal CF transcriptome reveals impaired RXR function***

To assess whether bacterial endotoxins also suppress FXR/RXR activity in the CF intestine, *in vivo*, we performed transcriptome sequencing, followed by Ingenuity® Pathway Analysis (IPA), to identify canonical signaling pathways that were differentially regulated in CF ileum, compared to control tissue. Our model predicts that Toll-like receptor (TLR)-mediated activation of the NFκB and cJun-N-terminal kinase (JNK) pathways not only attenuates FXR signaling, but also signaling through other RXR binding partners [27-29, 31]. Because RXR forms obligate heterodimers with most lipid-sensing nuclear receptors, loss of its function is expected to impinge on the transcriptional regulation of many genes involved in BA and lipid metabolism.

Firstly, the IPA confirmed that FXR signaling was impaired in CF mice, as many differentially regulated FXR target genes were identified, including *Fgf15* and *Shp* (Figure 5A,

Table S2). Further, it provided compelling evidence for the activation of an immune response in the CF intestine, as exemplified by the up-regulation of many genes involved in antigen presentation (Figure 5A, Table S2). In fact, many of the most strongly up-regulated genes in the CF ileum are involved in host-microbe interactions and host defense, including NFκB-inducible chemokines and acute phase proteins, the *alarmin* IL-33, and the fucosyltransferase 2, which is induced by bacterial colonization of the gut, and was previously shown to increase mucin fucosylation in CF mice (Figure 5B) [32-34]. In line with the up-regulation of these immune response markers, upstream regulator analysis (URA) indicated strong activation of LPS- and cytokine-mediated, NFκB-dependent pro-inflammatory signaling in the CF ileum (Figure 5C).

Importantly, URA also indicated a concomitant marked inactivation of RXR heterodimer nuclear receptors, and many genes involved in lipid metabolism and transport appear to be dysregulated in the CF ileum (Figure 5C, Table S2). Of interest, this set includes the peroxisome proliferator activated nuclear receptor γ (PPARγ), which inactivation has previously been linked to CF intestinal disease (Figure 5C, Figure S1) [35]. The IPA suggests that repression of RXR is triggered by exposure to LPS and pro-inflammatory cytokines (Figure 5D). These data imply that CF is associated with an overall reduction in RXR-dependent signaling, which extends to nuclear receptors that are activated by ligands other than (conjugated) BAs. However, the expression of these receptors was unaffected, except for *Ppara* (Figure S2).

To substantiate the role of the CF-related dysbiosis in the pathogenesis of impaired FXR/RXR signaling, we performed transcriptome sequencing and IPA/URA on tissue from mice that were treated with antibiotics. As already indicated by our analysis of *Fgf15* and *Shp* expression, antibiotic treatment enhanced FXR signaling in CF mice (Figure 6A, Table S3). Further, antibiotic treatment suppressed the inflammatory response in the CF intestine, as exemplified by the down-regulation of genes involved in antigen presentation (Figure 6A, Table S3), host-microbe interactions, and host defense (Figure 6B). As expected, antibiotic treatment also affected the innate and adaptive immune response in control mice, but its effect on gene expression was generally more moderate than in the CF mice (Figure 6B). In CF mice, repression/reversal of the immune response after antibiotic treatment was also evident from the URA, showing inactivation of LPS- and cytokine-mediated, NFκB-dependent pro-inflammatory signaling, whereas signaling through RXR heterodimer nuclear receptors was restored (Figure 6C). Accordingly, IPA indicated that antibiotic treatment alleviates the repression of RXR function, imposed by LPS and pro-inflammatory cytokines (Figure 6D, Table S3). These results suggest that a CF-related dysbiosis represses RXR function, and, consequently, FXR signaling.

In a murine colitis model, it was shown that glucuronic acid conjugation of BAs is enhanced in inflamed tissue and that this prevents FXR activation [22]. An up-regulation of UDP-glucuronosyltransferase encoding genes was shown to be the crucial step in this mechanism. To assess the role of glucuronic acid conjugation in the CF-related FXR signaling

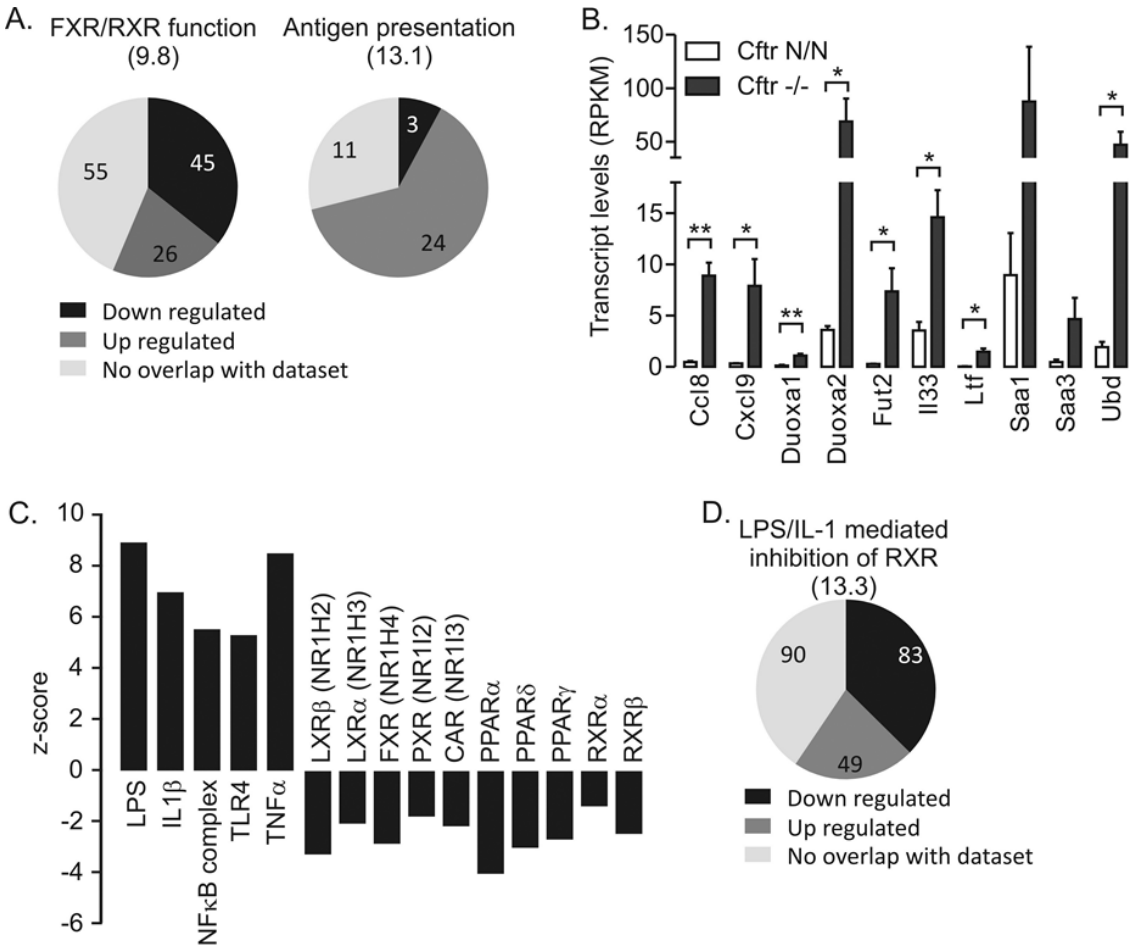


***Figure 5*** *Differentially regulated signal transduction pathways in the ileum of CF mice and controls. A. The ileal transcriptome of CF mice and controls was compared by IPA. Regulation of canonical pathways involving FXR/RXR function and antigen presentation were significantly affected by CF. B. Expression of genes involved in host-microbe interactions and host defense in the ileum of CF mice (Cftr -/-) and controls (Cftr N/N), assessed by transcriptome sequencing. Data depict reads per 1000 base pair transcript per million mapped reads (RPKM). *p < 0.05, **p < 0.01, n = 3. Ccl8: chemokine C-C motif ligand 8, Cxcl9: chemokine C-X-C motif ligand 9, Duoxa1/2: dual oxidase maturation factor A1/A2, Fut2: fucosyltransferase 2, Il33: Interleukin 33, Ltf: lactotransferrin, Saa1/3: serum amyloid A1/A3, Ubd: ubiquitin D (FAT10). C. URA based on ileal gene expression in CF mice, relative to controls. D. IPA indicates that repression of RXR in the CF ileum is triggered by LPS and IL-1β. Numerals in the pie charts refer to the number of genes represented by each segment. Numerals in parentheses are –log(overlap p-value).*

defect, we determined the level of UDP-glucuronosyltransferase-encoding transcripts in CF mice and controls. We found that none of the UDP-glucuronosyltransferases identified were up-regulated, suggesting that glucuronic acid conjugation of BAs is not enhanced in the CF intestine (Figure S3).

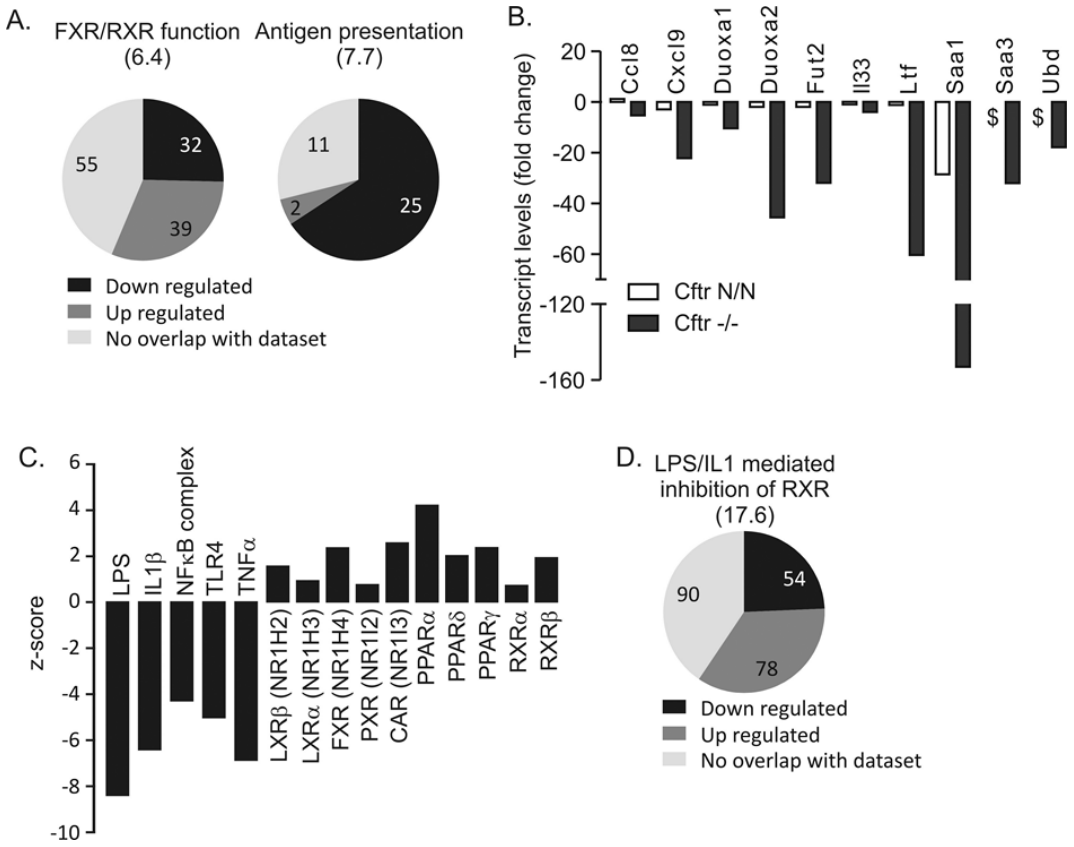


***Figure 6 Effect of antibiotic treatment on differentially regulated signal transduction pathways in the ileum of CF mice.*** *A. The ileal transcriptome of antibiotic-treated and conventionally reared CF mice was compared by IPA. Regulation of canonical pathways involving FXR/RXR function, and antigen presentation were significantly affected by antibiotic treatment. B. Effect of antibiotic treatment on the expression of genes involved in host-microbe interactions and host defense in CF mice (Cftr -/-) and controls (Cftr N/N), as assessed by transcriptome sequencing. Data denote fold change relative to the expression in conventionally reared animals. $Not detected in antibiotic treated tissue. C. URA based on ileal gene expression in antibiotic treated, relative to conventionally reared CF mice. D. IPA indicates that antibiotic treatment alleviates repression of RXR function in the CF ileum. Numerals in the pie charts refer to the number of genes represented by each segment. Numerals in parentheses are –log(overlap p-value).*

***Impaired intestinal FXR signaling reduces BA-dependent hepatic cell proliferation***

FGF15-dependent hepatic cell proliferation was shown to promote liver regeneration after injury, and it was proposed that this intestine-liver signaling axis also drives homeotrophic liver growth/repair [6, 7, 36]. It was shown that, through activation of this axis, dietary CA supplementation increases liver mass [36].

To investigate whether impaired FXR/RXR signaling in the CF intestine affects this intestine-liver signaling axis, we assessed the effect of dietary CA supplementation on liver mass, and intestinal and hepatic expression of FXR target genes. We found that CA supplementation induced *Fgf15*, and enhanced production of FGF15 protein in both genotypes, but that this effect was markedly more pronounced in control than in CF mice (Figures 7A, 7B). In control mice, the strong stimulation of FGF15 production elicited by CA supplementation was associated with a marked increase in liver mass (Figure 7C). In contrast, in CF mice, this trophic response was lost completely. In accord with the low FGF15 production observed in CF mice, *Cyp7a1* expression was much less effectively suppressed in CA fed CF mice than in controls (Figure 7D). However, the regulation of genes that are controlled (predominantly) through hepatic FXR was not affected: CA supplementation suppressed *Cyp8b1* expression, and induced hepatic *Shp*, to a similar extent in CF mice and controls (Figure 4D) [2, 5, 37].

These results demonstrate that dietary CA supplementation fails to correct FXR signaling in the ileum, but leads to apparently normal activation of hepatic FXR. The loss of intestinal FXR activity markedly reduced the trophic effect of BAs on the CF liver, and impaired the feedback regulation exerted on hepatic BA synthesis. Because the CA dose used in these experiments was >100-fold in excess of the estimated daily amount entering the intestine through biliary secretion and is predicted to saturate the capacity for intra-luminal conversion and absorption [38], these data further argue against the notion that biotransformation limits BA uptake and FXR activity in CF mice.

**Discussion**

This study shows that signaling through the BA-activated nuclear receptor FXR is markedly impaired in the distal small intestine of CF mice. Impaired intestinal FXR signaling compromised FGF15-dependent regulation of hepatic cell proliferation and BA synthesis. This defect was associated with an up-regulation of genes involved in the innate and adaptive immune response, and suppression of RXR signaling. Antibiotic treatment attenuated the immune response, and restored FXR and RXR activity in the CF ileum. Conversely, LPS treatment of non-CF ileum elicited a CF-like phenotype, i.e. strong repression of FXR-dependent *Fgf15*

induction. These data suggest that a CF-related inflammatory response suppresses signaling

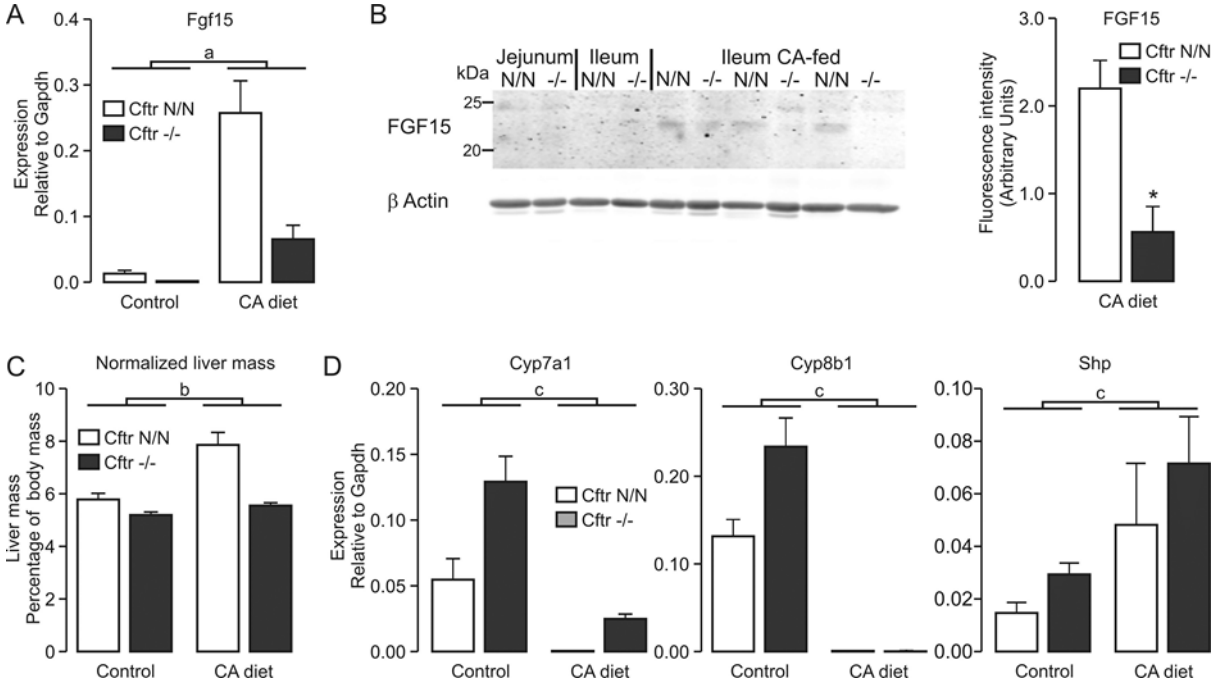


***Figure 7*** *The effect of dietary BA supplementation on FXR signaling. CF mice (Cftr -/-) and controls (Cftr N/N) were fed a CA-enriched or a conventional diet. A. Induction of intestinal Fgf15.* [a]*Two-way ANOVA indicated a significant interaction between CA intake and Cftr genotype for the effect on Fgf15 expression (p = 0.0001), implying that loss of CFTR affects the response to dietary CA supplementation. Control data as shown in Figure 3. n = 3-6. B. FGF15 protein was below detection levels in jejunal and ileal tissue of mice fed a control diet. CA feeding increased FGF15 levels in both CF mice and controls, but this effect was more pronounced in controls. Numerals to the left of the blot refer to the molecular mass (kDa) of protein standards. The bar diagram depicts the intensity of the fluorescent signal of the FGF15 band relative to the β-actin signal of the same sample. *p < 0.05, n = 3. C. Effect of CA supplementation on liver mass.* [b]*Two-way ANOVA indicated a statistically significant interaction between CA feeding and Cftr genotype for the effect on liver mass (p = 0.004), implying that loss of CFTR affects the response to dietary CA supplementation. n = 3-6. D. Effect of dietary BA supplementation on hepatic gene expression.* [c]*Two-way ANOVA indicated that CA feeding suppressed hepatic Cyp7a1 (p = 0.001) and Cyp8b1 (p = 0.0001) expression, but enhanced expression of Shp (p = 0.003).*

through these nuclear receptors.

It has been proposed that bacterial modification (deconjugation, dehydroxylation) of intraluminal BAs may reduce their uptake via ASBT and, consequently, FXR activity [20]. Because CF is associated with small intestinal bacterial overgrowth [24], this model accounts for the fact that FXR signaling is impaired in CF mice. Indeed, we observed that suppression of bacterial growth (by antibiotic treatment) enhanced FXR signaling, specifically in CF mice,

indicating that the CF microbiota does play a role in the down-regulation of FXR signaling. Because much of the microflora will be lost upon tissue isolation, this model also accounts for the observation that TC exposure triggered normal levels of *Fgf15* induction in tissue explants.

However, not all our results are consistent with the above model, suggesting that other factors play a more decisive role. Key to this notion was the observation that dietary CA supplementation induced some hepatic FXR target genes to a similar extent in CF mice and controls, which seems incongruent with low BA absorption, whereas the intestinal FXR signaling defect persisted. In fact, the dosage used in these experiments was projected to result in luminal BA levels well in excess of those occurring naturally, and it seems implausible that, under these conditions, microbial biotransformation could have such an overriding effect on BA uptake and intestinal FXR activity. Furthermore, the IPA showed that signaling through other RXR heterodimer forming nuclear receptors, that are activated by ligands other than BAs and are unlikely to be strongly affected by a purported reduction in BA uptake, was also down-regulated. This led us to consider that a common mechanism, unrelated to BA biotransformation, underlies the suppression of FXR and other ligand-dependent nuclear receptors in the CF ileum.

The acute activation of NFκB and JNK in response to bacterial LPS or pro-inflammatory cytokines plays a central role in the defense against pathogens. NFκB induces the transcription of an array of genes involved in the inflammatory response, and also modulates the activity of several nuclear receptors; its p65 subunit was shown to interact directly with RXR, to prevent binding of the PXR/RXR heterodimer to DNA regulatory sequences [29]. Activation of JNK was shown to induce phosphorylation of RXR, and reduce its nuclear localization [27, 28, 31]. Consistent with this role of NFκB and JNK in RXR repression, LPS treatment inhibited the activity of the RXR heterodimers of FXR and PXR in hepatocytes [21, 29, 39], and it was observed that TNFα and IL-1β, cytokines that trigger the canonical NFκB pathway, repress intestinal FXR/RXR activity [30]. In line with these data, we show here that LPS strongly repressed FXR-dependent *Fgf15* induction in non-diseased ileum, essentially mimicking the repression of FXR/RXR activity found *in vivo* in the CF intestine. These data indicate that a bacterial endotoxin-induced inflammatory response may impair FXR/RXR function in the gut. This notion is supported by the IPA, which revealed a marked activation of the innate and adaptive immune response, coinciding with impaired FXR and RXR signaling. The IPA indicated that repression of RXR is triggered by LPS and pro-inflammatory cytokines, leading to recruitment of TAK1 (TGFβ-activated kinase 1) and IKK (inhibitor of nuclear factor-κB kinase) complexes and subsequent activation of NFκB and JNK. Further, the IPA showed that antibiotic treatment ameliorated the inflammatory response, and restored FXR/RXR function in the CF

ileum. Therefore, we propose that local inflammation of the gut wall, most plausibly though activation of the NFκB and/or JNK pathways, suppresses RXR activity in the CF ileum, leading to a concomitant inhibition of FXR activity.

In mice, both complete FGF15 deficiency and suppression of FGF15 production by microbiota modification were shown to markedly enhance the fecal excretion of BAs [5, 20]. Our current findings indicate that the fecal BA wasting observed in CF mice may, similarly, result from low FGF15 production and impaired feedback regulation of BA synthesis (Figure S4). Consistent with this model, some studies have shown that biliary BA secretion is enhanced in CF mice [14, 15]. Because it does not imply an epithelial transport defect, this model also accounts for the fact that a correlation between enhanced excretion and reduced uptake of BAs has proved difficult to establish, in CF mice as well as in patients [40, 41]. It may also explain why the presentation of fecal BA wasting is quite variable between patients, as any factor that affects the gut microbiota and the host immune response (e.g. diet, antibiotic use, intestinal obstruction) may act to modulate FXR signaling and BA handling. The same probably holds true for CF mouse models. For instance, liquid diets or oral laxatives, often applied to prevent luminal dehydration and intestinal obstruction in CF mice, were shown to strongly affect the intestinal bacterial load [42]. Therefore, it is important to note that the animals used at present were reared on a solid diet and were withheld laxative several days before experimentation.

This model for the pathogenesis of CF-related fecal BA wasting shows distinct similarities to the one proposed for idiopathic BA malabsorption (chronic BA diarrhea). As for CF, anomalous BA handling in this syndrome was initially attributed to impaired reabsorption of BAs, although evidence for a primary defect in epithelial translocation proved elusive (reviewed by Hofmann, Mangelsdorf [43]). More recently, it has been linked to abnormally low plasma FGF19 levels, causing impaired feedback regulation of BA synthesis, enhanced intestinal BA delivery, saturation of ASBT, and increased spillage of BAs to the colon [44]. Upon entering the colon, BAs provoke secretory diarrhea via a CFTR-dependent mechanism (perhaps ironically, implying CF patients would not be afflicted). Whether in idiopathic BA malabsorption low plasma FGF19 levels are linked to changes in the gut microbiota, or even reduced intestinal FXR activity, has, however, not been established.

Although not the focus of the present investigation, we surmise that an intestinal FXR signaling defect may also be of consequence for the pathophysiology of CFLD. Firstly, by enhancing BA synthesis and reducing the capacity for homeostatic liver regeneration, repression of intestinal FXR/FGF19 signaling may contribute to the progression of the cholangiopathy typical of CF [8]. Secondly, impaired intestinal FXR signaling may enhance exposure of the

liver to endotoxins, as it was shown that FXR deficiency, in conjunction with dysbiosis, compromises epithelial barrier function [45]. Congruent with this scenario, it was shown that a chemically induced colitis exacerbates liver disease in CF mice, and a pathogenic role of gut-derived bacterial products was indicated [11]. Indeed, although focal biliary cirrhosis is thought to result primarily from the loss of local CFTR activity, it is also apparent that some gastrointestinal manifestations of CF, like pancreatic insufficiency and a history of meconium ileus, seem to predispose to the development of CFLD [10, 46, 47]. It is conceivable that such manifestations impact the gut microbiota and host-microbe interactions, potentially leading to inflammation of the gut wall and repression of FXR. Collectively, these data imply that intestinal inflammation and FXR dysfunction may contribute to the pathogenesis of biliary cirrhosis, suggesting that therapeutic interventions aimed at restoring FXR signaling may slow the progression of CFLD.

## Experimental procedures

### *Animal procedures and tissue collection*

CF mice (*Cftr*$^{tm1Cam}$; congenic FVB/n) and littermate controls were maintained in individually ventilated cages in an environmentally controlled facility at the Erasmus MC. Animals were reared on a low fiber diet (C1013; Altromin) and a polyethylene glycol/electrolyte dinking solution to prevent intestinal obstruction in early life [48]. In some instances, before further experimentation, animals were administered either a diet supplemented with CA (0.5%), or drinking water supplemented with ciprofloxacin (0.3 g/L) and metronidazole (0.5 g/L) for 15 days [25]. Intake of food and water was monitored during this period, and shown to be comparable between genotypes (not shown).

Before tissue collection, animals (13-22 weeks) were kept on normal drinking water (or, when applicable, drinking water supplemented with antibiotics) for >4 days, which is well tolerated by adult CF mice. Animals were anaesthetized (ketamine 120 mg/kg, xylazine 20 mg/kg; i.p.), and the intestinal tract and liver were collected, and flushed or rinsed, respectively, with ice-cold saline. Sampling from a CF animal and a sex-matched littermate control was performed within a time window of 20 min, and between 12:00-14:00h, to control for diurnal variations in gene expression. Experiments were approved by the Independent Committee on Ethical Use of Experimental Animals, Rotterdam, according to national guidelines (120-0402/0501/0503/0902; 141-1204/1208/1210).

***Intestinal and hepatic gene expression***

For gene expression studies, two ileal sections (3-5 mm in length) were collected, at 0.5-1.5 and 5-6 cm proximal to the ileocecal valve. Liver tissue was sampled from the right lobe. Tissue homogenization, RNA extraction, and quantitative PCR (primer sequences shown in Table S1) was performed as described elsewhere [49]. Median values of assays performed in triplicate were used to determine gene expression levels, relative to *Gapdh*. To correct for regional differences in gene expression in the distal small intestine, mean values of the relative expression levels at the 2 sampling locations are presented.

***Ex vivo FXR-dependent induction of intestinal gene expression***

For assessing BA-dependent induction of gene expression, 2 contiguous sections of the small intestine were collected, 3-5 cm proximal to the ileocecal valve. Mucosal tissue sheets were mounted in Ussing chambers and bathed in modified Meyler solution, gassed with 95% $O_2$-5% $CO_2$, at 37°C, as described previously [40]. After a 40 min equilibration period, the solution bathing the luminal side of one tissue sheet was supplemented with TC (0.25 mmol/L), while the other section served as vehicle (water) control. After 1h, tissue was collected and processed for RNA extraction (see above). For assessing the effect of bacterial LPS on FXR-dependent gene induction, ileal tissue sections were incubated for 18h with the FXR agonist GW4064 (1 µmol/L), in the presence or absence of LPS (*Salmonella enterica*; 10 µg/mL), in Dulbecco Modified Eagle's Medium, supplemented with fetal calf serum (10%), penicillin (50 U/mL), and streptomycin (0.005%), at 37°C, in 5% $CO_2$. Gene expression was assessed as outlined above.

***Transcriptome sequencing***

Transcriptome sequencing was performed at the Beijing Genomics Institute. In brief, mRNA was isolated from total tissue RNA extracts (200 ng), fragmented, and, subsequently used for cDNA synthesis. The resulting cDNA library was sequenced using an HiSeq 2000 sequencer (TruSeq SBS KIT-HS V3; Illumina). Data were processed using CLC genomic workbench 7.5 (CLC Bio), and the sequence reads were mapped to the Genome Reference Consortium (GRC) genome data set GRCm38.76, using default parameters.

***Detection of ASBT and FGF15 by Western analysis***

For ASBT detection, brush border membrane fractions were prepared from the distal 8 cm of the small intestine, as described in detail elsewhere [50]. For FGF15 detection, ileal tissue was excised 2-5 cm proximal to the ileocecal valve, and epithelial cells were gently scraped of the underlying connective tissue layers, using a glass cover slip. Cell and brush border

membrane preparations were lysed by brief sonication (3 15s bursts) in ice-cooled NaCl (150 mmol/L), Tris/HCl pH 7.6 (25 mmol/L), Triton X100 (1%), sodium deoxycholate (1%), sodium dodecylsulphate (0.1%), NaF (5 mmol/L), $Na_3VO_4$ (3 mmol/L), supplemented with a protease inhibitor cocktail. The resulting lysates were subjected to SDS-PAGE, and proteins were transferred to nitrocellulose membrane. ASBT was detected using a polyclonal antibody directed against hamster ASBT [51]. FGF15 was detected using a polyclonal antibody directed against an epitope of mouse origin (SC27177; Santa Cruz). A fluorescent dye-labeled secondary antibody and the Odyssey infrared imaging system (Application software 3, Licor Biosciences) were used for quantification of the FGF15 signal. Detection of β-actin served as loading control (SC47778; Santa Cruz).

***Immunohistochemistry***

Paraformaldehyde-fixed, paraffin-embedded tissue sections (5 µm) of the distal small intestine (excised 2-4 cm proximal to the ileocecal valve), were probed with ASBT antibody (see above), followed by an anti-rabbit IgG horseradish peroxidase-conjugated secondary antibody. Immune complexes were visualized by incubation with 3,3-diaminobenzidine tetrahydrochloride, and sections were counterstained with hematoxylin.

***Analysis of BA in luminal eluates and gastrointestinal tissues***

Tissue was collected from anesthetized animals, as outlined above. To collect its contents, the intestinal lumen was rinsed with 10 mL ice-cold phosphate buffered saline. The intestine was subsequently divided in a proximal section (2/3 of the entire length) and a distal section. Tissue samples and eluates were weighed and the former were homogenized in ice-cold phosphate buffered saline. After samples were saponified in NaOH (1 mol/L; in methanol), BAs were extracted on Sep-Pak C18 cartridges (Mallinckrodt Baker). BAs were analyzed as unconjugated, methyl ester-trimethylsilyl ether derivatives, by capillary gas chromatography [52].

***Data analysis***

The statistical significance of differences between mean levels of gene expression, FGF15 abundance and tissue BAs in CF and wildtype mice were analyzed by Student's *t* test (2 sided). The effect of BA and antibiotic treatment on gene expression in CF mice and controls was analyzed by 2-way ANOVA (Graphpad Prism 5, Graphpad Software). Data shown are means ± SE.

Transcriptome data were analyzed using the Ingenuity® software application (Version 1.10; Qiagen). IPA/URA was applied to identify differentially regulated pathways and their upstream modulators, as described in detail elsewhere [53]. For identification of canonical signaling pathways that were differentially regulated in the ileum of CF mice, compared to controls, transcriptome data from 3 sex-matched (2F/1M) littermate couples were used. For each couple and transcript, expression in the *Cftr* -/- animal was calculated relative to the respective *Cftr* N/N control. Identification of differentially regulated signaling pathways was based on those genes that, on average, were up- or down-regulated by a factor of ≥2. To assess the effect of the antibiotic treatment on ileal gene expression, for each genotype, the expression in one treated animal was expressed relative to the average expression level in the untreated animals, and the analysis was performed on genes that were up- or down-regulated by a factor of ≥2. To identify differentially regulated pathways, the enrichment of the dataset with up- or down-regulated genes comprised within a signal transduction network was assessed (overlap p-value). To assess the activation state of a pathway and its upstream regulator, the consistency of the match between the observed and the predicted (based on established interactions within a network) expression pattern was calculated (activation z-score). A positive z-score signifies a regulator in the active state, a negative score indicates that its activity is repressed.

**Acknowledgements**

The authors would like to thank Renze Boverhof (University Medical Center Groningen) for excellent technical assistance, and Dr. Luis B. Agellon (McGill University, Montréal, Canada) for kindly donating the ASBT antibody.

**References**

[1] Hofmann AF. Biliary secretion and excretion in health and disease: current concepts. Ann Hepatol. 2007;6:15-27.
[2] Kim I, Ahn SH, Inagaki T, Choi M, Ito S, Guo GL, et al. Differential regulation of bile acid homeostasis by the farnesoid X receptor in liver and intestine. J Lipid Res. 2007;48:2664-72.
[3] Jung D, Inagaki T, Gerard RD, Dawson PA, Kliewer SA, Mangelsdorf DJ, et al. FXR agonists and FGF15 reduce fecal bile acid excretion in a mouse model of bile acid malabsorption. J Lipid Res. 2007;48:2693-700.
[4] Song KH, Li T, Owsley E, Strom S, Chiang JY. Bile acids activate fibroblast growth factor 19 signaling in human hepatocytes to inhibit cholesterol 7alpha-hydroxylase gene expression. Hepatology. 2009;49:297-305.
[5] Inagaki T, Choi M, Moschetta A, Peng L, Cummins CL, McDonald JG, et al. Fibroblast growth factor 15 functions as an enterohepatic signal to regulate bile acid homeostasis. Cell Metab. 2005;2:217-25.
[6] Uriarte I, Fernandez-Barrena MG, Monte MJ, Latasa MU, Chang HC, Carotti S, et al. Identification of fibroblast growth factor 15 as a novel mediator of liver regeneration and its application in the prevention of post-resection liver failure in mice. Gut. 2013;62:899-910.
[7] Zhang L, Wang YD, Chen WD, Wang X, Lou G, Liu N, et al. Promotion of liver regeneration/repair by farnesoid X receptor in both liver and intestine in mice. Hepatology. 2012;56:2336-43.
[8] Modica S, Petruzzelli M, Bellafante E, Murzilli S, Salvatore L, Celli N, et al. Selective Activation of Nuclear Bile Acid Receptor FXR in the Intestine Protects Mice Against Cholestasis. Gastroenterology. 2012;142:355-U269.
[9] Staufer K, Halilbasic E, Trauner M, Kazemi-Shirazi L. Cystic fibrosis related liver disease: another black box in hepatology. Int J Mol Sci. 2014;15:13529-49.
[10] Lamireau T, Monnereau S, Martin S, Marcotte JE, Winnock M, Alvarez F. Epidemiology of liver disease in cystic fibrosis: a longitudinal study. J Hepatol. 2004;41:920-5.
[11] Fiorotto R, Scirpo R, Trauner M, Fabris L, Hoque R, Spirli C, et al. Loss of CFTR affects biliary epithelium innate immunity and causes TLR4-NF-kappaB-mediated inflammatory response in mice. Gastroenterology. 2011;141:1498-508.
[12] Strandvik B, Einarsson K, Lindblad A, Angelin B. Bile acid kinetics and biliary lipid composition in cystic fibrosis. J Hepatol. 1996;25:43-8.
[13] Bijvelds MJC, Bronsveld I, Havinga R, Sinaasappel M, de Jonge HR, Verkade HJ. Fat absorption in cystic fibrosis mice is impeded by defective lipolysis and post-lipolytic events. Am J Physiol. 2005;288:G646-G53.
[14] Freudenberg F, Broderick AL, Yu BB, Leonard MR, Glickman JN, Carey MC. Pathophysiological basis of liver disease in cystic fibrosis employing a DF508 mouse model. Am J Physiol. 2008;294:G1411-G20.
[15] Bodewes FA, Wouthuyzen-Bakker M, Bijvelds MJC, Havinga R, de Jonge HR, Verkade HJ. Ursodeoxycholate modulates bile flow and bile salt pool independently from the cystic fibrosis transmembrane regulator (Cftr) in mice. Am J Physiol. 2012;302:G1035-G42.
[16] Debray D, Rainteau D, Barbu V, Rouahi M, El Mourabit H, Lerondel S, et al. Defects in gallbladder emptying and bile Acid homeostasis in mice with cystic fibrosis transmembrane conductance regulator deficiencies. Gastroenterology. 2012;142:1581-91 e6.
[17] Bodewes FA, Bijvelds MJC, de Vries W, Baller JF, Gouw AS, de Jonge HR, et al. Cholic acid induces a Cftr dependent biliary secretion and liver growth response in mice. PLoS One. 2015;10:e0117599.
[18] Sayin SI, Wahlstrom A, Felin J, Jantti S, Marschall HU, Bamberg K, et al. Gut microbiota regulates bile acid metabolism by reducing the levels of tauro-beta-muricholic acid, a naturally occurring FXR antagonist. Cell Metab. 2013;17:225-35.

[19] Out C, Patankar JV, Doktorova M, Boesjes M, Bos T, de Boer S, et al. Gut microbiota inhibit Asbt-dependent intestinal bile acid reabsorption via Gata4. J Hepatol. 2015;63:697-704.
[20] Degirolamo C, Rainaldi S, Bovenga F, Murzilli S, Moschetta A. Microbiota modification with probiotics induces hepatic bile acid synthesis via downregulation of the Fxr-Fgf15 axis in mice. Cell Rep. 2014;7:12-8.
[21] Wang YD, Chen WD, Wang M, Yu D, Forman BM, Huang W. Farnesoid X receptor antagonizes nuclear factor kappaB in hepatic inflammatory response. Hepatology. 2008;48:1632-43.
[22] Zhou X, Cao L, Jiang C, Xie Y, Cheng X, Krausz KW, et al. PPARalpha-UGT axis activation represses intestinal FXR-FGF15 feedback signalling and exacerbates experimental colitis. Nat Commun. 2014;5:4573.
[23] Rau M, Stieger B, Monte MJ, Schmitt J, Jahn D, Frey-Wagner I, et al. Alterations in Enterohepatic Fgf15 Signaling and Changes in Bile Acid Composition Depend on Localization of Murine Intestinal Inflammation. Inflamm Bowel Dis. 2016;22:2382-9.
[24] Norkina O, Burnett TG, De Lisle RC. Bacterial overgrowth in the cystic fibrosis transmembrane conductance regulator null mouse small intestine. Infect Immun. 2004;72:6040-9.
[25] Lynch SV, Goldfarb KC, Wild YK, Kong W, De Lisle RC, Brodie EL. Cystic fibrosis transmembrane conductance regulator knockout mice exhibit aberrant gastrointestinal microbiota. Gut Microbes. 2013;4:41-7.
[26] Norkina O, Kaur S, Ziemer D, De Lisle RC. Inflammation of the cystic fibrosis mouse small intestine. Am J Physiol. 2004;286:G1032-G41.
[27] Ghose R, Zimmerman TL, Thevananther S, Karpen SJ. Endotoxin leads to rapid subcellular re-localization of hepatic RXRalpha: A novel mechanism for reduced hepatic gene expression in inflammation. Nucl Recept. 2004;2:4.
[28] Schneider Aguirre R, Karpen SJ. Inflammatory mediators increase SUMOylation of retinoid X receptor alpha in a c-Jun N-terminal kinase-dependent manner in human hepatocellular carcinoma cells. Mol Pharmacol. 2013;84:218-26.
[29] Gu X, Ke S, Liu D, Sheng T, Thomas PE, Rabson AB, et al. Role of NF-kappaB in regulation of PXR-mediated gene expression: a mechanism for the suppression of cytochrome P-450 3A4 by proinflammatory agents. J Biol Chem. 2006;281:17882-9.
[30] Gadaleta RM, Oldenburg B, Willemsen EC, Spit M, Murzilli S, Salvatore L, et al. Activation of bile salt nuclear receptor FXR is repressed by pro-inflammatory cytokines activating NF-kappaB signaling in the intestine. Biochim Biophys Acta. 2011;1812:851-8.
[31] Bruck N, Bastien J, Bour G, Tarrade A, Plassat JL, Bauer A, et al. Phosphorylation of the retinoid x receptor at the omega loop, modulates the expression of retinoic-acid-target genes with a promoter context specificity. Cell Signal. 2005;17:1229-39.
[32] Goto Y, Uematsu S, Kiyono H. Epithelial glycosylation in gut homeostasis and inflammation. Nat Immunol. 2016;17:1244-51.
[33] Reid-Yu SA, Tuinema BR, Small CN, Xing L, Coombes BK. CXCL9 contributes to antimicrobial protection of the gut during citrobacter rodentium infection independent of chemokine-receptor signaling. PLoS Pathog. 2015;11:e1004648.
[34] Thomsson KA, Hinojosa-Kurtzberg M, Axelsson KA, Domino SE, Lowe JB, Gendler SJ, et al. Intestinal mucins from cystic fibrosis mice show increased fucosylation due to an induced Fucalpha1-2 glycosyltransferase. Biochem J. 2002;367:609-16.
[35] Harmon GS, Dumlao DS, Ng DT, Barrett KE, Dennis EA, Dong H, et al. Pharmacological correction of a defect in PPAR-gamma signaling ameliorates disease severity in Cftr-deficient mice. Nat Med. 2010;16:313-8.
[36] Huang W, Ma K, Zhang J, Qatanani M, Cuvillier J, Liu J, et al. Nuclear receptor-dependent bile acid signaling is required for normal liver regeneration. Science. 2006;312:233-6.

[37] Kong B, Wang L, Chiang JY, Zhang Y, Klaassen CD, Guo GL. Mechanism of tissue-specific farnesoid X receptor in suppressing the expression of genes in bile-acid synthesis in mice. Hepatology. 2012;56:1034-43.
[38] Craddock AL, Love MW, Daniel RW, Kirby LC, Walters HC, Wong MH, et al. Expression and transport properties of the human ileal and renal sodium- dependent bile acid transporter. Am J Physiol. 1998;274:G157-G69.
[39] Zhou C, Tabb MM, Nelson EL, Grun F, Verma S, Sadatrafiei A, et al. Mutual repression between steroid and xenobiotic receptor and NF-kappaB signaling pathways links xenobiotic metabolism and inflammation. J Clin Invest. 2006;116:2280-9.
[40] Bijvelds MJC, Jorna H, Verkade HJ, Bot AGM, Hofmann F, Agellon LB, et al. Activation of CFTR by ASBT-mediated bile salt absorption. Am J Physiol. 2005;289:G870-G9.
[41] Thompson GN, Davidson GP. In vivo bile acid uptake from terminal ileum in cystic fibrosis. Pediatr Res. 1988;23:323-8.
[42] De Lisle RC, Roach E, Jansson K. Effects of laxative and N-acetylcysteine on mucus accumulation, bacterial load, transit, and inflammation in the cystic fibrosis mouse small intestine. Am J Physiol. 2007;293:G577-G84.
[43] Hofmann AF, Mangelsdorf DJ, Kliewer SA. Chronic diarrhea due to excessive bile acid synthesis and not defective ileal transport: a new syndrome of defective Fibroblast Growth Factor 19 release. Clin Gastroenterol Hepatol. 2009;7:1151-4.
[44] Walters JR, Tasleem AM, Omer OS, Brydon WG, Dew T, le Roux CW. A new mechanism for bile acid diarrhea: defective feedback inhibition of bile acid biosynthesis. Clin Gastroenterol Hepatol. 2009;7:1189-94.
[45] Inagaki T, Moschetta A, Lee YK, Peng L, Zhao G, Downes M, et al. Regulation of antibacterial defense in the small intestine by the nuclear bile acid receptor. Proc Natl Acad Sci U S A. 2006;103:3920-5.
[46] Wilschanski M, Rivlin J, Cohen S, Augarten A, Blau H, Aviram M, et al. Clinical and genetic risk factors for cystic fibrosis-related liver disease. Pediatrics. 1999;103:52-7.
[47] Colombo C, Battezzati PM, Crosignani A, Morabito A, Costantini D, Padoan R, et al. Liver disease in cystic fibrosis: a prospective study on incidence, risk factors, and outcome. Hepatology. 2002;36:1374-82.
[48] Xiao F, Li J, Singh AK, Riederer B, Wang J, Sultan A, et al. Cystic fibrosis transmembrane conductance regulator mutant F508del membrane expression rescues epithelial HCO3- secretion in murine intestine. J Physiol. 2012.
[49] Ikpa PT, Sleddens HFBM, Steinbrecher KA, Peppelenbosch MP, De Jonge HR, Smits R, et al. Guanylin and uroguanylin are produced by mouse intestinal epithelial cells of columnar and secretory lineage. Histochem Cell Biol. 2016;146:445-55.
[50] van Dommelen FS, Hamer CM, De Jonge HR. Efficient entrapment of large and small compounds during vesiculation of intestinal microvilli. Biochem J. 1986;236:771-8.
[51] Torchia EC, Stolz A, Agellon LB. Differential modulation of cellular death and survival pathways by conjugated bile acids. BMC Biochem. 2001;2:11.
[52] Gerhardt KO, Gehrke CW, Rogers IT, Flynn MA, Hentges DJ. Gas-liquid chromatography of fecal neutral steriods. J Chromatogr. 1977;135:341-9.
[53] Krämer A, Green J, Pollard J, Jr., Tugendreich S. Causal analysis approaches in Ingenuity Pathway Analysis. Bioinformatics. 2014;30:523-30.

**Supplementary data**

**Impaired intestinal farnesoid X receptor signaling in cystic fibrosis mice**

Pauline T. Ikpa, Marcela Doktorova, Kelly F. Meijsen, Natascha D. A. Nieuwenhuijze, Kalyan Dulla, Henkjan J. Verkade, Johan W. Jonker, Hugo R. de Jonge, Marcel J. C. Bijvelds

**Table S1 – Related to *Experimental procedures*.**

**Primer sequences**

| Protein | Gene | Forward primer | Reverse Primer |
|---|---|---|---|
| ASBT | *Slc10a2* | GGAACTGGCTCCAATATCCTG | GTTCCCGAGTCAACCCACAT |
| FXR | *Nr1h4* | CATCAAGGACAGAGAGGCGG | TCAGCGTGGTGATGGTTGAA |
| FGF15 | *Fgf15* | GTCCCTATGTCTCCAACTGCTTCCT | TTCCTCCCTGAAGGTACAGTCTTCC |
| SHP | *Nr0b2* | CGAATCCTCCTCATGGCCTC | TCCCATGATAGGGCGGAAGA |
| CYP7A1 | *Cyp7a1* | ACTCTCTGAAGCCATGATGCAA | AGCGTTAGATATCCGGCTTCAA |
| CYP8B1 | *Cyp8b1* | TTGCAAATGCTGCCTCAACC | TAACAGTCGCACACATGGCT |
| GAPDH | *Gapdh* | TTCCAGTATGACTCCACTCACGG | TGAAGACACCAGTAGACTCCACGAC |

**Table S2 – Related to Figure 5.**
**Differentially regulated signal transduction pathways in ileum of CF mice and controls.** Gene expression in *Cftr null* mice is depicted relative to the expression in wildtype mice.

| **LPS-IL1-RXR** | | | |
|---|---|---|---|
| Symbol | Entrez Gene Name | Gene Symbol - mouse (Entrez Gene) | Expr Fold Change |
| ABCA1 | ATP binding cassette subfamily A member 1 | Abca1 | -3.189 |
| ABCB1 | ATP binding cassette subfamily B member 1 | Abcb1a | -2.904 |
| ABCB9 | ATP binding cassette subfamily B member 9 | -- | |
| ABCC2 | ATP binding cassette subfamily C member 2 | Abcc2 | -2.237 |
| ABCC3 | ATP binding cassette subfamily C member 3 | -- | |
| ABCG1 | ATP binding cassette subfamily G member 1 | -- | |
| ABCG5 | ATP binding cassette subfamily G member 5 | Abcg5 | -2.198 |
| ABCG8 | ATP binding cassette subfamily G member 8 | Abcg8 | -2.677 |
| ACOX1 | acyl-CoA oxidase 1 | Acox1 | -1.771 |
| ACOX2 | acyl-CoA oxidase 2 | Acox2 | -2.524 |
| ACOX3 | acyl-CoA oxidase 3, pristanoyl | -- | |
| ACSL1 | acyl-CoA synthetase long-chain family member 1 | Acsl1 | -1.406 |
| ACSL3 | acyl-CoA synthetase long-chain family member 3 | -- | |
| ACSL4 | acyl-CoA synthetase long-chain family member 4 | -- | |
| ACSL5 | acyl-CoA synthetase long-chain family member 5 | -- | |
| ALAS1 | 5'-aminolevulinate synthase 1 | -- | |
| ALDH16A1 | aldehyde dehydrogenase 16 family member A1 | -- | |
| ALDH18A1 | aldehyde dehydrogenase 18 family member A1 | -- | |
| ALDH1A1 | aldehyde dehydrogenase 1 family member A1 | Aldh1a1 | -3.399 |
| ALDH1A2 | aldehyde dehydrogenase 1 family member A2 | Aldh1a2 | -1.867 |
| ALDH1A3 | aldehyde dehydrogenase 1 family member A3 | -- | |
| ALDH1B1 | aldehyde dehydrogenase 1 family member B1 | -- | |
| ALDH1L1 | aldehyde dehydrogenase 1 family member L1 | -- | |

| | | | |
|---|---|---|---|
| ALDH3A2 | aldehyde dehydrogenase 3 family member A2 | Aldh3a2 | -2.412 |
| ALDH3B1 | aldehyde dehydrogenase 3 family member B1 | -- | |
| ALDH4A1 | aldehyde dehydrogenase 4 family member A1 | Aldh4a1 | 2.137 |
| ALDH5A1 | aldehyde dehydrogenase 5 family member A1 | -- | |
| ALDH6A1 | aldehyde dehydrogenase 6 family member A1 | -- | |
| ALDH7A1 | aldehyde dehydrogenase 7 family member A1 | -- | |
| ALDH9A1 | aldehyde dehydrogenase 9 family member A1 | -- | |
| APOC2 | apolipoprotein C2 | Apoc2 | 1.983 |
| APOE | apolipoprotein E | Apoe | -1.182 |
| CAT | catalase | Cat | -3.622 |
| CD14 | CD14 molecule | Cd14 | 3.364 |
| CHST1 | carbohydrate sulfotransferase 1 | -- | |
| CHST3 | carbohydrate sulfotransferase 3 | Chst3 | 23.983 |
| CHST4 | carbohydrate sulfotransferase 4 | Chst4 | 3.539 |
| CHST10 | carbohydrate sulfotransferase 10 | Chst10 | 3.180 |
| CHST11 | carbohydrate sulfotransferase 11 | -- | |
| CHST12 | carbohydrate sulfotransferase 12 | -- | |
| CPT2 | carnitine palmitoyltransferase 2 | -- | |
| CPT1A | carnitine palmitoyltransferase 1A | -- | |
| CYP2B6 | cytochrome P450 family 2 subfamily B member 6 | Cyp2b10 | -2.566 |
| CYP2C9 | cytochrome P450 family 2 subfamily C member 9 | Cyp2c66 | -7.949 |
| CYP3A5 | cytochrome P450 family 3 subfamily A member 5 | Cyp3a11 | -12.095 |
| CYP3A7 | cytochrome P450 family 3 subfamily A member 7 | -- | |
| CYP4A11 | cytochrome P450 family 4 subfamily A member 11 | Cyp4a10 | -21.224 |
| ECSIT | ECSIT signalling integrator | -- | |
| FABP1 | fatty acid binding protein 1 | Fabp1 | -3.019 |
| FABP2 | fatty acid binding protein 2 | Fabp2 | -2.032 |
| FABP4 | fatty acid binding protein 4 | Fabp4 | 1.571 |
| FABP5 | fatty acid binding protein 5 | -- | |
| FABP6 | fatty acid binding protein 6 | Fabp6 | -4.583 |
| FMO1 | flavin containing monooxygenase 1 | Fmo1 | -1.677 |
| FMO2 | flavin containing monooxygenase 2 | Fmo2 | -2.230 |
| FMO4 | flavin containing monooxygenase 4 | -- | |
| FMO5 | flavin containing monooxygenase 5 | Fmo5 | -2.792 |
| GAL3ST2 | galactose-3-O-sulfotransferase 2 | Gal3st2 | -2.855 |
| GSTA3 | glutathione S-transferase alpha 3 | -- | |
| GSTA5 | glutathione S-transferase alpha 5 | Gm10639 | 2.343 |
| GSTK1 | glutathione S-transferase kappa 1 | -- | |
| GSTM1 | glutathione S-transferase mu 1 | -- | |
| GSTM2 | glutathione S-transferase mu 2 | -- | |
| Gstm3 | glutathione S-transferase, mu 3 | -- | |
| GSTM3 | glutathione S-transferase mu 3 | -- | |
| GSTM4 | glutathione S-transferase mu 4 | -- | |
| GSTM5 | glutathione S-transferase mu 5 | -- | |
| GSTO1 | glutathione S-transferase omega 1 | -- | |
| GSTP1 | glutathione S-transferase pi 1 | Gstp2 | 2.081 |
| GSTT2/GSTT2B | glutathione S-transferase theta 2 (gene/pseudogene) | -- | |
| HMGCS1 | 3-hydroxy-3-methylglutaryl-CoA synthase 1 | -- | |
| HMGCS2 | 3-hydroxy-3-methylglutaryl-CoA synthase 2 | -- | |
| HS2ST1 | heparan sulfate 2-O-sulfotransferase 1 | -- | |
| HS3ST1 | heparan sulfate-glucosamine 3-sulfotransferase 1 | -- | |
| HS6ST1 | heparan sulfate 6-O-sulfotransferase 1 | -- | |
| IL18 | interleukin 18 | Il18 | 1.276 |
| IL33 | interleukin 33 | Il33 | 4.208 |

| | | | |
|---|---|---|---|
| IL1R1 | interleukin 1 receptor type 1 | Il1r1 | 1.133 |
| IL1RL1 | interleukin 1 receptor like 1 | Il1rl1 | 2.470 |
| IL1RN | interleukin 1 receptor antagonist | Il1rn | 2.977 |
| IL4I1 | interleukin 4 induced 1 | Il4i1 | 2.834 |
| IRAK1 | interleukin 1 receptor associated kinase 1 | Irak1 | 1.142 |
| JUN | Jun proto-oncogene, AP-1 transcription factor subunit | Jun | -1.164 |
| LY96 | lymphocyte antigen 96 | -- | |
| MAOA | monoamine oxidase A | -- | |
| MAOB | monoamine oxidase B | Maob | -1.885 |
| MAP2K4 | mitogen-activated protein kinase kinase 4 | -- | |
| MAP2K7 | mitogen-activated protein kinase kinase 7 | -- | |
| MAP3K1 | mitogen-activated protein kinase kinase kinase 1 | -- | |
| MAPK8 | mitogen-activated protein kinase 8 | Mapk8 | 1.116 |
| MAPK9 | mitogen-activated protein kinase 9 | Mapk9 | -1.088 |
| MGMT | O-6-methylguanine-DNA methyltransferase | -- | |
| MGST1 | microsomal glutathione S-transferase 1 | -- | |
| MGST2 | microsomal glutathione S-transferase 2 | -- | |
| MGST3 | microsomal glutathione S-transferase 3 | -- | |
| MYD88 | myeloid differentiation primary response 88 | Myd88 | 1.492 |
| NCOA1 | nuclear receptor coactivator 1 | Ncoa1 | 1.035 |
| NDST1 | N-deacetylase and N-sulfotransferase 1 | Ndst1 | -1.163 |
| NDST2 | N-deacetylase and N-sulfotransferase 2 | -- | |
| NGFR | nerve growth factor receptor | Ngfr | -2.271 |
| NR0B2 | nuclear receptor subfamily 0 group B member 2 | Nr0b2 | -44.334 |
| NR1H2 | nuclear receptor subfamily 1 group H member 2 | Nr1h2 | -1.021 |
| NR1H3 | nuclear receptor subfamily 1 group H member 3 | Nr1h3 | -1.166 |
| NR1H4 | nuclear receptor subfamily 1 group H member 4 | Nr1h4 | 1.053 |
| NR1I2 | nuclear receptor subfamily 1 group I member 2 | Nr1i2 | -1.334 |
| NR1I3 | nuclear receptor subfamily 1 group I member 3 | Nr1i3 | -1.165 |
| NR5A2 | nuclear receptor subfamily 5 group A member 2 | Nr5a2 | -1.211 |
| PAPSS2 | 3'-phosphoadenosine 5'-phosphosulfate synthase 2 | -- | |
| PLTP | phospholipid transfer protein | -- | |
| PPARA | peroxisome proliferator activated receptor alpha | Ppara | -3.810 |
| PPARGC1A | PPARG coactivator 1 alpha | Ppargc1a | -1.557 |
| PPARGC1B | PPARG coactivator 1 beta | Ppargc1b | 1.133 |
| RARA | retinoic acid receptor alpha | Rara | -1.346 |
| RXRA | retinoid X receptor alpha | Rxra | -1.436 |
| SCARB1 | scavenger receptor class B member 1 | Scarb1 | -1.157 |
| SLC27A1 | solute carrier family 27 member 1 | -- | |
| SLC27A2 | solute carrier family 27 member 2 | -- | |
| SLC27A4 | solute carrier family 27 member 4 | -- | |
| SMOX | spermine oxidase | Smox | 2.001 |
| SOD3 | superoxide dismutase 3, extracellular | -- | |
| SREBF1 | sterol regulatory element binding transcription factor 1 | Srebf1 | -1.596 |
| SULT1B1 | sulfotransferase family 1B member 1 | -- | |
| SULT1C2 | sulfotransferase family 1C member 2 | Sult1c2 | -2.988 |
| Sult1d1 | sulfotransferase family 1D, member 1 | -- | |
| SULT2B1 | sulfotransferase family 2B member 1 | -- | |
| TNF | tumor necrosis factor | Tnf | 4.137 |
| TNFRSF11B | TNF receptor superfamily member 11b | -- | |
| TNFRSF1A | TNF receptor superfamily member 1A | Tnfrsf1a | 1.051 |
| TNFRSF1B | TNF receptor superfamily member 1B | Tnfrsf1b | 1.775 |
| TRAF2 | TNF receptor associated factor 2 | -- | |
| TRAF6 | TNF receptor associated factor 6 | Traf6 | -1.069 |

| XPO1 | exportin 1 | Xpo1 | 1.200 |
|---|---|---|---|
| **FXR-RXR** | | | |
| Symbol | Entrez Gene Name | GenBank/Gene Symbol - mouse (Entrez Gene) | Exp Fold Change |
| ABCC2 | ATP binding cassette subfamily C member 2 | Abcc2 | -2.237 |
| ABCG5 | ATP binding cassette subfamily G member 5 | Abcg5 | -2.198 |
| ABCG8 | ATP binding cassette subfamily G member 8 | Abcg8 | -2.677 |
| AGT | angiotensinogen | Agt | -2.902 |
| AKT1 | AKT serine/threonine kinase 1 | Akt1 | 1.149 |
| AKT2 | AKT serine/threonine kinase 2 | -- | |
| AKT3 | AKT serine/threonine kinase 3 | -- | |
| ALB | albumin | Alb | 285.441 |
| APOA1 | apolipoprotein A1 | Apoa1 | -1.490 |
| APOA4 | apolipoprotein A4 | Apoa4 | -2.237 |
| APOB | apolipoprotein B | -- | |
| APOC2 | apolipoprotein C2 | Apoc2 | 1.983 |
| APOE | apolipoprotein E | Apoe | -1.182 |
| BAAT | bile acid-CoA:amino acid N-acyltransferase | Baat | -2.022 |
| C3 | complement C3 | C3 | 1.307 |
| C4A/C4B | complement C4B (Chido blood group) | -- | |
| CLU | clusterin | Clu | 3.391 |
| CREBBP | CREB binding protein | Crebbp | -1.507 |
| CYP27A1 | cytochrome P450 family 27 subfamily A member 1 | Cyp27a1 | -1.494 |
| FABP6 | fatty acid binding protein 6 | Fabp6 | -4.583 |
| FASN | fatty acid synthase | -- | |
| FBP1 | fructose-bisphosphatase 1 | Fbp1 | -3.530 |
| FGF19 | fibroblast growth factor 19 | Fgf15 | -40.903 |
| FGFR4 | fibroblast growth factor receptor 4 | -- | |
| FOXA1 | forkhead box A1 | Foxa1 | -1.147 |
| FOXA2 | forkhead box A2 | Foxa2 | -1.275 |
| FOXA3 | forkhead box A3 | Foxa3 | 1.234 |
| FOXO1 | forkhead box O1 | Foxo1 | -1.196 |
| G6PC | glucose-6-phosphatase catalytic subunit | G6pc | -2.944 |
| G6PC3 | glucose-6-phosphatase catalytic subunit 3 | -- | |
| HNF1A | HNF1 homeobox A | Hnf1a | -1.318 |
| HNF4A | hepatocyte nuclear factor 4 alpha | Hnf4a | -1.060 |
| IL18 | interleukin 18 | Il18 | 1.276 |
| IL33 | interleukin 33 | Il33 | 4.208 |
| IL1RN | interleukin 1 receptor antagonist | Il1rn | 2.977 |
| LPL | lipoprotein lipase | Lpl | -1.100 |
| MAP2K4 | mitogen-activated protein kinase kinase 4 | -- | |
| MAPK8 | mitogen-activated protein kinase 8 | Mapk8 | 1.116 |
| MAPK9 | mitogen-activated protein kinase 9 | Mapk9 | -1.088 |
| MAPK12 | mitogen-activated protein kinase 12 | -- | |
| MLXIPL | MLX interacting protein like | Mlxipl | -2.124 |
| MTTP | microsomal triglyceride transfer protein | Mttp | -1.226 |
| NR0B2 | nuclear receptor subfamily 0 group B member 2 | Nr0b2 | -44.334 |
| NR1H3 | nuclear receptor subfamily 1 group H member 3 | Nr1h3 | -1.166 |
| NR1H4 | nuclear receptor subfamily 1 group H member 4 | Nr1h4 | 1.053 |
| NR1I2 | nuclear receptor subfamily 1 group I member 2 | Nr1i2 | -1.334 |
| NR5A2 | nuclear receptor subfamily 5 group A member 2 | Nr5a2 | -1.211 |
| PCK2 | phosphoenolpyruvate carboxykinase 2, mitochondrial | -- | |
| PCYOX1 | prenylcysteine oxidase 1 | -- | |
| PKLR | pyruvate kinase, liver and RBC | -- | |
| PLTP | phospholipid transfer protein | -- | |

| | | | |
|---|---|---|---|
| PON3 | paraoxonase 3 | -- | |
| PPARA | peroxisome proliferator activated receptor alpha | Ppara | -3.810 |
| PPARG | peroxisome proliferator activated receptor gamma | Pparg | 1.321 |
| PPARGC1A | PPARG coactivator 1 alpha | Ppargc1a | -1.557 |
| RARA | retinoic acid receptor alpha | Rara | -1.346 |
| RBP4 | retinol binding protein 4 | Rbp4 | 2.111 |
| RXRA | retinoid X receptor alpha | Rxra | -1.436 |
| SAA1 | serum amyloid A1 | Saa1 | 21.654 |
| SCARB1 | scavenger receptor class B member 1 | Scarb1 | -1.157 |
| SDC1 | syndecan 1 | -- | |
| SERPINA1 | serpin family A member 1 | Serpina1b | 4.477 |
| SERPINF1 | serpin family F member 1 | -- | |
| SLC10A2 | solute carrier family 10 member 2 | Slc10a2 | 2.290 |
| SLC4A2 | solute carrier family 4 member 2 | -- | |
| SLC51A | solute carrier family 51 alpha subunit | Slc51a | -1.869 |
| SLC51B | solute carrier family 51 beta subunit | Slc51b | -1.421 |
| SREBF1 | sterol regulatory element binding transcription factor 1 | Srebf1 | -1.596 |
| TF | transferrin | -- | |
| TNF | tumor necrosis factor | Tnf | 4.137 |
| TTR | transthyretin | Ttr | 11.339 |

| **Antigen presentation** | | | |
|---|---|---|---|
| Symbol | Entrez Gene Name | Gene Symbol - mouse (Entrez Gene) | Expr Fold Change |
| B2M | beta-2-microglobulin | B2m | 1.443 |
| CALR | calreticulin | -- | |
| CANX | calnexin | -- | |
| CD74 | CD74 molecule | Cd74 | 4.162 |
| CIITA | class II major histocompatibility complex transactivator | Ciita | 6.042 |
| HLA-A | major histocompatibility complex, class I, A | H2-Q7 | 2.267 |
| HLA-DMA | major histocompatibility complex, class II, DM alpha | H2-DMa | 5.015 |
| HLA-DMB | major histocompatibility complex, class II, DM beta | H2-DMb1 | 5.267 |
| HLA-DOA | major histocompatibility complex, class II, DO alpha | H2-Oa | 3.583 |
| HLA-DOB | major histocompatibility complex, class II, DO beta | H2-Ob | 2.444 |
| HLA-DQA1 | major histocompatibility complex, class II, DQ alpha 1 | H2-Aa | 3.854 |
| HLA-DQB1 | major histocompatibility complex, class II, DQ beta 1 | H2-Ab1 | 4.405 |
| HLA-DRA | major histocompatibility complex, class II, DR alpha | H2-Ea-ps | 3.037 |
| HLA-DRB5 | major histocompatibility complex, class II, DR beta 5 | H2-Eb1 | 5.732 |
| HLA-E | major histocompatibility complex, class I, E | -- | |
| HLA-F | major histocompatibility complex, class I, F | -- | |
| HLA-G | major histocompatibility complex, class I, G | H2-M3 | 2.341 |
| MR1 | major histocompatibility complex, class I-related | -- | |
| NLRC5 | NLR family CARD domain containing 5 | Nlrc5 | 8.639 |
| PDIA3 | protein disulfide isomerase family A member 3 | -- | |
| PSMB5 | proteasome subunit beta 5 | -- | |
| PSMB6 | proteasome subunit beta 6 | -- | |
| PSMB8 | proteasome subunit beta 8 | Psmb8 | 3.793 |
| PSMB9 | proteasome subunit beta 9 | Psmb9 | 3.547 |
| TAP1 | transporter 1, ATP binding cassette subfamily B member | Tap1 | 3.858 |
| TAP2 | transporter 2, ATP binding cassette subfamily B member | -- | |
| TAPBP | TAP binding protein | Tapbp | -1.004 |

**Figure S1 – Related to Figure 5C**

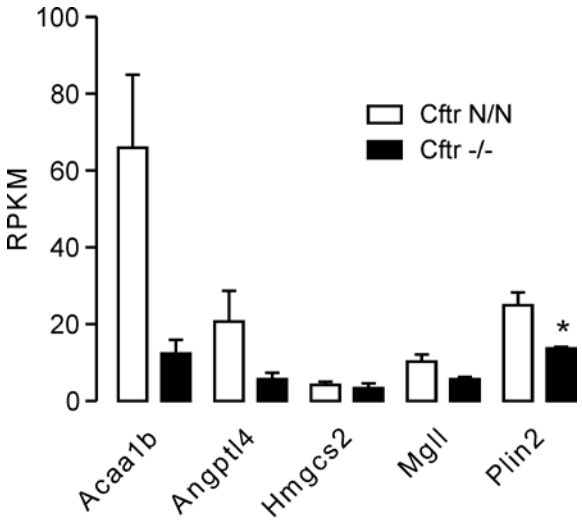


Expression of PPARγ target genes in the ileum of CF mice and controls. Transcript levels of genes that were previously analyzed to signal inactivation of PPARγ **(**Harmon et al. 2010). Data depict reads per 1000 base pair transcript per million reads mapped (RPKM). N=3. *p < 0.05

.

**Figure S2 – Related to Figure 5C**

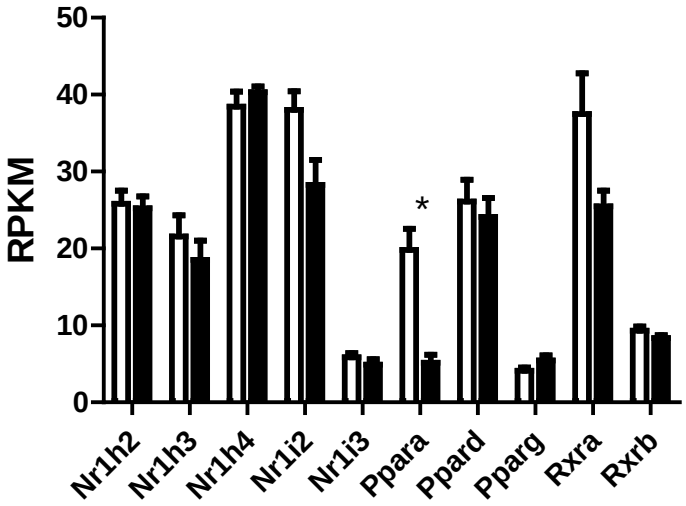


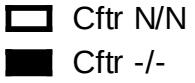


Expression of ligand-dependent nuclear receptors in ileum of CF mice and controls. Data depict reads per 1000 base pair transcript per million reads mapped (RPKM). N=3. *p < 0.05

**Table S3 – Related to Figure 6.**

**Effect of antibiotic treatment on differentially regulated signal transduction pathways in ileum of CF mice.** Gene expression after antibiotic treatment is depicted relative to the expression in non-treated animals.

| **ABX**<br>**LPS-IL1-RXR**<br>Symbol | Entrez Gene Name | GenBank/Gene Symbol - mouse (Entrez Gene) | Exp Fold Change |
|---|---|---|---|
| ABCA1 | ATP binding cassette subfamily A member 1 | Abca1 | 4.616 |
| ABCB1 | ATP binding cassette subfamily B member 1 | -- | |
| ABCB9 | ATP binding cassette subfamily B member 9 | -- | |
| ABCC2 | ATP binding cassette subfamily C member 2 | Abcc2 | 3.355 |
| ABCC3 | ATP binding cassette subfamily C member 3 | -- | |
| ABCG1 | ATP binding cassette subfamily G member 1 | -- | |
| ABCG5 | ATP binding cassette subfamily G member 5 | Abcg5 | 2.124 |
| ABCG8 | ATP binding cassette subfamily G member 8 | Abcg8 | 3.701 |
| ACOX1 | acyl-CoA oxidase 1 | Acox1 | 2.680 |
| ACOX2 | acyl-CoA oxidase 2 | Acox2 | 3.783 |
| ACOX3 | acyl-CoA oxidase 3. pristanoyl | -- | |
| ACSL1 | acyl-CoA synthetase long-chain family member 1 | -- | |
| ACSL3 | acyl-CoA synthetase long-chain family member 3 | Acsl3 | 2.497 |
| ACSL4 | acyl-CoA synthetase long-chain family member 4 | -- | |
| ACSL5 | acyl-CoA synthetase long-chain family member 5 | -- | |
| ALAS1 | 5'-aminolevulinate synthase 1 | -- | |
| ALDH16A1 | aldehyde dehydrogenase 16 family member A1 | -- | |
| ALDH18A1 | aldehyde dehydrogenase 18 family member A1 | -- | |
| ALDH1A1 | aldehyde dehydrogenase 1 family member A1 | Aldh1a1 | 6.046 |
| ALDH1A2 | aldehyde dehydrogenase 1 family member A2 | Aldh1a2 | -1.101 |
| ALDH1A3 | aldehyde dehydrogenase 1 family member A3 | Aldh1a3 | 2.093 |
| ALDH1B1 | aldehyde dehydrogenase 1 family member B1 | -- | |
| ALDH1L1 | aldehyde dehydrogenase 1 family member L1 | -- | |
| ALDH3A2 | aldehyde dehydrogenase 3 family member A2 | Aldh3a2 | 4.558 |
| ALDH3B1 | aldehyde dehydrogenase 3 family member B1 | -- | |
| ALDH4A1 | aldehyde dehydrogenase 4 family member A1 | -- | |
| ALDH5A1 | aldehyde dehydrogenase 5 family member A1 | -- | |
| ALDH6A1 | aldehyde dehydrogenase 6 family member A1 | -- | |
| ALDH7A1 | aldehyde dehydrogenase 7 family member A1 | -- | |
| ALDH9A1 | aldehyde dehydrogenase 9 family member A1 | -- | |
| APOC2 | apolipoprotein C2 | Apoc2 | 2.349 |
| APOE | apolipoprotein E | Apoe | 1.635 |
| CAT | catalase | Cat | 5.660 |
| CD14 | CD14 molecule | Cd14 | -2.802 |
| CHST1 | carbohydrate sulfotransferase 1 | -- | |
| CHST3 | carbohydrate sulfotransferase 3 | Chst3 | 2.121 |
| CHST4 | carbohydrate sulfotransferase 4 | Chst4 | -5.964 |
| CHST10 | carbohydrate sulfotransferase 10 | -- | |
| CHST11 | carbohydrate sulfotransferase 11 | -- | |
| CHST12 | carbohydrate sulfotransferase 12 | Chst12 | -2.049 |
| CPT2 | carnitine palmitoyltransferase 2 | -- | |
| CPT1A | carnitine palmitoyltransferase 1A | -- | |
| CYP2B6 | cytochrome P450 family 2 subfamily B member 6 | Cyp2b10 | 4.225 |
| CYP2C9 | cytochrome P450 family 2 subfamily C member 9 | Cyp2c66 | 17.276 |
| CYP3A5 | cytochrome P450 family 3 subfamily A member 5 | Cyp3a11 | 34.386 |
| CYP3A7 | cytochrome P450 family 3 subfamily A member 7 | Cyp3a13 | 2.157 |
| CYP4A11 | cytochrome P450 family 4 subfamily A member 11 | Cyp4a10 | 181.115 |
| ECSIT | ECSIT signalling integrator | Ecsit | -2.006 |

| | | | |
|---|---|---|---|
| FABP1 | fatty acid binding protein 1 | Fabp1 | 10.414 |
| FABP2 | fatty acid binding protein 2 | Fabp2 | 3.059 |
| FABP4 | fatty acid binding protein 4 | Fabp4 | -1.097 |
| FABP5 | fatty acid binding protein 5 | Fabp5 | -2.215 |
| FABP6 | fatty acid binding protein 6 | Fabp6 | -2.991 |
| FMO1 | flavin containing monooxygenase 1 | -- | |
| FMO2 | flavin containing monooxygenase 2 | Fmo2 | 2.962 |
| FMO4 | flavin containing monooxygenase 4 | -- | |
| FMO5 | flavin containing monooxygenase 5 | Fmo5 | 3.531 |
| GAL3ST2 | galactose-3-O-sulfotransferase 2 | Gal3st2 | 3.431 |
| GSTA3 | glutathione S-transferase alpha 3 | Gsta3 | 6.051 |
| GSTA5 | glutathione S-transferase alpha 5 | Gsta1 | 3.756 |
| GSTK1 | glutathione S-transferase kappa 1 | -- | |
| GSTM1 | glutathione S-transferase mu 1 | -- | |
| GSTM2 | glutathione S-transferase mu 2 | -- | |
| Gstm3 | glutathione S-transferase. mu 3 | Gstm3 | 2.386 |
| GSTM3 | glutathione S-transferase mu 3 | Gstm5 | -2.083 |
| GSTM4 | glutathione S-transferase mu 4 | -- | |
| GSTM5 | glutathione S-transferase mu 5 | Gstm1 | 4.264 |
| GSTO1 | glutathione S-transferase omega 1 | -- | |
| GSTP1 | glutathione S-transferase pi 1 | Gstp2 | -3.510 |
| GSTT2/GSTT2B | glutathione S-transferase theta 2 (gene/pseudogene) | -- | |
| HMGCS1 | 3-hydroxy-3-methylglutaryl-CoA synthase 1 | Hmgcs1 | -2.326 |
| HMGCS2 | 3-hydroxy-3-methylglutaryl-CoA synthase 2 | Hmgcs2 | 11.330 |
| HS2ST1 | heparan sulfate 2-O-sulfotransferase 1 | -- | |
| HS3ST1 | heparan sulfate-glucosamine 3-sulfotransferase 1 | Hs3st1 | -2.785 |
| HS6ST1 | heparan sulfate 6-O-sulfotransferase 1 | -- | |
| IL18 | interleukin 18 | Il18 | -1.853 |
| IL33 | interleukin 33 | Il33 | -3.934 |
| IL1R1 | interleukin 1 receptor type 1 | -- | |
| IL1RL1 | interleukin 1 receptor like 1 | Il1rl1 | -5.512 |
| IL1RN | interleukin 1 receptor antagonist | Il1rn | -2.753 |
| IL4I1 | interleukin 4 induced 1 | -- | |
| IRAK1 | interleukin 1 receptor associated kinase 1 | -- | |
| JUN | Jun proto-oncogene. AP-1 transcription factor subunit | Jun | 1.342 |
| LY96 | lymphocyte antigen 96 | -- | |
| MAOA | monoamine oxidase A | Maoa | 2.014 |
| MAOB | monoamine oxidase B | Maob | 2.385 |
| MAP2K4 | mitogen-activated protein kinase kinase 4 | Map2k4 | -1.300 |
| MAP2K7 | mitogen-activated protein kinase kinase 7 | -- | |
| MAP3K1 | mitogen-activated protein kinase kinase kinase 1 | Map3k1 | 1.204 |
| MAPK8 | mitogen-activated protein kinase 8 | Mapk8 | -1.073 |
| MAPK9 | mitogen-activated protein kinase 9 | Mapk9 | -1.165 |
| MGMT | O-6-methylguanine-DNA methyltransferase | -- | |
| MGST1 | microsomal glutathione S-transferase 1 | -- | |
| MGST2 | microsomal glutathione S-transferase 2 | -- | |
| MGST3 | microsomal glutathione S-transferase 3 | -- | |
| MYD88 | myeloid differentiation primary response 88 | Myd88 | -2.574 |
| NCOA1 | nuclear receptor coactivator 1 | Ncoa1 | -1.325 |
| NDST1 | N-deacetylase and N-sulfotransferase 1 | -- | |
| NDST2 | N-deacetylase and N-sulfotransferase 2 | -- | |
| NGFR | nerve growth factor receptor | Ngfr | 1.886 |
| NR0B2 | nuclear receptor subfamily 0 group B member 2 | Nr0b2 | 7.028 |
| NR1H2 | nuclear receptor subfamily 1 group H member 2 | Nr1h2 | 1.018 |

| | | | |
|---|---|---|---|
| NR1H3 | nuclear receptor subfamily 1 group H member 3 | Nr1h3 | 1.138 |
| NR1H4 | nuclear receptor subfamily 1 group H member 4 | Nr1h4 | -1.393 |
| NR1I2 | nuclear receptor subfamily 1 group I member 2 | Nr1i2 | 1.749 |
| NR1I3 | nuclear receptor subfamily 1 group I member 3 | Nr1i3 | 3.386 |
| NR5A2 | nuclear receptor subfamily 5 group A member 2 | Nr5a2 | -1.201 |
| PAPSS2 | 3'-phosphoadenosine 5'-phosphosulfate synthase 2 | -- | |
| PLTP | phospholipid transfer protein | -- | |
| PPARA | peroxisome proliferator activated receptor alpha | Ppara | 4.844 |
| PPARGC1A | PPARG coactivator 1 alpha | Ppargc1a | 1.675 |
| PPARGC1B | PPARG coactivator 1 beta | Ppargc1b | -2.336 |
| RARA | retinoic acid receptor alpha | Rara | -1.031 |
| RXRA | retinoid X receptor alpha | Rxra | 1.222 |
| SCARB1 | scavenger receptor class B member 1 | Scarb1 | 1.110 |
| SLC27A1 | solute carrier family 27 member 1 | -- | |
| SLC27A2 | solute carrier family 27 member 2 | Slc27a2 | 7.577 |
| SLC27A4 | solute carrier family 27 member 4 | -- | |
| SMOX | spermine oxidase | Smox | -2.796 |
| SOD3 | superoxide dismutase 3. extracellular | -- | |
| SREBF1 | sterol regulatory element binding transcription factor 1 | Srebf1 | 2.048 |
| SULT1B1 | sulfotransferase family 1B member 1 | -- | |
| SULT1C2 | sulfotransferase family 1C member 2 | -- | |
| Sult1d1 | sulfotransferase family 1D. member 1 | Sult1d1 | 3.399 |
| SULT2B1 | sulfotransferase family 2B member 1 | -- | |
| TNF | tumor necrosis factor | Tnf | -2.332 |
| TNFRSF11B | TNF receptor superfamily member 11b | -- | |
| TNFRSF1A | TNF receptor superfamily member 1A | Tnfrsf1a | 1.105 |
| TNFRSF1B | TNF receptor superfamily member 1B | -- | |
| TRAF2 | TNF receptor associated factor 2 | Traf2 | -1.139 |
| TRAF6 | TNF receptor associated factor 6 | -- | |
| XPO1 | exportin 1 | -- | |

| **ABX FXR-RXR** | | Gene Symbol - mouse (Entrez Gene) | Expr Fold Change |
|---|---|---|---|
| Symbol | Entrez Gene Name | | |
| ABCC2 | ATP binding cassette subfamily C member 2 | Abcc2 | 3.355 |
| ABCG5 | ATP binding cassette subfamily G member 5 | Abcg5 | 2.124 |
| ABCG8 | ATP binding cassette subfamily G member 8 | Abcg8 | 3.701 |
| AGT | angiotensinogen | Agt | 1.113 |
| AKT1 | AKT serine/threonine kinase 1 | Akt1 | -1.128 |
| AKT2 | AKT serine/threonine kinase 2 | -- | |
| AKT3 | AKT serine/threonine kinase 3 | -- | |
| ALB | albumin | Alb | 8.857 |
| APOA1 | apolipoprotein A1 | Apoa1 | 1.608 |
| APOA4 | apolipoprotein A4 | Apoa4 | 7.796 |
| APOB | apolipoprotein B | Apob | 3.440 |
| APOC2 | apolipoprotein C2 | Apoc2 | 2.349 |
| APOE | apolipoprotein E | Apoe | 1.635 |
| BAAT | bile acid-CoA:amino acid N-acyltransferase | -- | |
| C3 | complement C3 | -- | |
| C4A/C4B | complement C4B (Chido blood group) | -- | |
| CLU | clusterin | Clu | 2.124 |
| CREBBP | CREB binding protein | Crebbp | -1.068 |
| CYP27A1 | cytochrome P450 family 27 subfamily A member 1 | Cyp27a1 | 4.105 |
| FABP6 | fatty acid binding protein 6 | Fabp6 | -2.991 |
| FASN | fatty acid synthase | -- | |
| FBP1 | fructose-bisphosphatase 1 | Fbp1 | 2.632 |

| | | | |
|---|---|---|---|
| FGF19 | fibroblast growth factor 19 | Fgf15 | 54.014 |
| FGFR4 | fibroblast growth factor receptor 4 | Fgfr4 | -1.319 |
| FOXA1 | forkhead box A1 | Foxa1 | -1.184 |
| FOXA2 | forkhead box A2 | Foxa2 | -1.481 |
| FOXA3 | forkhead box A3 | Foxa3 | -1.696 |
| FOXO1 | forkhead box O1 | Foxo1 | 1.446 |
| G6PC | glucose-6-phosphatase catalytic subunit | G6pc | 5.422 |
| G6PC3 | glucose-6-phosphatase catalytic subunit 3 | -- | |
| HNF1A | HNF1 homeobox A | Hnf1a | 1.011 |
| HNF4A | hepatocyte nuclear factor 4 alpha | Hnf4a | 1.037 |
| IL18 | interleukin 18 | Il18 | -1.853 |
| IL33 | interleukin 33 | Il33 | -3.934 |
| IL1RN | interleukin 1 receptor antagonist | Il1rn | -2.753 |
| LPL | lipoprotein lipase | Lpl | -1.638 |
| MAP2K4 | mitogen-activated protein kinase kinase 4 | Map2k4 | -1.300 |
| MAPK8 | mitogen-activated protein kinase 8 | Mapk8 | -1.073 |
| MAPK9 | mitogen-activated protein kinase 9 | Mapk9 | -1.165 |
| MAPK12 | mitogen-activated protein kinase 12 | Mapk12 | 1.248 |
| MLXIPL | MLX interacting protein like | Mlxipl | 2.314 |
| MTTP | microsomal triglyceride transfer protein | Mttp | 1.985 |
| NR0B2 | nuclear receptor subfamily 0 group B member 2 | Nr0b2 | 7.028 |
| NR1H3 | nuclear receptor subfamily 1 group H member 3 | Nr1h3 | 1.138 |
| NR1H4 | nuclear receptor subfamily 1 group H member 4 | Nr1h4 | -1.393 |
| NR1I2 | nuclear receptor subfamily 1 group I member 2 | Nr1i2 | 1.749 |
| NR5A2 | nuclear receptor subfamily 5 group A member 2 | Nr5a2 | -1.201 |
| PCK2 | phosphoenolpyruvate carboxykinase 2. mitochondrial | -- | |
| PCYOX1 | prenylcysteine oxidase 1 | -- | |
| PKLR | pyruvate kinase. liver and RBC | -- | |
| PLTP | phospholipid transfer protein | -- | |
| PON3 | paraoxonase 3 | -- | |
| PPARA | peroxisome proliferator activated receptor alpha | Ppara | 4.844 |
| PPARG | peroxisome proliferator activated receptor gamma | Pparg | -1.331 |
| PPARGC1A | PPARG coactivator 1 alpha | Ppargc1a | 1.675 |
| RARA | retinoic acid receptor alpha | Rara | -1.031 |
| RBP4 | retinol binding protein 4 | -- | |
| RXRA | retinoid X receptor alpha | Rxra | 1.222 |
| SAA1 | serum amyloid A1 | Saa1 | -152.960 |
| SCARB1 | scavenger receptor class B member 1 | Scarb1 | 1.110 |
| SDC1 | syndecan 1 | -- | |
| SERPINA1 | serpin family A member 1 | Serpina1b | 5.082 |
| SERPINF1 | serpin family F member 1 | -- | |
| SLC10A2 | solute carrier family 10 member 2 | Slc10a2 | -13.666 |
| SLC4A2 | solute carrier family 4 member 2 | -- | |
| SLC51A | solute carrier family 51 alpha subunit | Slc51a | -1.753 |
| SLC51B | solute carrier family 51 beta subunit | -- | |
| SREBF1 | sterol regulatory element binding transcription factor 1 | Srebf1 | 2.048 |
| TF | transferrin | Trf | 2.432 |
| TNF | tumor necrosis factor | Tnf | -2.332 |
| TTR | transthyretin | -- | |

**ABX**
**Antigen presentation**

| Symbol | Entrez Gene Name | Gene Symbol - mouse (Entrez Gene) | Expr Fold Change |
|---|---|---|---|
| B2M | beta-2-microglobulin | B2m | -1.642 |
| CALR | calreticulin | -- | |

| | | | |
|---|---|---|---|
| CANX | calnexin | -- | |
| CD74 | CD74 molecule | Cd74 | -3.127 |
| CIITA | class II major histocompatibility complex transactivator | Ciita | -3.153 |
| HLA-A | major histocompatibility complex. class I. A | H2-Q1 | 2.735 |
| HLA-DMA | major histocompatibility complex. class II. DM alpha | H2-DMa | -3.570 |
| HLA-DMB | major histocompatibility complex. class II. DM beta | H2-DMb1 | -3.932 |
| HLA-DOA | major histocompatibility complex. class II. DO alpha | -- | |
| HLA-DOB | major histocompatibility complex. class II. DO beta | -- | |
| HLA-DQA1 | major histocompatibility complex. class II. DQ alpha 1 | H2-Aa | -2.418 |
| HLA-DQB1 | major histocompatibility complex. class II. DQ beta 1 | H2-Ab1 | -3.070 |
| HLA-DRA | major histocompatibility complex. class II. DR alpha | -- | |
| HLA-DRB5 | major histocompatibility complex. class II. DR beta 5 | H2-Eb1 | -3.064 |
| HLA-E | major histocompatibility complex. class I. E | H2-T23 | -2.179 |
| HLA-F | major histocompatibility complex. class I. F | Gm11127 | -2.413 |
| HLA-G | major histocompatibility complex. class I. G | -- | |
| MR1 | major histocompatibility complex. class I-related | -- | |
| NLRC5 | NLR family CARD domain containing 5 | Nlrc5 | -3.498 |
| PDIA3 | protein disulfide isomerase family A member 3 | -- | |
| PSMB5 | proteasome subunit beta 5 | -- | |
| PSMB6 | proteasome subunit beta 6 | -- | |
| PSMB8 | proteasome subunit beta 8 | Psmb8 | -2.825 |
| PSMB9 | proteasome subunit beta 9 | Psmb9 | -4.378 |
| TAP1 | transporter 1. ATP binding cassette subfamily B member | Tap1 | -4.269 |
| TAP2 | transporter 2. ATP binding cassette subfamily B member | -- | |
| TAPBP | TAP binding protein | Tapbp | -1.159 |

**Figure S3 – Related to Figure 5.**

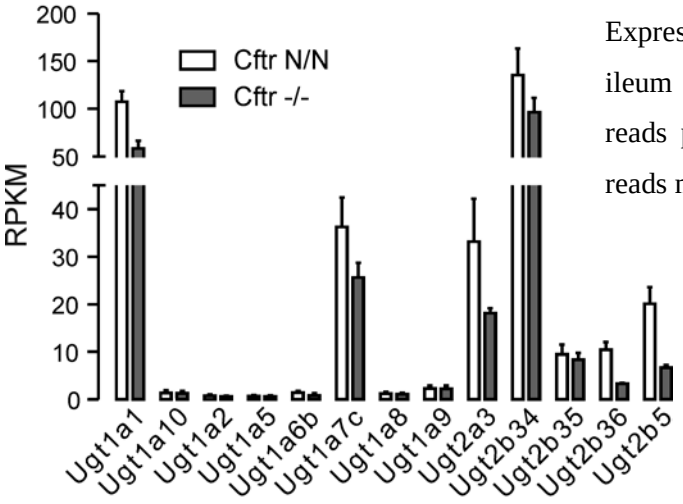


Expression of UDP glucuronosyltransferases in ileum of CF mice and controls. Data depict reads per 1000 base pair transcript per million reads mapped (RPKM). N=3.

**Figure S4 – Related to Discussion (Graphical abstract)**

Impaired feedback regulation of hepatic BA synthesis in CF. BAs are synthesized in hepatocytes and secreted across the canalicular membrane by the bile salt export pump (BSEP). BAs that enter the intestine through biliary secretion are reabsorbed in the distal small intestine via ASBT. In intestinal cells, BAs activate the nuclear receptor FXR. Activated FXR dimerizes with its heterodimer binding partner RXR to induce several genes involved in BA metabolism, including FGF19. FGF19, via activation of its hepatic receptor (FGFR4), represses expression of the gene encoding the rate-limiting enzyme in hepatic BA synthesis, CYP7A1. In addition, FGF19 has trophic actions in the liver and supports liver regeneration after injury. BAs are exported from intestinal cells via OSTα/β, after which they are shuttled back to the liver. In CF, a dysbiosis triggers inflammation of the gut wall, leading to post-translational modification and inactivation of RXR. The attendant reduction in FXR activity leads to reduced FGF19 induction/production. Low portal FGF19 levels increase hepatic CYP7A1 expression, leading to enhanced BA synthesis and biliary secretion. When intestinal BA delivery exceeds the capacity for re-uptake, fecal excretion increases. Low FGF19 production will also decrease hepatocyte proliferation and reduce the capacity for homeostatic liver regeneration.

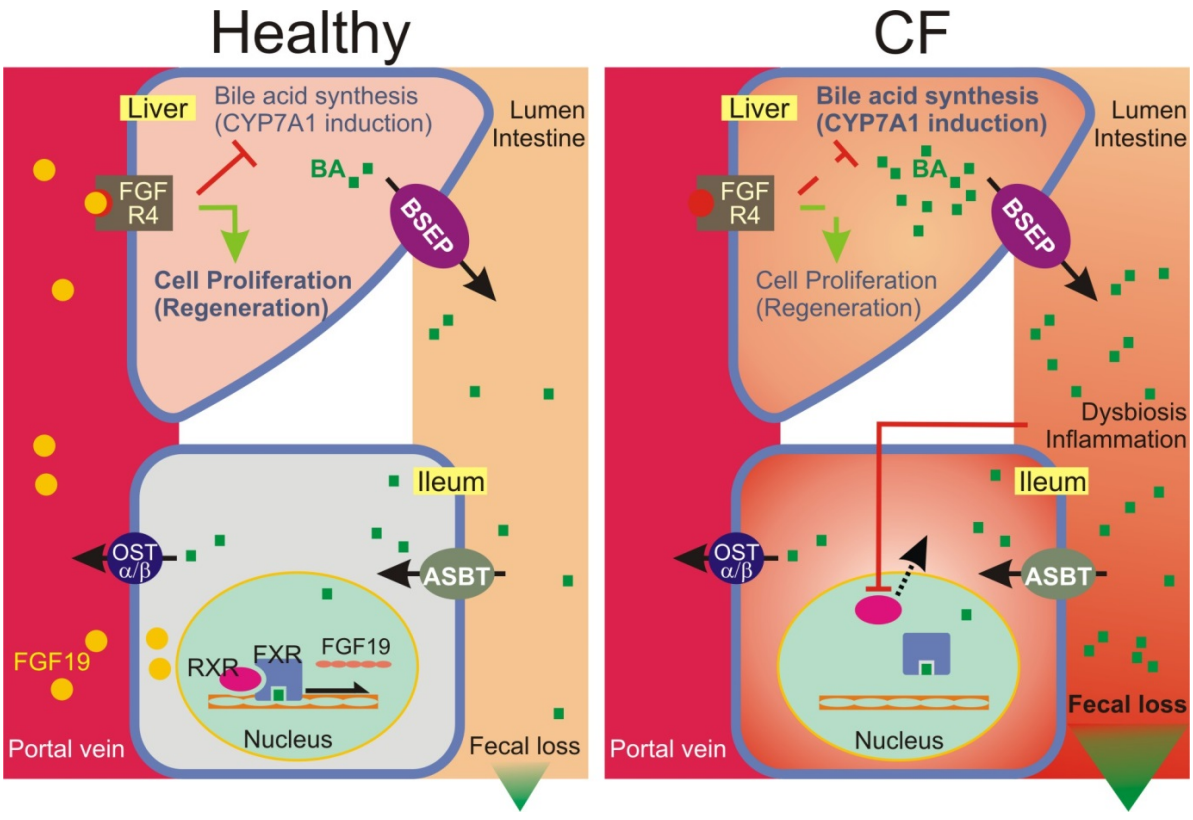

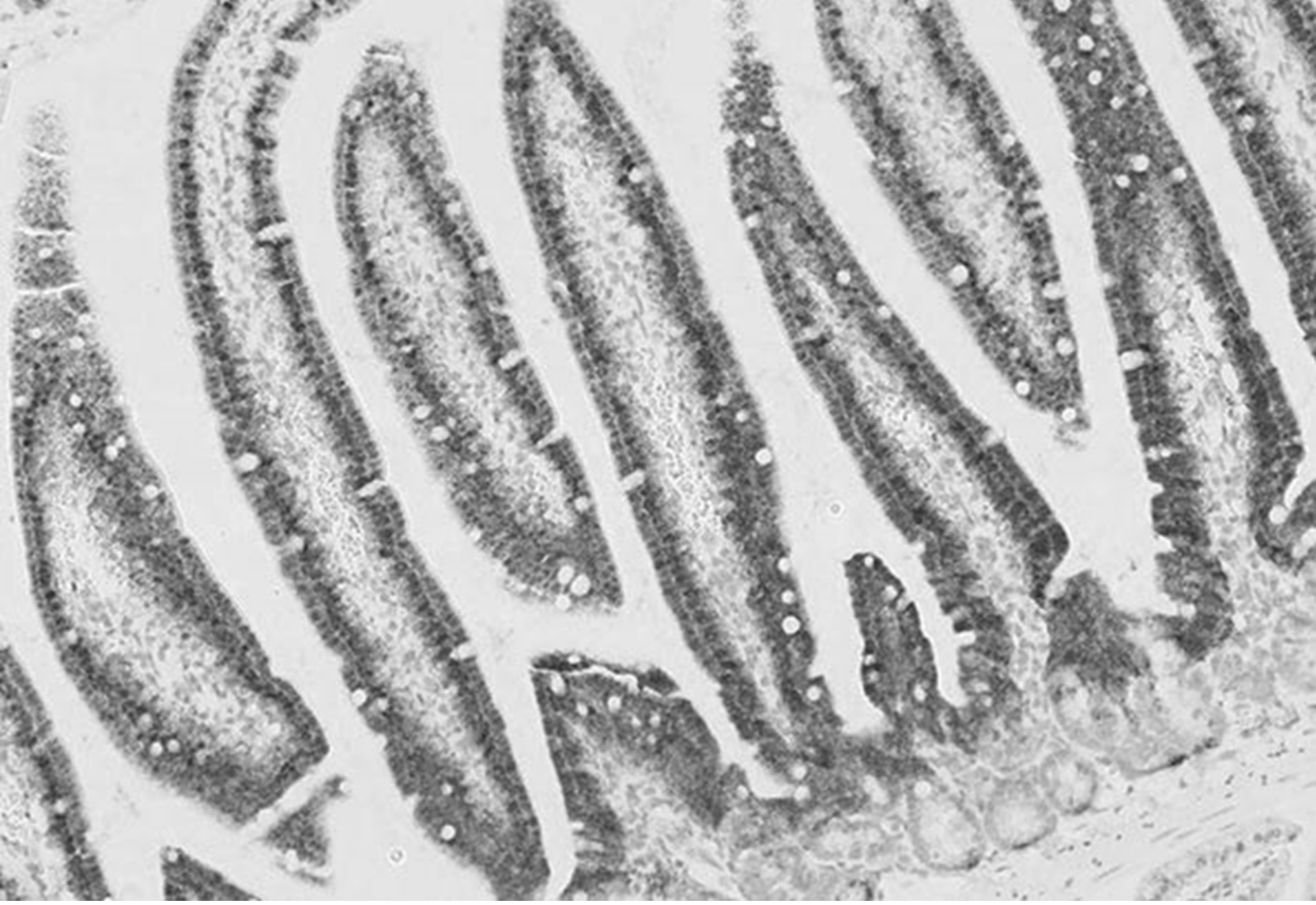

# Chapter 7

# Summary and future perspectives

**Summary**

The primary disease-causing consequences of CFTR dysfunction are dehydration and acidification of the luminal surface of CFTR-expressing epithelia. Combined, these factors lead to accretion of viscous mucus and inspissation of the contents of exocrine pancreatic and biliary ducts, and the gut lumen [1, 2]. Exocrine pancreatic dysfunction, the resultant maldigestion, and mucus plugging, precipitate bacterial colonization of the upper intestinal tract, i.e. small intestinal bacterial overgrowth (SIBO), which may further nutrient malabsorption [1, 3, 4]. Although nowadays rarely fatal, these gastrointestinal complication of CF are a significant cause of morbidity and distress among patients. Abdominal pain and discomfort affects many CF patients throughout their lives, and has a strong bearing on the perceived quality of life [1-5].

In addition, principally because of its impact on nutritional status, CF-related gastrointestinal disease is an important determinant of disease progression and prognosis, and its clinical management remains one of the mainstays of patient care. Mainly due to such careful clinical management, the life expectancy of CF patients has increased dramatically over the past few decades [6, 7]. As treatment of CF lung disease becomes more effective and the life expectancy of CF patients increases, the non-pulmonary complication of CF, such as distal intestinal obstructive syndrome (DIOS) and CF-related liver disease (CFLD), are expected to become a prominent cause of morbidity and mortality in CF patients [8, 9]. Therefore, there remains an unmet need for effective treatment of the pulmonary as well as the non-pulmonary (gastrointestinal) complications of CF. Recently developed therapies directed at correcting the basic molecular defect in CFTR anion channel function may in future meet this need (Chapter 2) [10]. Ever expanding knowledge of the molecular structure of CFTR has made it possible to model the impact of the most common disease-causing mutation on the structure and the function of CFTR. A sub-division in mutation classes, based on these structural and functional consequences, provides a rationale for the development of CFTR-targeted drug therapies. This development is aided by improved diagnostic tools which are used to monitor the efficacy of novel CFTR-targeted pharmacotherapies.

However, currently, these novel therapies are still incompletely developed and only effective in correcting the activity of specific CFTR mutants, which makes them applicable to

only a subset of patients [10]. Moreover, the currently (July 2017) approved drugs are prohibitively expensive, which further limits their application in a wider group of patients, especially in less affluent nations [11]. Therefore, a search for cost-effective, so-called mutation-agnostic therapies, which rely on improving symptomatic treatment and/or on alternative strategies to correct the luminal dehydration/acidification defect, is still warranted.

One such strategy entails the modulation of other ion transport mechanisms, of which the (in)activation may counteract the phenotypic consequences of CFTR dysfunction. Most work in this area has centered on the (hyper)activation of alternative anion channels in the apical plasma membrane of airway epithelia cells, including $Ca^{2+}$-activated $Cl^-$ channels [12] and the CFTR-associated SLC26A9 [13]. However, these channels are expressed at only low levels in the gut, or their subcellular localization precludes a role in anion secretion [14, 15] . Therefore, as the options for increasing anion secretion in the CF intestine appear to be limited, we surmise that improving luminal hydration by reducing $Na^+$-coupled water absorption may have more therapeutic potential. For instance inhibition of apically located $Na^+$ channels (i.e. ENaC) or $Na^+/H^+$ exchangers, in particular NHE3, the major nutrient-independent absorptive transporter of $Na^+$ in the intestine, is a potentially viable approach to prevent epithelial dehydration in the absence of CFTR function [16].

To further improve care and management of CF patients, a thorough understanding of the pathophysiological mechanisms that spring from the primary dehydration/acidification defect is crucial. As the gastrointestinal pathophysiology results from an intricate interplay between the combined effects of pancreatic, biliary and intestinal CFTR dysfunction, the causality of, and relation between, separate disease phenomena can be difficult to fathom. For instance, CF-related SIBO will impact host-microbe interactions, which, in turn may have profound effects on many physiological processes within and outside of the intestinal tract [17, 18]. To gain more insight in this complex pathophysiology, we applied transcriptome analysis to systematically chart the changes in gene expression resulting from loss of CFTR function in the distal small **(Chapter 3).** This allowed us to identify cellular signal transduction routes that are dysregulated in CF and may, therefore, be considered therapeutic targets. One of the striking findings of this analysis was that the CF condition has a wide-ranging impact on gene expression, and affects an array of cellular function. The analysis provided clear evidence for intestinal dysbiosis, leading up to an altered host-microorganism interaction and inflammation of the gut wall. In turn, this leads to repression of ligand-dependent nuclear receptor signaling, dysregulation of genes involved in intestinal lipid, sterol, bile acid, and xenobiotic metabolism and in nutrient and solute absorption [19, 20].

In **Chapter 4 and 5,** we focused on the therapeutic potential of a class of endogenous inhibitors of NHE3, the peptides guanylin and uroguanylin, which have the unique ability to activate a readily accessible luminal surface receptor in the intestine, the guanylyl cyclase C (GCC). Activation of GCC by orally administered (uro)guanylin (mimetic) peptides is predicted to result in retention of salt and water in the intestinal lumen by blockade of NHE3-mediated $Na^+$ absorption. In addition, in the subset of patients with residual CFTR activity, it may stimulate low levels of chloride/bicarbonate secretion.

Firstly, we charted the cellular origin of these two luminocrine peptides using an improved in situ hybridization technique, RNAscope **(Chapter 4).** The expression patterns of uroguanylin and guanylin were distinct, although there also was considerable overlap in some regions. Both guanylin and uroguanylin transcripts were found in cells of the secretory lineage, as well as in columnar absorptive cells (enterocytes). Guanylin and uroguanylin were expressed by the Paneth cells that neighbor the intestinal stem cells in the crypts of Lieberkühn, suggesting a role in host defense and, possibly, cell cycle control. Expression in the brush cells in the duodenal villi suggests that these peptides are involved in the regulation of duodenal bicarbonate secretion and luminal pH. GCC transcript was found in epithelial cells along the entire rostrocaudal axis of the intestines. In addition, GCC transcript was found in the duodenal (Brunner) glands. These results suggest that (uro)guanylin (mimetic peptides) may have an additional beneficial action on the CF gut: by triggering CFTR-independent $HCO_3^-$ release from GCC-containing columnar cells, they may promote the expansion of the condensed mucins and their detachment from goblet cells, and restore the protective mucus layer covering the epithelium.

Next, we demonstrated that, in line with the transcriptome data, the production of guanylin and uroguanylin is reduced in CF mice **(Chapter 5)**. This repression of the (uro)guanylin/GCC signaling axis appears to result from SIBO and inflammation of the gut wall, as antibiotic treatment could correct this defect. Reduced GCC activity may exacerbate the fluid secretory defect in CF, and contribute to luminal dehydration and acidification by relieving the repression imposed by cGMP signaling on NHE3 activity. Because of the role of GCC signaling in host defense, lowered (uro)guanylin production may also contribute to intestinal dysbiosis in CF. [21, 22].

The transcriptome analysis indicated that the SIBO found in CF mice is associated with repression of ligand-dependent nuclear receptor signaling. Consistent with this analysis, we observed that intestinal farnesoid X receptor (FXR) signaling in CF mice was markedly impaired, and FXR targets such as *Fgf15* and *Nr0b2* (*Shp*) rank among the most down-

regulated genes in the CF intestine **(Chapter 6).** Antibiotic treatment corrected FXR signaling suggesting that a CF-related inflammatory response suppresses FXR activity. Repression of FXR signaling enhanced de novo bile acid (BA) synthesis, which may culminate in enhanced fecal bile acid excretion, as is present in *Cftr* and *Fgf15 null* mice and in CF patients [1, 23, 24]. Because intestinal FXR activity appears to be crucial for intestinal barrier function and checks the development of certain cholangiopathies, it is conceivable that the loss of its activity in CF plays a role in the etiology of CFLD [25-28]. These results suggest that therapies aimed at restoring FXR function may improve lipid metabolism in CF and slow the development in CFLD. FXR targeted therapy may also improve hepatic glucose and energy metabolism in CF patients [29, 30].

**Future perspective**

The presently prioritized CF therapies are the CFTR-targeted, personalized therapies which are mostly based on mutation-specific small molecule drugs [10].

However, because of the large number of disease-causing mutations in CF (http://www.genet.sickkids.on.ca/app) and their complex effects on CFTR expression and function [31], there remains an interest in therapies that do not rely mainly or solely on restoration of CFTR function, but aim to restore intestinal fluid balance by modulating the activity of other principal intestinal ion transport mechanisms. Our study provides a rationale for targeting the intestinal (uro)guanylin/GCC signaling axis to counteract the CF-typical fluid secretory defect. A similar approach may also be used to treat other complications of CF intestinal disease, including SIBO, gut wall inflammation and DIOS.

The intestinal microbiome is crucial for maintaining health and intestinal dysbiosis has been associated with local gastroenterologic disorders, as well as disease of other organs [32]. To what extent SIBO contributes to the general CF pathology is still unclear, but it has been reported that both intestinal dysbiosis and inflammation are associated with poor nutritional status in patient [33-35]. Our data indicate that dysbiosis and inflammation have a marked effect on intestinal gene expression, and repress the GCC- and ligand-dependent nuclear receptor signaling. Our finding that bacterial lipopolysaccharide (LPS) appears to be a key trigger of the CF-typical immune response suggests that gram-negative bacteria contribute to SIBO. Therapies aimed at reducing colonization of the gut by gram-negative bacteria may attenuate the host immune response and reduce the deleterious effect of gut wall inflammation [36-39]. Because prolonged use of antibiotics is undesirable (e.g. because of potential side effects and development of antibiotics resistance), one possible direction that

may be pursued is the application of probiotics to favor proliferation of bacterial species that repress inflammation (*Lactobacillus murinis*) and epithelial damage (*Lactobacillus plantaram*) [40-47].

**References**

[1] Assis DN, Freedman SD. Gastrointestinal Disorders in Cystic Fibrosis. Clin Chest Med. 2016;37:109-18.
[2] Quinton PM. Role of epithelial HCO3(-) transport in mucin secretion: lessons from cystic fibrosis. Am J Physiol Cell Physiol. 2010;299:C1222-33.
[3] Fridge JL, Conrad C, Gerson L, Castillo RO, Cox K. Risk factors for small bowel bacterial overgrowth in cystic fibrosis. J Pediatr Gastroenterol Nutr. 2007;44:212-8.
[4] Haller W, Ledder O, Lewindon PJ, Couper R, Gaskin KJ, Oliver M. Cystic fibrosis: An update for clinicians. Part 1: Nutrition and gastrointestinal complications. J Gastroenterol Hepatol. 2014;29:1344-55.
[5] Gelfond D, Borowitz D. Gastrointestinal complications of cystic fibrosis. Clin Gastroenterol Hepatol. 2013;11:333-42; quiz e30-1.
[6] Dodge JA, Lewis PA, Stanton M, Wilsher J. Cystic fibrosis mortality and survival in the UK: 1947-2003. Eur Respir J. 2007;29:522-6.
[7] Davis PB. Cystic fibrosis since 1938. Am J Respir Crit Care Med. 2006;173:475-82.
[8] Chryssostalis A, Hubert D, Coste J, Kanaan R, Burgel PR, Desmazes-Dufeu N, et al. Liver disease in adult patients with cystic fibrosis: a frequent and independent prognostic factor associated with death or lung transplantation. J Hepatol. 2011;55:1377-82.
[9] Dray X, Bienvenu T, Desmazes-Dufeu N, Dusser D, Marteau P, Hubert D. Distal intestinal obstruction syndrome in adults with cystic fibrosis. Clin Gastroenterol Hepatol. 2004;2:498-503.
[10] Hanrahan JW, Sampson HM, Thomas DY. Novel pharmacological strategies to treat cystic fibrosis. Trends Pharmacol Sci. 2013;34:119-25.
[11] Cohen D, Raftery J. Paying twice: questions over high cost of cystic fibrosis drug developed with charitable funding. BMJ. 2014;348:g1445.
[12] Pedemonte N, Galietta LJ. Structure and function of TMEM16 proteins (anoctamins). Physiol Rev. 2014;94:419-59.
[13] Mall MA, Galietta LJ. Targeting ion channels in cystic fibrosis. J Cyst Fibros. 2015;14:561-70.
[14] Liu X, Li T, Riederer B, Lenzen H, Ludolph L, Yeruva S, et al. Loss of Slc26a9 anion transporter alters intestinal electrolyte and HCO3(-) transport and reduces survival in CFTR-deficient mice. Pflugers Arch. 2015;467:1261-75.
[15] Schreiber R, Faria D, Skryabin BV, Wanitchakool P, Rock JR, Kunzelmann K. Anoctamins support calcium-dependent chloride secretion by facilitating calcium signaling in adult mouse intestine. Pflugers Arch. 2015;467:1203-13.
[16] Bradford EM, Sartor MA, Gawenis LR, Clarke LL, Shull GE. Reduced NHE3-mediated Na+ absorption increases survival and decreases the incidence of intestinal obstructions in cystic fibrosis mice. Am J Physiol Gastrointest Liver Physiol. 2009;296:G886-98.
[17] Le Chatelier E, Nielsen T, Qin J, Prifti E, Hildebrand F, Falony G, et al. Richness of human gut microbiome correlates with metabolic markers. Nature. 2013;500:541-6.
[18] Ha CW, Lam YY, Holmes AJ. Mechanistic links between gut microbial community dynamics, microbial functions and metabolic health. World Journal of Gastroenterology. 2014;20:16498-517.
[19] Heijerman H. Infection and inflammation in cystic fibrosis: a short review. J Cyst Fibros. 2005;4 Suppl 2:3-5.
[20] Brady MS, Rickard K, Yu PL, Eigen H. Effectiveness of Enteric Coated Pancreatic-Enzymes Given before Meals in Reducing Steatorrhea in Children with Cystic-Fibrosis. J Am Diet Assoc. 1992;92:813-7.
[21] Speck K, Charles A. Distal intestinal obstructive syndrome in adults with cystic fibrosis - A surgical perspective. Arch Surg-Chicago. 2008;143:601-3.

[22] van der Doef HP, Kokke FT, van der Ent CK, Houwen RH. Intestinal obstruction syndromes in cystic fibrosis: meconium ileus, distal intestinal obstruction syndrome, and constipation. Curr Gastroenterol Rep. 2011;13:265-70.
[23] Inagaki T, Choi M, Moschetta A, Peng L, Cummins CL, McDonald JG, et al. Fibroblast growth factor 15 functions as an enterohepatic signal to regulate bile acid homeostasis. Cell Metabolism. 2005;2:217-25.
[24] Bijvelds MJ, Bronsveld I, Havinga R, Sinaasappel M, de Jonge HR, Verkade HJ. Fat absorption in cystic fibrosis mice is impeded by defective lipolysis and post-lipolytic events. Am J Physiol Gastrointest Liver Physiol. 2005;288:G646-53.
[25] Degirolamo C, Rainaldi S, Bovenga F, Murzilli S, Moschetta A. Microbiota modification with probiotics induces hepatic bile acid synthesis via downregulation of the Fxr-Fgf15 axis in mice. Cell Rep. 2014;7:12-8.
[26] Zhou M, Learned RM, Rossi SJ, DePaoli AM, Tian H, Ling L. Engineered fibroblast growth factor 19 reduces liver injury and resolves sclerosing cholangitis in Mdr2-deficient mice. Hepatology. 2016;63:914-29.
[27] Modica S, Petruzzelli M, Bellafante E, Murzilli S, Salvatore L, Celli N, et al. Selective Activation of Nuclear Bile Acid Receptor FXR in the Intestine Protects Mice Against Cholestasis. Gastroenterology. 2012;142:355-U269.
[28] Inagaki T, Moschetta A, Lee YK, Peng L, Zhao GX, Downes M, et al. Regulation of antibacterial defense in the small intestine by the nuclear bile acid receptor. P Natl Acad Sci USA. 2006;103:3920-5.
[29] Zollner G, Marschall HU, Wagner M, Trauner M. Role of nuclear receptors in the adaptive response to bile acids and cholestasis: pathogenetic and therapeutic considerations. Mol Pharm. 2006;3:231-51.
[30] Nguyen A, Bouscarel B. Bile acids and signal transduction: role in glucose homeostasis. Cell Signal. 2008;20:2180-97.
[31] Veit G, Avramescu RG, Chiang AN, Houck SA, Cai Z, Peters KW, et al. From CFTR biology toward combinatorial pharmacotherapy: expanded classification of cystic fibrosis mutations. Mol Biol Cell. 2016;27:424-33.
[32] Lynch SV, Pedersen O. The Human Intestinal Microbiome in Health and Disease. New Engl J Med. 2016;375:2369-79.
[33] Kraemer R, Rudeberg A, Hadorn B, Rossi E. Relative underweight in cystic fibrosis and its prognostic value. Acta Paediatr Scand. 1978;67:33-7.
[34] Brzostek K, Ukleja A. [The importance of a well-balanced diet in the comprehensive treatment of cystic fobrosis] Znaczenie odpowiedniego zywienia w kompleksowym leczeniu mukowiscydozy. Pol Merkur Lekarski. 2017;42:51-6.
[35] Bouquet J, Sinaasappel M, Neijens HJ. Malabsorption in cystic fibrosis: mechanisms and treatment. J Pediatr Gastroenterol Nutr. 1988;7 Suppl 1:S30-5.
[36] Cheng J, Ringel-Kulka T, Heikamp-de Jong I, Ringel Y, Carroll I, de Vos WM, et al. Discordant temporal development of bacterial phyla and the emergence of core in the fecal microbiota of young children. Isme J. 2016;10:1002-14.
[37] Human Microbiome Project C. Structure, function and diversity of the healthy human microbiome. Nature. 2012;486:207-14.
[38] Hollister EB, Riehle K, Luna RA, Weidler EM, Rubio-Gonzales M, Mistretta TA, et al. Structure and function of the healthy pre-adolescent pediatric gut microbiome. Microbiome. 2015;3:36.
[39] Claesson MJ, Jeffery IB, Conde S, Power SE, O'Connor EM, Cusack S, et al. Gut microbiota composition correlates with diet and health in the elderly. Nature. 2012;488:178-84.

[40] Lynch SV, Goldfarb KC, Wild YK, Kong W, De Lisle RC, Brodie EL. Cystic fibrosis transmembrane conductance regulator knockout mice exhibit aberrant gastrointestinal microbiota. Gut Microbes. 2013;4:41-7.
[41] del Campo R, Garriga M, Perez-Aragon A, Guallarte P, Lamas A, Maiz L, et al. Improvement of digestive health and reduction in proteobacterial populations in the gut microbiota of cystic fibrosis patients using a Lactobacillus reuteri probiotic preparation: a double blind prospective study. J Cyst Fibros. 2014;13:716-22.
[42] Atarashi K, Tanoue T, Oshima K, Suda W, Nagano Y, Nishikawa H, et al. Treg induction by a rationally selected mixture of Clostridia strains from the human microbiota. Nature. 2013;500:232-6.
[43] Ahern PP, Faith JJ, Gordon JI. Mining the human gut microbiota for effector strains that shape the immune system. Immunity. 2014;40:815-23.
[44] Braat H, Rottiers P, Hommes DW, Huyghebaert N, Remaut E, Remon JP, et al. A phase I trial with transgenic bacteria expressing interleukin-10 in Crohn's disease. Clin Gastroenterol Hepatol. 2006;4:754-9.
[45] Steidler L, Hans W, Schotte L, Neirynck S, Obermeier F, Falk W, et al. Treatment of murine colitis by Lactococcus lactis secreting interleukin-10. Science. 2000;289:1352-5.
[46] Manor O, Levy R, Pope CE, Hayden HS, Brittnacher MJ, Carr R, et al. Metagenomic evidence for taxonomic dysbiosis and functional imbalance in the gastrointestinal tracts of children with cystic fibrosis. Sci Rep. 2016;6:22493.
[47] Bruzzese E, Callegari ML, Raia V, Viscovo S, Scotto R, Ferrari S, et al. Disrupted intestinal microbiota and intestinal inflammation in children with cystic fibrosis and its restoration with Lactobacillus GG: a randomised clinical trial. PLoS One. 2014;9:e87796.

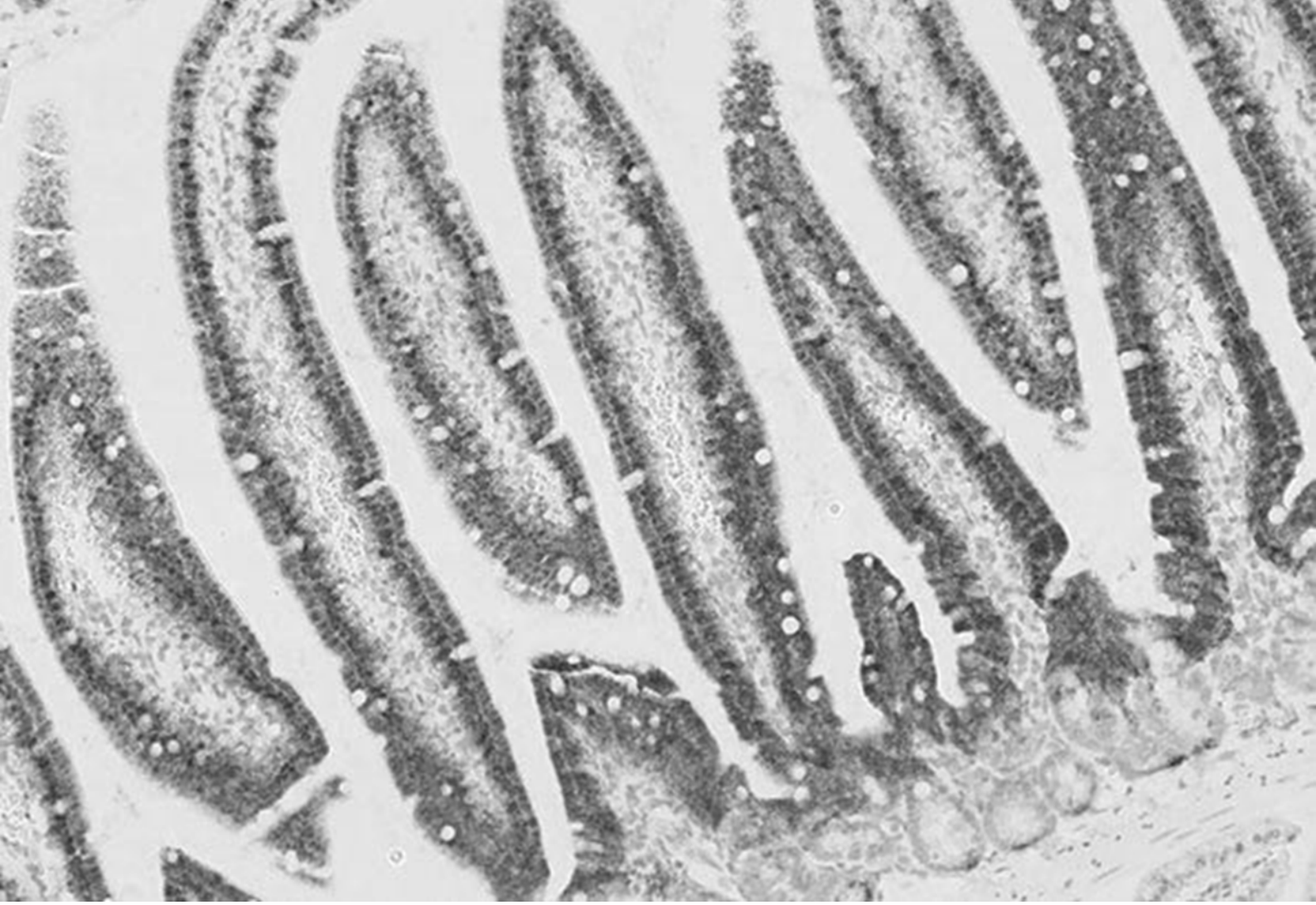

# Chapter 8

# Appendices

**Dutch Summary (Nederlandse Samenvatting)**

**Curriculum Vitae**

**PhD Portfolio**

**Acknowledgements**

**Samenvatting**

Cystic fibrosis (CF; taaislijmziekte) is een erfelijke ziekte die wordt veroorzaakt door mutaties in het CF gen. Dit leidt tot verlies van functie van het CFTR eiwit, dat een belangrijke rol speelt in het transport van zouten en water over de slijmvliezen van (onder andere) de luchtwegen en het darmstelsel. CF wordt gekenmerkt door uitdroging van deze slijmvliezen en de ophoping van viskeus (*taai*) slijm in deze orgaansystemen. Als gevolg hiervan is de spijsvertering verstoord en is de capaciteit voor de opname van voeding verminderd. De combinatie van deze factoren leidt onder meer tot een groeiachterstand bij kinderen, vet-diarree en darmverstoppingen. Deze gastro-intestinale complicaties, alhoewel zelden direct levensbedreigend, zijn zeer belastend voor de patiënt en beïnvloeden het algehele ziekteverloop en de levensverwachting. Om deze redenen is de behandeling van deze gastro-intestinale complicaties een belangrijk onderdeel van de zorg voor patiënten. Mede door dit beleid is de levensverwachting van CF patiënten over de laatste decennia aanzienlijk toegenomen. Desalniettemin blijft er behoefte aan meer effectieve behandelmethoden. De nieuwe medicijnen die op dit ogenblik worden ontwikkeld om het basis-defect in de functie van het CFTR eiwit te corrigeren zullen mogelijk in de toekomst in deze behoefte kunnen voorzien. Deze ontwikkelingen zijn het onderwerp van **hoofdstuk 2** van dit proefschrift. Tot het zo ver is blijft er echter behoefte aan andere, betaalbare, behandelmethoden die toepasbaar zijn in een brede groep CF patiënten.

Om verder inzicht te krijgen in hoe de verschillende gastro-intestinale complicaties van CF zich ontwikkelen vanuit het primaire defect in CFTR functie, is in **hoofdstuk 3** onderzocht wat het effect is van het verlies van CFTR activiteit op de expressie van genen in het laatste deel van de dunne darm. Deze zogenaamde transcriptoom-analyse toont aan dat CF een breed scala van processen in het darmslijmvlies beïnvloedt. De analyse geeft eenduidig bewijs voor de aanwezigheid van bacteriële overgroei en ontsteking van de darmwand, die vervolgens leidt tot een verstoorde regulatie van de opname en verwerking van vetten en andere essentiële voedingsstoffen. De studie laat verder zien dat een gerichte bestrijding van de bacteriële overgroei deze defecten grotendeels herstelt.

Een nieuwe aanpak ter bestrijding van zulke gastro-intestinale CF complicaties die in dit proefschrift wordt verkend is gericht op het verminderen/voorkomen van de CF-kenmerkende uitdroging van de darmslijmvliezen. Deze aanpak heeft niet tot doel de CFTR functie te verbeteren, maar probeert de zout- en waterbalans in de darm te herstellen door de absorptie van zouten en water uit de darm te verminderen. Het is al langer bekend dat de darm twee hormonen produceert, guanyline en uroguayline, die netto transport van zouten en water naar het darmlumen stimuleren door activering van een receptor op het darmslijmvlies. Met het oog op de mogelijke toepassing van

(uro)guanyline-achtige receptor-activators in de behandeling van CF patiënten, werd deze hormonale route verder onderzocht in de hoofdstukken 4 en 5.

Allereerst werd onderzocht in welke celtypen guanyline en uroguanyline worden aangemaakt en welke celtypen van het darmslijmvlies de receptor produceren en dus gevoelig zijn voor (uro)guanyline stimulatie (**hoofdstuk 4**). Uit dit onderzoek bleek dat de beide hormonen slechts in bepaalde celtypen en op specifieke locaties in het darmkanaal worden aangetroffen, terwijl de receptor over de gehele lengte van de dunne en dikke darm, en ook in duodenale klieren, aanwezig is. Dit wijst er op dat stimulatie van deze receptor door een oraal toegediende activator over de gehele lengte van de darm een gunstig effect op de vochtbalans zal hebben. Omdat deze receptor ook betrokken is bij de neutralisatie van het maagzuur in het bovenste deel van de dunne darm, zou stimulatie ook een gunstig effect op de zuur-base balans en de daarmee samenhangende viscositeit van de slijmlaag kunnen hebben. In **hoofdstuk 5** wordt bovendien aangetoond dat de productie van guanyline en uroguanyline is verlaagd in CF. Dat suggereert dat een verminderde stimulering van de (uro)guanyline receptor bijdraagt aan de CF-typische uitdroging van het darmslijmvlies, en dat dit defect kan worden gecompenseerd door toediening van stoffen die de werking van (uro)guanyline imiteren.

Uit de transcriptoom analyse (hoofdstuk 3) was gebleken dat de opname en verwerking van lipiden is verstoord in CF. In **hoofdstuk 6** is dit verder onderzocht en werd aangetoond dat bacteriële overgroei en het onstekingsproces de activiteit van de galzout-receptor FXR onderdrukt. Deze remming van FXR in de darm leidt tot een verhoogde synthese van galzouten in de lever. Mogelijk draagt dit bij aan de verhoogde fecale excretie van galzouten, kenmerkend voor CF, en aan de ontwikkeling van CF-gerelateerde leverziekte.

De ontwikkeling van nieuwe CF therapieën is nu sterk gericht op het identificeren van stoffen die via een directe interactie de functie van het defecte CFTR eiwit verbeteren. Dit leidt doorgaans tot de ontdekking van stoffen die enkel het effect van specifieke mutaties corrigeren en daarom niet in alle patiënten toepasbaar zijn. Mede omdat het aantal verschillende CF-veroorzakende mutaties zo hoog is, blijft er behoefte aan middelen die niet gericht zijn op de correctie van een specifieke defect in de structuur van het CFTR eiwit en daardoor breed inzetbaar zijn binnen de populatie van CF patiënten. Het in dit proefschrift beschreven onderzoek biedt aanknopingspunten voor de ontwikkeling van dergelijke therapieën. Deze zijn gericht op het verbeteren van de vochtbalans in de darm en het voorkomen van de complicaties die, direct of indirect, voortvloeien uit het verlies van CFTR activiteit.

**Curriculum vitae**

Pauline Ikpa was born in Lagos Nigeria on the 22nd of January 1975. She attended and finished her primary school education in Lagos and was enrolled in a boarding school in Ijebu-Ode Ogun state Nigerian for her secondary school education.

In 1993 she was admitted into Nigeria's premiere university, the University of Ibadan for her Bachelors in Biochemistry which she completed in 1999. Thereafter, she enrolled for the compulsory Nigerian National Youth Service for 1 year. She later returned to the university of Ibadan in the year 2000 to complete an academic Master Degree in Biochemistry and Molecular Biology which she completed in 2002.

In 2003 she got married and decided to pursue a career in medical diagnostic for which she followed a compulsory medical laboratory certification course for 2 years (2003 – 2005) in the Nigeria's prestigious Lagos University Teaching Hospital. She worked as a certified medical laboratory scientist from 2005 – 2007.

In 2007, during her time working in Nigeria she obtained a research masters scholarship from the Vrije Universteit Amsterdam to study Biomolecular Science which she completed in 2009. She did her final internship at the Netherlands Cancer Institute Antoni van Leeuwenhoek Hospital in Amsterdam and she then worked as a research technician at the Department of Genetics and Radiation Oncology at Erasmus Medical Center in Rotterdam, the Netherlands, a position she held from 2009 - 2011.

In 2011 she started her PhD program in the Department of Gastroenterology and Hepatology also at the Erasmus Medical Center in Rotterdam with the research group of Prof Hugo de Jonge studying diarrhea diseases, intestinal bowel syndrome and cystic fibrosis under the supervision of Dr Marcel Bijvelds. Her project focused on cystic fibrosis defect in intestinal bile acid and guanylin signaling and aimed to discover novel therapeutic targets for the alleviation of cystic fibrosis intestinal pathology.

Presently, she works as a post-doc, a research position within the same group were she is looking at new approaches to improve gut health in cystic fibrosis.

**PhD Portfolio**

**Name:** Pauline T. Ikpa

**Department:** Gastroenterology and hepatology

**PhD Period:** July 2011- June 2015

**Promotor:** Prof. Dr. Maikel P. Peppelenbosch

**Copromotoren:** Dr. Marcel J.C. Bijvelds and Dr. Hugo R. de Jonge

**Courses**:

- Article 5b: Competence to work with radioactivity in the Netherlands.
- Article 9: Competence to work with laboratory animal science.
- BioBusiness Summer School 2016

**Conferences*:***

- 2014, The 28th Annual North American Cystic Fibrosis Conference Atlanta Georgia (2014)

**Posters:** 1) Impaired FXR signaling in the CF intestine.

2) Validation of (Uro)guanylin treatment as a novel therapeutic option in Cystic Fibrosis.

- 2015, The 19th Annual Molmed day, Erasmus Medical Center Molecular Medicine day Postgraduate School, Rotterdam, The Netherlands.

**Posters:** 1) Impaired FXR signaling in the CF intestine

**List of publications*:***

- **Ikpa PT,** Jonge HR, Peppelenbosch MP, Bijvelds MJ. Impaired FXR signaling in cystic fibrosis mice (Manuscript to be submitted).
- **Ikpa PT**, Jonge HR, Sleddens H, Peppelenbosch MP, Bijvelds MJ. Impaired intestinal guanylyl cyclase C signaling in cystic fibrosis mice (Manuscript to be submitted).
- **Ikpa PT,** Dulla K**,** Jonge HR, Peppelenbosch MP, Bijvelds MJ. Transcriptome analysis of the distal small intestine of *Cftr* null mice (Manuscript to be submitted).
- **Ikpa PT,** Jonge HR, Steinbrecher CKA, Sleddens HFBM, Peppelenbosch M, Smit R, Bijvelds MJ. Guanylin and uroguanylin are produced by mouse intestinal epithelial cells of columnar and secretory lineage Histochem Cell Biol. 2016 Oct:146(4):445-55.

- **Ikpa PT,** Bijvelds MJ, de Jonge HR. Cystic fibrosis: toward personalized therapies *Int J Biochem Cell Biol. 2014 Jul;52:192-200.*
- Hermans N, Laffeber C, Cristovão M, Artola-Borán M, Mardenborough Y, **Ikpa P**, Jaddoe A, Winterwerp HH, Wyman C, Jiricny J, Kanaar R, Friedhoff P, Lebbink JH. Dual daughter strand incision is processive and increase the efficiency if DNA mismatch repair. Nucleic Acids Res. 2016 Aug 19;44(14):6770-86.
- Mattiroli F, Vissers JH, van Dijk WJ, **Ikpa P,** Citterio E, Vermeulen W, Marteijn JA, Sixma TK. RNF168 ubiquitinates K13-15 on H2A/H2AX to drive DNA damage signaling. *Cell. 2012 Sep 14;150(6):1182-95*.

**Acknowledgements**

At last my thesis is ready after a journey of a lifetime, glory to God Almighty! During this journey a lot of friendship were made and also many sacrifices were inevitable. Therefore, I would like to thank my fellow colleagues, friends and family.

**To my husband Abraham and kids, Andria and Alex;** I appreciated all your support and patience.

**To my promoter Prof. Maikel P Peppelenbosch,** thank you for the opportunity to carry out my research in your Lab and all the support you rendered over the years. My deepest gratitude goes to **Prof Hugo de Jonge** who made this journey possible by giving me the opportunity to work in his group, without which I will not be in this position today. Hugo, words cannot explain my gratitude. To my co-promoter **Marcel Bijvelds** thank you very much for your supervision and willingness to share your knowledge, thank you for your patience and stimulation to work. To **Ron (Smits)** thank you for your guidance, willingness to share ideas and render support when necessary.

**Jaap, Luc, Henneke, Andre, Andrea** even though we never really worked together, I would like to say thank you for providing a conducive working atmosphere as leaders. To CFTR ladies **Kelly and Natascha** thanks for all the support and I am looking forward to working with you again. To my office mates Na1001 (2017: **Vincent, Wen, Hakim, Yingying, Sunrui, Thijmen, Andiaan, Suk Lee Lam**) thank you for all the encouragement, jokes and laughs. I wish you all success! To **Auke, Pan (Abdullah), Monique, Henk** at some point during my time in the lab I had the opportunity to talk to you and I want to thank you all for the warm reception.

**To Isaac (Ishaku)** my brother in Christ and fellow Nigeria. A big thank you for all your support, your joining the group was like having a brother around. Thanks again!!

**Petra, Paula, Anthonie** Thanks a lot and I must say your guys are multitalented from music to photography and arts!! **Jan,** thanks for everything, because of you my Dutch improved in a short while. **Jun,** thanks for your help in introducing me to IPA. **Juan Li (Amy)** you are a nice person, things are going to get better (Urbesth!!!) **Kim, Gertine, Shanta, Patrick, Martine, Frances, Buddy, Aniek, Marieke** thanks for putting everything in place and at the same time assisting when necessary**.**

To all my past **(Effie, Cindy, Yeubang, Wenshi),** present Chinese colleagues especially, **Wanlu, Estella, Wenhui, Changbo,Shan, Pengyu** thank you all for being good

company**.** To **Gwenny,** thanks a lot for a good introduction to the lab; it was a good start and I enjoyed all the other conversations. **Greta** thanks for all the smiles!

**Asma,** thanks a lot my friend and sister, to us the project was a humble beginning**. Werner, Evelyn, Dowty, Jasper, Wadaq, Wesley, Rik, Renee, Elmer, Rajesh, Haziz, Angela, Xiaolei, Veda, Jasper, Elke.** I learnt a lot form you guys**. Raymond and Leonie** thanks for being so helpful with my administration and computer**. To Francesca, Joyce and Prof Titia** thanks for the opportunity to start in your labs. **To my Vrije Universiteit M.Sc colleages Jai, Laurens, Nawal, Paula, Dr Jan, Dr Bert and Dr Ingrid** thanks for all your support. On the last note I would like to say thank you with a shout of Hallelujah!!! To all "The Predestined Foundation family" (www.thepredestined.org), Neo-Tresax international family and my entire RCCG family.